

12-2014

# Development of a Hydrologic Model for an Urban Headwater Stream: The Influence of Pervious Surface Properties on Runoff Dynamics

Dawn A. Farver

University of Arkansas, Fayetteville

Follow this and additional works at: <http://scholarworks.uark.edu/etd>

 Part of the [Fresh Water Studies Commons](#), [Hydraulic Engineering Commons](#), and the [Hydrology Commons](#)

---

## Recommended Citation

Farver, Dawn A., "Development of a Hydrologic Model for an Urban Headwater Stream: The Influence of Pervious Surface Properties on Runoff Dynamics" (2014). *Theses and Dissertations*. 2060.  
<http://scholarworks.uark.edu/etd/2060>

This Dissertation is brought to you for free and open access by ScholarWorks@UARK. It has been accepted for inclusion in Theses and Dissertations by an authorized administrator of ScholarWorks@UARK. For more information, please contact [scholar@uark.edu](mailto:scholar@uark.edu), [ccmiddle@uark.edu](mailto:ccmiddle@uark.edu).

Development of a Hydrologic Model for an Urban Headwater Stream: The Influence  
of Pervious Surface Properties on Runoff Dynamics

Development of a Hydrologic Model for an Urban Headwater Stream: The Influence  
of Pervious Surface Properties on Runoff Dynamics

A dissertation submitted in partial fulfillment  
of the requirements for the degree of  
Doctor of Philosophy in Civil Engineering

by

Dawn Ann Farver  
The Ohio State University  
Bachelor of Science in Food, Agricultural, and Biological Engineering, 2001  
The Ohio State University  
Master of Science in Food, Agricultural, and Biological Engineering, 2004

December 2014  
University of Arkansas

This dissertation is approved for recommendation to the Graduate Council.

---

Dr. Rodney D. Williams  
Dissertation Director

---

Dr. Kristofor Brye  
Committee Member

---

Dr. John C. Dixon  
Committee Member

---

Dr. Jason A. Tullis  
Committee Member

## Abstract

A hydrologic model was developed for the Mullins Creek (MC) catchment located on the University of Arkansas campus in Fayetteville, Arkansas. The MC catchment is a small, dynamic urban stream system with a range of land use/land cover (LULC), an extensive and well-developed stormwater drainage network, and extensive urbanization (over 90% developed, and almost 50% impervious surface area (ISA)). Selected datasets provided information on the stormwater drainage network, the physical attributes of the catchment and receiving waterway (i.e. drainage area, slope, etc.), infiltration potential of soil map units, LULC, and percent ISA. These datasets were analyzed to provide input parameters and develop a Storm Water Management Model (SWMM) for the MC catchment. To more accurately characterize the infiltration potential of the pervious areas of the catchment, infiltration testing was performed in the field to compare infiltration in paired highly maintained and minimally maintained sites in the same soil map unit in or near the catchment. As a component of the modeling process, a sensitivity analysis was run on two sets of parameters: percent ISA and Horton infiltration rates. The sensitivity of the model output to changes in percent ISA and changes in infiltration rates varied based on storm event size. The MC SWMM model was most sensitive to changes in percent impervious surface for small storm events (25 – 50 mm), while the model was most sensitive to changes in infiltration rates for moderate to large storm events ( $\geq 150$  mm). In an effort to test the utility of developing a hydrologic model of this type for other small, urban drainage systems, the uncalibrated model was validated using selected storm events. Observed storm hydrograph data were downloaded from a USGS gaging station located at the outlet of the catchment. Overall, the MC model performed well for the selected storm events, although it performed best for the storms that occurred closest to when the LULC data were collected. The uncalibrated model outputs were most accurate when observed soil infiltration data were incorporated into the model, and when the percent ISA in the model was set equal to total impervious area.

## Acknowledgments

First, I'd like to thank my dissertation committee. This has definitely been a process, and I appreciate all of your support, guidance, and patience. Especially to Dr. Kris Brye for lending me an ear, field equipment, and field help.

I would also like to thank Dr. Patricia Koski and all the Graduate School staff for their help and support throughout my time here at the University of Arkansas. You all care about our graduate students and respect us for the researchers, teachers, students, and people that we are.

My journey to Arkansas has brought many special people into my life. My fellow graduate students who shared their own trials and tribulations, stories of success, advice, support, and were my partners in crime. Some of you have finished and moved on, and provided me with much needed encouragement when things were tough. Some of you are still working on your degrees. Best of luck. Thank you for being my family and community when I was so far from home. Special thanks to Stephanie Shepherd, Byron Winston, Kathy Knierim, Dorine Reed Bower, Tammy Overacker, Liz Brandt, Lora Streeter, Marie Karlsson, Rodica Lisnic and all my friends and colleagues from the GDSAB.

Thank you to everyone who helped me out in the field: Stephanie Shepherd, Lisa Wood, Doug Wolf, Kathy Knierim, and Richard McMullen. Not to mention my husband and daughter who joined me on many a field outing. Thank you to Scott Becton for sharing much needed field supplies, moral support, and data collection advice. Thank you to Dr. Van Brahana, Dr. Charles Leflar, and Dr. Julian Archer for allowing me access to collect soil samples and infiltration data.

Thank you to my first stream teachers – Dr. Andrew Ward, Dan Mecklenburg, and Dr. Lance Williams, who helped me appreciate streams and taught me how to study and understand these amazing systems, fish, bugs and all. Finally, to the original stream geomorph crew: Jessica D'Ambrosio, Jon Witter, and Anand Jayakaran.

## **Dedication**

This dissertation is dedicated to all my friends and family who supported me throughout this journey, even when you had no idea what I was doing, or why I was doing it...and listened and believed in me when I had my own doubts.

Especially to my mom – Sandra Farver, my original and loudest cheerleader, to my husband – Chad Kirkpatrick, for...everything...there are not enough words, to my daughter – Aurora Sage, for your patience and love and beautiful artwork, and to my dogs – Raine and Parker, for spending many late nights and early mornings with me.

## Table of Contents

<b>Chapter 1. Introduction</b>	<b>1</b>
Dissertation Format	1
Study Justification	2
Problem Statement	6
Research Hypotheses	7
<b>Chapter 2. Literature Review</b>	<b>8</b>
Urbanization	8
Impervious Surface Area	13
Effective Impervious Area (EIA)	15
Relationship between Total Impervious Area and Effective Impervious Area	18
Summary of Urbanization Impacts	18
Infiltration and Compaction	20
Infiltration	20
Estimating Infiltration Rates	22
Horton Infiltration Method	22
Green and Ampt Infiltration Model	25
NRCS Curve Number Method	26
Summary	30
Infiltration in Urbanized/Developed Areas	30
Soil Compaction	33
Soil Compaction During Development	35
Measuring Soil Compaction/Infiltration Capacity	35
Hydrologic Modeling	36
Historical Perspective	36
Purpose of Hydrological Models	37
Modeling Process	38
Types of Hydrologic Models	40
Lumped vs. Distributed Hydrologic Models	42
Stochastic vs. Deterministic vs. Parametric	42
Event-based vs. Continuous	42
Summary	43
About the EPA's Storm Water Management Model (SWMM)	43
Subcatchments	46
Infiltration	48
Flow Routing	48
Applicability of SWMM in small urban watersheds	50
<b>Chapter 3. Site Description/Characterization</b>	<b>55</b>
Physical Characteristics	58
Land Use/Land Cover (LULC) and Imperviousness	60
Stormwater Drainage Network	64
USGS Gaging Station	64
Soils Data	68

<b>Chapter 3. cont.</b>	
Subcatchments	68
Summary/Discussion	72
<b>Chapter 4. Mullins Creek Soil Characterization</b>	<b>74</b>
Introduction	74
Soils in the Mullins Creek Catchment	75
Methods	78
Infiltration Testing	78
Moisture Content	83
Bulk Density	83
Particle-size Analysis	85
Data Analysis	90
Results	90
Bulk Density	90
Infiltration Rate/Moisture Content/Horton Parameters	93
Particle-size Analysis/Color Analysis	95
Discussion	101
<b>Chapter 5. Storm Water Management Model (SWMM) Parameterization</b>	<b>106</b>
Introduction	106
Physical Subcatchment Characteristics	106
Land Use/Land Cover (LULC) and Percent Impervious Surface	114
Subcatchment Infiltration Parameters	114
Impervious Surface	121
Discussion	125
<b>Chapter 6. Mullins Creek SWMM Sensitivity Analysis</b>	<b>127</b>
Introduction	127
SWMM Sensitivity Analysis Model Runs	128
Results	133
Percent Impervious Area	133
Horton Infiltration Parameters	140
Discussion	143
<b>Chapter 7. Mullins Creek Uncalibrated SWMM Model Validation</b>	<b>151</b>
Introduction	151
Methods	153
Observed Runoff Data	154
Precipitation Data	154
SWMM Model Runs	158
Results and Discussion	158
<b>Chapter 8. Summary and Conclusions</b>	<b>168</b>
<b>References</b>	<b>174</b>



Appendix A. Observed infiltration parameters from field data collection	182
Appendix B. Rainfall distribution for selected storm events	194
Appendix C. Infiltration and impervious surface inputs for model validation	203
Appendix D. Predicted versus observed runoff for selected storm events	211

## List of Tables

Table 1.1. Land use/land cover (LULC) data for the Mullins Creek catchment	5
Table 2.1. Two examples of stream health thresholds for percent impervious surface area (ISA)	16
Table 2.2. Relationship between land use and imperviousness	19
Table 2.3. Percent effective impervious area for different categories of impervious surface	19
Table 2.4. Common ranges of accepted parameter values for the Horton Infiltration Equation	24
Table 2.5. Horton parameters for selected soil types under bluegrass turf land cover	24
Table 2.6. Characteristics of soils in each hydrologic soil group (HSG)	28
Table 2.7. Assessing quality of land cover	28
Table 2.8. Curve numbers for land use, condition, and hydrologic soil group for average conditions	29
Table 2.9. Curve numbers for AMC II, and conversion factors to convert from AMC II to AMC I and/or AMC III	31
Table 2.10. Parameter values for various soil texture classes for use with the Green-Ampt equation	31
Table 2.11. Horton infiltration parameter input descriptions for the SWMM	32
Table 2.12. Green-Ampt infiltration parameter input descriptions for the SWMM	32
Table 2.13. Levels of complexity for hydrologic models	41
Table 2.14. Comparison of temporal and spatial resolution for event-based versus continuous simulation runs in SWMM	47
Table 3.1. Geomorphology data summary on the Mullins Creek main catchment central reach	61
Table 3.2. Bed material characteristics of the middle reach of Mullins Creek determined by a pebble count pre-2012 restoration	61
Table 3.3. Land use/land cover (LULC) and percent total impervious surface (TIA) data for Mullins Creek for 2010	62

## List of Tables (cont.)

Table 3.4. Land Use/Land Cover (LULC) for the Mullins Creek catchment in 2010, and percent impervious surface	63
Table 3.5. Subcatchment data summary for the main subcatchments A through D	73
Table 3.6. of values for select subcatchment parameters divided by primary subcatchment	73
Table 4.1. Recommended infiltration rates for the Horton Infiltration Equation based on hydrologic soil group (HSG)	76
Table 4.2. Descriptions of soil series associated with the Mullins Creek catchment area	76
Table 4.3. Mullins Creek soil map unit descriptions and percentages in the catchment	79
Table 4.4. Field infiltration testing sites and locations	79
Table 4.5. Bulk density results for each pair of sampling locations	91
Table 4.6. Initial moisture content and infiltration results for all sites sampled	94
Table 4.7. Predicted and observed texture classes for Mullins Creek soils	96
Table 4.8. Results from particle size analysis: percent sand, clay, and silt for each soil sample	97
Table 4.9. Munsell color classifications for saturated soil samples in the Mullins Creek catchment	100
Table 5.1. Physical parameters extracted for each subcatchment in ArcGIS to be used as inputs to the SWMM model	111
Table 5.2. Percent impervious surface in each Mullins Creek subcatchment	115
Table 5.3. Land use land cover (LULC) categories for each subcatchment used in the SWMM model	117
Table 5.4. Observed and predicted Horton infiltration parameters used to determine the infiltration characteristics of each subcatchment in SWMM	120
Table 5.5. Predicted and observed Horton infiltration parameter inputs into SWMM using soil texture and observed field data	122
Table 5.6. Land use/land cover categories extracted from 2010 LULC dataset for each subcatchment	124

## List of Tables (cont.)

Table 6.1. Parameters entered into each SWMM model run for each subcatchment to test the sensitivity of the model to percent impervious surface under different storm intensity scenarios	129
Table 6.2. Parameters entered into each SWMM model runs for each subcatchment to test the sensitivity of the model to changes in Horton Infiltration parameters	131
Table 6.3. Table of peak discharge predictions (cms) for a range of storm event sizes and over a range of impervious surface percentages for the Mullins Creek catchment model in SWMM	136
Table 6.4. Table of total runoff predictions (m <sup>3</sup> ) for a range of storm event sizes and over a range of impervious surface percentages for the Mullins Creek catchment model in SWMM	138
Table 6.5. Table of peak discharge predictions (cms) for a range of storm event sizes and over a range of infiltration values for the Mullins Creek catchment model in SWMM	144
Table 6.6. Table of total runoff predictions (m <sup>3</sup> ) for a range of storm event sizes and over a range of infiltration values for the Mullins Creek catchment model in SWMM	146
Table 7.1. The average infiltration rates and percent impervious surface for three different infiltration/impervious surface scenarios for each main subcatchment	155
Table 7.2. Summary of observed storm events used for model validation purposes	156
Table 7.3. Observed vs. predicted SWMM model results for the first infiltration scenario	162
Table 7.4. Observed vs. predicted SWMM model results for the second infiltration scenario	162
Table 7.5. Observed vs. predicted SWMM model results for the third infiltration scenario	163
Table 7.6. Observed vs. predicted SWMM model results for the fourth infiltration scenario	163
Table C.1. Input parameters for each subcatchment for model scenario 1: predicted infiltration based on soil texture, and percent impervious area equal to percent directly connected impervious area	203
Table C.2. Input parameters for each subcatchment for model scenario 2: predicted infiltration based on soil texture, and percent impervious area equal to percent total impervious area	205

## List of Tables (cont.)

Table C.3. Input parameters for each subcatchment for model scenario 3: predicted infiltration based on observed soil infiltration characteristics, and percent impervious area equal total impervious area	207
Table C.4. Input parameters for each subcatchment for model scenario 4: predicted infiltration based on observed soil infiltration characteristics, and percent impervious area equal total impervious area	209

## List of Figures

Figure 1.1. Aerial map of the Mullins Creek catchment located on the University of Arkansas Fayetteville campus	5
Figure 2.1. Illustration of the balance between biological, chemical, and physical components of a stream system	9
Figure 2.2. Hypothetical storm hydrographs demonstrating the change in channel response to urbanization	12
Figure 2.3. The relationship between impervious cover and surface runoff for increasingly concentrated urban development	14
Figure 2.4. As the depth of the water table decreases in response to reduced infiltration in a catchment, a stream can go from being a “gaining” reach (a) to a “losing” reach (b), decreasing baseflow conditions during dry periods	21
Figure 2.5. A theoretical infiltration curve for a silt-loam soil using the Horton Equation	24
Figure 2.6. The modeling process	39
Figure 2.7. Conceptual model of surface runoff from subcatchments in SWMM	47
Figure 2.8. Conceptual model of rectangular subcatchment runoff from pervious and impervious surfaces	49
Figure 3.1. A graphic of the geology of the Ozark Plateau Region, including the Boston Mountains, Springfield Plateau, and Salem Plateau sub regions	56
Figure 3.2. Map of Beaver Lake Reservoir watershed composed of seven major catchments spanning five counties in Arkansas	57
Figure 3.3. The study area, Mullins Creek catchment, is located in Washington County in Northwest Arkansas	59
Figure 3.4. Land Use/Land Cover (LULC) for the Mullins Creek catchment in 2010, and percent impervious surface	62
Figure 3.5. Stormwater drainage network under the Mullins Creek catchment	65
Figure 3.6. Total length of stormwater drainage pipe by diameter	66
Figure 3.7. USGS Gaging Station (07048480) “College Branch at MLK Blvd at Fayetteville, AR” is located where Mullins Creek runs under Martin Luther King, Jr. Boulevard	67
Figure 3.8. Relationship between rainfall and runoff for all storm events with a peak flow greater than 100 cfs (2.8 cms) that occurred between 2008 and 2011	69

## List of Figures (cont.)

Figure 3.9. Relationship between rainfall and runoff for all storm events with a peak flow greater than 100 cfs (2.8 cms).	70
Figure 3.10. Main subcatchments in the Mullins Creek catchment: A, B, C, and D, and the higher spatial resolution subcatchment delineation used for hydrologic modeling parameterization.	71
Figure 4.1. Soil map units in the Mullins Creek catchment and the Hydrologic Soil Group (HSG) distribution in the catchment	77
Figure 4.2. Layout of double-infiltrometer rings and locations for field testing	80
Figure 4.3. Photograph of a double-ring infiltrometer used in the study, manufactured by Turftec International.	80
Figure 4.4. Sample field data collection sheet used for recording infiltration testing results	82
Figure 4.5. Photographs of theta probe used to measure initial moisture content of the soil at each site before infiltration testing was performed	84
Figure 4.6. Bulk density sample collected in the field from the Oakland-Zion site	84
Figure 4.7. Soil samples were ground to a uniform size and passed through a 2-mm sieve to obtain a sample for analysis	86
Figure 4.8. One liter sedimentation cylinder with hydrometer present for reading	88
Figure 4.9. Photograph of particle settling in sedimentation cylinder	89
Figure 4.10. Graph of the bulk density of highly maintained pairs of sites versus the bulk density of minimally maintained sites excluding the results for the sites characterized as HSG D	92
Figure 4.11. Texture triangle of AASHTO, USDA, and Unified Classification Systems	96
Figure 4.12. Bulk density core sample from The Garden SW field location	98
Figure 4.13. Photograph of sedimentation cylinders with incorporated samples	99
Figure 4.14. Example of a construction site near the Lot 56B infiltration sampling site	102
Figure 4.15. Photograph of a highly maintained site (South Lot 56B) on the University of Arkansas campus	103
Figure 4.16. Example of predicting Horton Infiltration parameters from observed data	105

## List of Figures (cont.)

Figure 5.1. Example of a raster digital elevation model (DEM) grid that is converted from elevation data to flow direction	108
Figure 5.2. Sample flow accumulation layer that results from the Elevation layer to the left after flow direction is calculated for each pixel	108
Figure 5.3. Example of a flow accumulation layer from ArcGIS	109
Figure 5.4. Geoprocessing model for delineating subcatchments in ArcGIS	113
Figure 5.5. Geoprocessing model for extracting raster datasets	118
Figure 6.1. Map of SCS rainfall distributions for the United States	134
Figure 6.2. Distribution of a 100 mm, SCS Type III, 24 hour storm event	135
Figure 6.3. Table of peak discharge predictions (cms) for a range of storm event sizes and over a range of impervious surface percentages for the Mullins Creek catchment model in SWMM	137
Figure 6.4. Relationship between total runoff predictions for the Mullins Creek catchment and percent impervious area over a range of SCS Type III, 24 hr design storm events	139
Figure 6.5. Sensitivity of the peak discharge output to changes in percent impervious surface for different storm intensities	141
Figure 6.6. Sensitivity of the total runoff output to changes in percent impervious surface for different storm intensities	142
Figure 6.7. Relationship between peak discharge predictions for the Mullins Creek catchment and percent of maximum Horton infiltration parameters over a range of SCS Type III, 24 hr design storm events	145
Figure 6.8. Relationship between total runoff predictions for the Mullins Creek catchment and percent of maximum Horton infiltration parameters over a range of SCS Type III, 24 hr design storm events	147
Figure 6.9. Relationship between total runoff predictions for the Mullins Creek catchment and percent of maximum Horton infiltration parameters over a range of SCS Type III, 24 hr design storm events	148
Figure 6.10. Sensitivity of the total runoff output to changes in percent of maximum Horton infiltration parameters for different storm intensities	149
Figure 7.1. Graph of total runoff (m <sup>3</sup> ) versus total rainfall (mm) for the storm events selected for validation of the SWMM model	157



## List of Figures (cont.)

Figure 7.2. A system precipitation hyetograph based on NEXRAD Level III radar data and processed using a Radar Acquisition and Processing (RAP) Project in PCSWMM	159
Figure 7.3. Observed versus predicted storm hydrograph from SWMM model	160
Figure 7.4. Predicted versus observed runoff for Mullins Creek catchment (Scenario 4: 27 June 2010)	165
Figure 7.5. Predicted versus observed runoff for Mullins Creek catchment (Scenario 4: 5 August 2009)	166
Figure 8.1. Mullins Creek SWMM modeling scenarios for validation of the uncalibrated model	171
Figure A.1. Graph of observed Horton infiltration data points and the best-fit Horton infiltration curve developed from the observed dataset for the Fayetteville High School (FHS) sampling location.	182
Figure A.2. Graph of observed Horton infiltration data points and the best-fit Horton infiltration curve developed from the observed dataset for the Leflar sampling location	183
Figure A.3. Graph of observed Horton infiltration data points and the best-fit Horton infiltration curve developed from the observed dataset for the Maple Hill sampling location	184
Figure A.4. Graph of observed Horton infiltration data points and the best-fit Horton infiltration curve developed from the observed dataset for the Lewis Avenue sampling location	185
Figure A.5. Graph of observed Horton infiltration data points and the best-fit Horton infiltration curve developed from the observed dataset for the Reynold's Center sampling location	186
Figure A.6. Graph of observed Horton infiltration data points and the best-fit Horton infiltration curve developed from the observed dataset for the Pratt Place sampling location	187
Figure A.7. Graph of observed Horton infiltration data points and the best-fit Horton infiltration curve developed from the observed dataset for the SW Gardens sampling location	188
Figure A.8. Graph of observed Horton infiltration data points and the best-fit Horton infiltration curve developed from the observed dataset for the SW Gardens sampling location	189

## List of Figures (cont.)

Figure A.9. Graph of observed Horton infiltration data points and the best-fit Horton infiltration curve developed from the observed dataset for the Central Gardens sampling location	190
Figure A.10. Graph of observed Horton infiltration data points and the best-fit Horton infiltration curve developed from the observed dataset for the Mullins Creek South sampling location	191
Figure A.11. Graph of observed Horton infiltration data points and the best-fit Horton infiltration curve developed from the observed dataset for the Lot 56B sampling location	192
Figure A.12. Graph of observed Horton infiltration data points and the best-fit Horton infiltration curve developed from the observed dataset for the Oakland-Zion sampling location	193
Figure B.1. Rainfall hyetograph for Mullins Creek catchment from PCSWMM system results, NEXRAD Level III inputs, 12 April 2009 storm event	194
Figure B.2. Rainfall hyetograph for Mullins Creek catchment from PCSWMM system results, NEXRAD Level III inputs, 05 August 2009 storm event	195
Figure B.3. Rainfall hyetograph for Mullins Creek catchment from PCSWMM system results, NEXRAD Level III inputs, 10 August 2009 storm event	196
Figure B.4. Rainfall hyetograph for Mullins Creek catchment from PCSWMM system results, NEXRAD Level III inputs, 21 September 2009 storm event	197
Figure B.5. Rainfall hyetograph for Mullins Creek catchment from PCSWMM system results, NEXRAD Level III inputs, 08 October 2009 storm event	198
Figure B.6. Rainfall hyetograph for Mullins Creek catchment from PCSWMM system results, NEXRAD Level III inputs, 29 October 2009 storm event	199
Figure B.7. Rainfall hyetograph for Mullins Creek catchment from PCSWMM system results, NEXRAD Level III inputs, 27 June 2010 storm event	200
Figure B.8. Rainfall hyetograph for Mullins Creek catchment from PCSWMM system results, NEXRAD Level III inputs, 27 February 2011 storm event	201
Figure B.9. Rainfall hyetograph for Mullins Creek catchment from PCSWMM system results, NEXRAD Level III inputs, 22 September 2011 storm event	202
Figure D.1a. Predicted versus observed runoff for Mullins Creek catchment (Scenario 1: 12 April 2009)	211
Figure D.1b. Predicted versus observed runoff for Mullins Creek catchment (Scenario 2: 12 April 2009)	212

## List of Figures (cont.)

Figure D.1c. Predicted versus observed runoff for Mullins Creek catchment (Scenario 3: 12 April 2009)	213
Figure D.1d. Predicted versus observed runoff for Mullins Creek catchment (Scenario 4: 12 April 2009)	214
Figure D.2a. Predicted versus observed runoff for Mullins Creek catchment (Scenario 1: 05 August 2009)	215
Figure D.2b. Predicted versus observed runoff for Mullins Creek catchment (Scenario 2: 05 August 2009)	216
Figure D.2c. Predicted versus observed runoff for Mullins Creek catchment (Scenario 3: 05 August 2009)	217
Figure D.2d. Predicted versus observed runoff for Mullins Creek catchment (Scenario 4: 05 August 2009)	218
Figure D.3a. Predicted versus observed runoff for Mullins Creek catchment (Scenario 1: 10 August 2009)	219
Figure D.3b. Predicted versus observed runoff for Mullins Creek catchment (Scenario 2: 10 August 2009)	220
Figure D.3c. Predicted versus observed runoff for Mullins Creek catchment (Scenario 3: 10 August 2009)	221
Figure D.3d. Predicted versus observed runoff for Mullins Creek catchment (Scenario 4: 10 August 2009)	222
Figure D.4a. Predicted versus observed runoff for Mullins Creek catchment (Scenario 1: 21 September 2009)	223
Figure D.4b. Predicted versus observed runoff for Mullins Creek catchment (Scenario 2: 21 September 2009)	224
Figure D.4c. Predicted versus observed runoff for Mullins Creek catchment (Scenario 3: 21 September 2009)	225
Figure D.4d. Predicted versus observed runoff for Mullins Creek catchment (Scenario 4: 21 September 2009)	226
Figure D.5a. Predicted versus observed runoff for Mullins Creek catchment (Scenario 1: 08 October 2009)	227
Figure D.5b. Predicted versus observed runoff for Mullins Creek catchment (Scenario 2: 08 October 2009)	228

## List of Figures (cont.)

Figure D.5c. Predicted versus observed runoff for Mullins Creek catchment (Scenario 3: 08 October 2009)	229
Figure D.5d. Predicted versus observed runoff for Mullins Creek catchment (Scenario 4: 08 October 2009)	230
Figure D.6a. Predicted versus observed runoff for Mullins Creek catchment (Scenario 1: 29 October 2009)	231
Figure D.6b. Predicted versus observed runoff for Mullins Creek catchment (Scenario 2: 29 October 2009)	232
Figure D.6c. Predicted versus observed runoff for Mullins Creek catchment (Scenario 3: 29 October 2009)	233
Figure D.6d. Predicted versus observed runoff for Mullins Creek catchment (Scenario 4: 29 October 2009)	234
Figure D.7a. Predicted versus observed runoff for Mullins Creek catchment (Scenario 1: 27 June 2010)	235
Figure D.7b. Predicted versus observed runoff for Mullins Creek catchment (Scenario 2: 27 June 2010)	236
Figure D.7c. Predicted versus observed runoff for Mullins Creek catchment (Scenario 3: 27 June 2010)	237
Figure D.7d. Predicted versus observed runoff for Mullins Creek catchment (Scenario 4: 27 June 2010)	238
Figure D.8a. Predicted versus observed runoff for Mullins Creek catchment (Scenario 1: 27 February 2011)	239
Figure D.8b. Predicted versus observed runoff for Mullins Creek catchment (Scenario 2: 27 February 2011)	240
Figure D.8c. Predicted versus observed runoff for Mullins Creek catchment (Scenario 3: 27 February 2011)	241
Figure D.8d. Predicted versus observed runoff for Mullins Creek catchment (Scenario 4: 27 February 2011)	242
Figure D.9a. Predicted versus observed runoff for Mullins Creek catchment (Scenario 1: 22 September 2011)	243
Figure D.9b. Predicted versus observed runoff for Mullins Creek catchment (Scenario 2: 22 September 2011)	244

## List of Figures (cont.)

Figure D.9c. Predicted versus observed runoff for Mullins Creek catchment (Scenario 3: 22 September 2011)	245
Figure D.9d. Predicted versus observed runoff for Mullins Creek catchment (Scenario 4: 22 September 2011)	246

## **Chapter 1. Introduction**

### **Dissertation Format**

Because of the nature of this project and its multi-component nature where independent studies feed data into other portions of the project, this dissertation is presented in a non-traditional format. The layout of the chapters and organization of the document is outlined below.

Chapter 1, the introduction, provides basic background, justification, and the overall goals of the project for the reader. Chapter 2 is the literature review which presents a comprehensive summary of the literature relevant to the topics studied/presented in the document. Chapter 3, the site characterization chapter, presents information about the study site and location, in addition to relevant datasets, references used to extract information about the site, and is referenced through the document where appropriate. Chapters 4, 5, and 6 present the main body of research.

In chapter 4, the reader will find information on the field soil infiltration analysis research that was performed and data that were collected to better understand existing conditions in the study area. These data were also incorporated into the hydrologic model to more accurately parameterize the infiltration to match existing conditions.

Methods and the process of parameterizing the hydrologic model are discussed in Chapter 5. Available datasets and how they were analyzed, are addressed as well as the discretization of the catchment into subcatchments.

Chapter 6 discusses the sensitivity of the Mullins Creek Storm Water Management Model (SWMM) to changes in key parameters: infiltration rates for pervious surfaces, and percent impervious surface.

Chapter 7 explores validating the uncalibrated SWMM model to examine the accuracy/utility of the model in ungaged urban catchments. Whether or not an uncalibrated model can be used for assessing the conditions of a small urban catchment, and further be used for hydrologic response to change in the catchment will be discussed.

An overall summary of the previously presented research, and general conclusions about the work and analyses completed are discussed in Chapter 8.

### **Study Justification**

Headwater streams are like the capillaries of a river network. As most of the nutrient, oxygen, and waste exchange in the human body happens in the capillaries, the same holds true for river networks. The headwater streams are a direct connection between the aquatic and terrestrial environments, and important processes take place in headwater streams that affect the health of the overall system. Natural headwater systems, relatively narrow, with extensive riparian vegetation, are the primary source of “energy” into the stream network through detrital inputs, for example, leaves falling off trees into the waterway. The system is shaded, stabilizing temperatures, and limiting autotrophic production (Vannote, et al., 1980). The detritus provides an energy source for bacteria, fungi, meiofauna, and macroinvertebrates who break down the detritus and convert it to biomass. These organisms then become an energy source for higher level predators moving up the food chain and downstream.

As humans move into an area that has a headwater stream system, these systems are immediately disturbed. Riparian corridors are removed, detrital inputs are reduced, temperature fluctuations in the stream increase, channel stability decreases, water quality decreases, etc. Because of the small size of some of these systems, and an effort to reduce/control flooding, they are diverted underground into pipes. Often the streams that are not “piped” are widened, deepened, and straightened (aka. channelized). Development/urbanization also means the construction of transportation infrastructure (i.e. bridges, culverts), which affect channel stability and flow dynamics, and stormwater drainage networks which affect infiltration, stormwater runoff efficiency, and groundwater recharge.

Changes to one or two headwater streams in a network may not result in large changes downstream, but as more and more headwater stream catchments in a network become urbanized, the cumulative effect downstream becomes magnified. Severe disruption of the natural system and aquatic ecosystem is observed downstream of these affected areas. As the cumulative effects of urbanization and development have become better understood, city planners and watershed managers have begun looking for more effective ways to manage stormwater runoff. One of the ways stormwater runoff has become better managed is by “disconnecting” the impervious areas of the catchment from the receiving water, and decreasing runoff by increasing infiltration through the implementation of low impact development (LID) technologies.

Accurate hydrologic modeling of urban headwater stream systems is important to understanding the impacts of different activities/changes in a catchment. Being able to quantify the existing rainfall/runoff relationship dynamics of a headwater stream catchment provides a baseline for predicting how changes in the catchment will affect future rainfall/runoff dynamics. These changes could be a result of increasing impervious surface (infilling), or predicting the effect of introducing LID technologies. A hydrologic model could also be used to determine the most effective LID technologies for a catchment to obtain the greatest decrease in runoff, or the best location for a selected LID technology in a catchment, for example, determining the best location for a rain garden installation.

While the catchment changes that are a part of the urbanization process are well known – increase in impervious surfaces, drastic alteration of natural drainage pathways, etc. – and the effects of these changes on the receiving stream – altered flow dynamics, increased runoff, aquatic habitat degradation, etc. – more research is needed on “developed pervious” areas in a catchment and their influence on flow dynamics.

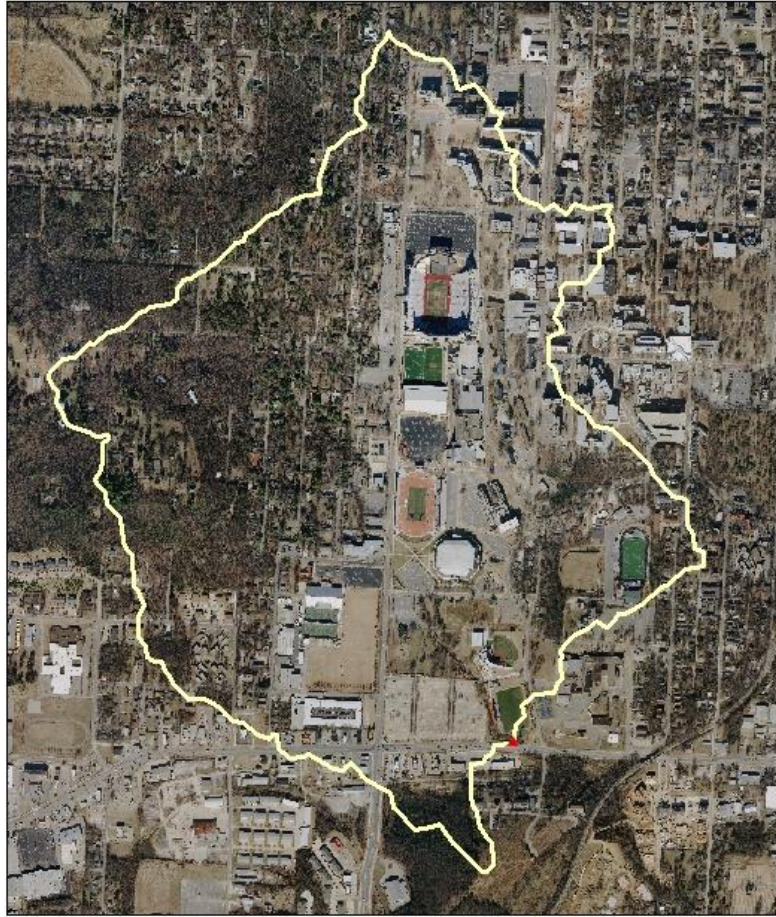
“Developed pervious” surfaces, while technically pervious, have been drastically altered from their natural state during construction/development. Hydrologic models have traditionally



used infiltration characteristics of native, undisturbed soils to predict runoff from pervious areas. However, natural soils are compacted, stripped, replaced, and natural vegetation is removed and replaced with landscaping and turf grass during development. Few studies have examined the behavior/characteristics of these pervious surfaces post-development, even though researchers like Wigmosta, et al. (1994) have observed that impervious surfaces have only about 20% greater runoff than pervious areas categorized as “sodded lawns.” Even less is known about how similar these soils are to their undisturbed counterparts, or if they resemble the natural soil type at all when it is possible that the surface material is an imported soil with different characteristics.

Mullins Creek is a small urban catchment (222.7 ha) that drains much of the University of Arkansas, Fayetteville main campus, located in Washington County, Arkansas (Figure 1.1). The catchment is located in the Boston Mountains Plateau physiographic province which is part of the larger Ozark Plateau region. Mullins Creek is a tributary to the West Fork of the White River which ultimately drains into Beaver Reservoir, the primary drinking water source for much of Northwest Arkansas. The West Fork of the White River has been listed on the U.S. Environmental Protection Agency’s 303(d) list, a list of impaired waterways, for high levels of turbidity and excessive silt loads. In a report published by the Arkansas Department of Environmental Quality (ADEQ), Formica, et al. (2004) estimated that about 66% of the sediment load in the West Fork of the White River was attributed to stream bank erosion, 17% was attributed to roadways and ditches, and almost 11% was attributed to construction in urban areas.

The land use/land cover distribution in the Mullins Creek catchment is shown in Table 1.1. It is important to note the high percentage of high intensity urban and the percentage of the catchment that is designated as “roads.” The vast majority of the watershed, over 90%, could be considered developed in some way.



0 250 500 Meters

Figure 1.1. Aerial map of the Mullins Creek catchment (outlined in cream) located on the University of Arkansas Fayetteville campus, Fayetteville, Arkansas, Washington County. The red triangle represents the outlet for the catchment.

Table 1.1. Land use/land cover (LULC) data for the Mullins Creek catchment for 2010 (Gorham, 2012b) extracted using ArcGIS (ESRI, 2014).

Mullins Creek Land Use/Land Cover (2010)	
LULC Description	Percent
Roads	10.4
Agriculture/Grass	2.6
Forest /Woodland	3.4
Urban Low Intensity	49.1
Urban High Intensity	34.4

An extensive stormwater drainage network is also a part of the catchment. In 2009, the University of Arkansas developed a stormwater management plan to assist the City of Fayetteville in meeting Non-Point Source Discharge Elimination System (NPDES) permitting requirements for communities regulated as Small Municipal Separate Storm Sewer Systems (MS4s). Part of the Stormwater Management Plan (SWMP) developed by the University of Arkansas included a goal of developing “a storm sewer system map, showing the location of all outfalls and the names and location of all waters that receive discharges from those outfalls” (UA, 2009). The availability of this dataset allows for the development of a hydrologic model that looks at surface drainage as well as water movement through the stormwater drainage network. All of these factors, plus the presence of a USGS gaging station at the outlet of the catchment, make this an ideal site to study to help understand the impacts of urbanization on small catchments. It also provides the opportunity to determine factors/methods/processes/datasets/data analysis necessary to accurately model condition in catchments like Mullins Creek.

### **Problem Statement**

With the continuing growth of the U.S. Population, and urban sprawl as cities grow and spread, more and more headwater streams and tributaries are being affected, both directly and indirectly, by development and urbanization. While the contribution of flow from one headwater stream to the larger system may be small, the combined contribution from multiple headwater streams is what creates large rivers. As these systems are developed, small channels are rerouted into pipes, pervious surfaces are paved over with impervious, natural drainage is replaced with underground stormwater networks, and the flow regime drastically changes. When enough of these headwater systems are so affected, the impacts to flows in the receiving waterways downstream can be huge leading to increased flow velocity, storm peak, erosion, and channel instability. A key component to better manage these systems to offset stressors of development and urbanization, is to understand

the response of the system to these stressors. As computing power has increased, and remote sensing and Geographic Information Systems (GIS) technologies have improved, and as necessary datasets have become more widely available, the ability to accurately model these urban systems has increased greatly over the last 30 to 40 years. Developing and parameterizing a model for the Mullins Creek catchment, and analyzing the results, can aid in the understanding of how these systems can be modeled to better predict changes and management options for similar sites.

### **Research Hypotheses**

1. There was a significant difference in soil characteristics for soil map units under minimally maintained versus highly maintained land use. Bulk density values were predicted to be higher for highly maintained sites, and infiltration rates were predicted to be lower.
2. The sensitivity of the SWMM model to changes in percent impervious surface was predicted to vary based on storm event size and percent impervious coverage in the catchment.
3. The sensitivity of the SWMM model to changes in Horton infiltration parameters was predicted to vary based on storm event size and infiltration potential.
4. It was predicted that an uncalibrated Storm Water Management Model (SWMM) could be developed for the Mullins Creek catchment that would reasonably predict peak discharge and total runoff for observed storm events.
5. Including observed soil infiltration data in the SWMM model parameterization process was predicted to improve the accuracy of the model output.

## Chapter 2. Literature Review

### Impact of Development/Urbanization on Stream Health

The health of a stream system is measured by the relationship/balance between physical, chemical, and biological components of the system (Figure 2.1). Stream health includes many components related to stream ecosystems (habitat structure, flow regime, water quality, energy sources, biotic interactions) that represent a good summary of stream health. The focus of this research is on the “flow regime” component, but again, it is important to note the relationship between all of the ecosystem components and their response to urbanization.

As stated by Konrad and Booth (2005, p.160), “few studies definitively make the link between hydrologic alteration and biological responses in urban streams, in part *because urban development affects nearly all aspects of fluvial ecosystems.*” (Emphasis added by author) This section of the literature review defines urbanization, and types of impervious surfaces, and includes a discussion of the impacts of development on a receiving waterway. These changes affect all the components of stream health shown in Figure 2.1 can induce changes in water quality, ecosystem health, and hydrologic response of a receiving waterway.

### Urbanization

*Of all land-use changes affecting the hydrology of an area, urbanization is by far the most forceful (Leopold, 1968, p.1).*

In the mid- to late-1960s, urban hydrology was starting to become an area of interest for hydrologists and civil engineers. Leopold (1968) discussed “four interrelated but separable” effects that land use changes have on hydrology, but note the effects listed include variables that could also be related to chemical and biological health of a stream system: peak flow characteristics, total runoff, water quality, and “hydrologic amenities.” According to Leopold (1968) “hydrologic

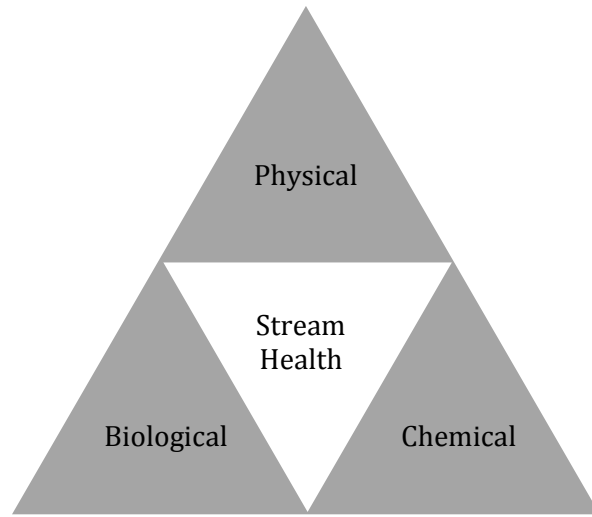


Figure 2.1. Illustration of the balance between biological, chemical, and physical components of a stream system.

amenities” can mean everything from stream stability, habitat diversity, erosion, to how appealing the stream appears to be to the casual observer. The focus of this research is on the effects of urbanization on the hydrology of a small, urban watershed. As defined by Konrad and Booth (2005, p.157),

*“Urbanization” is not a single condition; instead, it is a collection of actions that lead to recognizable landscape forms, and, in turn, to changes in stream conditions. No single change defines urbanization, but the cumulative effect of human activities in urban basins profoundly influences streams and their biota.*

Urbanization represents a disturbance of natural cover and landscapes, converting natural (forest, meadow, prairie) and agriculturally managed (pasture, cropland) vegetated areas to residential, commercial, and industrial land use. These natural areas are lost and replaced with impermeable surfaces and compacted, highly managed, pervious areas (Shuster, et al., 2005; Roy, et al., 2003; Grimm, et al., 2000; Booth and Jackson, 1997). Urbanized landscapes are also characterized by dramatically altered natural flow paths for water. Marshes and wetland areas are ditched, channelized, and drained. Constructed stormwater drainage systems are designed to replace/bypass natural drainage networks, and increase the hydraulic efficiency of the catchment (Walsh and Kunapo, 2009; Bedient, et al., 2008; Booth, 1990). As urbanization increases in a catchment, there is an increase in imperviousness, which leads to altered hydrology in the catchment, and more efficient transport of non-point source pollutants to the receiving waterway (Bedient, et al., 2008; Roy, et al., 2003). Modifications to a catchment that happen during urbanization can lead to overland flow and increases in stream flow for smaller, less intense rainfall events that prior to development would have infiltrated and been stored in the landscape (Booth and Jackson, 1997).

The characterization/prediction of hydrological effects of urbanization is the focus of this modeling project and dissertation work. Leopold (1968) discussed the influence of two factors that affect the stream response to urbanization: 1. The percent of imperviousness which is determined

by the land use/land cover, and 2. The rate of water transmission from the catchment to the receiving waterway, which is related to the characteristics of the drainage network. The process of urbanization, and the resulting changes to the catchment exert multiple pressures on the hydrologic cycle including increased hydraulic efficiency, decreased infiltration capacity, increased runoff potential, shorter time of concentration/lag time, decreased groundwater recharge/base flow, increased peak flow, increased total runoff, and increased “flashiness” (Leopold, 1968; Booth, 1991; Arnold and Gibbons, 1996; Konrad and Booth, 2005; Shuster, 2005; Fletcher, et al., 2013). While not a scientific term, the flashiness of stream is a description of how the stream response changes in a urbanized watershed. In an urban stream, especially in small, urban, headwater streams, the rate of stream flow rises more rapidly during, and recedes more rapidly after, a precipitation event (Konrad and Booth, 2005). An increased frequency of “sediment-transporting” and “habitat-disturbing” flows have also been observed pre- and post-development (Booth, 1991). Figure 2.2 shows a comparison in theoretical storm hydrographs and how they change in response to urbanization in a catchment.

One of the unique challenges that modeling a catchment like Mullins Creek poses, is that it is a dynamic urban system. Even though the catchment could be considered “developed” and has been for a number of decades, it is still in a constant state of change that is different from a traditional urban system.

Several comprehensive review papers have been published that discuss the relationship between percent urban/impervious land cover to overall stream system response including hydrology, geomorphology, habitat quality, water quality, aquatic biology, and changes to the overall stream ecosystem (Shuster, et al., 2005; Walsh, et al., 2005b; Brabec, et al., 2002; Paul and Meyer, 2001; Arnold and Gibbons, 1996; Schueler, 1994).



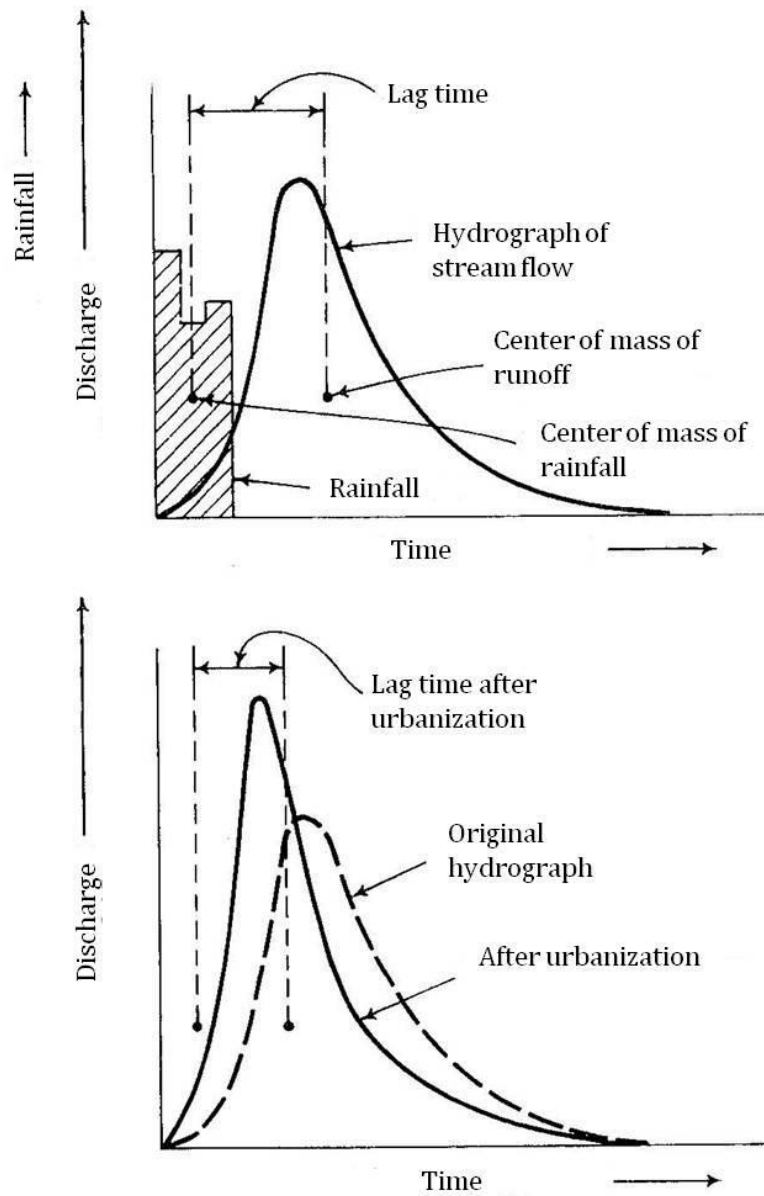


Figure 2.2. Hypothetical storm hydrographs demonstrating the change in channel response to urbanization (adapted from Leopold, 1968).

## **Impervious Surface Area (ISA) (aka. Imperviousness, Impervious Surfaces)**

Impervious surfaces in a watershed can be defined as any surface cover that prevents the infiltration of water into the soil. Technically this can mean anthropogenic or natural surfaces (i.e. exposed bedrock). The research in this dissertation is focused on the impervious surfaces constructed by humans, and how these impervious surfaces, through the prevention of infiltration, and decrease in infiltration capacity of the catchment, change the flow dynamics of stormwater runoff (Slonecker, et al., 2001). Since at least the mid-1960s, impervious surfaces have been identified as a neutral measurement of the intensity of urban development in an area (Walsh, et al., 2002; Slonecker, et al., 2001; Stankowski, 1972; Espy, et al., 1966), and in the mid-1990s, impervious surfaces were being recognized as an important environmental indicator of the health of a receiving waterway (Arnold and Gibbons, 1996; Schueler, 1994). The “imperviousness” of a catchment can be described more specifically as the sum of roads, parking lots, driveways, sidewalks, rooftops, tennis/basketball courts, and “other impermeable surfaces of urban landscapes” (Schueler, 1994). Schueler (1994) divides impervious surface areas into two primary categories: rooftops, and impervious surfaces related to transportation systems (i.e. roads, parking lots, driveways, etc.). A higher percentage of impervious surface area (ISA) can generally be attributed to transportation systems as opposed to rooftops. Schueler (1994) attributes this difference to strict zoning laws related to number and density of rooftops (structures) in urban/suburban areas, while transportation systems are under no such regulation. The changing dynamics of water flow through the different parts of the hydrologic cycle in response to urbanization and an increase in imperviousness is shown in Figure 2.3.

Many researchers across a wide range geographical areas, using many different metrics/methods/variables, and studying different components of stream systems (i.e. channel stability, habitat quality, biotic integrity, etc.), have found that stream health, especially physical and biological components, can be found to degrade at a threshold as low as 10% impervious

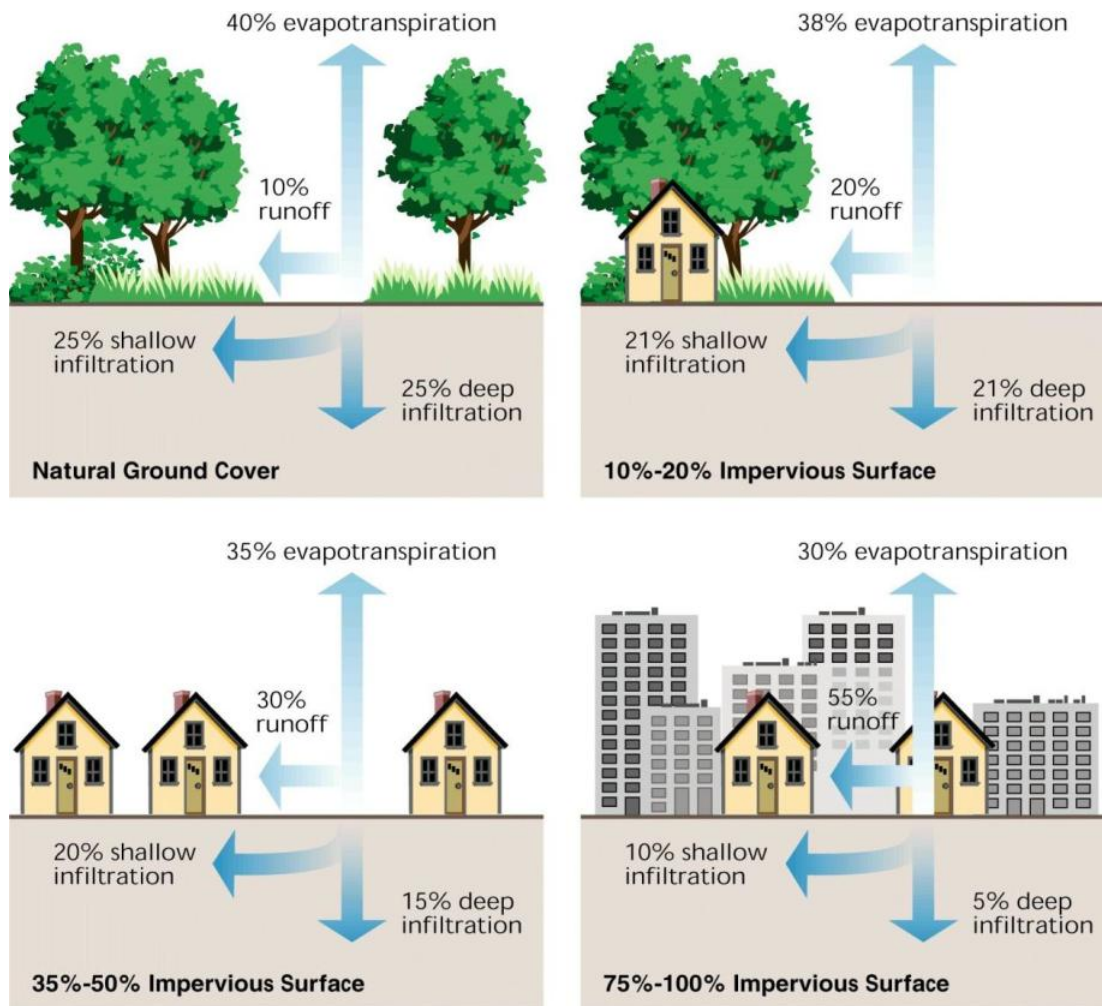


Figure 2.3. The relationship between impervious cover and surface runoff for increasingly concentrated urban development (Adapted from FISRWG, 1998).

surface area (May, et al.,1997; Schueler, 1994). These studies show definitively that there is a strong correlation between the imperviousness of a catchment and the health of the receiving stream (Arnold and Gibbons, 1996). For various applications, researchers have developed thresholds for impervious surface area (ISA) related to stream health and management. For example, Table 2.1 shows thresholds and descriptions of streams from two review papers.

### **Effective Impervious Area (EIA)**

Effective impervious area (EIA), also known as directly-connected impervious area (DCIA) represents a subset of total impervious area (TIA). There are two types of impervious areas that make up TIA: effective impervious areas and “ineffective” impervious areas. Effective impervious areas are impervious surfaces that are hydraulically connected to a drainage system/network. Precipitation that falls on these surfaces does not encounter a pervious surface in its journey from initial contact with the surface, to discharging into the receiving waterway. EIA leads to enhanced conveyance of water away from an area of concern (e.g. roadway or housing development). On the contrary, ineffective impervious areas are impervious surfaces that drain to pervious surfaces. A good example of a common ineffective impervious surface is a roof in a residential neighborhood that has gutters that drain to a garden or lawn (Shuster, et al., 2005; Alley and Veenhuis, 1982). Any potential storage available in the surrounding landscape is bypassed by EIA, leading to a concentration of flow and contaminants being directed to surface waters (Lee and Heaney, 2003). Very little precipitation is needed on a surface, like a parking lot, for overland flow to be observed. When these parking lots are designed to drain into a stormwater drainage network, it takes very minimal rainfall volumes to introduce significant amounts of flow to a receiving waterway – flow that previously would have infiltrated and stored in the soil matrix to be used by surrounding vegetation and released to the atmosphere through evapotranspiration (ET) (Booth and Jackson, 1997).

Table 2.1. Two examples of stream health thresholds for percent impervious surface area (ISA)

Schueler (1994)		Arnold and Gibbons (1996)	
Description	Percent ISA	Description	Percent ISA
Sensitive streams	1 -10	Protected	< 10
Impacted	11-25	Impacted	10-30
Non-supporting	26-100	Degraded	> 30

Studies that simply examine the effects of “impervious surfaces” on stream health and catchment response, without identifying the ISA as effective or noneffective, are providing the reader with limited information. If the authors specify that they are working with percent TIA to explain changes in the resulting health of the receiving waterway, the researchers are using a “hydrologically incomplete” definition. The issue is two-fold. Authors are not only including impervious surfaces in their analysis that may contribute zero flow to stormwater response in a receiving waterway (i.e. a basketball court in the middle of a city park surrounded by grass), they are also ignoring “nominally pervious surfaces” with high levels of compaction, assuming that all pervious surfaces will allow for significant infiltration (Booth and Jackson, 1997). In reality, the compaction of a natural soil can greatly reduce infiltration capacity (see section on Compaction).

Thresholds of stream health degradation have also been determined for EIA. Channel instability has been observed at levels of EIA above ten percent, leading to a decline in fish habitat quality. In King County, Washington, a category of protected waterways, Regionally Significant Resource Areas (RSRAs), have been identified. These areas are characterized by a high level of aquatic system function – presence of exceptional species, high level of habitat diversity/abundance – as compared to aquatic/terrestrial systems of similar size and structure in the region (King County, 1993). The majority of RSRAs had three percent or less EIA in their respective catchments. In general, Booth and Jackson (1997) found that “noteworthy accumulations of physical and biological effects” were observed in catchments which were near or above ten percent EIA.

Other authors also have noted changes in stream health as a result of EIA. Greatly reduced quality of macroinvertebrate assemblages were noted above 6 to 14 percent EIA (Walsh et al., 2005) and for fish assemblages over eight to ten percent EIA (Wang, et al. 2001). Other researchers noted a loss of sensitive fish species at rates of just two to four percent EIA (Wenger, et al. 2008), and negative water quality effects were noted at one to five percent EIA (Walsh, et al., 2005b).

## Relationship between Total Impervious Area (TIA) and Effective Impervious Area

Multiple researchers have examined the quantitative relationship between total impervious area (TIA) and effective impervious area (EIA) in urban catchments. One of the first relationships was developed by Alley and Veenhuis (1982).

$$EIA = 0.15 TIA^{1.41} \quad (1)$$

Other relationships have been developed more recently by Wenger et al. (2008),

$$EIA = 1.046 TIA - 6.23\% \quad (2)$$

and Roy and Shuster (2009).

$$EIA = 0.627 TIA - 1.86\% \quad (3)$$

Another researcher used the relationship developed by Alley and Veenhuis (1982) to extrapolate the percent TIA and percent EIA for different land use and land cover categories (Table 2.2).

Researchers also found that the majority of EIA was identified as “transportation-related” impervious surfaces (97.2%) (Lee and Heaney, 2003). Table 2.3 summarizes the percent of TIA that is EIA for different types of impervious surfaces.

These relationships add to the discussion of differences observed for the types of impervious surfaces (i.e. transportation-related versus rooftops) and the effects of these surfaces on hydrologic stream response receiving waterways. Not only is there a higher percent of impervious surfaces that can be categorized as “transportation-related,” a higher percent of transportation-related ISA can be categorized as effective.

## Summary of Urbanization Impacts

The impacts of urbanization on a stream catchment and the receiving waterway are well known and well documented, however, the increasing availability of data, and increasing

Table 2.2. Relationship between land use and imperviousness (from Dinicola, 1989).

Land Use Description	TIA (%)	EIA (%)	EIA/TIA
Low Density Residential (2 - 5 acre lots)	10	4	0.40
Medium Density Residential (1 acre lots)	20	10	0.50
"Suburban" Density Residential (1/4 acre lots)	35	24	0.69
High Density/Multi-family Residential (8+ units per acre)	60	48	0.80
Commercial/Industrial	90	86	0.96

Table 2.3. Percent effective impervious area for different categories of impervious surface (from Lee and Heaney, 2003).

Type of Impervious Surface	Percent Effective Impervious Area (EIA)
Streets/Roadways	68.9
Driveways	28.3
Sidewalks	68.2
Rooftops	2.9



capabilities of hydrologic models are continually allowing researchers to improve upon previous research. This can lead to better model development through validation and calibration, and lead to better prediction for changing land use/land cover effects for watershed management purposes. Increasing level of detail in these models, including impervious surface mapping, delineation of TIA and EIA, and knowledge of stormwater drainage networks, is increasing the accuracy and utility of these models to engineers and planners.

### **Infiltration and Compaction**

When developing a stormwater model, a researcher is modeling the interaction between different components of the hydrologic cycle, and the interaction between water and the earth's surface. For this research project, a model is being used to predict the stream response in a small, urban watershed (Mullins Creek) to actual precipitation events. One of the most important components of the model is the information on what happens once the precipitation reaches the surface of the catchment. Impervious surface coverage, and condition of pervious areas lead to predictions in volume of precipitation that runs off the surface into the stormwater drainage network and into the receiving waterway. This section of the literature review discusses how urbanization affects the infiltration potential or infiltration capacity of pervious surfaces in a catchment, and the importance of entering accurate parameters for infiltration into a hydrologic model.

### **Infiltration**

One of the main processes in the hydrologic cycle, infiltration is downward movement of water through the surface of the soil into the soil profile. This process is essential for water availability for plant growth, and the recharge of groundwater. Groundwater levels are directly related to baseflow conditions of a stream. As the depth of groundwater in an aquifer decreases, a corresponding drop in baseflow occurs as well (Figure 2.4). Infiltration of water during a storm

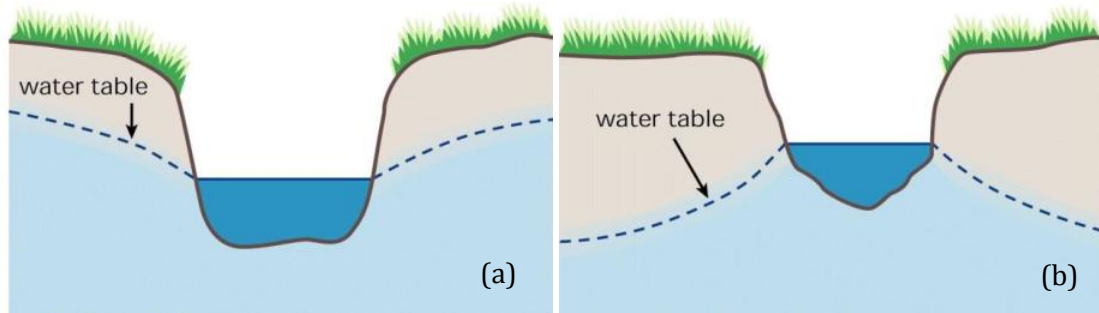


Figure 2.4. As the depth of the water table decreases in response to reduced infiltration in a catchment, a stream can go from being a “gaining” reach (a) to a “losing” reach (b), decreasing baseflow conditions during dry periods (from FISRWG, 1998).

event decreases surface runoff, decreases erosion, and reduces the movement of sediment and other pollutants from the land surface into receiving waterways (Ward and Trimble 2004). In modeling storm runoff, infiltration is considered to be a loss or abstraction. The amount of precipitation that falls, minus the amount that infiltrates into the soil, equals the amount of runoff for a given storm event (Bedient, et al., 2008).

The infiltration rate, often expressed as millimeters per hour (mm/hr) is the rate at which water moves through the soil surface into the soil profile. The infiltration rate can be dependent on the soil texture (percent sand, silt and clay), bulk density, porosity, heterogeneity, preferential flow paths, surface conditions, antecedent moisture conditions, and the presence of organic matter (USDA 2008; Wolkowski and Lowery 2008; Ward and Trimble, 2004).

### Estimating Infiltration Rates

Many methods have been developed to estimate infiltration rates, and better predict runoff from storm events. A few of the more commonly used and widely accepted methods are summarized below, keeping in mind that each method has its benefits and limitations.

*Infiltration divides rainfall into two parts, which thereafter pursue different courses through the hydrologic cycle. One part goes via overland flow and stream channels to the sea as surface runoff; the other goes initially into the soil and thence through the ground-water again to the stream or else is returned to the air by evaporative processes (Horton, 1933, p. 446).*

### Horton Infiltration Method

In Horton (1939), the Horton Infiltration Equation was first introduced:

$$f = f_c + (f_o - f_c)e^{-kt} \quad (4)$$

Where,  
 $f$  = infiltration rate at time,  $t$  (mm/hr)  
 $f_o$  = infiltration rate at time, 0 (mm/hr)  
 $f_c$  = final constant infiltration capacity (mm/hr)  
 $k$  = best fit empirical parameter (hr<sup>-1</sup>)

The process of infiltration described by the Horton Equation is that water infiltrates into the soil at a rate that decreases over time when the rainfall rate ( $i$ ), exceeds the infiltration rate ( $f$ ). In other words, when there is an excess of rainfall,  $i > f$ , the infiltration capacity decreases with time until it reaches a constant rate,  $f_c$  (Figure 2.5). This constant rate is reached when the soil pores have been filled and the capillary suction is reduced. In different soil types, the curve will be different. The decrease in infiltration rate is more rapid and the final infiltration rate is lower in a soil that is high in clay content versus a soil that is high in sand (Bedient et al., 2008).

Horton's concept of infiltration capacity is empirically based on observations measured at the ground surface. Each of the parameters in the Horton Infiltration Equation is a function of surface texture and vegetative cover type. The infiltration rate can also vary with slope (McCuen, 2005).

A typical range of values for the parameters in the Horton Infiltration Equation are presented in Table 2.4 along with typical values for different soil types under bluegrass turf land cover (Table 2.5).

The advantages of using the Horton Infiltration Equation are that it is a relatively simple equation to use and results obtained tend to fit well to measured data. A disadvantage is that it has no physical significance and field data are required to validate the results (Ward and Trimble, 2004). Another disadvantage is that the equation assumes that the rate of precipitation is always greater than the rate of infiltration. This may occur rarely in practice in well drained soils with high infiltration capacities, or during relatively small storm events (Bedient, et al., 2008). A key disadvantage that is part of the basis for this research is that the Horton parameters for natural soils are generally not applicable to disturbed soils in urbanized areas (Bedient, et al. 2008).

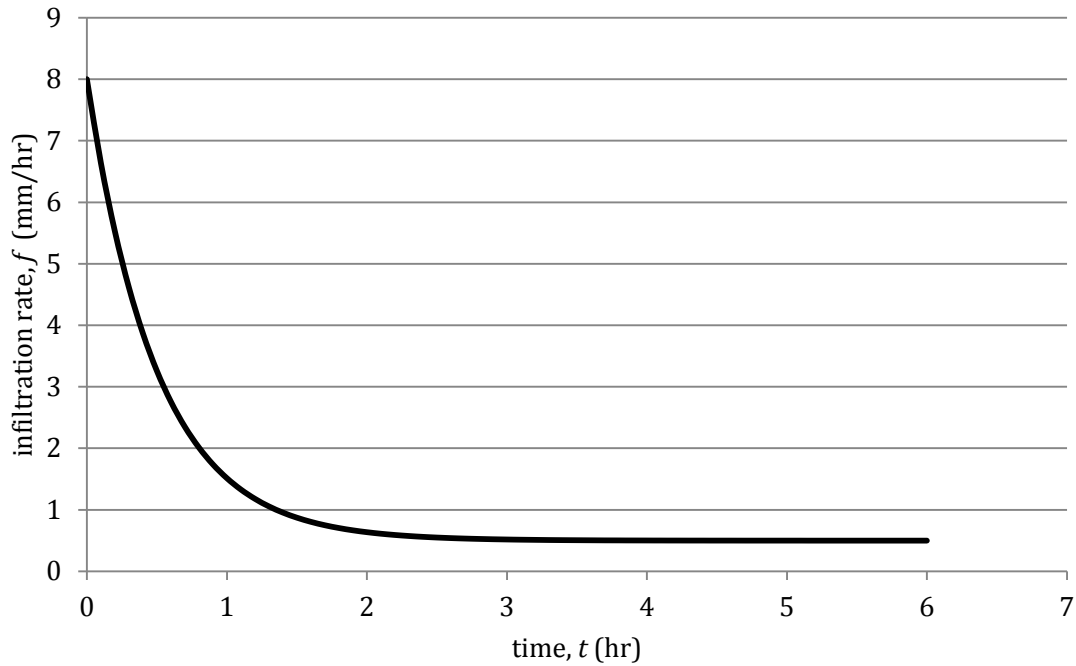


Figure 2.5. A theoretical infiltration curve for a silt-loam soil using the Horton Equation.

Table 2.4: Common ranges of accepted parameter values for the Horton Infiltration Equation (McCuen, 2005).

Description	Parameter	Range of Values
Final Infiltration Rate	$f_c$	0.25 – 50.8 mm/hr
Initial Infiltration Rate	$f_o$	0.76 – 254 mm/hr
Empirical Best Fit Parameter	$k$	1 - 20 hr <sup>-1</sup>

Table 2.5. Horton parameters for selected soil types under bluegrass turf land cover (Adapted from Terstriep and Stall, 1974).

Soil type	$f_o$ (mm/hr)	$f_c$ (mm/hr)	$k$ (hr <sup>-1</sup> )
Clay loam, silty clay loam, sandy clay loam, silty clay, clay	76.2	2.54	2
Sandy clay loam	127.0	6.35	2
Silt loam, loam	203.2	12.7	2
Sand, loamy sand, sandy loam	254.0	25.4	2

## Green and Ampt Infiltration Model

The Green-Ampt Infiltration Equation (Equation 5), first published by Green and Ampt (1911) was developed from Darcy's law and assumes capillary flow in a porous soil (Ward and Trimble, 2004). The Green-Ampt equation is a widely accepted method used to predict cumulative water infiltration into the soil as a function of time partly because of the wide availability of soil parameter data necessary to use the method (Bedient, et al. 2008).

$$f = K_s \left( 1 - \frac{M_d \psi}{F} \right) \quad (5)$$

Where,  
 $f$  = Infiltration rate  
 $K_s$  = Vertical saturated hydraulic conductivity  
 $M_d$  = Moisture deficit  
 $\psi$  = Wetting front suction head (cm of water)  
 $F$  = Cumulative depth of water infiltrated into soil

In the Green-Ampt equation, the capillary suction, vertical saturated hydraulic conductivity, and the moisture deficit must be estimated. The vertical saturated hydraulic conductivity,  $K_s$ , is dependent on pore size and grain size properties of the soil. The moisture deficit,  $M_d$ , is a function of effective porosity and the initial saturation of the soil, and the suction head,  $\psi$ , is the difference between atmospheric and hydrostatic pressure at a given site.

Just as with the Horton Equation described in the previous section, the Green-Ampt Equation operates on a series of assumptions (from Ferguson, 1994):

1. The soil is homogenous and stable. The effects of macropores and preferential flow pathways found in natural soils are not considered.
2. The supply of ponded water on the soil surface is unlimited.
3. A distinct wetting front exists and advances at the same rate at any depth, similar to piston flow.

4. The capillary suction just below the wetting front is uniform throughout the soil profile and is constant with respect to time.
5. The volumetric water contents remain constant above and below the wetting front as it advances into the soil profile.

### **NRCS Curve number Method**

The Natural Resources Conservation Service (NRCS, formerly Soil Conservation Service (SCS)) Curve Number method is most commonly used method in the United States to determine the volume of runoff (aka. rainfall excess). The curve number (CN) is used to combine infiltration losses with surface storage, to determine what portion of rainfall will runoff (Ward and Trimble, 2004). The CN method is based on the dimensionless unit hydrograph, and was developed from the measurement of unit hydrographs from a wide range of gaged watersheds which varied in catchment size and geographic location. It assumes a relationship between accumulated storm total rainfall ( $P$ ), runoff ( $Q$ ), and infiltration plus initial abstraction ( $F + I_a$ ). The value,  $S$ , calculated using the curve number, is known as the “potential abstraction” (Bedient, et al., 2008). For the purpose of examining infiltration only, and not runoff, the focus is on the first part of the calculation of runoff:

$$S = \frac{1000}{CN} - 10 \quad (6)$$

Where,  $S$  = potential abstraction  
 $CN$  = the SCS Curve Number

The SCS Curve Number (CN) is an index that uses one number to reflect a combination of factors that affect runoff potential from a given land surface. It is a function of three main factors:

- Hydrologic Soil Group (HSG)

- Land use/land cover type and characteristics
- Antecedent Moisture Conditions (AMC)

### **Hydrologic Soil Group (HSG)**

Each natural soil type can be categorized into a hydrologic soil group (HSG) based on the runoff potential of the soil. Table 2.6 shows characteristics of soils in each group.

### **Role of land use and land cover (LULC)**

Not only is the type of LULC important, but there are other complex variables that go along with it. For example, the land cover might be an agricultural crop (e.g. corn), but the runoff behavior will be different for a row crop style planting versus contour planting. The curve numbers that have been developed, also take into account the approximate percent of impervious surface area for a given LULC, specifically for urbanized/urbanizing areas. The condition of the land cover, and quality of land management is also important. In an urban setting there can be varying levels of quality on a lot based on the percent of ground surface covered with vegetation, and the density of the ground cover (Table 2.7). There are over 20 general land use classes that have been assigned curve numbers by the USDA-SCS (1986). Table 2.8 presents a selected list of curve numbers for urban/developed LULC types.

Finally, the curve number can also be adjusted for the antecedent moisture condition (AMC), how wet the soils were at the time that rainfall for a given storm began. Antecedent soil moisture has been shown to have a significant effect on the volume and rate of surface runoff. The NRCS has published a series of adjustment factors for the curve numbers based on the AMC. All numbers presented in Table 2.8 assume AMC II, or average soil moisture conditions. If the soils are dryer than average at the start of the rain event (AMC I), the curve numbers will be adjusted to a lower number correlating to higher infiltration and lower surface runoff. If the soils are already wet at the beginning of a rainfall event (AMC III), the adjustment factor will increase the curve number



Table 2.6. Characteristics of soils in each hydrologic soil group (HSG) (from Ward and Trimble, 2004; McCuen, 2005).

Hydrologic Soil Group	Relative Infiltration Rate	General Characteristics	Final Infiltration Rate (mm/hr)
A	low runoff potential	Soils with high infiltration rates even when thoroughly wetted. Deep sand.	> 7.6
B	moderately low runoff potential	Moderate infiltration rates when thoroughly wetted. Sandy loam.	3.8 – 7.6
C	moderately high runoff potential	Slow infiltration rates when thoroughly wetted. Clay loams.	1.3 – 3.8
D	high runoff potential	Soils with very slow infiltration rates and significant swelling when thoroughly wetted. Heavy, plastic, clays.	< 1.3

Table 2.7. Assessing quality of land cover (from McCuen, 2005).

Quality	Cover Characteristics	Relative Cover
Poor	Heavily grazed or regularly burned	Less than 50% of ground surface protected by plant cover or shrub/tree canopy
Fair	Moderate cover	50 - 75% of ground surface protected
Good	Heavy to dense cover	More than 75% of ground surface protected

Table 2.8: Curve numbers for land use, condition, and hydrologic soil group for average conditions (USDA-NRCS, 2004).

Land Use Description	Hydrologic Soil Group			
	A	B	C	D
<b>Fully developed urban areas (vegetation established)</b>				
Lawns, open spaces, parks, golf courses, cemeteries, etc.				
Good condition (grass cover more than 75% of the area)	39	61	74	80
Fair condition (grass cover on 50 - 75% of the area)	49	69	79	84
Poor condition (grass cover on less than 50% of the area)	68	79	86	89
<b>Paved parking lots, roofs, driveways</b>				
Streets and roads				
Paved with curb and gutter design	98	98	98	98
Gravel	76	85	89	91
Dirt	72	82	87	89
Paved with open ditches	83	89	92	93
<b>Commercial and business areas (85% impervious)</b>				
<b>Industrial districts (72% impervious)</b>				
Row houses, townhouses, residential with lot sizes 1/8 acre or less (65% impervious)				
Residential (average lot size)				
1/4 acre (38% impervious)	61	75	83	87
1/2 acre (25% impervious)	54	70	80	85
1 acre (20% impervious)	51	68	79	84
2 acres (12% impervious)	46	65	77	82
<b>Developing urban areas (no vegetation established)</b>				
Newly graded, bare dirt				
	77	86	91	94

correlating to lower infiltration capacity and higher runoff potential. Table 2.9 shows a list of curve numbers and their adjustment factors for AMC I and III.

### **Infiltration estimation methods summary**

The three infiltration estimation methods summarized above, the Horton equation, the Green-Ampt equation and the CN method, are the three methods that a user can select from in the Storm Water Management Model (SWMM) to estimate infiltration for a catchment. The reality is that no single method works well for all situations. It can depend on the data that are available to the user as well as the conditions at a given site. A list of accepted values for use in populating the Green-Ampt infiltration parameter values in SWMM is presented in Table 2.10.

Descriptions/definitions of the required SWMM inputs for the Horton Infiltration method and the Green-Ampt infiltration method are presented in Table 2.11 and Table 2.12, respectively.

### **Infiltration in Urbanized/Developed areas**

A significant reduction in the natural infiltration rate that has been observed in urban areas is caused by:

- Introduction of impervious surfaces/decreased exposed pervious surfaces
- Removal of surface soils
- Introduction of non-native soils
- Compaction during earth moving and construction (disruption of soil structure)
- Urban activities that continue post-development:
  - Maintenance of landscaped areas
  - Parking cars on grass
  - Compaction of playing fields (Pitt, et al., 2008; Pitt, et al., 2002)

Table 2.9: Curve numbers for AMC II, and conversion factors to convert from AMC II to AMC I and/or AMC III (adapted from Ward and Trimble, 2004).

CN	Conversion Factors		
	AMC II	AMC I (dry)	AMC III (wet)
20	0.45	2.22	
40	0.55	1.5	
60	0.67	1.3	
80	0.79	1.14	
100	1.00	1.00	

Table 2.10. Parameter values for various soil texture classes for use with the Green-Ampt equation (adapted from Rawls, et al., 1983).

Soil Texture Class	Saturated Hydraulic Conductivity (mm/hr)	Suction Head (mm)	Porosity (fraction)	Field Capacity (fraction)	Wilting Point (fraction)
Sand	120.0	50.0	0.437	0.062	0.024
Loamy Sand	30.0	60.0	0.437	0.105	0.047
Sandy Loam	11.0	110.0	0.453	0.19	0.085
Loam	3.5	90.0	0.463	0.232	0.116
Silt Loam	6.5	170.0	0.501	0.284	0.135
Sandy Clay Loam	1.5	220.0	0.398	0.244	0.136
Clay Loam	1.0	210.0	0.464	0.31	0.187
Silty Clay Loam	1.0	270.0	0.471	0.342	0.21
Sandy Clay	0.5	240.0	0.43	0.321	0.221
Silty Clay	0.5	290.0	0.479	0.371	0.251
Clay	0.3	320.0	0.475	0.378	0.265

Table 2.11. Horton infiltration parameter input descriptions for the SWMM (Rossman, 2010)

Parameter	Description
Max. Infil. Rate	Maximum infiltration rate on the Horton curve (in/hr or mm/hr) (see table below)
Min. Infil. Rate	Minimum infiltration rate on the Horton curve (in/hr or mm/hr). Equivalent to the saturated hydraulic conductivity. See the Soil Characteristics Table for typical values.
Decay Const.	Infiltration rate decay constant for the Horton curve (1/hours). Typical values range between 2 and 7.
Drying Time	Time in days for a fully saturated soil to dry completely. Typical values range from 2 to 14 days.
Max. Infil. Vol.	Maximum infiltration volume possible (inches or mm, 0 if not applicable). Can be estimated as the difference between a soil's porosity and its wilting point times the depth of the infiltration zone.

Table 2.12. Green-Ampt infiltration parameter input descriptions for the SWMM (Rossman, 2010)

Parameter	Description
Suction Head	Average value of soil capillary suction along the wetting front (inches or mm)
Conductivity	Soil saturated hydraulic conductivity (in/hr or mm/hr)
Initial Deficit	Fraction of soil volume that is initially dry (i.e., difference between soil porosity and initial moisture content)

While a great number of studies have been undertaken that examine the link and effects of impervious surface area in a watershed, and while this relationship is fairly well known, the additional effects of disturbing the remaining pervious areas where infiltration can occur are rarely considered (Pitt, et al., 2008; Hamilton and Waddington, 1999; Booth, et al., 2002; also see section on soil compaction in literature review).

The limited number of studies that have been conducted to examine the infiltration characteristics of developed pervious areas have observed/measured/reported a significant reduction in infiltration rates (Pitt, et al., 1999). Even today, more research is needed that focuses on the effect of urbanization on the remaining pervious areas in a watershed. Most of the pervious areas in a watershed (50 – 70%) are composed of lawns planted with turfgrass (Schueler, 2000; Hamilton and Waddington, 1999). Studies of the soil characteristics under maintained lawns in residential and urban areas have found that these soils typically have low infiltration capacity and high bulk densities (Hamilton and Waddington, 1999; Oliveira and Merwin, 2001).

### **Soil Compaction**

Soil compaction has been studied for decades with regard to its effect on agricultural production. Compaction can come from farm equipment or livestock and can have a detrimental effect on crop yields and growth of grass/hay in areas where livestock graze. Once the bulk density of a soil exceeds  $1.6 \text{ g/cm}^3$ , it becomes difficult for roots to grow, plants that do grow are more prone to drought, and the need for supplemental irrigation is increased, especially for non-native plants (Schueler, 2000). The study of hydrological impacts of soil compaction in an urban environment is much younger and is still being developed.

As discussed above, infiltration is a major process that affects the volume of water that runs off during a storm event. Many hydrologic models and the modelers who use them, relate infiltration to the soil map unit present in the catchment/area of study. For example, the Natural

Resource Conservation Service Curve Number method uses a runoff coefficient, CN, which takes into account the land use/land cover, soil type (hydrologic soil group, infiltration/runoff potential of a particular soil), and antecedent moisture condition (AMC) of an area of the catchment to help predict detention, infiltration potential, and runoff volume over the area. What it does not take into account, is the current condition of the developed landscape with regard to the underlying soils and how they may have been changed/altered/affected during development.

*Very large errors in soil infiltration rates can easily be made if published soil maps are used in conjunction with most available models for typically disturbed urban soils, as these tools ignore the effects of soil compaction (Pitt, et al., 2008, p.657).*

According to Horton (1933), when assessing the role of infiltration in the hydrologic cycle, two cases must be considered when discussing infiltration-capacity: 1) natural soils, and 2) soils which have recently been cultivated. Examining the affects of development on natural soils, it increasingly makes sense to consider a third case: soils which have been developed.

During the process of urbanization/development, the conversion of forested, natural grassland/meadow, or agricultural land to residential/commercial, there are many intended and unintended effects the process has on the underlying native soil.

During development, the following things can and often do occur in preparing the area:

- Topsoil removal
- Regrading
- Partial or complete vegetation removal/clearing
- Introduction of a different (non-native) soil with more desirable characteristics for the purpose of the contractor and different properties from the native soil
- Intentional and unintentional compaction of the soil with heavy machinery

Often during development, the native topsoil and associated vegetation is removed. The property in question is often regraded and leveled resulting in a change in the natural contours of

the site, non-native soil may be imported to the site, new top soil may be imported or the original may be replaced and sod is laid down to replace the vegetation that was lost. At the very least, the native soil becomes compacted to a much higher bulk density with a much lower percentage of pore space, or it is stripped and replaced. Often the developed area will have a land cover that is impervious (house, driveway, sidewalk, parking lot, road) or maintained developed (lawn, landscaping).

### **Soil Compaction during Development**

During the construction/development process, soil compaction occurs in different ways, both intentional and unintentional. When topsoil is removed, a more compacted subsoil with decreased infiltration capacity is exposed. As heavy machinery is used throughout the area of development, the soil under the machines can be compacted several feet down. There is also intentional compaction along the road right of way, around the foundation of buildings, and in the preparation/construction of stormwater detention ponds (Schueler, 2000; Gregory, et al., 2006).

### **Measuring Soil Compaction/Infiltration Capacity in Developed Soils**

Various characteristics of urban soils have been studied and used to predict infiltration capacity and other soil characteristics. One of the most common measurements of a soil is bulk density. Bulk density is the density of a known volume of soil as it exists *in situ* and includes air space and organic material (Gardiner and Miller, 2004). It can be a useful indicator of existing soil structure and can be used to help predict different soil characteristics including: porosity, permeability, infiltration rate, and water storage capacity. As the bulk density increases, the infiltration capacity is reduced and more surface runoff will be generated from a given storm event. While the bulk density of natural, undisturbed surface soils can range from 1.1 to 1.4 g/cm<sup>3</sup>, urban soils have a much higher bulk density, occasionally approaching the bulk density of concrete. These compacted soils have a tendency to behave more like impervious surfaces during large storm



events than their undeveloped pervious counterparts (Scheuler, 2000). In one study, Wigmosta, et al. (1994) found that compacted soils in a small urbanized catchment can contribute 40 – 60% of annual runoff to the receiving waterway.

Another factor that can complicate the study of urban soils is the high level of spatial variability of these soils as compared to their undeveloped counterparts. This makes it difficult to describe the characteristics of a “typical” urban soil (Hamilton and Waddington, 1999; Pouyat, et al., 2007).

### **Summary of Urbanization on Compaction**

Based on the review of research in this area, there needs to be more time spent studying the effects of development and urbanization on pervious surface properties to more accurately model runoff conditions in urban catchments. Developed pervious surfaces can contribute a large amount of runoff that may be closer to estimations of runoff from impervious areas than from undeveloped pervious areas.

### **Hydrologic Modeling**

#### **Historical perspective**

While simple hydrologic models that generally focus on one part of the hydrologic cycle have existed for generations (e.g. rational method, Horton infiltration equation), comprehensive watershed models that attempt to describe all parts of the hydrologic cycle were developed more recently. The inception of hydrological modeling can be traced to the development of civil engineering as a discipline. It is historically linked to the design of roads (and associated culverts, bridges), canals, sewers, drainage systems, water supply systems, dams, etc. (Singh and Woolhiser, 2002). The first comprehensive watershed model that was available for use was the Stanford Watershed Model (SWM) developed through a multi-organizational effort between Harvard

University, Stanford University, and the Army Corps of Engineers (ACOE) (Crawford and Linsley, 1966). Over time the SWM has evolved into the Hydrologic Simulation Program – FORTRAN (HSPF) (Johanson, et al., 1980).

When it comes to the treatment/control/study of urban stormwater, research and practice has moved from simple flood control – remove the water from developed areas as quickly as possible – to recognizing that there is a need to understand the effect that runoff removal systems have on a receiving waterway, tied/linked/associated with efforts to preserve the stability of these systems (Nix, 1994).

The increase in computer processing and data storage capabilities, along with an increase in available datasets from more intensive monitoring and field data collection, allowed hydrologic model development and modeling efforts to increase in complexity and capability in the 1970s covering applications from urban stormwater to agricultural drainage to reservoir design and river basin management. However, much of the early model development was because of an interest in examining the water quality of urban runoff (Bedient, et al., 2008).

### **Purpose of hydrological models**

Precipitation that falls on an urban watershed is transported through a very complex hydrologic and hydraulic system as it moves from ground surface to receiving waterway (Nix, 1994). As noted by Singh and Woolhiser (2002), watershed models are an important key to understanding the dynamic interactions between rainfall and runoff as they occur in a watershed. They are important for assessing the quality, quantity, and availability of water resources, and predicting the effects of development and other land use changes. Watershed models can help to scientifically study and examine the relationship between human activities and the conditions that exist in the receiving waterways. As defined by Bedient, et al. (2008, p.312):

*Hydrologic models incorporate equations to describe hydrologic transport processes and storages to account for water balances in space and time.*

Hydrologic simulation models have generally been developed to meet one of two goals, although in some instances the model can serve both purposes (Beven, 1989):

1. To explore existing conditions and how making assumptions/simplification of certain parameters reflects the nature of the real-world system
2. To predict the behavior of an existing real-world system under different sets of circumstances

### **Modeling Process**

A generic modeling process is presented in Figure 2.6. Each modeler must start with an objective, and the level of detail/complexity of the model will then be based on available time, data, and funding/budget. With so many widely accepted, tested, and supported hydrologic models available to hydrologists, engineers, and watershed planners, few new models are being developed. It makes more sense for an engineer to select an existing model that works for the system to be modeled and meets the objectives of the study (Bedient, et al., 2008).

The steps in watershed modeling as outlined by Bedient, et al. (2008) are shown below.

1. Select model based on study objectives and watershed characteristics, availability of data, and project budget.
2. Obtain all necessary input data – rainfall, infiltration physiography, land use, channel characteristics, streamflow, design floods, and reservoir data.
3. Evaluate and refine study objectives in terms of simulations to be performed under various watershed conditions.
4. Choose methods for determining subbasin hydrographs and channel routing.

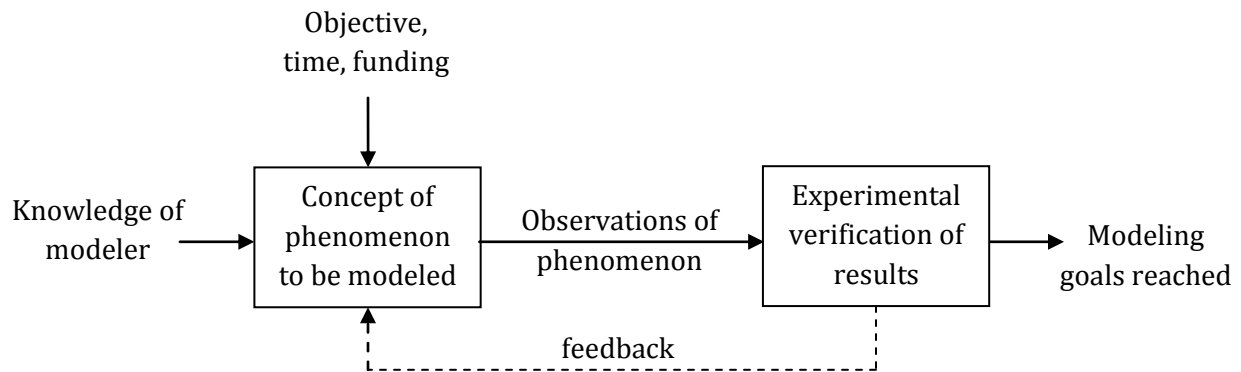


Figure 2.6. The modeling process (adapted from Overton and Meadows, 1976)

5. Calibrate model using historical rainfall, streamflow, and existing watershed conditions. Verify model using other events under different conditions while maintaining same calibration parameters.
6. Perform model simulations using historical or design rainfall, various conditions of land use, and various control schemes for reservoirs, channels or diversions.
7. Perform sensitivity analysis on input rainfall, routing parameters, and hydrograph parameters as required.
8. Evaluate usefulness of the model and comment on needed changes or modifications.

Calibration and validation of a watershed model are integral to the process of modeling. Each model that is developed is an imperfect representation of the actual watershed system. Calibration is the process of adjusting the model within the natural range of each parameter, and comparing the results to field data and actual storm events if available. The goal of calibration is to simulate observed conditions as accurately as possible (Bedient, et al., 2008; DeBarry, 2004). Validation is the “process of collecting data to describe inputs and outputs to a watershed for a wide range of conditions and adjusting the model parameters so the model adequately replicates the watershed as depicted.” (Nix, 1994).

### **Types of Hydrologic Models**

Hydrologic models can be classified according to a wide range of characteristics starting with level of detail/complexity. There are three general levels of detail (Table 2.13) for hydrologic/watershed models as described by Nix (1994). As the level of complexity of a model increases, there is a corresponding increase in the dataset input requirements, the knowledge/capability of the modeler, and in the cost to develop the model.

Table 2.13. Levels of complexity for hydrologic models (adapted from Nix, 1994).

	Characteristics/Description	Examples
Level I	Very simple models Do not route flows through watershed Require little input data Minimal (if any) computer assistance required	SWMM Level I
Level II	Computer-executed models  Generate runoff hydrographs at one or only a few points Continuous, long term modeling Allow simple routing of flow through channels/storage basins	STORM, HSPF
Level III	Computer-executed models Capable of routing flows through gutters, channels, and sewers Highest data input requirements Continuous and/or event based modeling Produce runoff hydrographs at various locations in system	SWMM MIKE-SHE

## **Lumped vs. Distributed Hydrologic Models**

In a lumped model, all parameters of the watershed, i.e. slope, land use/land cover, soil characteristics, etc., are averaged over the entire watershed, while distributed models take spatial variability into account. When using a distributed model, the parameters for a watershed will change based on location within the watershed (Nix, 1994). These models attempt to describe physical processes and hydrologic mechanisms as they change in space. Distributed models have also been described as “physics-based” models and have a high data input requirement. Although technological capabilities and dataset availability are improving, in the past, there were generally not enough data available to properly calibrate/validate these models (Bedient, et al., 2008). In reality, it is impossible to have a completely distributed model that changes in response to each small adjustment in spatial location, but some models allow for more complexity than others.

## **Stochastic vs. Deterministic vs. Parametric**

A stochastic model takes randomness into account when modeling a watershed system as a representation of the uncertainty in these systems. In the case of a strictly stochastic model, the same input parameters will provide varied results. On the other hand, a deterministic (or mechanistic) model will always produce the same output for a given set of inputs. Parametric models include both deterministic and stochastic traits. In practice, most urban hydrologic models are “parametric models that feel deterministic” with varying levels of uncertainty embedded, or “pseudo-deterministic”, “pseudo-distributed” models (Butler and Davies, 2004; Nix, 1994).

## **Event-based vs. Continuous**

Watershed models can also be classified by the timeframe to which the models are applied. Single-event models can examine the behavior of the watershed over a single rainfall-runoff event, while continuous models simulate watershed behavior over many sequential events (Nix, 1994).

While some models are limited in their ability to simulate over one timeframe versus another, some current models can do one or both (i.e. SWMM, Rossman, 2010).

### **Summary of Hydrologic Modeling**

There are definite advantages and limitations to using a hydrologic model. Any model output is only as good as the quality of the inputs. Aka. “garbage in, garbage out” The utility/quality of the output can also be dependent on the skill and knowledge of the modeler. The potential benefits of using a more complex model can be lost if data are missing or inadequate to properly run the model, let alone for calibration/validation purposes.

One advantage of hydrologic modeling and going through the modeling process is the insight gained by the user during the process of gathering and organizing the data input requirements for a model. Once a system is successfully modeled (including calibration/validation), it can be used to rapidly examine alternatives for watershed management, water supply systems, flood control options, etc. and compare results. A serious limitation can result when using a model when required input datasets are missing or not available, thus not allowing for effective calibration/validation of the model (Bedient, et al., 2008).

Even with the limitations of using a hydrologic model, these models “provide the most logical and scientifically advanced approach to understanding the hydrologic behavior of complex watershed and water resources systems” (Bedient, et al., 2008).

### **About the U.S. Environmental Protection Agency’s (EPA’s) Storm Water Management Model (SWMM)**

The Storm Water Management Model (SWMM) was first developed by the U.S. Environmental Protection Agency (USEPA) in conjunction with other entities in 1971. Since that time SWMM has undergone several major upgrades as data availability, the state of the science of hydrologic modeling, and computer technology/capabilities have improved (Huber and Dickinson,



1992). The most recent version of SWMM is version 5.1 which became available in March 2014 (Lewis Rossman, personal communication, 27 March 2014). When version 5.0 was released, it was a complete rewrite of the previous release and included many upgrades, added flexibility, and improved capabilities for modeling Low Impact Development (LID) technologies (Rossman, 2010).

For the most current and comprehensive information about SWMM (version 5.0), see Rossman (2010). Much of the content in this section is information distilled from the User Manual that is applicable to this dissertation research.

From Rossman (2010), SWMM conceptualizes drainage systems as a series of water/material flows between several major environmental compartments. The major compartments that are applicable to this project are summarized below:

**Atmosphere.** Precipitation falls onto the land surface. Rain gage “objects” represent rainfall inputs which can be uploaded historical rainfall data, or user defined synthetic rain events.

**Land Surface.** The land surface is represented by subcatchments where the inflow is the precipitation from the atmosphere compartment. Outflow leaves the land surface compartment and is sent to the groundwater compartment via infiltration, and to the transport compartment via surface runoff.

**Groundwater.** The groundwater compartment receives inflow from infiltration via the land surface compartment. A portion of flow input via infiltration is sent via outflow to the transport compartment.

**Transport.** The transport compartment is made up of conveyance elements including channels (natural and man-made), pipes, pumps, regulators, etc. Inflows come from surface runoff, groundwater interflow, and user-defined hydrographs. Components of the transport compartment are modeled using node and link objects (i.e. conduits, junctions).

According to Rossman (2010), "SWMM is a physically based, discrete-time simulation model. It employs principles of conservation of mass, energy, and momentum wherever appropriate." SWMM can be used to model stormwater runoff through multiple physical hydrologic cycle processes including surface runoff, groundwater, flow routing, infiltration, and surface ponding.

The highest levels of technical ability in SWMM are invested around four hydrologic/hydraulic processes (from Akan and Houghtalen, 2003):

**Precipitation.** The user can use either historical precipitation event information, or use a design (synthetic) storm as an input into the model as a hyetograph.

**Rainfall losses.** Rainfall losses are subtracted from the precipitation input to produce rainfall excess or runoff. These losses, also known as abstractions, include evaporation, depression storage/interception, and infiltration.

**Runoff transformation.** Runoff transformation is the process of converting the rainfall excess into a hydrograph leaving each subcatchment as defined by the user. In this step, SWMM combines mass balance equations with Manning's equation (using the Manning's roughness coefficient,  $n$ ) to obtain the hydrograph characteristics at the outflow of the subcatchment.

**Flow Routing.** Flow routing is the process of moving each hydrograph downstream through a system of pipes, channels, and/or ponds. As discussed above, either TRANSPORT or EXTRAN can be used, however, EXTRAN is the more sophisticated of the two allowing for calculation of backwater conditions, storage and pipe networking within a stormwater drainage system.

Several computation blocks (or subroutines) can be simulated separately, so for example, a user can enter a synthetic hydrograph and examine the results from the EXTRAN block with regard to flow routing for the system of interest (Wang and Altunkaynak, 2012).

SWMM can also be run either continuously (over a period of years), or as an event-based simulation (over a period of a few hours/days). For small urban catchments like the one in this study, the ability to model hydrologic response for individual events is important to accurately characterize these complex environments. A comparison of event-based simulation runs versus continuous simulation runs are presented in Table 2.14. Stream response to a storm event can be very rapid in a small, urban catchment which requires a shorter time step and greater level of detail to develop an accurate representation of the stream response (Tsihrintzis and Hamid, 1998). The time of concentration ( $t_c$ ) or the time it takes for rainfall to travel through the catchment to the receiving waterway, can be reduced from hours to minutes for a small catchment after development.

### **Subcatchments**

It is recommended that a catchment of interest be delineated into multiple subcatchments so each subcatchment has relatively homogeneous physical characteristics. Information characterizing each subcatchment including area, width, average slope, percent imperviousness, surface roughness, infiltration capacity, and surface storage potential are used by SWMM to develop a runoff hydrograph (Temprano, et al., 2006). Flow inputs into each subcatchment are limited to precipitation and/or “designated upstream subcatchments.” Outflows from each subcatchment are more complex and include infiltration, evaporation, and surface runoff (Figure 2.7). The capacity of the subcatchment “reservoir” is equal to the maximum depression storage of the subcatchment including ponding, surface wetting, and interception (Rossman, 2010).

Table 2.14. Comparison of temporal and spatial resolution for event-based versus continuous simulation runs in SWMM (Tsihrintzis and Hamid, 1998).

	<b>Event-Based Simulation</b>	<b>Continuous Simulation</b>
Simulation Time	Short (hours)	Long (years)
Simulation Time Step	Short (minutes)	Long (hours)
Detail of catchment representation (i.e. Drainage Network)	High level of detail and more representative of a distributed model	Low level of detail, more representative of a lumped model

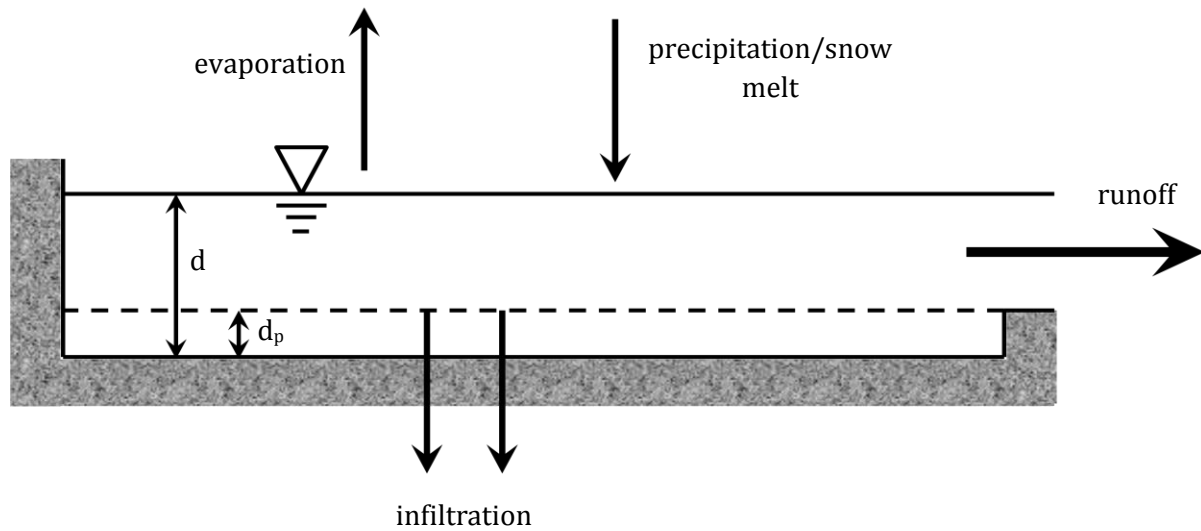


Figure 2.7. Conceptual model of surface runoff from subcatchments in SWMM (adapted from Rossman, 2010). Surface runoff begins when the depth of water in the subcatchment “reservoir” ( $d$ ) exceeds the maximum depression storage ( $d_p$ ).

In SWMM, each subcatchment delineated is modeled as a rectangular, nonlinear reservoir, employing a combination of the continuity equation and Manning's equation on each for the given conditions (Figure 2.8). Each subcatchment will have its own fraction of impervious and pervious surface, infiltration capacity, roughness, storage potential, slope, etc. (Sun et al., 2014). As with this study, the majority of required parameters for a hydrologic model are generally extracted from GIS layers (MacArthur and DeVries, 1993).

### **Infiltration**

The process of infiltration, rainfall penetrating the ground surface into the unsaturated soil zone in pervious areas of a catchment, was discussed in more detail in the infiltration section of the literature review. SWMM provides the opportunity to select one of three methods to model infiltration: Horton Infiltration Method, Green-Ampt, and the Natural Resource Conservation Service (NRCS) Curve Number (CN) Method. These methods were discussed in detail in the infiltration section of the literature review.

### **Flow Routing**

Flow routing in SWMM is "governed by conservation of mass and momentum equations for gradually varied, unsteady flow" (Rossman, 2010). As with infiltration, multiple options are available for the user to route hydrographs through channels, pipes, ponds, etc. The first option, steady flow, is the most simplified option and for all intents and purposes, represents no routing. This means that the hydrograph will not change from one end of a conveyance feature to another. The kinematic wave method employs the continuity equation and simplified momentum equation. The dynamic wave method provides the user with the most theoretically accurate results using a complete set of one-dimensional Saint Venant flow equations (Rossman, 2010).

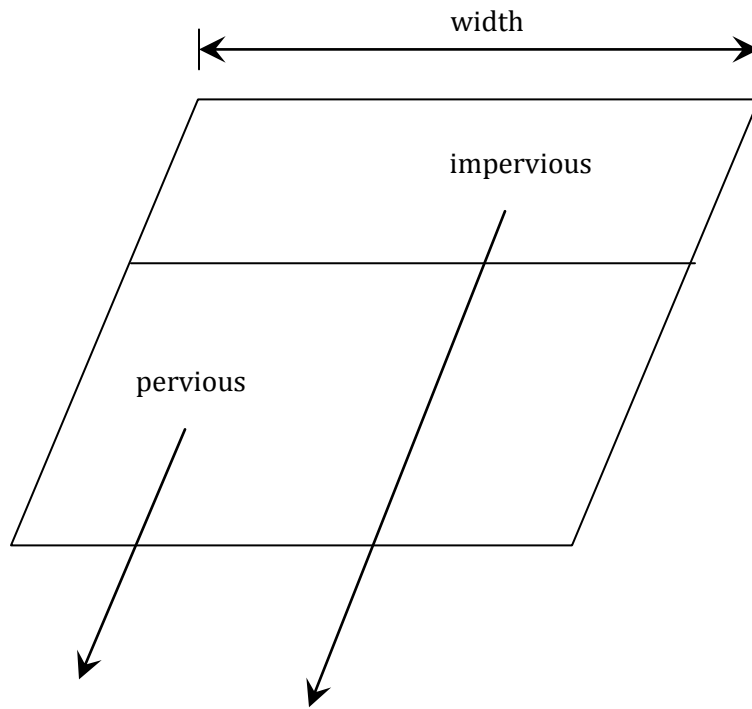


Figure 2.8. Conceptual model of rectangular subcatchment runoff from pervious and impervious surfaces (adapted from Rossman, 2010)

SWMM has three primary computational blocks for modeling runoff and downstream transport of water and water quality constituents: RUNOFF, TRANSPORT, and EXTRAN. At the most basic level, the RUNOFF block transforms rainfall into runoff and develops a storm hydrograph for a given rainfall event and physical characteristics of each subcatchment. It can also model overland flow and has limited channel routing capabilities. The TRANSPORT and EXTRAN computational blocks take the hydrograph developed in the RUNOFF block and route the hydrograph through pipes, channels, and ponds. EXTRAN is the more sophisticated of the two computational blocks with regard to hydraulics simulation important for accurate modeling of stormwater drainage networks. The TRANSPORT block is less robust, but includes the capability to route water quality constituents (aka. pollutographs) through the drainage system (Wang and Altnkayanak, 2012; Akan and Houghtalen, 2003).

### **Applicability of SWMM in small urban watersheds**

Before the late 1990s, research studies that used the U.S. Environmental Protection Agency's (EPA's) Storm Water Management Model (SWMM) were concentrated on studying large, urban catchments using continuous simulation. With advances in the availability of high spatial resolution of imagery, as well as analysis capabilities of GIS, along with the availability of detailed stormwater drainage network information, it has become easier to obtain necessary inputs to model small, urban watersheds. This section of the literature review will summarize a selection of research studies that used SWMM to model stormwater quantity and quality in small, urban watersheds located around the world.

In their study, Tsihrintzis and Hamid (1998) used SWMM to model the quantity and quality of stormwater runoff from four small urban sites in Florida ranging from 5.97 to 23.56 ha in area. In their study, each catchment was characterized by one dominant urban land use (i.e. low density residential, commercial). The objective of their study was to test the applicability of SWMM to

small, subtropical urban catchments, and provide modelers with a method to select appropriate input parameters for their watersheds to be entered into SWMM. Per the discussion in the previous section about event-based versus continuous simulation, event-based simulation was selected for this watershed because of the dynamic nature and rapid response of small urban watersheds to precipitation events. Tsihrintzis and Hamid (1998) found that SWMM generally performed well in predicting water quantity and quality in their selected watersheds, but with little research on the use of SWMM in smaller watersheds, questioned the efficacy of SWMM in small versus large catchments.

Lee and Heaney (2003) used SWMM to estimate runoff from a small urban watershed (5.81 ha) located in Miami, Florida. Their goal was to accurately characterize the impervious surfaces in the watershed using increasing levels of effort to obtain increased levels of detail. The researchers started with impervious surface area estimates from remote sensing data only, and moved up to ground referencing surveys where the gutter outlets for each rooftop were located and characterized. They were also looking to accurately quantify the effect of accurately characterizing directly-connected impervious areas (DCIA) versus Total Impervious Area (TIA) in their spatial analysis of urban imperviousness. In their results, Lee and Heaney (2003) found that higher levels of effort in characterizing impervious surface areas resulted in a decrease in the estimated DCIA, which led to decreases in predicted storm peaks and runoff volumes for a given storm event when modeled in SWMM.

Temprano, et al. (2006) were interested in modeling water quality on a small urban catchment (56 ha) in Northern Spain. While the researchers noted that there were several different mathematical models available to study water quality in urban catchments with combined sewer systems (CSSs) during “rainy weather” (SWMM, STORM, DR3M-QUAL, MOUSE, etc.), the authors selected SWMM because it was “one of the most complete and widely used throughout the world” (Temprano, et al., 2006). In their study, Temprano, et al. (2006) divided their watershed into 246



subcatchments, and demonstrated that SWMM had a high predictive capability, able to simulate the total volume of a storm even within four percent of measured.

A small urban catchment (65% imperviousness, 11.35 ha) in Pavia, Italy was modeled to examine the rainfall-runoff relationship by Wang and Altunkaynak (2012). Their objective was to compare modeling results from SWMM and using a fuzzy logic approach. By using the OPTIMIZATION block in SWMM to automatically calibrate their runoff parameters, Wang and Altunkaynak (2012) found that SWMM and the fuzzy logic approach both showed comparable results for storm events less than 25 mm total precipitation, but that SWMM had a tendency to over predict runoff for storm events with rainfall totals greater than 25 mm.

A small urban catchment (13.65 ha) in Macau, China was modeled by Zhao, et al. (2013) using SWMM to examine the results of popular likelihood functions used in hydrological models. Goldstein, et al. (2010) discuss the use of SWMM to model a “block-scale” (2.66 ha) urban catchment to examine the sensitivity of runoff predictions to input parameters, e.g. percent impervious surface area, depression storage, Manning’s n values, etc.

The potential effect of climate change on small urban catchments was studied by Denault, et al. (2006) by modeling a small urban catchment (~45% TIA, 440 ha) in North Vancouver, British Columbia. The researchers used SWMM to evaluate the effects of increased rainfall intensity on design peak flows to discuss potential issues for future drainage system capacity in the catchment. Wu, et al. (2013) also were interested in likely impacts of climate change as well as land use change, increased storm intensity, and total precipitation, in the Midwest. In their study, five headwater streams, ranging in size from 61.8 to 195 ha, were studied in Polk County, Iowa. The percent of impervious surface area ranged from 5.3 to 37.1% in these watersheds, and the researchers found that the location of the ISA had a greater effect on the timing of runoff (i.e. time to peak flow) than total volume of runoff. They also predicted that small basins may experience greater impacts from climate and land use/land cover change than larger basins.

Meierdiercks, et al. (2010) discussed research that took place in three headwater subbasins ranging from 1.3 to 1.9 km<sup>2</sup> to examine stormwater drainage networks. Using SWMM, the researchers were interested in determining the level of stormwater network detail needed to accurately predict hydrologic response. By identifying patterns in drainage networks, their goal was to simplify model inputs without sacrificing accuracy of the model predictions. Another study examining spatial resolution of drainage networks on the accuracy of SWMM model results was described by Park et al. (2008). In their study, they studied a 73 ha catchment and modeled storm events in SWMM using different levels of spatial resolution for the drainage network. While they found a decrease in pollutant loads with decreasing drainage network resolution, they reported little change in the hydrograph as resolution decreased.

When examining potential effects of land use change/development on stream response, it is common for two different models with two different levels of capability/complexity, for pre- and post-development. For example, a more simplified model, like the NRCS Curve Number Method will be used for pre-development, while a more complex hydrologic model, like SWMM, will be used for the post-development predictions (Jang, et al., 2007). Jang, et al. (2007) proposed using the same model for pre- and post-development hypothesizing that the results will be more consistent and match up better with expected results. In an effort to recreate conditions that could happen in watershed planning, Jang, et al. (2007) examined results for an uncalibrated SWMM model to simulate using the model on an unaged watershed, and found that SWMM performed well for a pre-development watershed, and using the model for pre-and post-development conditions did lead to more consistent/expected results. This research was performed in Korea on watersheds ranging from 8.5 to 56 km<sup>2</sup>.

Bhaduri, et al. (2001) presented research on two urban subbasins (221 and 95 acres) using two different models: SWMM and L-THIA. L-THIA is a simple, user friendly, model that uses the CN method for runoff calculations. While SWMM can perform more sophisticated runoff calculations, it

requires a large amount of information to run a model. It is a complex model that is data intensive and requires a high level of expertise. Developing and running a model in L-THIA can take a number of hours, while creating the same model in SWMM can take weeks or months depending on expertise of the user and availability of necessary parameter data. The researchers determined that L-THIA tended to overestimate runoff as compared with SWMM, and while it should not be used for modeling results of a final design, can provide a method to perform an initial assessment of hydrologic impacts of land use and/or climate change.

In a very recent publication, Sun, et al. (2014) examined the importance/affect on model accuracy depending on the level of catchment discretization (the level of spatial resolution of the subcatchments in a given study area). They looked at two urban watersheds, 46.7 ha and 17.75 ha, and determined that the higher the level of discretization, the more homogeneous each subcatchment was, the more accurate the results of the model. Ideally, the authors suggested that each type of land use/land cover/soil type combination should be represented as individual subcatchments, although this level of detail can be time consuming to extract from remote sensing datasets.

From this summary of selected research articles on the use of SWMM in small, urban watersheds, it is possible to see the wide range of applications to small, urban watersheds from the United States (Iowa, Florida, New York) to British Columbia, to Europe (Italy, Spain), Australia, and Asia (China, Korea). SWMM is a widely used, highly respected, and comprehensive model that can be used to accurately model conditions in small urban watersheds with extensive stormwater drainage networks.

### Chapter 3. Site Description/Characterization

Mullins Creek is a small urban catchment (approximately 220 ha) that drains much of the University of Arkansas, Fayetteville (UA) main campus, located in Washington County, Arkansas. The catchment is located in the Boston Mountains Plateau physiographic province which is part of the larger Ozark Plateau region (Arkansas Geological Survey, 2014; Figure 3.1). Mullins Creek is a tributary to the West Fork of the White River which ultimately drains into Beaver Reservoir, the primary drinking water source for much of Northwest Arkansas (Figure 3.2). Beaver Lake Reservoir provides drinking water for approximately 420,000 people over five counties in Northwest Arkansas, which equals about one in seven Arkansans. Preserving the quality of water in the Mullins Creek catchment and other tributaries, Beaver Lake Reservoir source-water protection, is of great concern and importance (Beaver Water District, 2010, 2014). The West Fork of the White River has been listed on the U.S. Environmental Protection Agency's 303(d) list, a list of impaired waterways, for high levels of turbidity and excessive silt loads. In a report published by the Arkansas Department of Environmental Quality (ADEQ), Formica, et al. (2004) estimated that about 66% of the sediment load in the West Fork of the White River was attributed to stream bank erosion, 17% was attributed to roadways and ditches, and almost 11% was attributed to construction in urban areas.

Mullins Creek is representative of many small streams located in dynamically changing urban environments. Urban streams are "flashy", exposed more frequently to changing conditions in the catchment (i.e. construction/development), exposed to more direct interference in the form of flood and erosion protection (i.e. channelization, rip-rap), and are constrained by existing infrastructure (i.e. roads, extensive underground drainage networks, buildings). Small urban catchments are also locations where research has led to an increase in stream restoration projects and implementation of Low Impact Development (LID) practices/techniques in the catchment. The Mullins Creek catchment has also experienced a great deal of land use/land cover change as the

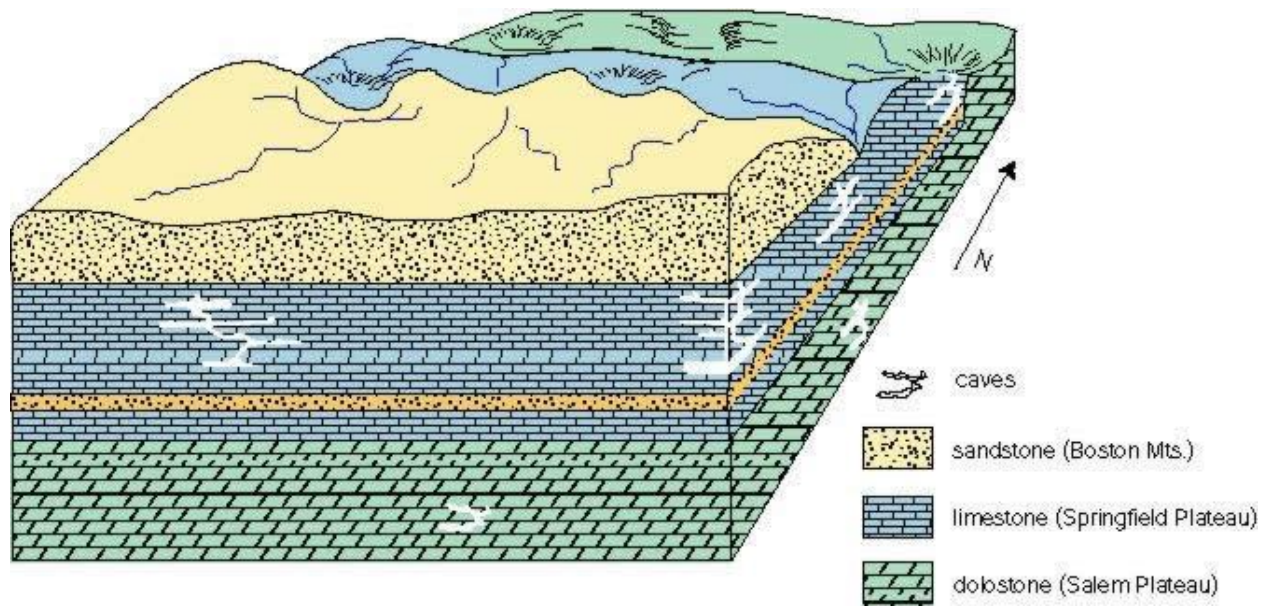


Figure 3.1. A graphic of the geology of the Ozark Plateau Region, including the Boston Mountains, Springfield Plateau, and Salem Plateau subregions. The Mullins Creek catchment is predominantly located in the Boston Mt. Plateau, characterized by the surface deposition of sandstones and shales on top of the limestone layer characterized by the Springfield Plateau subregion (Arkansas Geological Survey, 2014).

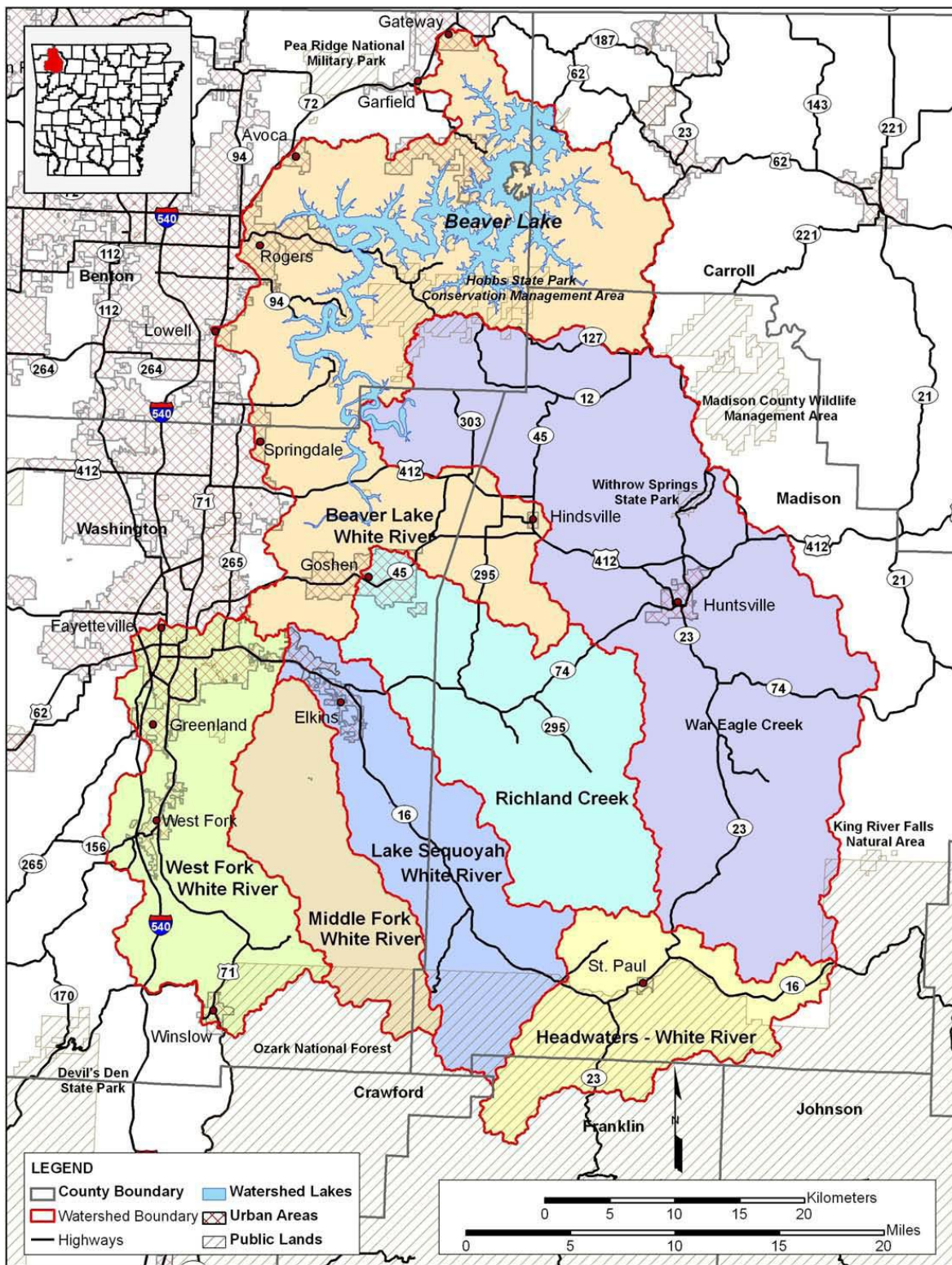


Figure 3.2. Map of Beaver Lake Reservoir watershed composed of seven major catchments spanning five counties in Arkansas. Mullins Creek is a tributary to the West Fork White River catchment. (BWD, 2010).

University of Arkansas (UA) continues to grow its student population and must construct additional buildings and infrastructure to keep up with demand. In the past decade this has included the razing of many buildings including a dormitory complex along the edges of Mullins Creek as well as construction of a new dormitory complex, a new softball stadium, and new training facilities for UA athletics, just in the Mullins Creek catchment. In 2008, the campus was home to over 19,000 students in addition to almost 850 faculty (UA, 2009).

### **Physical Characteristics**

Mullins Creek is located on the University of Arkansas campus in Fayetteville, Arkansas and drains a significant portion of the main campus including a majority of the athletic facilities on campus (Figure 3.3). The Mullins Creek catchment drains an area of approximately 220 ha and includes land uses from forested to high intensity urban. The main channel begins where flow leaves drainage pipes that collect runoff from University of Arkansas parking lots. It flows south to Maple Avenue where it is directed underground into a large concrete box culvert that runs underneath the University of Arkansas football stadium, football practice fields, track, and men's basketball area (Bud Walton Arena). The creek daylightes again south of Leroy Pond Road and runs through The Garden, a park-like tailgating area with a pavilion and gazebos, runs under Lady Razorback Road, and runs between the Lady Razorbacks soccer stadium and a large parking lot until it takes a 90 degree turn to the east, and another 90 degree turn back to the south to run under Martin Luther King, Jr. Boulevard.

In 2012, a stream restoration project was undertaken by the University of Arkansas and the Watershed Conservation Resource Center (WCRC) to help address flooding and erosion issues in the reach south of Leroy Pond Drive and North of Lady Razorback Road (Matt VanEps, WCRC, personal communication. 21 July 2014). The research described in this project is focused on the stream and existing land use before the 2012 restoration. Prior to the restoration project in 2012, a

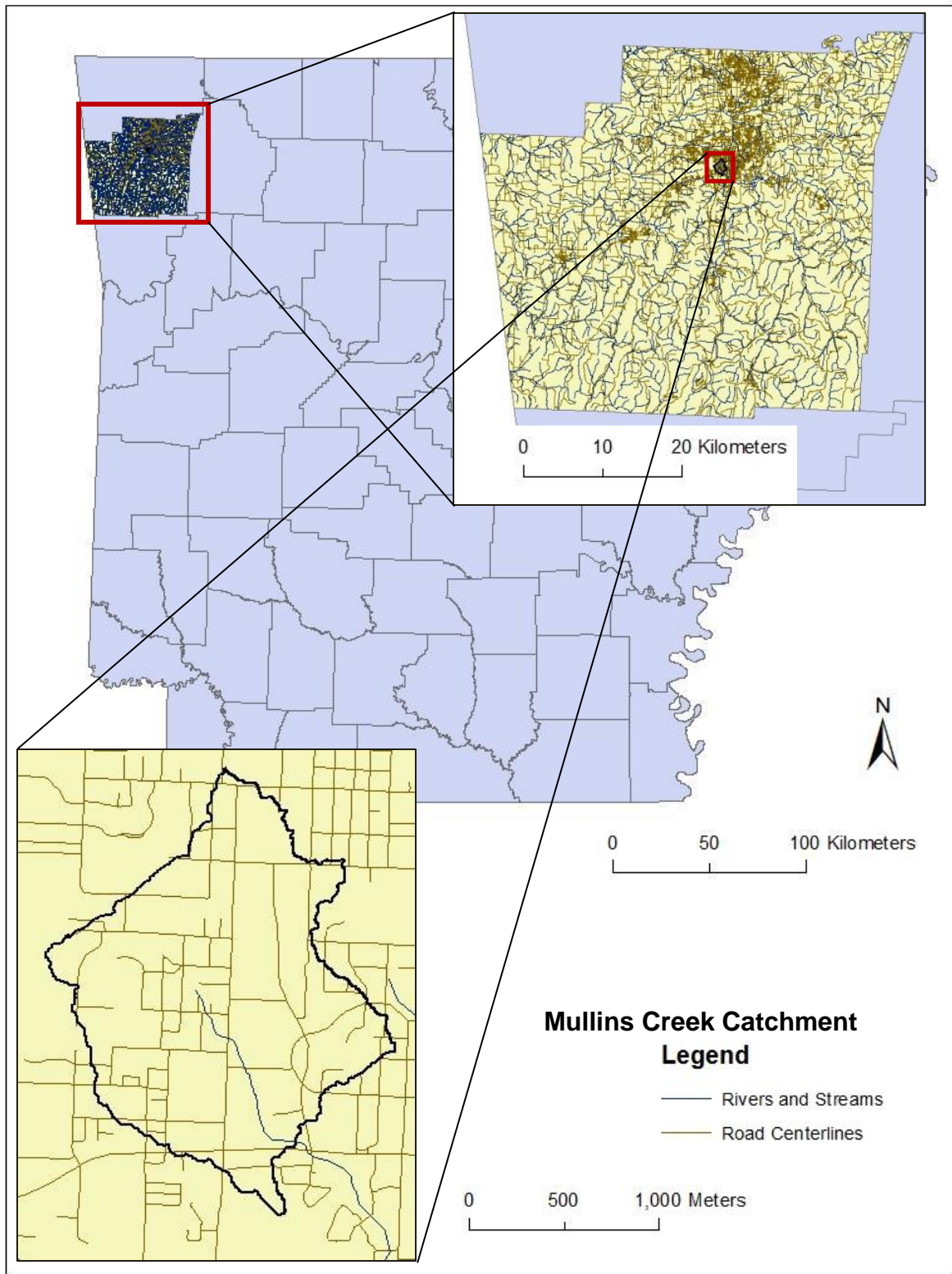


Figure 3.3. The study area, Mullins Creek catchment, is located in Washington County in Northwest Arkansas (ASLB, 2014; USGS, 2009).



stream survey was performed to quantify existing conditions including cross-sectional area, location of the bankfull elevation, and a bed material characterization. The raw survey data were analyzed to determine average conditions for the reach (Table 3.1 and 3.2).

### **Land Use/Land Cover (LULC) and Imperviousness**

Mullins Creek, even though it is a highly developed catchment, has a wide range of LULC conditions throughout the catchment. The western half of the catchment is predominantly pervious surfaces characterized as forested, and low intensity urban land use, while the central portion of the catchment, along the main flow path of the stream, is characterized by high intensity urban development (Figure 3.4). The most highly concentrated development and impervious surface coverage is located just to the east of Razorback Road which bisects the catchment. The land use/land cover distribution in the Mullins Creek catchment is shown in Table 3.3. It is important to note the high percentage of high intensity urban and the percentage of the catchment that is designated as “roads.”

The main land use/land cover categories that were important to this study were pervious (grass or forest) and then impervious. The impervious surfaces were categorized as rooftop, road, or driveway/parking lot to estimate percent of directly connected impervious area (DCIA). To determine percentages of grass, forest, rooftop, and driveway/parking lot for the two categories of urban intensity, a series of point in a rough grid pattern were selected throughout each category and were ground-referenced to an aerial map of the area to determine the land use/land cover (Table 3.4). Based on the LULC data, the vast majority of the watershed, over 90%, could be considered developed in some way, and 32% of the catchment has been categorized as 100% impervious (Gorham, 2012a; Gorham, 2012b).

Table 3.1. Geomorphology data summary on the Mullins Creek main catchment central reach (Matt VanEps, WCRC, personal communication, 13 December 2013). The cross-sectional dimension values are the average of the nine cross-sections surveyed.

Mullins Creek Geomorphology Plan/Profile	
Cross-sectional Area (m <sup>2</sup> )	6.0
Width (m)	8.8
Mean Depth (m)	0.69
Max Depth (m)	1.38
Hydraulic Radius (m)	0.60
Width to Depth Ratio	13.3
Slope (m/m)	0.00895
Sinuosity	1.03

Table 3.2. Bed material characteristics of the middle reach of Mullins Creek determined by a pebble count pre-2012 restoration (Matt VanEps, WCRC, personal communication, 13 December 2013)

Bed Material Characterization	Riffle (mm)	Reach (mm)
d <sub>16</sub>	6.9	9.2
d <sub>35</sub>	18	17
d <sub>50</sub>	31	28
d <sub>84</sub>	90	78
d <sub>95</sub>	130	120

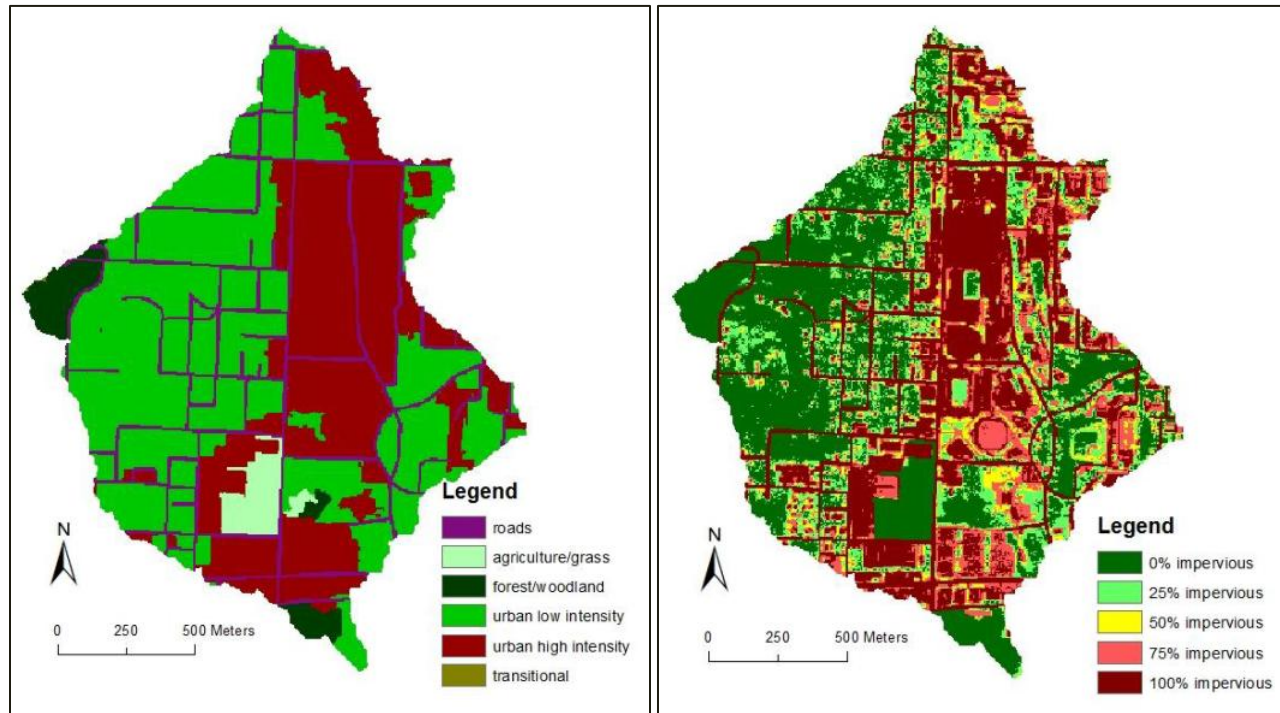


Figure 3.4. Land Use/Land Cover (LULC) for the Mullins Creek catchment in 2010, and percent impervious surface (Gorham, 2012a; Gorham, 2012b). Note the concentration of high intensity urban LULC and 100% impervious surface concentrations (identified in red) in the eastern and southern portions of the catchment.

Table 3.3. Land use/land cover (LULC) and percent total impervious surface (TIA) data for Mullins Creek for 2010 (Gorham, 2012a; Gorham, 2012b)

LULC Description	Percent
Roads	10.4
Agriculture/Grass	2.6
Forest /Woodland	3.4
Urban Low Intensity	49.1
Urban High Intensity	34.4
Total Impervious Area	48.5

Table 3.4. Pervious and impervious surface categories for High Intensity and Low Intensity Urban LULC Categories.

	LULC Category	
	High Intensity Urban	Low Intensity Urban
Total Area (ha)	75.7	108.0
Number of Samples	230	355
Driveway/Parking Lot (%)	34.7	7.9
Rooftop/Other (%)	34.8	18.1
Lawn (%)	27.0	53.0
Forest (%)	0.4	19.1

## **Stormwater Drainage Network**

The catchment is also characterized by an extensive stormwater drainage network that increases stormwater runoff efficiency. A significant length of the main channel is routed underground into a concrete box culvert running underneath the main athletic facilities on campus. (Figure 3.5). In 2009, the University of Arkansas developed a stormwater management plan to assist the City of Fayetteville in meeting Non-Point Source Discharge Elimination System (NPDES) permitting requirements for communities regulated as Small Municipal Separate Storm Sewer Systems (MS4s). Part of the Stormwater Management Plan (SWMP) developed by the University of Arkansas included a goal of developing “a storm sewer system map, showing the location of all outfalls and the names and location of all waters that receive discharges from those outfalls” (UA, 2009). The availability of this dataset allows for the development of a hydrologic model that looks at surface drainage as well as water movement through the stormwater drainage network. While the location of pipes and lengths, etc. were mapped for this purpose, more detailed analysis and measurement of the drainage network on the UA campus was performed by Koehn et al. (2011).

As a part of the National Pollutant Discharge Elimination System (NPDES) permitting program, the University of Arkansas and the City of Fayetteville were required to file for permits and to map their stormwater drainage systems . Overall, there are approximately 11035 m of pipes running under the Mullins Creek Catchment for a stormwater drainage density of 50.2 m of pipe per hectare. The distribution of pipe sizes shows that 18 in (45.7 cm) diameter pipes are the most predominant size in the catchment (Figure 3.6) made primarily of corrugated steel, ductile iron, and reinforced concrete (City of Fayetteville, 2014; Koehn, et al., 2011).

## **USGS Gaging Station**

The U.S. Geological Survey (USGS) installed a gaging station where Mullins Creek flows under Martin Luther King, Jr. Boulevard in Fayetteville, Arkansas (Figure 3.7). The USGS began real

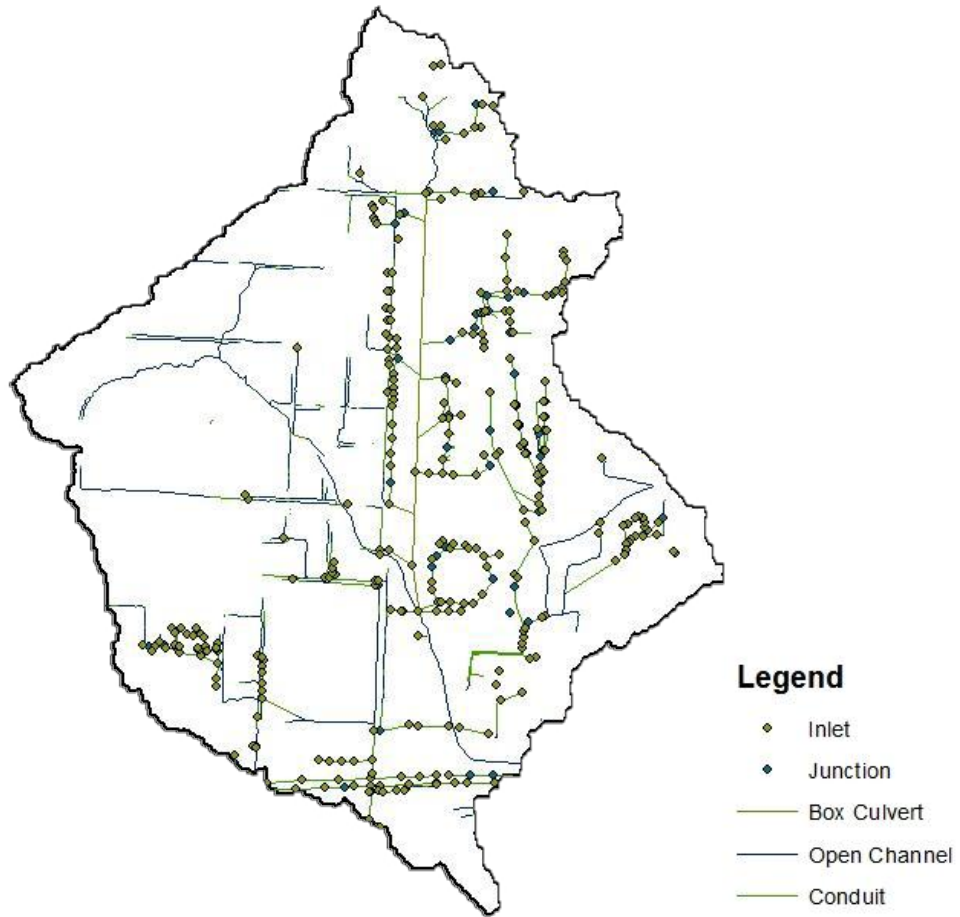


Figure 3.5. Stormwater drainage network under the Mullins Creek catchment (COF, 2014)

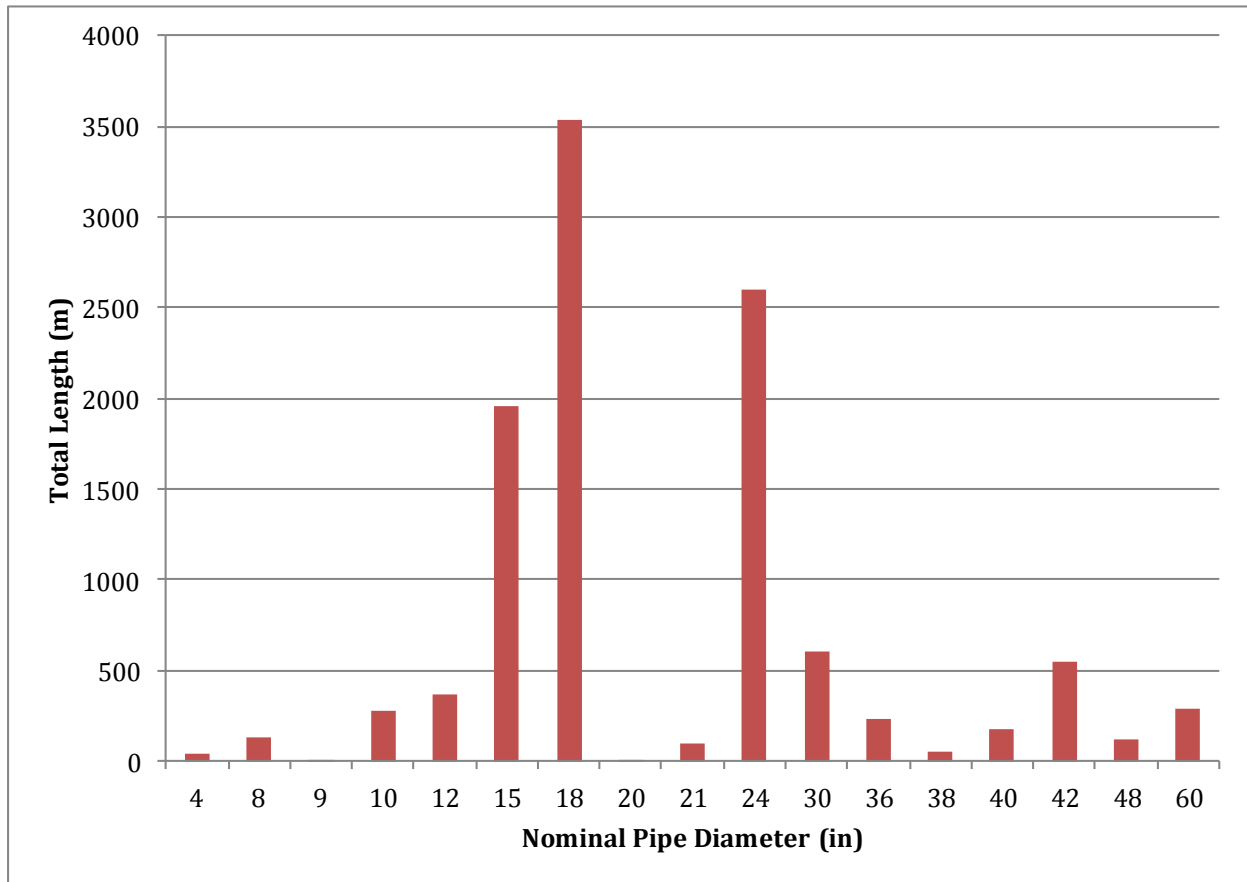


Figure 3.6. Total length of stormwater drainage pipe by diameter. At over 3500 m, the 18 in diameter pipe was the most common pipe size in the network, followed by 24 in diameter pipe (over 2500 m) (COF, 2014; Koehn, et al., 2011).



Figure 3.7. USGS Gaging Station (07048480) "College Branch at MLK Blvd at Fayetteville, AR" located where Mullins Creek runs under Martin Luther King, Jr. Boulevard (road to the right of the photo). Mullins Creek is flowing from left to right under the road in this photograph. (Unless otherwise noted, all photographs in this document were taken by the author.)



time data collection in September 1996 and discharge (cfs) and gage height (ft) are reported for the location every five minutes. Data can be downloaded from their website from October 2007 to present, and can be downloaded from the Instantaneous Data Archive (IDA) if the data were recorded in water year 2007 or earlier. All storm events with a peak flow greater than 100 cfs were identified for 2008 – 2010 and the total runoff was plotted versus total precipitation as a representation of the rainfall/runoff relationship (Figure 3.8).

### **Soils Data**

There are 11 different soil map units in the Mullins Creek catchment from eight different soil series: Enders (Fine, mixed, active, thermic Typic Hapludults), Fayetteville (Fine-loamy, mixed, active, thermic Rhodic Paleudults), Hector (Loamy, siliceous, subactive, thermic Lithic Dystrudepts), Johnsborg (Fine-silty, mixed, active, mesic Aquic Fragiudults), Leaf (Fine, mixed, active, thermic Typic Albaquults), Linker (Fine-loamy, siliceous, semiactive, thermic Typic Hapludults), Sloan Fine-loamy, mixed, superactive, mesic Fluvaquentic Endoaquolls), and Savannah (Fine-loamy, siliceous, semiactive, thermic Typic Fragiudults) (NRCS, 2014c). These soil series represent three different hydrologic soil groups (HSG) ranging from moderately well drained (B) to poorly drained (D) (Figure 3.9). The majority of soils in the catchment fall into the HSG C category. For more information on HSG and infiltration characteristics of soils in the Mullins Creek catchment, please see Chapters 2 and 4.

### **Subcatchments**

The Mullins Creek catchment was delineated into subcatchments based on surface water hydrology and the digital elevation model for the catchment for hydrological modeling purposes. Initially the catchment was broken up into four main subcatchments, A, B, C, and D, and then each of those subcatchments was further divided for a total of 49 subcatchments (Figure 3.10).

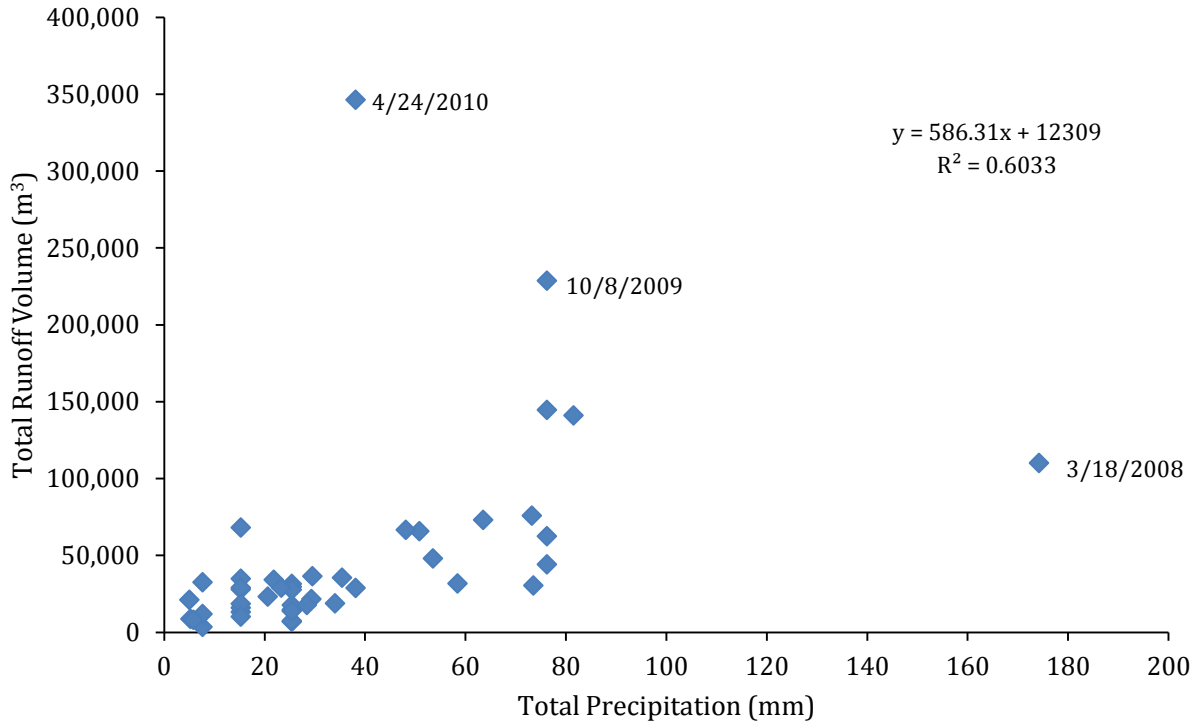


Figure 3.8. Relationship between rainfall and runoff for all storm events with a peak flow greater than 100 cfs (2.8 cms) that occurred between 2008 and 2011. Total runoff for each storm (m<sup>3</sup>) is plotted versus total precipitation for the event (mm). The points furthest away from the main cluster of data points are identified by the date of the event. The equation on the graph represents the linear relationship between runoff volume and total precipitation with outlying data points removed (USGS, 2014; NCDC, 2014).

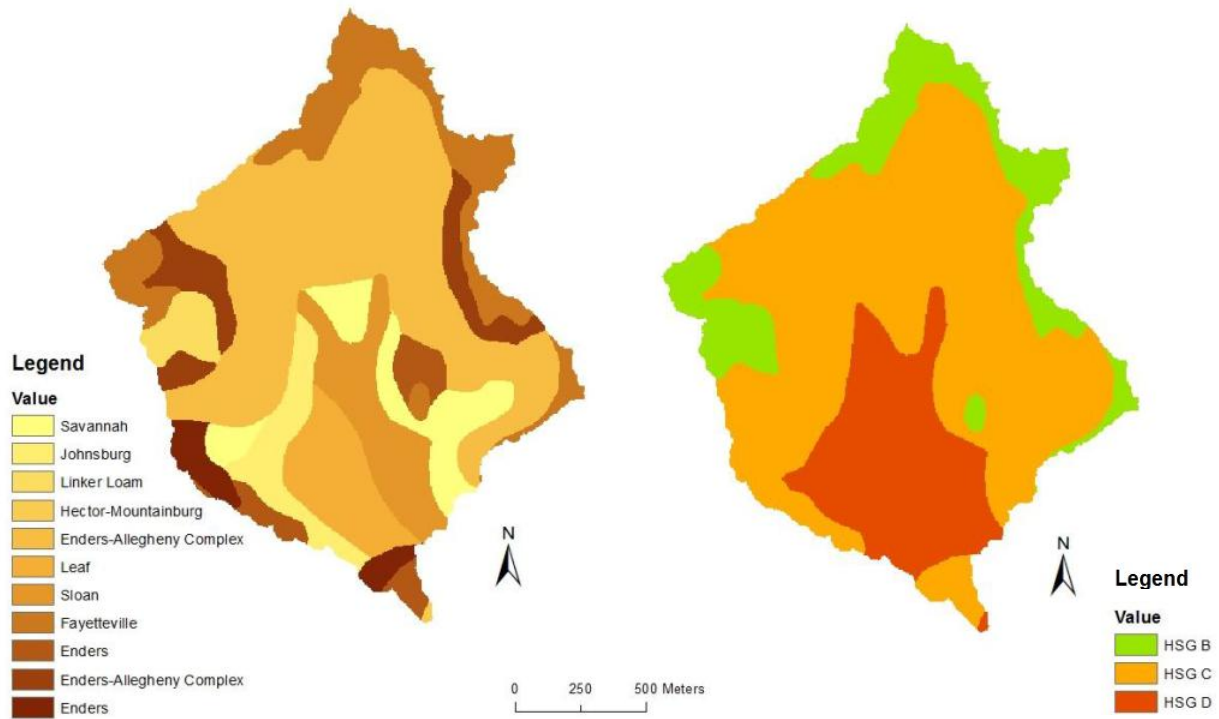


Figure 3.9. Soil map units in the Mullins Creek catchment and the Hydrologic Soil Group (HSG) distribution in the catchment. More detail about soil characteristics in the Mullins Creek catchment are presented in Chapter 4 (NRCS, 1994).

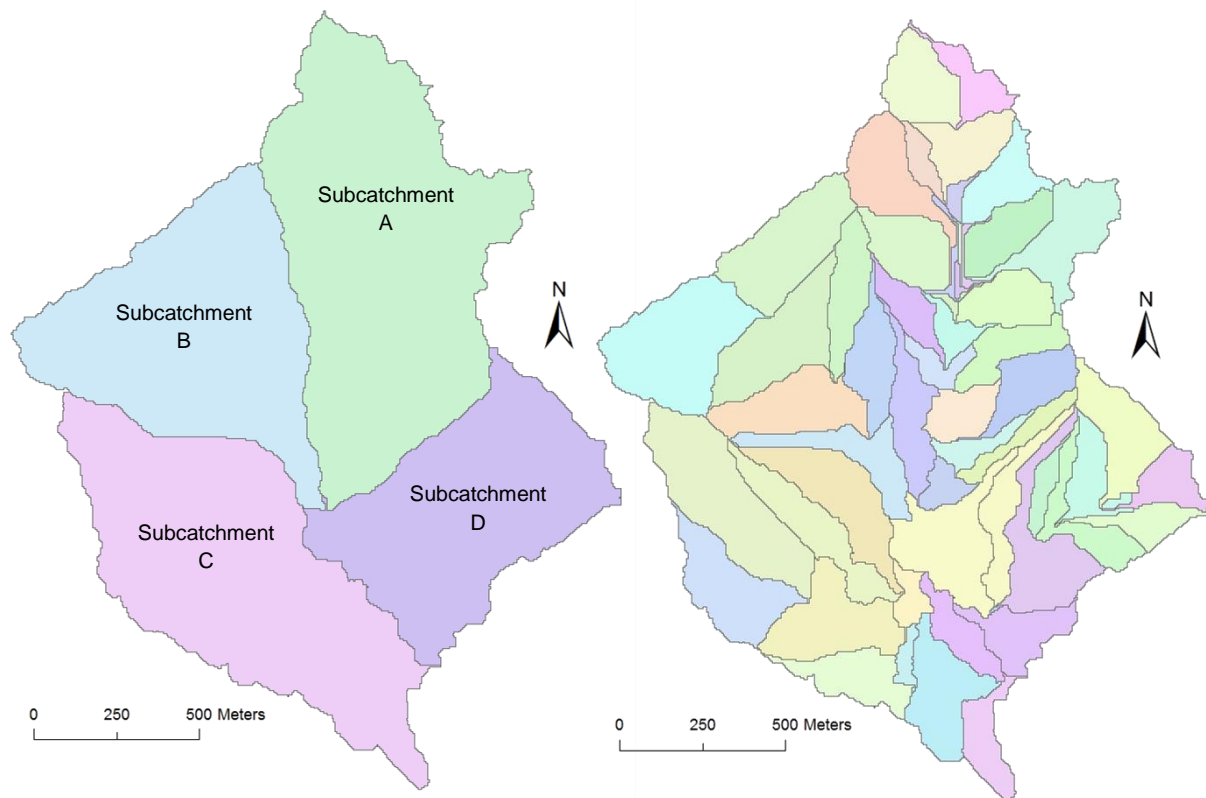


Figure 3.10. Main subcatchments in the Mullins Creek catchment: A, B, C, and D (left), and the higher spatial resolution subcatchment delineation used for hydrologic modeling parameterization (right). While over 50 subcatchments were originally delineated, a few subcatchments were combined because of size and proximity.

Average parameters for each subcatchment were determined/measured/calculated using ArcGIS (Table 3.5). The subcatchments ranged in their drainage area, primary hydrologic soil group, slope, and other parameters (Table 3.6). For a complete list of subcatchments and their extracted parameters, please see Chapter 5.

### **Summary/Discussion**

The information presented above was used to calculate/measure/predict additional variables for each subcatchment to complete the parameterization of the SWMM model in addition to the data collected and analyzed on soil infiltration in Chapter 4. This catchment is representative of many small, urban catchments that are affected by highly extensive and efficient stormwater drainage networks, and high levels of development and impervious surfaces. Data available online from remote sensing sources was paired with ground referenced data to present an accurate representation of the catchment and delineated subcatchments in the SWMM model. More information on the model parameterization process and how data were analyzed/interpreted for input into the model is presented in Chapter 5.

Table 3.5. Subcatchment data summary for the main subcatchments A through D.

	Physical Characteristics		Land Use/Land Cover (Gorham, 2012a,b)						Soil Infiltration (NRCS, 1994)		
	Area (ha)	% Slope	% IMP	% Roads	% Grass	% Forested	% LIU	% HIU	%B	%C	%D
SC-A	70.2	3.57	70.1	10.0	0.0	0.0	27.0	62.9	25.8	67.8	6.4
SC-B	48.9	4.66	21.8	10.8	0.1	9.8	78.2	1.1	18.1	72.3	9.6
SC-C	58.9	4.00	44.6	10.6	8.3	4.1	47.1	29.9	6.6	44.4	49.0
SC-D	41.7	0.01	48.8	10.3	1.7	0.9	55.0	32.1	13.0	66.2	20.8

Table 3.6. Range of values for select subcatchment parameters divided by primary subcatchment. A minimum value, maximum value, and average value were calculated for each parameter.

	Subcatchment A			Subcatchment B			Subcatchment C			Subcatchment D		
	Min	Max	Avg	Min	Max	Avg	Min	Max	Avg	Min	Max	Avg
Area (ha)	0.55	7.02	3.49	4.26	12.08	6.96	0.80	12.38	5.61	1.40	7.56	4.27
% Slope	1.5	13.4	7.1	1.3	8.8	6.0	0.8	8.8	4.0	0.8	15.7	7.4
% IMP	46.9	99.3	72.7	11.9	49.4	25.6	25.0	85.6	50.4	22.1	68.2	47.6
% Roads	0.0	19.7	9.3	7.1	18.7	12.1	0.5	41.9	12.3	4.1	18.5	10.1
% Grass	0.0	0.0	0.0	0.0	39.5	5.8	0.0	57.7	11.3	0.0	9.6	1.0
% Forested	0.0	0.0	0.0	0.0	52.0	7.5	0.0	23.0	4.6	0.0	4.2	0.4
% LIU	0.0	68.8	22.5	0.0	92.9	73.0	0.0	85.2	33.2	26.7	87.9	59.7
% HIU	11.6	99.8	68.2	0.0	10.9	1.6	2.1	75.7	38.6	6.4	68.9	28.8
%B	0.0	84.9	18.5	0.0	49.1	12.5	0.0	29.2	3.1	0.0	42.1	15.6
%C	15.1	100.0	73.2	30.3	99.9	74.0	0.0	85.4	38.8	26.6	100.0	69.9
%D	0.0	55.3	8.3	0.0	67.3	13.6	7.5	100.0	58.1	0.0	73.3	14.5

## Chapter 4: Mullins Creek Soil Characterization

### Introduction

Traditionally in watershed/hydrologic modeling, when predicting the runoff potential of a specific area, the modeler is looking at certain characteristics of the surface of the area of interest. These include any parameters/variables that would affect the infiltration capacity/rate of the area including: surface cover (i.e., impervious, grass, crop, forest, etc.), quality of cover, percent vegetative coverage versus exposed soil, and infiltration characteristics of the soils present in the area. The infiltration rate can be dependent on the soil texture (percent sand, silt and clay), bulk density, porosity, heterogeneity, preferential flow paths, surface conditions, antecedent moisture conditions, and the presence of organic matter (USDA, 2008; Wolkowski and Lowery, 2008; Ward and Trimble, 2004).

The Natural Resource Conservation Service (NRCS) developed a method to categorize different soils based on runoff potential and called the classification system the hydrologic soil group (HSG). The HSG is one of the parameters used by the NRCS Curve Number (CN) Method to calculate runoff for a catchment (NRCS, 2004). For more information on HSGs, see the infiltration section in the Literature Review (Chapter 2).

Other methods can be used to predict the infiltration rate/capacity of a specific soil, like the Horton Infiltration method or the Green-Ampt Infiltration method. The NRCS Curve Number method, in addition to the Horton and Green-Ampt methods, are the three options to predict infiltration used in the U.S. Environmental Protection Agency's Storm Water Management Model (SWMM) (Rossman, 2010). However, potential values for the variables in the Horton Infiltration equation [i.e., initial infiltration rate ( $f_0$ ), final infiltration rate ( $f_c$ ), and decay coefficient ( $k$ )] are rarely published in the literature as it is highly recommended that these values be developed for each site/soil by performing field testing. One example of recommended infiltration rates to be

used in the Horton Equation was published by the Urban Drainage and Flood Control District (UDFCD) (2007) and are shown in Table 4.1.

### **Soils in the Mullins Creek Catchment**

The Mullins Creek catchment is located in Washington County, Arkansas and drains a portion of the University of Arkansas, Fayetteville campus. Using data from the STATSGO Soils database published by the NRCS (1994) and importing the information into ArcGIS, it was determined that the catchment is composed of 11 different soil map units from nine different soil series (Table 4.2). The distribution of each soil map unit and the HSG is presented in Figure 4.1.

One of the hypotheses of this study was that the existing soils in the same map unit, but with different land use/land cover and maintenance regimes, could be significantly different than what is predicted. Many times during construction top soil is removed and replaced at a later time, sometimes by non-native soil. The texture of the soil can have a large effect on infiltration rate at the location. This would potentially make the use of infiltration parameters associated with a soil map unit in a hydrologic model inaccurate.

The purpose of this study was to observe/quantify/measure the characteristics of different soils under different land use conditions. Primarily, the study examines the differences between a specific soil under highly maintained (HM) conditions (i.e., turfgrass) and under minimally maintained (MM) conditions (i.e., forest, scrub/shrub, bunchgrass). The following hypotheses were addressed during the study:

1. Highly maintained sites would have lower infiltration rates than minimally maintained sites
2. Measurements would identify higher bulk densities in highly maintained sites versus minimally maintained sites
3. For all of the sites, infiltration rate will decrease as bulk density increases



Table 4.1. Recommended infiltration rates for the Horton Infiltration Equation based on hydrologic soil group (HSG) (UDFCD, 2007).

HSG	Initial Infiltration Rate ( $f_0$ ), (mm/hr)	Final Infiltration Rate ( $f_c$ ), (mm/hr)	Decay Coefficient ( $k$ ) (1/hr)
A	127.0	25.4	2.52
B	114.3	15.2	6.48
C/D	76.2	12.7	6.48

Table 4.2. Descriptions of soil series associated with the Mullins Creek catchment area. Data were obtained online from the NRCS Official Soil Descriptions website (NRCS, 2014c).

Series	Taxonomic Class	Texture Class	Permeability Description	Permeability (mm/hr)	HSG
Allegheny	Fine-loamy, mixed, semiactive, mesic Typic Hapludults	Loam	NA		NA
Enders	Fine, mixed, active, thermic Typic Hapludults	Gravelly fine sandy loam	Deep, well-drained, very slowly permeable	< 1.5	C
Fayetteville	Fine-loamy, mixed, active, thermic Rhodic Paleudults	Fine sandy loam	Deep, well-drained, moderately permeable	15.0 - 50.0	B
Hector	Loamy, siliceous, subactive, thermic Lithic Dystrudepts	Gravelly fine sandy loam	Shallow, well-drained, moderately rapidly permeable	<1.5	D
Johnsburg	Fine-silty, mixed, active, mesic Aquic Fragiudults	Silt Loam	Very deep, somewhat poorly drained	<1.5	D
Leaf	Fine, mixed, active, thermic Typic Albaquults	Silt Loam	Very deep, poorly drained, very slowly permeable	< 1.5	D
Leesburg	Fine-loamy, siliceous, semiactive, thermic Typic Paleudults	Gravelly sandy loam	Very deep, well drained, moderately permeable	15.0 - 50.0	B
Linker	Fine-loamy, siliceous, semiactive, thermic Typic Hapludults	Fine sandy loam	NA	15.0 - 50.0	B
Mountainburg	Loamy-skeletal, siliceous, subactive, thermic Lithic Hapludults	Cobbly fine sandy loam	NA	< 1.5	D
Savannah	Fine-loamy, siliceous, semiactive, thermic Typic Fragiudults	Fine sandy loam	Very deep, moderately well drained, moderately slowly permeable	15.0 - 50.0	C
Sloan	Fine-loamy, mixed, superactive, mesic Fluvaquentic Endoaquolls	Silty clay loam	Very deep, poorly drained soils	< 1.5	D

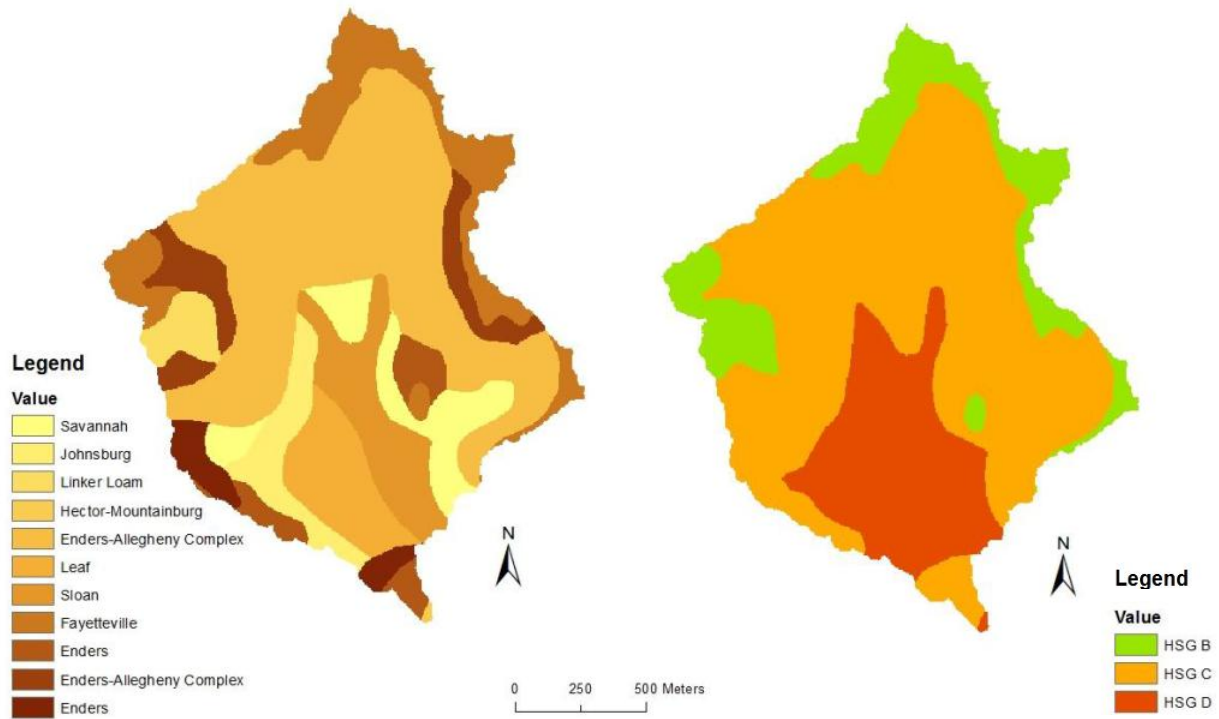


Figure 4.1. Soil map units in the Mullins Creek catchment and the Hydrologic Soil Group (HSG) distribution in the catchment (NRCS, 1994).

4. Differences in appearance (i.e. wet and dry soil color, distinct layers, presence of roots and organic matter) and soil texture would be observed in the highly maintained versus the minimally maintained sites.

## **Methods**

After identifying the soils that make up the Mullins Creek catchment, pairs of sites were selected in areas that represented five of the 11 soil map units (Table 4.3), and 78.5% of the catchment area. Two pairs of sites were located in the Enders-Allegheny complex (ErE) area since it represented over 40% of the catchment area. One of the pairs was located in an area that was highly maintained as turf grass, and the other was located in an area that was possibly developed at some point, but had been minimally maintained for approximately the last 20 years.

Table 4.4 presents a list of the sites with descriptions and the location where each set of measurements were conducted. For a few of the soil map units, a minimally maintained site for the pairing was unable to be located within the watershed, but a suitable site was located within 10 to 15 km of the watershed in a similar geographic region.

## **Infiltration testing**

In the field, infiltration rate over time was measured using double-ring infiltrometers (Figure 4.2). Three infiltrometers were installed at each study site in a triangular configuration with 3 to 4 m between infiltrometers where it was feasible (Figure 4.3).

The double-ring infiltrometer was pounded into the ground using a board and a mallet so the rings were below the surface of the soil approximately 5 cm to prevent leakage of water out of the ring or between rings. The outer ring was filled with water to check for leaks, and to help minimize the lateral movement of water as it infiltrated vertically into the soil from the inner ring. At the start of data collection, the inner ring of the infiltrometer was filled as closely to the top as

Table 4.3. Mullins Creek soil map unit descriptions and percentages in the catchment (NRCS, 1994).

Soil Map Unit Name	Map Unit Abbreviation	Percent of Catchment
Enders gravelly loam, 3 to 8 percent slopes	EnC	3.7
Enders gravelly loam, 8 to 12 percent slopes	EnD	2.9
Enders-Allegheny complex, 8 to 20 percent slopes (Leesburg)	ErE	40.8
Enders-Allegheny complex, 20 to 40 percent slopes (Leesburg)	ErF	6.7
Fayetteville fine sandy loam, 3 to 8 percent slopes eroded	FaC2	13.8
Hector-Mountainburg gravelly fine sandy loam, 3 to 8 percent slopes	HmC	0.1
Johnsburg silt loam	Jo	5.4
Leaf silt loam	Le	7.1
Linker loam, 3 to 8 percent slopes eroded	LkC2	2.7
Savannah fine sandy loam, 3 to 8 percent slopes, eroded	SfC2	8.1
Sloan silt loam	Sn	8.7

Table 4.4. Field infiltration testing sites and locations.

Site Name	Soil Map Unit	Level of Disturbance	Hydrologic Soil Group	Location	
				Latitude	Longitude
FHS	ErE	High	C	36.060492	-94.17206
Leflar	ErE	Low	C	36.061913	-94.18596
Maple Hill	ErE	High	C	36.070632	-94.1792
Lewis Avenue	ErE	Low	C	36.075735	-94.18362
Reynold's Center	FaC2	High	B	36.06444	-94.17281
Pratt Place	FaC2	Low	B	36.065371	-94.19194
SW Gardens	Le	High	D	36.058811	-94.18019
UA Chicken Farm	Le	Low	D	36.093072	-94.18315
Central Gardens	Sn	High	D	36.059149	-94.17943
Mullins Creek South	Sn	Low	D	36.057233	-94.17676
Lot 56B	SfC2	High	C	36.059904	-94.17649
Oakland-Zion	SfC2	Low	C	36.116235	-94.10513

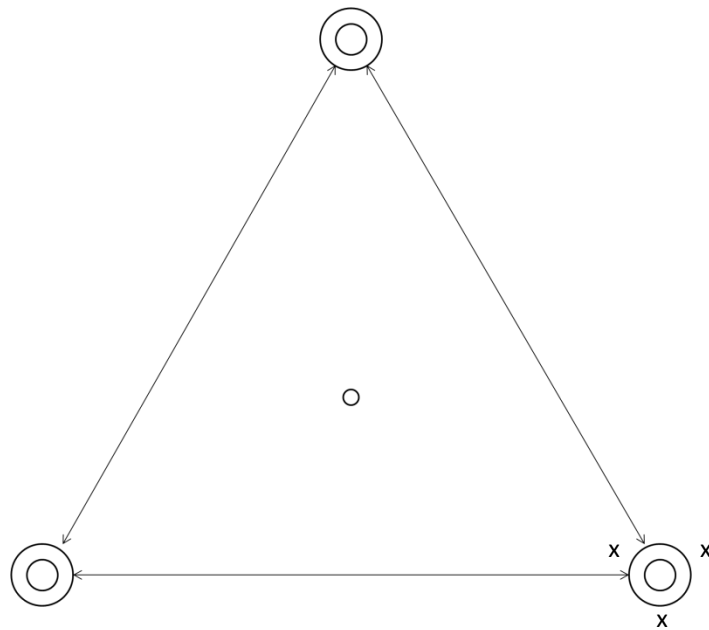


Figure 4.2. Layout of double-infiltration rings and locations for field testing. The double circles represent the location of each double-ring infiltration ring. The circle in the center of the layout represents the approximate location where a bulk density sample was collected, and the x's around the perimeter of the infiltration ring in the lower right corner represent the locations where moisture content was measured around each ring.



Figure 4.3. Photograph of a double-ring infiltration ring used in the study, manufactured by Turftec International. The diameter of the inside ring is 15.24 cm (6 in), and the diameter of the outer ring is 30.5 cm (12 in). The height of the ring is 10.2 cm (4 in).

possible, and measurements were taken at the time intervals listed on the data collection sheet (Figure 4.4) by measuring the distance from the top of the inner ring to the water surface. The measurement recorded at each time was the distance from the top of the inner ring to the water surface. Data points were collected starting at time,  $t = 0$  (initial water level),  $t = 1$  min, 2 min, 3 min, 4 min, 5 min, 7 min, 9 min, 11 min, 13 min, 15 min, 18 min, 21 min, 24 min, 27 min, 30 min, 35 min, 40 min, 45 min, and 50 min. The last data point was collected at  $t = 40$  to 50 min depending on the conditions at the site.

Field infiltration testing was used to determine observed initial infiltration rate ( $f_o$ , mm/hr), final infiltration rate ( $f_c$ , mm/hr) and overall infiltration rate (mm/hr), total depth of infiltration divided by the total amount of time for the test. Results can also be used to determine the observed decay constant,  $k$  (1/hr) used with the Horton Infiltration method. Overall infiltration rate was calculated by dividing the total depth of water infiltrated (mm) by the total time of the test (hr). The initial infiltration rate was the highest observed infiltration rate, the infiltration at the beginning of the test. The final infiltration rate was the rate of infiltration at the end of the test when the rate had evened out and reached an approximate equilibrium state. The observed Horton decay constant,  $k$  (1/hr) was also calculated for each site by solving the Horton Infiltration Equation for  $k$  (Equation 6).

$$k = -\frac{\ln\left(\frac{f - f_c}{f_o - f_c}\right)}{t} \quad (6)$$

Where,  $k$  = decay constant (1/hr)  
 $f$  = infiltration rate (mm/hr)  
 $f_o$  = initial infiltration rate (mm/hr)  
 $f_c$  = final infiltration rate (mm/hr)  
 $t$  = time (hr)



## **Moisture Content**

To quantify the moisture content of the soil before infiltration testing began, the moisture content of the soil was measured in triplicate around the edge of each infiltrometer. The moisture content was measured using a TH<sub>2</sub>O™ Portable Soil Moisture Meter made by Dynamax, Inc. (Figure 4.5) fitted with an HH2 Moisture Meter digital readout screen. The goal was that each infiltration test would be conducted when the soils had similar field moisture contents since soil moisture content greatly affects the soil's hydraulic conductivity. In addition, each highly maintained/minimally maintained pair of sites was tested on the same day to limit variations in infiltration results because of antecedent moisture.

## **Bulk Density**

This study used bulk density, the dry weight of a soil sample divided by the volume of the sample, to compare the level of compaction of the minimally maintained versus the highly maintained sites. One bulk density sample was collected per site from a central location relative to the three infiltration measurement locations. The ring used (shown with a sample inside in Figure 4.6) was 6.0 cm in diameter and 5.1 cm tall. Before the ring was installed, the surface organic material was removed using shears. The ring was then pounded into the soil to collect a clean sample. If large gravel and rocks were encountered, the ring was moved until a complete sample could be collected.

The bulk density sample was weighed (wet weight) and then dried in a drying oven at 60°C for a minimum of 72 hr. Once the sample was dry, the sample was reweighed to obtain a dry weight. Given the known volume of the bulk density ring (144.2 cm<sup>3</sup>) and the dry weight, the soil bulk density was then calculated using Equation 7. The soil from the bulk density sample was retained for use in a particle-size analysis.





Figure 4.5. Photographs of theta probe used to measure initial moisture content of the soil at each site before infiltration testing was performed.



Figure 4.6. Bulk density sample collected in the field from the Oakland-Zion site.

$$\rho_{dry} = \frac{m_s}{V_t} \quad (7)$$

Where,  
 $\rho_{dry}$  = the dry bulk density of the soil (g/cm<sup>3</sup>)  
 $m_s$  = the mass of the soil (g)  
 $V_t$  = the total volume of the sample (cm<sup>3</sup>)

### Particle-size Analysis and Visual Observation

The percent of silt, sand, and clay in each soil sample was determined using the hydrometer method outlined in the Soil Test Methods from the Southeastern United States manual published by the Southern Extension and Research Activity Information Exchange Group (2014).

The basic steps used to determine the soil texture are outlined below. For a more detailed description of the process, please see SERA (2014) in the References section. During the process of preparing the soil samples for conducting the particle-size analysis in the lab, visual observations were made about the samples, their textures, color when moist, presence of organic matter, presence of distinct layers, etc. Each soil sample was ground to a fine texture using a mortar and pestle until the entire sample was broken down to a uniform size. Following the grinding process, the soil sample was passed through a 2-mm sieve to remove all larger fragments of stone and pieces of organic matter (i.e., roots) (Figure 4.7). Fifty grams of the sieved sample were weighed out and placed into a 300-mL Erlenmeyer flask with water and 50 mL of dispersing agent (sodium hexametaphosphate), stirred, and allowed to equilibrate for 20 minutes. The sample was transferred to a 1-L sedimentation cylinder, and the cylinder was then filled with tap water up to the 1-L mark on the cylinder.

The Munsell color classification was used to classify each soil sample as it appeared when the sample was mixed into solution in the sedimentation cylinders during the particle size analysis in the lab. To determine the Munsell color of each sample, photographs were analyzed, the (red, green, blue) R,G,B color of each sample was determined (Adobe Photoshop), and a conversion table (Centore, 2013) was used to convert the R,G,B value to the Munsell color value for each sample. The



Figure 4.7. Soil samples were ground to a uniform size and passed through a 2-mm sieve to obtain a sample for analysis.

Munsell color of each soil is described by three characteristics: hue, value, and chroma. The hue is the primary color of the sample (red, yellow, blue, or green) along the visible spectrum. The value represents how “bright” the color is based on the amount of reflected light. The chroma is a value that represents the brilliance, or how pure, the color is (Gardiner and Miller, 2004). Photographs were taken of each sedimentation cylinder with the sample to record the color of each sample and to allow comparisons between paired sites.

Using a plunger, each sample was mixed thoroughly, and a hydrometer, with a Bouyoucos scale, reading was recorded at  $t = 40$  s after mixing (Figure 4.8). This reading was repeated three times for each sample including a blank. The blank was a 1-L sedimentation cylinder with water and dispersing agent, but no soil. Bouyoucos readings (g/L) were repeated and recorded for each sample at  $t = 2$  hr after completion of the last mixing (Figure 4.9). As the sample sits, the larger particles settle out from the water column first, followed by continually finer particles.

Using the relationship between the hydrometer readings for each sample and the blank at  $t = 40$  s and  $t = 2$  hr, the percent of silt, sand, and clay in each sample was calculated using the following equations with slight adjustments made for temperature of the suspension:

$$\% \text{ sand} = 100 - \left( \frac{(R_{1st} - R_{C1})}{\text{sample weight (g)}} \times 100 \right) \quad (8)$$

$$\% \text{ clay} = \frac{(R_{2nd} - R_{C2})}{\text{sample weight (g)}} \times 100 \quad (9)$$

$$\% \text{ silt} = 100 - \% \text{ sand} - \% \text{ clay} \quad (10)$$

Where,  $R_{1st}$  = The average of the three hydrometer readings taken at  $t = 40$  s (g/L)  
 $R_{C1}$  = The hydrometer reading for the blank at  $t = 40$  s (g/L)  
 $R_{2nd}$  = The hydrometer reading for the sample at  $t = 2$  hr (g/L)  
 $R_{C2}$  = The hydrometer reading for the blank at  $t = 2$  hr (g/L)

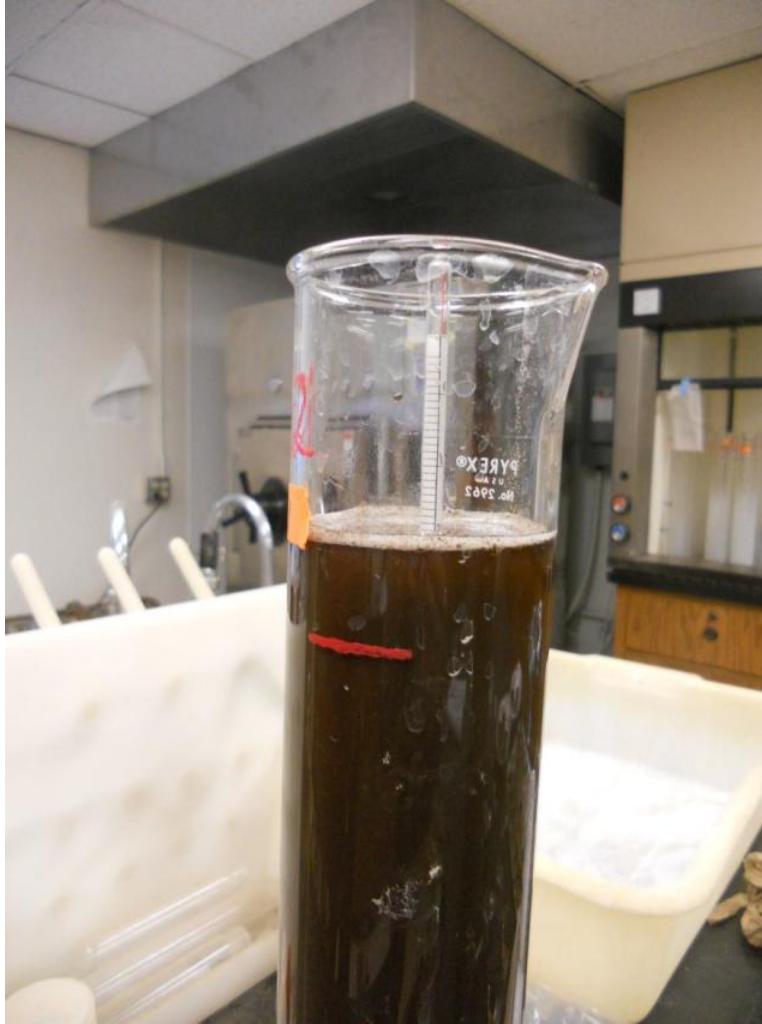


Figure 4.8. One liter sedimentation cylinder with hydrometer present for reading. The reading is the value on the hydrometer where it meets the sample surface.



Figure 4.9. Photograph of particle settling in sedimentation cylinder. As the sample sits after mixing, the larger sediments settle and collect at the bottom of the cylinder. As the larger particles settle out, the hydrometer reading reflects the change in density of the column of liquid.

At the completion of field data collection and data analysis, the soil map unit, infiltration rate over time, bulk density, particle distribution, texture class, and field moisture content for each site were measured and recorded.

## **Data Analysis**

A paired t-test assuming equal variance was used to determine if a statistical difference existed between the highly maintained and minimally maintained sites over a range of variables. The variables tested included infiltration rates, bulk density, moisture content, and percent of sand, silt, and clay. Microsoft Excel 2007 was used to expedite the calculation of the t-value for each variable pairing. Statistical significance was tested against a P-value of 0.05.

## **Results**

### **Bulk Density**

As hypothesized, the majority of the disturbed soils had greater bulk densities than the unmaintained sites (Table 4.5). This is likely a result of compaction during development/construction and during maintenance and/or as a result of vehicle traffic (e.g. parking for football games, tailgating). The two sites that were mapped as having soils in hydrologic soil group D (i.e., very low infiltration/high runoff potential soils) showed similar bulk densities between the maintained/unmaintained sites, although the maintained sites had a slightly numerically lower mean bulk density.

Using a paired t-test, the differences between the bulk densities of the highly maintained versus minimally maintained sites differed significantly ( $P > 0.05$ ). When the bulk density results for the two pairs of HSG D sites were removed from the dataset, a good relationship between the bulk density of the maintained sites and the unmaintained sites resulted when they were plotted against each other (Equation 11) with an  $R^2$  of 0.8121 (Figure 4.10). These data were plotted to

Table 4.5. Bulk density results for each pair of sampling locations.

Site Name	Level of Maintenance	Initial Moisture Content (m <sup>3</sup> /m <sup>3</sup> )	Bulk Density (g/cm <sup>3</sup> )
FHS	High	0.280	1.10
Leflar	Minimal	0.310	0.98
Maple Hill	High	0.340	1.19
Lewis Avenue	Minimal	0.306	0.94
Reynold's Center	High	0.308	1.29
Pratt Place	Minimal	0.302	1.05
SW Gardens	High	0.480	1.12
UA Chicken Farm	Minimal	0.290	1.15
Central Gardens	High	0.448	1.18
Mullins Creek South	Minimal	0.351	1.21
Lot 56B	High	0.290	1.43
Oakland-Zion	Minimal	0.269	1.32



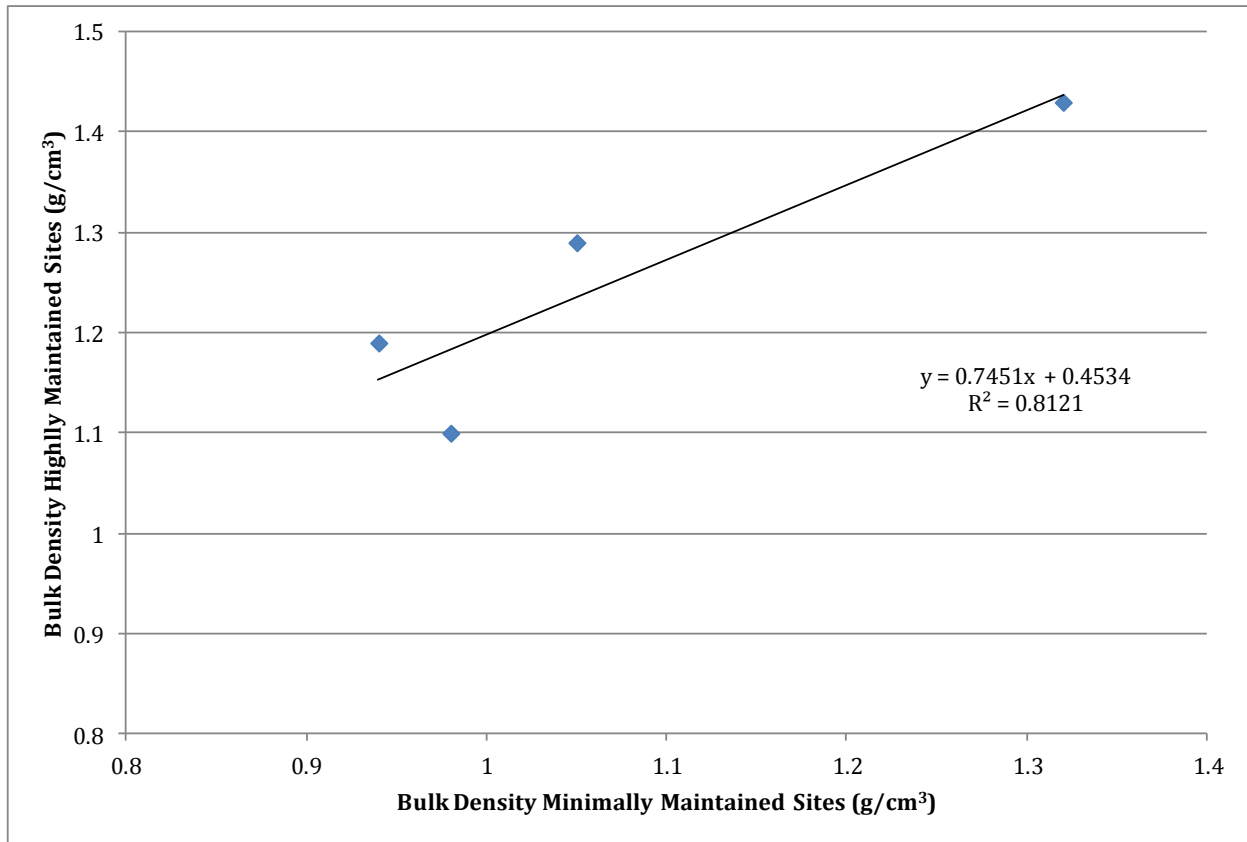


Figure 4.10. Graph of the bulk density of highly maintained pairs of sites versus the bulk density of minimally maintained sites excluding the results for the sites characterized as HSG D.

determine if a relationship between bulk density and infiltration rate could be determined for the catchment. More sampling would need to be done to determine if a good relationship exists, and how that relationship may change based on soil map unit and/or other soil characteristics.

$$\rho_{hm} = 0.745 * \rho_{mm} + 0.4534 \quad (11)$$

Where,  $\rho_{hm}$  = bulk density of the highly maintained site (g/cm<sup>3</sup>)  
 $\rho_{mm}$  = bulk density of the minimally maintained site (g/cm<sup>3</sup>)

### **Infiltration Rate/Moisture Content/Horton Parameters**

Because infiltration rate can be strongly affected by the moisture content of the soil, sampling at each pair of sites was performed on the same day, and moisture content was measured at multiple locations at each site. A paired t-test was performed on the average moisture content measurements between the minimally maintained and highly maintained sites. The differences between the moisture content datasets were not statistically significant ( $P < 0.05$ ) and it can be reasonably assumed that the moisture content did not have a significant effect on the infiltration test results measured in the field. The infiltration rates of the highly maintained sites were lower than the minimally maintained paired sites in each infiltration test (Table 4.6). In a paired t-test, the difference in infiltration rates (i.e., initial, final, and overall) between the highly maintained and minimally maintained sites were statistically significant ( $P > 0.05$ ).

When plotted against each other, a strong correlation did not exist ( $R^2 = 0.245$ ) between bulk density and infiltration rate, however, the trend matched the hypothesis that an increase in bulk density is related to a decrease in infiltration rate.

Table 4.6. Initial moisture content and infiltration results for all sites sampled. Pairs of sites are presented in succession.

Site Name	Level of Maintenance	Observed Overall Infiltration Rate (mm/hr)	Observed Initial Infiltration Rate (mm/hr)	Observed Final Infiltration Rate (mm/hr)	Observed Decay Constant (1/hr)
FHS	High	32.8	152.4	12.7	7.7
Leflar	Minimal	585.0	889.0	381.0	4.5
Maple Hill	High	14.5	81.3	5.1	7.0
Lewis Avenue	Minimal	437.9	762.0	342.9	4.6
Reynold's Center	High	15.5	76.2	5.1	5.9
Pratt Place	Minimal	109.7	203.2	88.9	4.7
SW Gardens	High	8.4	63.5	5.1	5.9
UA Chicken Farm	Minimal	20.3	88.9	7.6	4.7
Central Gardens	High	1.5	5.1	0.5	6.9
Mullins Creek South	Minimal	112.8	355.6	88.9	1.1
Lot 56B	High	42.7	88.9	30.5	6.1
Oakland-Zion	Minimal	270.5	457.2	203.2	4.7

## Particle-size Analysis/Color Analysis

A soil sample from each infiltration testing site was analyzed to determine the percent of sand, silt, and clay. Once the percentages were determined, it was possible to determine the soil texture class for the soil and compare the soil texture class of the mapped soil series (predicted) of the minimally maintained sites to the highly maintained sites (observed). The soil textural classes were determined by using the online soil texture class analyzer developed by the NRCS (NRCS 2014b), where values for percentages of each size class are plotted on a USDA Texture Triangle (Figure 4.11). While there were some differences in predicted and observed soil textures for the sites sampled (Table 4.7), none of the differences were statistically significant. Statistical analysis determined that there were not significant differences between the percents of silt, sand, and clay observed in the highly maintained samples versus the minimally maintained samples (Table 4.8). This was an unexpected result given the other observed differences between the minimally maintained and highly maintained sites.

Visual observations made during the particle-size analysis were recorded for the soil samples. One observation was that the highly maintained sites were more likely to have two distinct layers within the sample, the top layer was looser and had numerous plant roots, while the lower layer was more clay-like, appeared to be more compact and did not have as many roots (Figure 4.12a,b).

Other observations were made about the color of the samples once they were incorporated into the cylinders for analysis. Some of the pairs of sites were visibly different colors when suspended in the cylinders (Figure 4.13). A Munsell color classification was performed for each sample based on photographs taken of the samples in the sedimentation cylinders. Results of the Munsell color classification are presented in Table 4.9. The first two pairs of sites (samples 1 and 2, and 3 and 4), the minimally maintained site was darker in color than the highly maintained site. This can be indicative of a higher percent of organic matter which would be expected from

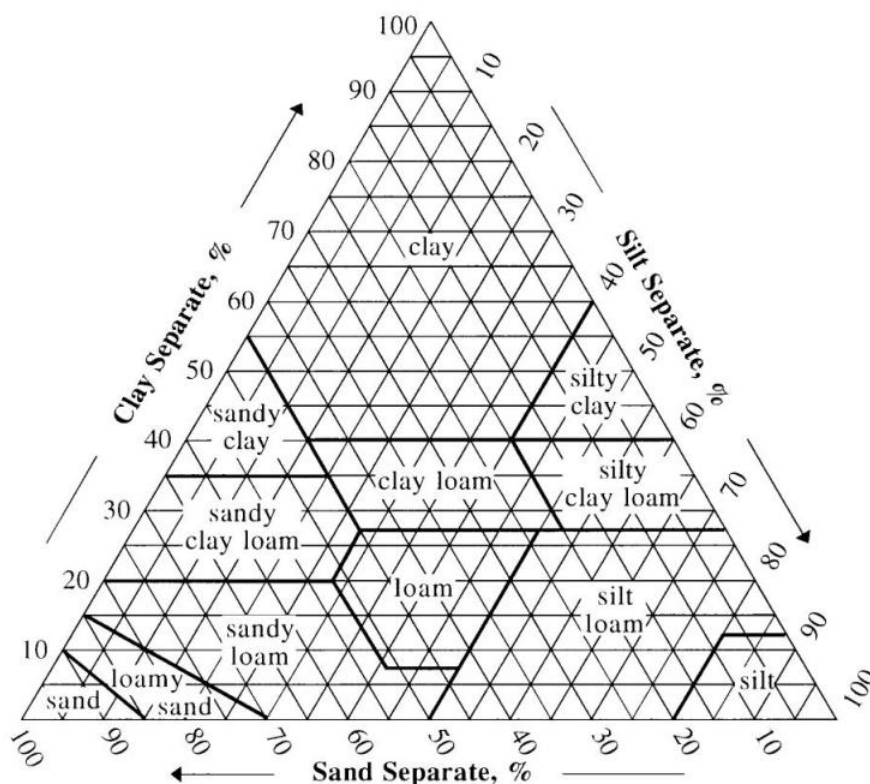


Figure 4.11. Texture triangle of AASHTO, USDA, and Unified Classification Systems (NRCS 2014c)

Table 4.7. Predicted and observed texture classes for Mullins Creek soils. Predicted texture classes were determined from soil series data sheets (NRCS 2014a). Observed texture classes were determined using the NRCS Soil Texture Calculator (NRCS 2014b).

Site Name	Soil Type	Predicted Texture Class	Observed Texture Class
FHS	ErE	Gravelly fine sandy loam	Loamy Fine Sand
Leflar	ErE	Gravelly fine sandy loam	Loam
Maple Hill	ErE	Gravelly fine sandy loam	Sandy Loam
Lewis Avenue	ErE	Gravelly fine sandy loam	Sandy Loam
Reynold's Center	FaC2	Fine sandy loam	Loam
Pratt Place	FaC2	Fine sandy loam	Loamy Fine Sand
SW Gardens	Le	Silt Loam	Sandy Loam
UA Chicken Farm	Le	Silt Loam	Loam
Central Gardens	Sn	Silty clay loam	Silt loam
Mullins Creek South	Sn	Silty clay loam	Loam
Lot 56B	SfC2	Fine sandy loam	Loam
Oakland-Zion	SfC2	Fine sandy loam	Sandy Loam

Table 4.8. Results from particle size analysis: percent sand, clay, and silt for each soil sample. The soil texture was calculated using the NRCS Soil Texture Calculator (NRCS, 2014b).

Soil Map Unit	Soil Sample	Site Name	% sand	% clay	% silt	NRCS Soil Texture Calculator
Enders-Allegheny	1	FHS	75.6	2.0	22.3	Loamy Fine Sand
Enders-Allegheny	2	Leflar	48.7	10.0	41.3	Loam
Enders-Allegheny	3	Maple Hill	56.6	16.0	27.3	Sandy Loam
Enders-Allegheny	4	Lewis Ave	53.7	8.0	38.3	Sandy Loam
Fayetteville	5	Reynold's Center	40.6	14.0	45.3	Loam
Fayetteville	6	Pratt Place	77.7	3.0	19.3	Loamy Fine Sand
Sloan	7	The Garden SW	60.3	7.0	32.7	Sandy Loam
Sloan	8	U of A Farm	39.3	13.0	47.7	Loam
Leaf	9	The Garden Central	39.0	10.0	51.0	Silt Loam
Leaf	10	Mullins Creek South	38.3	18.0	43.7	Loam
Savannah	11	Lot 56B	48.6	15.0	36.3	Loam
Savannah	12	Oakland-Zion	53.7	4.0	42.3	Sandy Loam















Figure 4.12. a) Bulk density core sample from The Garden SW field location. The top of the sample is to the right, and the lower layer is to the left. b) After the sample was initially broken up, netting was observed to be in the sample between the two layers of soil.



Figure 4.13. Photograph of sedimentation cylinders with incorporated samples. Each pair of cylinders (starting left to right) represents a pair of soils from the same soil type on the soils map, but one is from a highly maintained site, and one is from a minimally maintained site. Pairs 3-4, 5-6, and 7-8 were visibly different in color. The two most different (highlighted by the red rectangle) are sample 3, which is a wheat color, and sample 4 which is much darker.



Table 4.9. Munsell color classifications for saturated soil samples in the Mullins Creek catchment. R,G,B colors were extracted from photographs of samples in sedimentation cylinders taken in the laboratory and converted to Munsell colors.

Site No.	Site Name	Observed R,G,B			Color	Munsell Classification		
		R	G	B		R,G,B	Hue	Value
1	FHS	43	19	2		1.2R	1.0	3.4
2	Leflar	68	46	8		5.2Y	2.2	4.5
3	Maple Hill	138	91	29		1.5Y	3.8	5.5
4	Lewis Ave	55	30	2		3.7Y	1.4	3.1
5	Reynold's Center	126	79	19		2.4Y	3.8	6.5
6	Pratt Place	106	52	7		6.7YR	2.7	6.7
7	The Garden SW	92	58	15		8.8YR	2.5	4.7
8	U of A Farm	120	81	26		1.5Y	3.8	5.5
9	The Garden Central	128	83	30		1.5Y	3.8	5.5
10	Mullins Creek South	126	82	28		1.5Y	3.8	5.5
11	Lot 56B	111	76	24		7.5YR	3.4	6.8
12	Oakland-Zion	124	77	19		2.4Y	3.8	6.5

minimally maintained, especially forested, sites. The differences in color for the two samples may have also meant that the origins of each soil were different even though they were from the same soil map unit. It was possible that the top soil of the highly maintained sites was not native to the area.

## **Discussion**

There can be several issues with using an infiltration method to predict infiltration and runoff in a hydrologic model without collecting ground-reference data in the field. One issue is that the actual soil present at a developed site may not be the same soil as identified using the soil map. Native soils commonly have the top soil stripped during development/construction and may be replaced by non-native soils, and are commonly compacted (both intentionally and unintentionally) by construction equipment (Figure 4.14). Even if the location has not been stripped and cleared for development, if it is located near a construction site, it is possible that the soil surface has been compacted by heavy equipment traffic and may not behave as an undisturbed native soil would. The highly maintained sites in this study were located very near to multiple buildings and other structures (Figure 4.15). It is highly unlikely that a disturbed soil will exhibit the same characteristics as the mapped soil unit. It may have a lower infiltration capacity and greater bulk density, and may behave as if it belongs to a more water-movement-restrictive hydrologic soil group (i.e., HSG D vs. B).

While the collection of ground-reference data can be time intensive, some fairly simple sampling and testing can result in more accurate runoff predictions than using mapped information alone. Using characteristics of soil map units, especially in developed areas, can result in overestimation of infiltration and an underestimation of runoff from a given catchment. Changes to the soil infiltration characteristics are associated with development and construction of a site. Compaction, removal of native soil and replacement with non-native soil, frequent management



Figure 4.14. Example of a construction site near the Lot 56B infiltration sampling site. Topsoil has been removed and non-native soils have been introduced to the site and compacted.

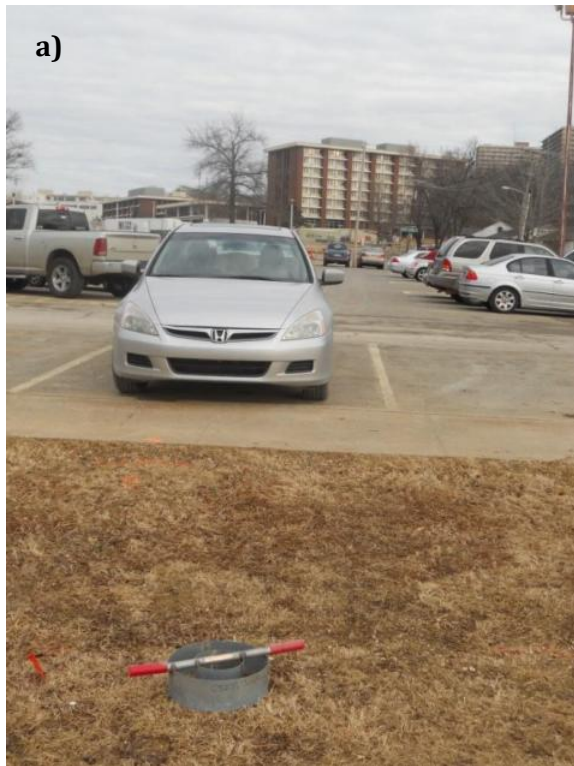


Figure 4.15. Photograph of a highly maintained site (South Lot 56B) on the University of Arkansas campus. a) Facing north toward a parking lot and dormitory, and b) facing south toward the Lady Razorbacks Softball Stadium.

that continues to compact the soil, all affect the infiltration potential and structure/behavior of the native soil. Ignoring the changes in pervious surface infiltration capacity post-development can also lead to inaccurate predictions of effects of development for watershed management and planning purposes, and an underestimation of runoff prediction in flood forecasting. This would potentially make the use of infiltration parameters associated with a soil map unit in a hydrologic model inaccurate.

Since a statistically significant difference in infiltration rates existed between the highly maintained and the minimally maintained site for the same soil map unit, it is believed that more accurate hydrologic modeling results would be obtained if these differences were taken into account in the infiltration component of the model. To test the difference in the modeling results, and the sensitivity of the model to changes in infiltration parameters, the results from the infiltration tests for the highly maintained sites were used to parameterize the Horton Infiltration module in the EPA's Storm Water Management Model (SWMM). Figure 4.16 shows an example of a graph of observed infiltration rate data, and the Horton infiltration curve that was developed for the Maple Hill testing site. Initial and final infiltration rates ( $f_o$  and  $f_c$  respectively), and the decay constant ( $k$ ) were all calculated from the observed infiltration data collected in the field. Figures for of observed infiltration curves for the remainder of the field sites are presented in Appendix A. Complete results for each site are presented in Appendix A. Results from the model runs are presented in Chapter 6 and Chapter 7.

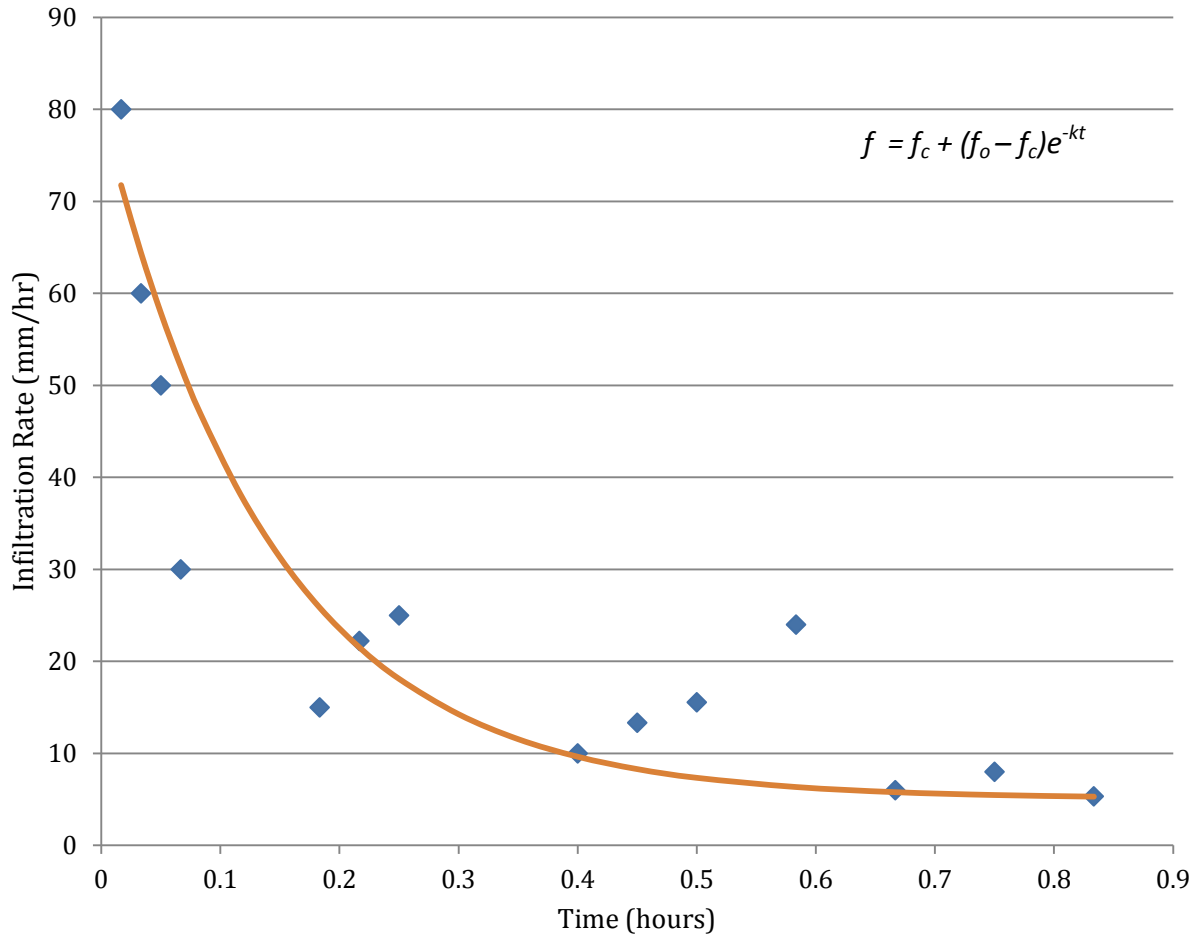


Figure 4.16. Example of predicting Horton Infiltration parameters from observed data. The points are observed infiltration rates during the test, and the line is a best-fit Horton infiltration curve. In this example,  $f_c = 5.1$  mm/hr,  $f_o = 80.0$  mm/hr, and  $k = 7.0$  1/hr

## **Chapter 5. Storm Water Management Model (SWMM) Parameterization**

### **Introduction**

An Environmental Protection Agency (EPA) Storm Water Management Model (SWMM) was developed to predict the hydrologic (rainfall/runoff) response of the Mullins Creek catchment. Two primary parameters were of interest for this study: infiltration, and impervious surface coverage.

Initially, the model had to be parameterized to reflect what was known/observed about the existing catchment. These parameters included the physical characteristics of the subcatchments including drainage area, width, hydraulic length, and slope. Land use land cover (LULC) datasets including the percent of total impervious area (TIA), directly-connected impervious area (DCIA), and the characteristics of the pervious areas were also necessary for accurately parameterizing the model. Information on the soil map units in each subcatchment helped with determining infiltration potential of pervious surfaces. Finally, the drainage efficiency, how quickly water is drained from the catchment, was characterized using the stormwater drainage network information from the City of Fayetteville and the University of Arkansas. Much of the data collected on the stormwater drainage network on the University of Arkansas campus including invert/rim elevations, pipe characteristics, diameter of conduits , etc. were collected and presented by Koehn, et al. (2011). Cross-section data for the main Mullins Creek channel pre-2012 restoration were obtained from Van Eps (Personal Communication, 13 December 2013), and McCoy (Personal Communication, 27 January 2014).

### **Physical Subcatchment Characteristics**

To determine the physical characteristics of each subcatchment as required by SWMM, the Mullins Creek catchment was delineated into 49 subcatchments based on the surface hydrology as defined by the digital elevation model (DEM; ASLIB, 2007), and flow accumulation estimates. The digital elevation model (DEM) downloaded and used for the hydrologic analysis was produced by

the Arkansas State Land Information Board (ASLIB) and the Arkansas Geographic Information Office (AGIO) as a part of the 2006 Arkansas Digital Orthophotography Program. The data collected to develop the DEM was acquired between 15 January 2006 and 31 March 2006. When selecting a DEM, a higher spatial resolution dataset was preferred because of the potential of obtaining more accurate results than for lower spatial resolution products (Teegavarapu, et al., 2006). The spatial resolution of the DEM was also the spatial resolution of the data layers that were subsequently extracted for the subcatchment making a higher spatial resolution more desirable. After each subcatchment was delineated, the resulting area was used as a mask in ArcGIS to extract necessary information (i.e. percent imperviousness, soil map unit, etc.). Lower spatial resolution DEMs were available for download from the United States Geological Survey (USGS) (1/3 arc-sec and 1 arc-sec, which are approximately 10 m and 30 m resolution respectively), but the units were angular which does not allow for using a mask (in linear units) to extract data.

For each tributary, an outlet point was selected, generally where the channel flowed into another channel, or at a confluence between two channels. This outlet point is known as a pour point in ArcGIS. The DEM that was used in this analysis was derived from LIDAR data, and is a raster dataset where each pixel is assigned an elevation value (ASLIB, 2007). A series of tools/processes are run on the DEM in ArcGIS (ESRI, 2014) to extract desired hydrologic information about a catchment. The first step is to determine the flow direction for each pixel in the DEM. The direction that a drop of water will flow from a pixel of interest is determined by analyzing the surrounding pixels (Figure 5.1). Once the flow direction is determined for each pixel in the dataset, the flow accumulation tool can be run. The flow accumulation tool determines how many pixels will cumulatively flow to each pixel in the catchment based on the results from the flow direction layer (Figure 5.2).

The flow accumulation layer is displayed as a gradient where the “brighter” a pixel is, closer to white (RGB: 255,255,255), the greater the number of pixels draining to that point (Figure 5.3). In



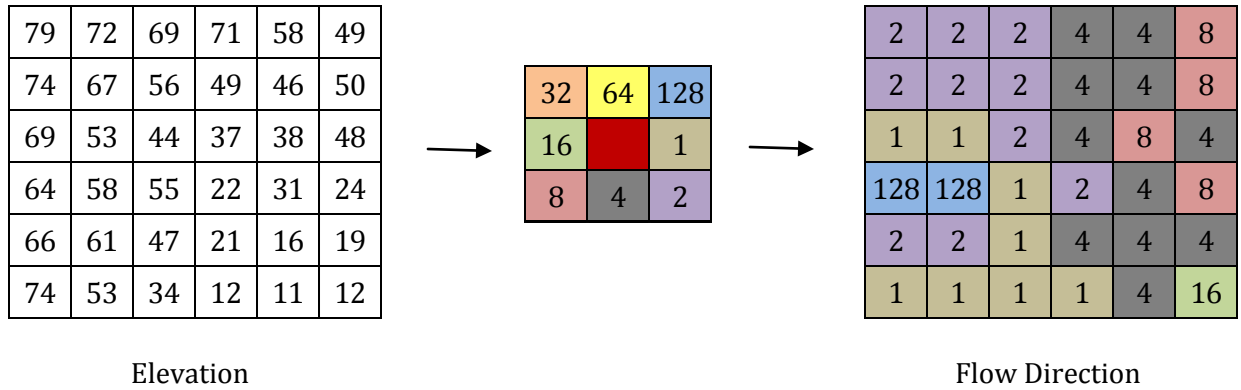


Figure 5.1. Example of a raster digital elevation model (DEM) grid that is converted from elevation data to flow direction. The grid in the middle shows the value assigned each pixel based on the direction water would flow from the pixel based on elevation data (adapted from ESRI, 2008).

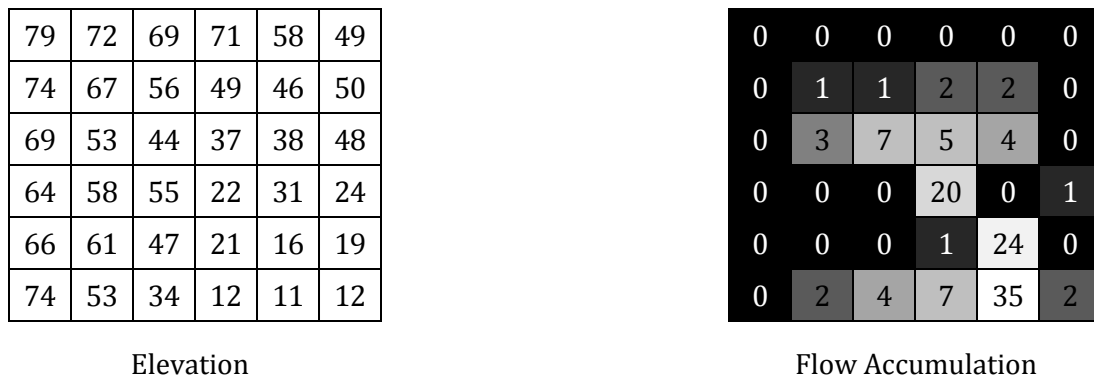


Figure 5.2. Sample flow accumulation layer that results from the Elevation layer to the left after flow direction is calculated for each pixel. The lighter the pixels, the more pixels flow to that point (adapted from ESRI, 2008). Note that the pixel with the lowest elevation in the figure on the left is 11. This is the same pixel in the graphic to the right that has the greatest flow accumulation value.

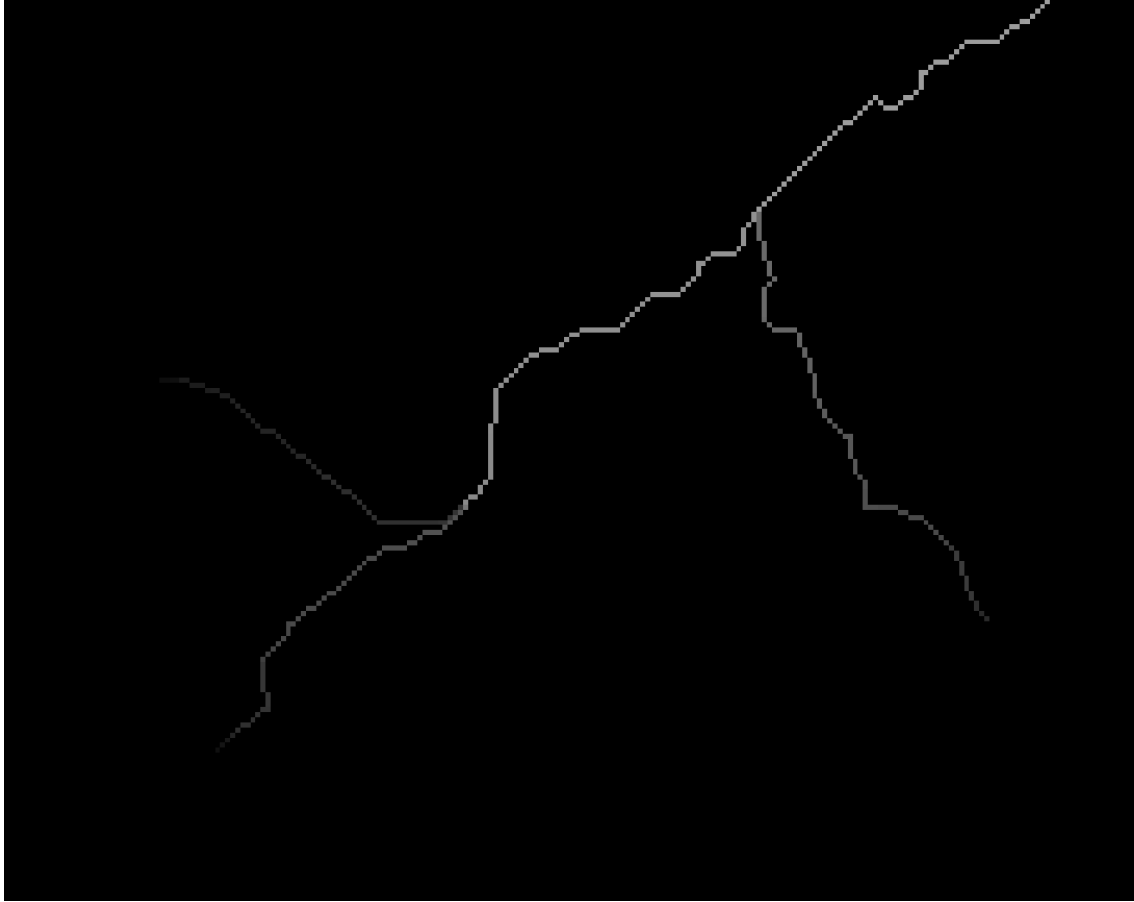


Figure 5.3. Example of a flow accumulation layer from ArcGIS. The brighter the pixel, the higher the flow accumulation value. The tributaries and headwater streams are lighter in color than the main branches of the system.

the figure, the drainage network can be observed with the pixels getting brighter as the waterways increase in drainage area and more pixels flow downstream.

A pour point must be selected for each subcatchment of interest. The catchment can then be delineated in ArcGIS using the watershed tool which delineates the catchment by including each pixel that ultimately drains to the selected outlet point. After each subcatchment has been delineated, the subcatchment layer can then be used as a “mask” in ArcGIS to extract individual datasets from layers that can then be used to describe that catchment. The subcatchment masks in ArcGIS were used to extract data from the LULC, percent impervious, soil map unit, and DEM layers.

Physical characteristics of the catchments that were needed to parameterize the SWMM model included drainage area, hydraulic length (the longest distance a drop of water would travel through the catchment to the outlet), width (drainage area divided by hydraulic length), and slope. The drainage area was calculated from each subcatchment as it was delineated in ArcGIS. After the subcatchment was delineated, the total number of pixels that made up each subcatchment, the “count,” were listed in the attribute table for the layer. The dimensions of each pixel were then multiplied by the count to obtain an area for the subcatchment. The length tool was used to determine/measure the hydraulic length of the subcatchment. The width was a parameter used by SWMM to determine the approximate dimensions of the catchment, and is commonly used as a calibration parameter by the model. Subcatchment width is calculated by dividing the drainage area by the hydraulic length of the catchment. The slope was determined by dividing the difference between the maximum and minimum elevation for each subcatchment by the hydraulic length. Physical parameters for each subcatchment are presented in Table 5.1. The geoprocessing model for delineating subcatchments in ArcGIS is presented in Figure 5.4.

Table 5.1. Physical parameters extracted for each subcatchment in ArcGIS to be used as inputs to the SWMM model.

Subcatchment	Drainage Area (ha)	Hydraulic Length (m)	Width (m)	Slope (%)
SA1a	4.86	411.2	118.2	5.2
SA1b	2.84	430.3	66.0	5.0
SA1	4.09	179.6	227.7	7.1
SA2	1.39	44.6	311.8	10.1
SA3	0.55	150.7	36.5	2.5
SA4	3.76	370.4	101.5	7.8
SA5	3.95	361.7	109.2	9.6
SA6	6.34	634.0	100.0	6.4
SA7,8,11,12	1.25	150.1	83.3	6.5
SA9	4.74	353.5	134.1	12.1
SA10	6.03	437.9	137.7	11.0
SA13	3.9	388.1	100.5	9.9
SA14,16	1.83	156.0	117.3	4.0
SA15	2.54	369.7	68.7	11.6
SA17	3.49	461.6	75.6	10.0
SA18	1.56	56.3	277.1	3.2
SA19	4.15	538.3	77.1	9.3
SA20	2.87	180.1	159.4	2.5
SA21,22	3.63	352.4	103.0	13.4
SA23	4.47	692.0	64.6	5.3
SA24	1.48	188.8	78.4	1.5
SB1	12.08	600.4	201.2	8.1
SB2	8.72	539.6	161.6	7.9
SB3	4.26	560.5	76	8.8
SB4	7.93	269.9	293.8	5.1
SB5	4.31	549.0	78.5	8.6
SB6	6.68	230.7	289.5	2.2
SB7	4.74	318.3	148.9	1.3

Table 5.1. cont.

Subcatchment	Drainage Area (ha)	Hydraulic Length (m)	Width (m)	Slope (%)
SC1	7.04	583.7	120.6	6.9
SC2	12.38	841.6	147.1	7.7
SC3	7.33	704.8	104.0	8.8
SC4	5.86	715.5	81.9	8.8
SC5	1.38	106.9	129.1	0.8
SC6	7.39	336.4	219.7	1.2
SC7	4.44	360.7	123.1	4.3
SC8	0.80	135.6	59.0	2.0
SC9	2.94	369.3	79.6	1.4
SC10	6.02	250.4	240.4	0.9
SC11	6.11	88.3	692.0	1.4
SD1	5.68	543.5	104.5	8.7
SD2	2.79	261.2	106.8	10.0
SD3	2.53	239.1	105.8	12.7
SD4	3.04	470.0	64.7	0.9
SD5	1.40	348.3	40.2	9.5
SD6	5.27	208.2	253.1	0.8
SD7	3.87	744.0	52.0	15.7
SD8	6.83	283.5	240.9	1.1
SD10	7.56	452.4	167.1	1.2
SD11	3.71	284.0	130.6	0.9

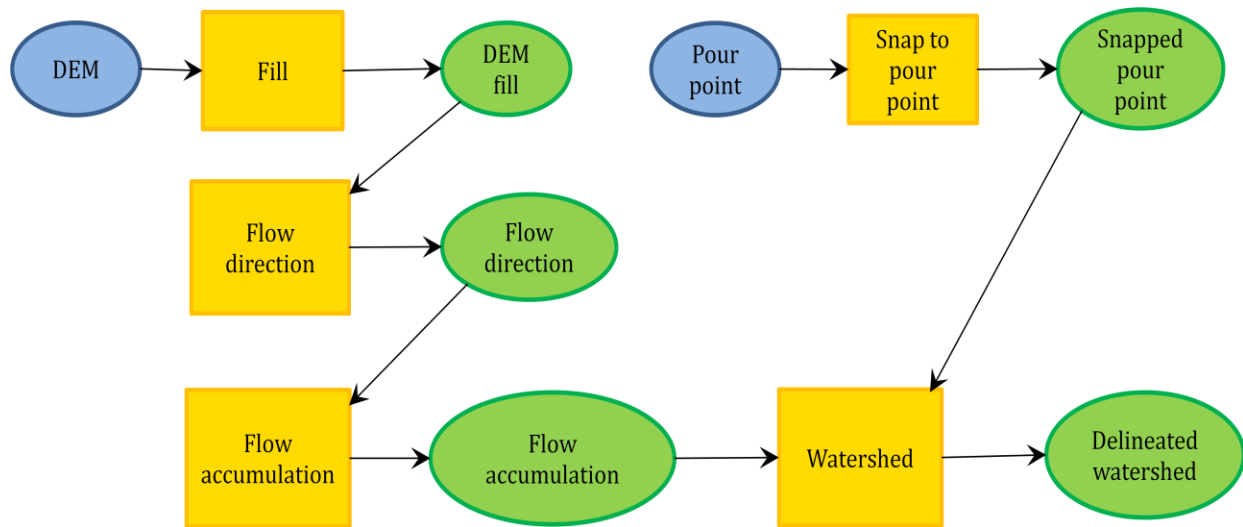


Figure 5.4. Geoprocessing model for delineating subcatchments in ArcGIS. The blue ovals represent data inputs, the yellow rectangles are processes, and the green ovals are process outputs.

## **Land Use/Land Cover (LULC) and Percent Impervious Surface**

The LULC and percent impervious surface were determined by extracting the data for each subcatchment and then analyzing the attribute table results for the extracted layer. The percent of total impervious area (TIA) was calculated for each subcatchment using the 2010 Percent Impervious raster layer (Gorham, 2012a). The percent TIA for each subcatchment is presented in Table 5.2. Subcatchment A had the greatest percent of TIA at almost 68% while subcatchment D had the lowest at just over 25%. Even at 25% TIA, the system was expected to show instability in response to the land use in the catchment. The percentages of each LULC category in each subcatchment are presented in Table 5.3. The same trend appeared for the LULC categories for the subcatchments as for the percent TIA. Subcatchment A was 73.0 % high intensity urban LULC. More information for parameterizing the model was needed regarding the makeup of the high intensity urban and low intensity urban categories. Pixels characterized as high intensity and low intensity urban were analyzed (as described in Chapter 3) to determine percent grass, percent forest/woodland, and percent impervious surface coverage. The percent impervious surface coverage was further delineated into rooftop, and driveway/parking lots to better estimate directly connected impervious area (DCIA) in each subcatchment. An example of the geoprocessing model used to extract data from LULC, percent impervious surface, and soil map unit datasets is presented in Figure 5.5.

The soil maps units for each subcatchment were also extracted, and percentages of soils in each hydrologic soil group for each subcatchment were determined along with soil texture. For more information on hydrologic soil groups, see Chapter 2.

## **Subcatchment Infiltration Parameters**

The Horton infiltration method was selected as the preferred infiltration method in SWMM because the values can be readily measured in the field. Because these values, initial infiltration rate

Table 5.2. Percent impervious surface in each Mullins Creek subcatchment from Gorham (2012a), percent Total Impervious Area (TIA) calculated from extracted data.

Subcatchment	100% Pervious	75% Pervious	50% Pervious/ 50% Impervious	75% Impervious	100% Impervious	%TIA
A1a	28.8	22.5	10.1	9.6	29.0	46.9
A1b	4.1	7.6	14.1	24.8	49.5	77.0
A1	19.7	17.0	11.6	15.2	36.6	58.0
A2	29.2	22.7	7.4	9.0	31.6	47.7
A3	18.8	22.2	12.4	13.9	32.6	54.8
A4	2.6	9.0	8.5	14.0	65.9	82.9
A5	9.6	18.6	8.5	11.2	52.1	69.4
A6	5.4	9.5	7.4	29.9	47.8	76.3
A7	7.0	13.0	7.8	22.7	49.5	73.6
A8	14.9	19.0	11.4	13.6	41.0	61.7
A9	14.1	17.5	8.5	7.0	53.0	66.8
A10	30.0	18.8	8.2	9.4	33.6	49.4
A11	23.0	18.2	8.3	8.3	42.2	57.1
A12	11.7	16.5	9.9	16.8	45.2	66.8
A13	8.4	11.9	5.4	11.3	62.9	77.1
A14	14.5	16.6	9.3	14.2	45.4	64.8
A15	9.6	9.2	8.0	16.2	57.1	75.5
A16	14.0	16.1	8.9	13.8	47.2	66.0
A17	5.7	10.3	10.8	18.4	54.8	76.5
A18	13.8	15.6	8.7	13.6	48.3	66.7
A19	12.9	14.8	8.7	14.1	49.5	68.1
A20	0.3	1.9	5.9	11.7	80.2	92.4
A21	6.8	10.4	9.1	27.0	46.7	74.1
A22	11.8	14.6	8.9	14.5	50.2	69.2
A23	3.5	11.2	8.3	14.6	62.3	80.3
A24	0.0	20.9	24.5	25.0	29.7	65.9
Average	12.3	14.8	9.6	15.4	47.8	67.9

Subcatchment	100% Pervious	75% Pervious	50% Pervious/ 50% Impervious	75% Impervious	100% Impervious	%TIA
B1	80.5	9.2	1.0	0.8	8.5	11.9
B2	71.0	16.6	2.5	1.7	8.2	14.9
B3	52.7	19.5	5.6	5.2	17.0	28.5
B4	74.3	11.3	2.1	2.1	10.1	15.6
B5	43.4	21.8	7.1	6.8	20.8	34.9
B6	54.9	23.0	5.7	3.5	12.8	24.1
B7	32.0	17.3	7.8	7.3	35.7	49.4
Average	58.4	17.0	4.5	3.9	16.2	25.6



Table 5.2. cont.

Subcatchment	100% Pervious	75% Pervious	50% Pervious/ 50% Impervious	75% Impervious	100% Impervious	%TIA
C1	39.2	22.1	9.0	9.0	20.6	37.4
C2	47.0	8.0	2.9	29.6	12.5	38.2
C3	42.8	15.9	6.4	6.9	28.0	40.3
C4	53.7	10.4	3.7	11.6	20.7	33.8
C5	59.0	16.7	5.4	3.1	15.8	25.0
C6	30.0	6.6	4.6	9.4	49.4	60.4
C7	2.3	7.6	4.7	16.3	69.1	85.6
C8	4.7	20.2	11.5	21.5	42.1	69.0
C9	22.7	9.5	6.2	33.1	28.4	58.8
C10	23.6	3.6	5.9	24.3	42.6	64.7
C11	44.4	8.7	4.6	22.0	20.4	41.3
Average	33.6	11.8	5.9	17.0	31.8	50.4

Subcatchment	100% Pervious	75% Pervious	50% Pervious/ 50% Impervious	75% Impervious	100% Impervious	%TIA
D1	31.0	11.1	7.5	17.1	33.3	52.6
D2	24.9	15.8	11.6	22.2	25.6	52.0
D3	31.1	15.8	12.8	21.8	18.5	45.2
D4	59.6	17.1	7.1	7.6	8.5	22.1
D4d	36.1	14.1	8.5	16.4	24.9	45.0
D4u	27.9	13.0	9.0	19.5	30.6	53.0
D5	32.9	23.6	12.5	11.8	19.1	40.2
D6	26.3	19.2	12.3	18.7	23.4	48.4
D7	6.1	10.1	15.6	41.5	26.7	68.2
D8	24.8	22.6	7.8	19.1	25.7	49.6
D10	25.3	13.0	11.7	20.0	30.1	54.1
D11	25.2	28.4	9.5	18.7	18.2	44.1
Average	29.3	17.0	10.5	19.5	23.7	47.9

Table 5.3. Land use land cover (LULC) categories for each subcatchment used in the SWMM model. Extracted from 2010 LULC layer (Gorham, 2012b).

2010 Mullins Creek LULC Categories (percent)					
Subcatchment	Roads	Grass	Forest	Low Intensity Urban	High Intensity Urban
A1a	13.2	0.0	0.0	67.0	19.8
A1b	5.5	0.0	0.0	10.4	84.1
A1	4.3	0.0	0.0	59.7	36.0
A2	19.7	0.0	0.0	68.8	11.6
A3	10.9	0.0	0.0	6.4	82.7
A4	12.8	0.0	0.0	2.9	84.3
A5	6.8	0.0	0.0	0.0	93.2
A6	11.1	0.0	0.0	40.2	48.7
A7	0.0	0.0	0.0	0.0	100.0
A8	0.0	0.0	0.0	0.0	100.0
A9	9.5	0.0	0.0	36.1	54.4
A10	14.8	0.0	0.0	62.8	22.3
A11	0.5	0.0	0.0	0.0	99.5
A12	0.0	0.0	0.0	0.0	100.0
A13	6.3	0.0	0.0	0.0	93.7
A14	0.0	0.0	0.0	0.0	100.0
A15	19.3	0.0	0.0	41.1	39.6
A16	0.6	0.0	0.0	0.0	99.4
A17	8.7	0.0	0.0	0.3	91.0
A18	5.5	0.0	0.0	13.8	80.7
A19	11.6	0.0	0.0	0.8	87.6
A20	8.9	0.0	0.0	0.0	91.1
A21	7.4	0.0	0.0	17.5	75.1
A22	3.8	0.0	0.0	0.0	96.2
A23	17.7	0.0	0.0	35.8	46.6
A24	0.0	0.0	0.0	39.5	60.5
Average	7.7	0.0	0.0	19.3	73.0

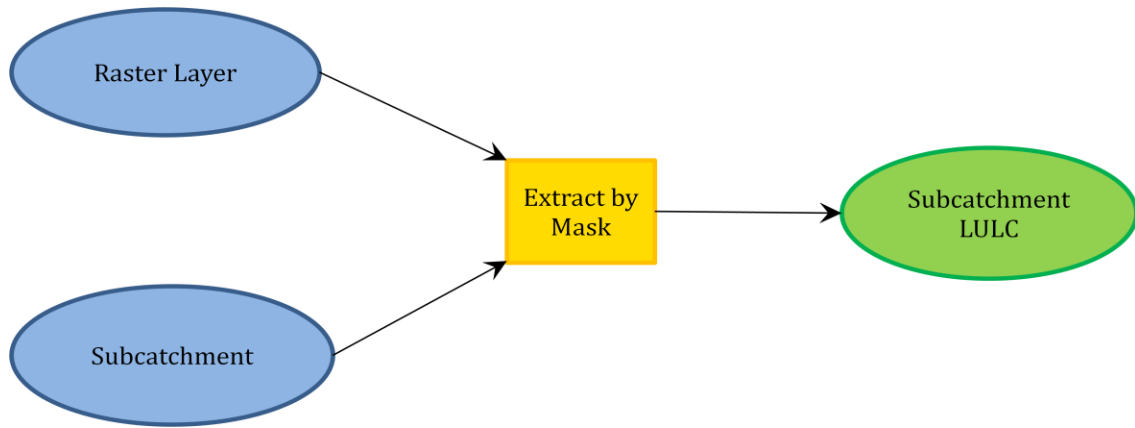


Figure 5.5. Geoprocessing model for extracting raster data, for example from a land use/land cover dataset, using a subcatchment as a mask. The blue ovals represent data inputs, the yellow rectangles are processes, and the green ovals are process outputs.

( $f_o$ ), final infiltration rate ( $f_c$ ), and decay constant ( $k$ ), are determined empirically, and can vary greatly between sites, it is difficult to locate “characteristic” values in the literature. Infiltration characteristics of soils in the Mullins Creek catchment were measured and described in detail in Chapter 4. To examine the effects of using predicted versus observed infiltration values for different soil map units under different LULC conditions on the hydrologic response of the catchment, the SWMM model was run multiple times with all parameters held constant except for the Horton infiltration parameters. To determine the appropriate Horton infiltration parameters for each soil map unit, each soil map unit was categorized by texture class, in this case, silt loam or sandy loam, and then by hydrologic soil group (B, C, or D). Silt loams tend to have lower infiltration rates than sandy loams, and hydrologic soil groups were categorized as B, C, or D in order of decreasing infiltration potential. Ultimately, the soil map units were divided into two categories: sandy loam and silt loam + HSG D. One of the soil map units, while categorized as a sandy loam, was categorized as HSG D because of other variables and was deemed to have low infiltration/high runoff potential. Table 5.4 presents the predicted and observed Horton Infiltration parameters used for each category of soil: sandy loam (highly maintained and minimally maintained LULC), and silt loam + HSG D (highly maintained and minimally maintained LULC).

In the first SWMM model run, the assumption with regard to infiltration was that all soil map units in pervious areas behaved as undisturbed soils. Values used to populate the model were in the maximum range recommended in the SWMM User’s Manual (Rossman, 2010) and were pulled from Terstreip and Stall (1974) for silt loam and sandy loam soil textures under turfgrass land cover.

Field measurements/data were collected to determine Horton infiltration parameters that represented conditions in the catchment. Minimally maintained sites in selected soil map units were paired with highly maintained sites (generally frequently mowed turfgrass cover). Infiltration rates were measured using a double-ring infiltrometer, moisture contents were measured, and bulk

Table 5.4. Observed and predicted Horton infiltration parameters used to determine the infiltration characteristics of each subcatchment in SWMM. The values used for the minimally maintained sites were from values published by Terstreip and Stall (1974). The values used for the highly maintained sites were from observed field data in the catchment.

Soil Texture	Pervious Surface Maintenance	$f_o$ (mm/hr)	$f_c$ (mm/hr)	$k$ (1/hr)
Sandy Loam	Minimally maintained	254.0	25.4	2.0
Sandy Loam	Highly maintained	101.6	12.7	6.9
Silt Loam + HSG D	Minimally maintained	203.2	12.7	2.0
Silt Loam + HSG D	Highly maintained	38.1	2.5	4.6

density samples were collected and dried. Bulk density samples were also analyzed to determine soil texture for each location (% sand, % silt, % clay). For more information on infiltration data collection and results, please see Chapter 4.

The same initial infiltration rate, final infiltration rate, and decay constants were used for minimally maintained pervious areas of each catchment, but new values were determined for highly maintained areas of each catchment using empirical data from field measurements/analysis. Both infiltration scenarios were run using actual storm event data, and compared to observed runoff data to determine if an increase in accuracy of the storm prediction was achieved using observed vs. predicted infiltration data. Table 5.5 presents the Horton infiltration parameters for each subcatchment based on texture, HSG, and LULC characteristics.

### **Impervious Surface**

Two different scenarios were also compared with regard to impervious surface coverage. (Results from these simulations were presented in Chapter 7.) Using the infiltration data collected in the field to populate the Horton Infiltration parameters, two different values were used for percent impervious area as defined by the model. Initially, percent impervious area was set to equal the percent of directly connected impervious area (DCIA) based on the type of impervious area: rooftop, driveway/parking lot and road. The percent DCIA for each impervious surface category was adapted from the relationships developed by Lee and Heaney (2003). Roads were categorized as 89.2% DCIA, parking lots and driveways were categorized as 61.6% DCIA, and rooftops were categorized as 67.0% DCIA. Larger values were selected in favor of lower values because most of the driveways identified in this catchment were for campus buildings where extensive stormwater drainage networks exist to drain them as opposed to residential driveways. The same was true for rooftops of campus buildings. Land use/land cover categories including more detailed analysis of the high intensity and low intensity urban layers are presented in Table 5.6 including an estimated

Table 5.5. Predicted and observed Horton infiltration parameter inputs into SWMM using soil texture and observed field data.

Subcatchment	Soil Texture/Infiltration Category		Horton Parameters (Predicted)			Horton Parameters (Observed)		
	% sandy loam	% silt loam + HSG D	$f_o$ (mm/hr)	$f_c$ (mm/hr)	$k$ (1/hr)	$f_o$ (mm/hr)	$f_c$ (mm/hr)	$k$ (1/hr)
A1a	100.0	0.0	254.0	25.4	2.0	131.3	15.2	5.9
A1b	100.0	0.0	254.0	25.4	2.0	108.3	13.3	6.7
A1	100.0	0.0	254.0	25.4	2.0	127.6	14.9	6.1
A1d	100.0	0.0	254.0	25.4	2.0	125.3	14.7	6.1
A1u	100.0	0.0	254.0	25.4	2.0	124.0	14.6	6.2
A2	100.0	0.0	254.0	25.4	2.0	133.0	15.3	5.9
A3	100.0	0.0	254.0	25.4	2.0	106.4	13.1	6.7
A3d	100.0	0.0	254.0	25.4	2.0	125.5	14.7	6.1
A3u	100.0	0.0	254.0	25.4	2.0	126.1	14.7	6.1
A4	100.0	0.0	254.0	25.4	2.0	104.5	12.9	6.8
A5	100.0	0.0	254.0	25.4	2.0	102.8	12.8	6.9
A6	100.0	0.0	254.0	25.4	2.0	121.9	14.4	6.2
A7,8,11,12	100.0	0.0	254.0	25.4	2.0	102.8	12.8	6.9
A9	100.0	0.0	254.0	25.4	2.0	120.1	14.2	6.3
A10	100.0	0.0	254.0	25.4	2.0	130.3	15.1	6.0
A13	100.0	0.0	254.0	25.4	2.0	102.8	12.8	6.9
A14,16	96.6	3.4	252.3	25.0	2.0	100.6	12.4	6.8
A15	99.1	0.9	253.5	25.3	2.0	122.8	14.4	6.2
A17	97.6	2.4	252.8	25.1	2.0	101.4	12.6	6.8
A18	71.9	28.1	239.7	21.8	2.0	92.3	10.5	6.0
A19	100.0	0.0	254.0	25.4	2.0	103.2	12.8	6.8
A20	60.9	39.1	234.1	20.4	2.0	77.9	8.8	6.0
A21,22	93.9	6.1	250.9	24.6	2.0	104.1	12.6	6.6
A23	68.3	31.7	237.9	21.4	2.0	101.4	11.0	5.6
A24	44.7	55.3	225.9	18.4	2.0	86.0	8.5	5.2
Average	93.3	6.7	250.6	24.6	2.0	111.3	13.2	6.3
B1	100.0	0.0	254.0	25.4	2.0	187.5	19.9	4.1
B2	100.0	0.0	254.0	25.4	2.0	137.1	15.7	5.8
B3	100.0	0.0	254.0	25.4	2.0	136.7	15.6	5.8
B4	100.0	0.0	254.0	25.4	2.0	137.0	15.7	5.8
B5	84.6	15.4	246.2	23.4	2.0	127.3	14.0	5.5
B6	87.6	12.4	247.7	23.8	2.0	129.5	14.3	5.5
B7	32.7	67.3	219.8	16.9	2.0	110.3	9.4	4.3
Average	86.4	13.6	247.1	23.7	2.0	137.9	14.9	5.3

Table 5.5. cont.

Subcatchment	Soil Texture/Infiltration Category		Horton Parameters (Predicted)			Horton Parameters (Observed)		
	% sandy loam	% silt loam + HSG D	$f_o$ (mm/hr)	$f_c$ (mm/hr)	$k$ (1/hr)	$f_o$ (mm/hr)	$f_c$ (mm/hr)	$k$ (1/hr)
C1	85.4	14.6	246.6	23.5	2.0	126.2	13.9	5.6
C2	92.5	7.5	250.2	24.4	2.0	132.2	14.8	5.6
C3	39.8	60.2	223.4	17.8	2.0	88.4	8.3	5.0
C4	51.1	48.9	229.1	19.2	2.0	92.4	9.3	5.3
C5	0.0	100.0	203.2	12.7	2.0	47.3	3.1	4.5
C6	14.8	85.2	210.7	14.6	2.0	58.2	4.7	4.7
C7	82.1	17.9	244.9	23.1	2.0	98.2	11.5	6.3
C8	29.5	70.5	218.2	16.5	2.0	57.9	5.6	5.3
C9	0.0	100.0	203.2	12.7	2.0	69.1	4.5	4.1
C10	24.0	76.0	215.4	15.7	2.0	116.9	9.2	3.9
C11	41.5	58.5	224.3	18.0	2.0	115.4	10.3	4.4
Average	41.9	58.1	224.5	18.0	2.0	91.1	8.7	5.0
D1	100.0	0.0	254.0	25.4	2.0	122.4	14.4	6.2
D2	100.0	0.0	254.0	25.4	2.0	122.7	14.5	6.2
D3	100.0	0.0	254.0	25.4	2.0	134.6	15.5	5.8
D4	100.0	0.0	254.0	25.4	2.0	135.7	15.5	5.8
D5	100.0	0.0	254.0	25.4	2.0	133.2	15.3	5.9
D6	100.0	0.0	254.0	25.4	2.0	133.2	15.3	5.9
D7	78.4	21.6	243.0	22.7	2.0	102.2	11.6	6.0
D8	97.3	2.7	252.6	25.1	2.0	125.8	14.6	6.0
D10	26.7	73.3	216.8	16.1	2.0	84.2	7.2	4.6
D11	52.6	47.4	229.9	19.4	2.0	103.5	10.2	5.0
Average	85.5	14.5	246.6	23.6	2.0	119.7	13.4	5.8



Table 5.6. Land use/land cover categories extracted from 2010 LULC dataset for each subcatchment. Impervious and pervious surface distribution was extracted from the High Intensity Urban and Low Intensity Urban categories to more specifically determine types of impervious and pervious surface throughout the catchment. These categories were then used in conjunction with research from Lee and Heaney (2003) to estimate directly connected impervious area (DCIA) for the catchment.

Subcatchment	Transportation-related Impervious Surface (%)	Rooftops, Other Impervious Surface (%)	Lawn (%)	Forested (%)	% DCIA
A1a	25.8	19.4	41.7	13.1	32.6
A1b	36.5	32.1	29.0	2.4	45.5
A1	22.0	23.9	42.3	11.8	30.8
A2	29.6	16.7	40.2	13.4	35.0
A3	41.2	30.8	26.4	1.6	49.1
A4	43.4	30.7	25.0	0.9	50.9
A5	40.3	33.4	25.9	0.4	49.1
A6	31.9	24.8	35.3	8.1	39.4
A7,8,11,12	35.9	35.8	27.8	0.4	46.2
A9	32.0	26.1	34.6	7.3	39.9
A10	28.1	19.5	40.1	12.3	34.5
A11	36.1	35.7	27.7	0.4	46.3
A12	35.8	35.9	27.9	0.4	46.1
A13	40.0	33.6	26.0	0.4	48.9
A14,16	36.2	35.7	27.7	0.4	46.4
A15	37.0	21.7	33.1	8.2	42.8
A17	41.5	32.6	25.4	0.4	49.9
A18	35.5	31.5	29.9	3.0	44.5
A19	43.3	31.5	24.7	0.5	51.0
A20	41.7	32.6	25.3	0.4	50.1
A21,22	36.9	32.1	28.8	2.2	45.9
A23	37.4	23.2	32.2	7.2	43.6
A24	24.8	29.0	38.3	8.0	34.7
Average	35.4	29.0	31.1	4.5	43.6
B1	8.2	0.1	39.5	52.2	7.4
B2	14.7	17.1	50.1	18.1	22.5
B3	21.9	15.7	45.9	16.5	28.2
B4	16.2	16.8	49.2	17.7	23.7
B5	22.9	15.5	45.3	16.3	28.9
B6	18.6	16.3	47.8	17.3	25.6
B7	25.6	14.9	37.3	22.2	30.5
Average	18.3	13.8	45.0	22.9	23.8

Table 5.6. cont.

Subcatchment	Transportation-related Impervious Surface (%)	Rooftops, Other Impervious Surface (%)	Lawn (%)	Forested (%)	% DCIA
C1	22.2	17.1	45.1	15.6	28.8
C2	20.2	16.4	46.5	16.9	26.9
C3	21.3	18.2	49.2	11.3	27.8
C4	20.1	18.1	51.7	10.1	26.5
C5	18.2	6.3	71.0	4.5	19.3
C6	28.6	18.2	48.8	4.4	33.3
C7	40.5	29.3	27.5	2.7	48.0
C8	63.2	20.6	16.0	0.2	64.5
C9	27.6	27.8	32.6	12.1	35.7
C10	33.5	24.0	18.6	23.8	39.4
C11	22.3	22.1	33.1	22.5	29.4
Average	28.9	19.8	40.0	11.3	34.5

Subcatchment	Transportation-related Impervious Surface (%)	Rooftops, Other Impervious Surface (%)	Lawn (%)	Forested (%)	% DCIA
D1	37.1	22.3	32.8	7.8	43.0
D2	33.4	23.6	34.7	8.2	40.3
D3	14.9	19.6	48.9	16.6	23.4
D4	15.1	18.5	49.2	17.1	23.3
D5	27.4	17.3	41.5	13.8	33.3
D6	19.7	19.6	45.7	15.0	27.5
D7	31.2	29.6	33.6	5.5	40.3
D8	30.1	21.2	38.0	10.7	36.8
D10	23.4	21.3	42.8	12.5	30.5
D11	21.1	19.8	44.6	14.4	28.8
Average	25.3	21.3	41.2	12.2	32.7

percent DCIA from values discussed above. For the second run, the percent impervious area in each subcatchment was set to equal the total impervious area as measured using the percent impervious layer (Gorham, 2012a). Again, this modified scenario was run using actual storm events to determine whether an improvement in rainfall/runoff relationship was observed.

## **Discussion**

All of these values were extracted, measured, collected, analyzed to ensure that the Mullins Creek SWMM model best reflected the reality of the existing catchment given the data available. These values determined using a highly detailed analysis were then used to test the sensitivity of the model to changes in percent impervious surface (Chapter 6), and the validity of using an uncalibrated model to predict rainfall/runoff response in a small urban catchment where observed data are often not available (Chapter 7).

## Chapter 6. Mullins Creek Storm Water Management Model (SWMM) Sensitivity Analysis

### Introduction

An important part of understanding a model is understanding the sensitivity of the model to changes in different parameters. Multiple studies have focused on and/or included a discussion of sensitivity of the SWMM model to changes in specific parameters. Often these are the same parameters used for calibration of the model. Some parameters, for example percent impervious area, are fairly easy to measure accurately and can be a parameter that the model has a high level of confidence in. Other parameters, like detention depth for pervious and impervious areas, are more difficult to quantify/measure/estimate and therefore the modeler has less confidence in the values assigned.

The sensitivity of SWMM to changes in different parameters is also related to the conditions that the parameters are being tested in. For example, the model may be more sensitive to changes for smaller storm events rather than larger storm events. The model may also be more sensitive in the maximum ranges of the parameter of interest than in the lower ranges. These differences will be discussed further in the results section of this chapter.

Because the SWMM output is made up of multiple components including peak discharge, total runoff, time to peak, etc. it is useful to examine how different parameters affect different components of the output. For example, Temprano, et al. (2006) reported that total volume and peak runoff outputs were most sensitive to percent impermeable surface. The researchers showed that SWMM was sensitive to changes in other parameters, including slope, width, and Manning's  $n$ , but that those parameters affected the time to peak more so than peak and total discharge.

Multiple studies/researchers reported that the SWMM outputs are most sensitive to changes in percent impervious surface (Zhao, et al., 2013; Goldstein, et al., 2010; Barco, et al, 2008; Temprano, et al., 2006), as well as parameters related to impervious surfaces characteristics including roughness, and depression storage. As for SWMM output sensitivity to infiltration, only

one paper mentioned infiltration as a “sensitive parameter” but that was after discussion of the model being most sensitive to impervious depression storage when the percent impervious surface is known and fixed (Tsihrintzis and Hamid, 1998). Another study that examined infiltration parameters with regard to model sensitivity stated that SWMM was relatively “insensitive” to changes in slope and infiltration rates (Peterson and Wicks, 2006).

For this research project, the sensitivity of the SWMM model that was developed for the Mullins Creek catchment was studied for two specific parameters/sets of parameters: percent impervious surface and Horton infiltration inputs. Many other studies have examined what parameters SWMM outputs are most sensitive to, where small changes in a parameter can equal large changes in model predictions. Because of the interest in the parameters listed above, all other parameters were entered to represent the existing system, catchment, watershed as accurately as possible, and were held constant throughout the rest of the study.

As a part of this study, the sensitivity of the Mullins Creek Storm Water Management Model (SWMM) to two selected parameters was studied: Horton infiltration parameters, and percent impervious surface.

### **SWMM Sensitivity Analysis Model Runs**

The model was initially run holding the infiltration parameters constant and equal to the observed values after the incorporation of data collected and described in Chapter 4. The percent of impervious surface area was varied for each model run from 0% at 20% intervals up to 100% and including 95% impervious surface area. Values used for each subcatchment in the models to assess sensitivity to changes in percent impervious surface are presented in Table 6.1. When studying the sensitivity of the model to changes in the Horton infiltration parameters, all other parameters were held constant including the percent of impervious surface. Table 6.2 outlines the different Horton parameters (and other parameters) used in the different infiltration scenarios. The first scenario used the maximum accepted Horton infiltration parameters as defined by McCuen (2005). Each

Table 6.1. Parameters entered into each SWMM model run for each subcatchment to test the sensitivity of the model to percent impervious surface under different storm intensity scenarios.

SC	Initial Infiltration Rate, $f_0$ (mm/hr)	Final Infiltration Rate, $f_c$ (mm/hr)	Decay Constant, $k$ (hr <sup>-1</sup> )	1	2	3	4	5	6	7
				% ISA	% ISA	% ISA	% ISA	% ISA	% ISA	% ISA
SA1a	131.3	15.2	5.9	0	20	40	60	80	95	100
SA1b	108.3	13.3	6.7	0	20	40	60	80	95	100
SA1	127.6	14.9	6.1	0	20	40	60	80	95	100
SA2	133	15.3	5.9	0	20	40	60	80	95	100
SA3	106.4	13.1	6.7	0	20	40	60	80	95	100
SA4	104.5	12.9	6.8	0	20	40	60	80	95	100
SA5	102.8	12.8	6.9	0	20	40	60	80	95	100
SA6	121.9	14.4	6.2	0	20	40	60	80	95	100
SA7,8,11,12	102.8	12.8	6.9	0	20	40	60	80	95	100
SA9	254	25.4	2	0	20	40	60	80	95	100
SA10	137.2	15.2	2	0	20	40	60	80	95	100
SA13	104.1	12.7	2	0	20	40	60	80	95	100
SA14,16	100.6	12.4	6.8	0	20	40	60	80	95	100
SA15	122.8	14.4	6.2	0	20	40	60	80	95	100
SA17	101.4	11	5.6	0	20	40	60	80	95	100
SA18	92.3	10.5	6	0	20	40	60	80	95	100
SA19	103.2	12.8	6.8	0	20	40	60	80	95	100
SA20	77.9	8.8	6	0	20	40	60	80	95	100
SA21,22	104.1	12.6	6.6	0	20	40	60	80	95	100
SA23	101.4	11	5.6	0	20	40	60	80	95	100
SA24	86	8.5	5.2	0	20	40	60	80	95	100
SB1	187.5	19.9	4.1	0	20	40	60	80	95	100
SB2	137.1	15.7	5.8	0	20	40	60	80	95	100
SB3	136.7	15.6	5.8	0	20	40	60	80	95	100
SB4	137	15.7	5.8	0	20	40	60	80	95	100
SB5	127.3	14	5.5	0	20	40	60	80	95	100
SB6	129.5	14.3	5.5	0	20	40	60	80	95	100
SB7	110.3	9.4	4.3	0	20	40	60	80	95	100

Table 6.1. cont.

SC	Initial Infiltration Rate, $f_0$ (mm/hr)	Final Infiltration Rate, $f_c$ (mm/hr)	Decay Constant, $k$ (hr <sup>-1</sup> )	1	2	3	4	5	6	7
				% ISA	% ISA	% ISA	% ISA	% ISA	% ISA	% ISA
SC1	126.2	13.9	5.6	0	20	40	60	80	95	100
SC2	132.2	14.8	5.6	0	20	40	60	80	95	100
SC3	88.4	8.3	5	0	20	40	60	80	95	100
SC4	92.4	9.3	5.3	0	20	40	60	80	95	100
SC5	47.3	3.1	4.5	0	20	40	60	80	95	100
SC6	58.2	4.7	4.7	0	20	40	60	80	95	100
SC7	98.2	11.5	6.3	0	20	40	60	80	95	100
SC8	57.9	5.6	5.3	0	20	40	60	80	95	100
SC9	69.1	4.5	4.1	0	20	40	60	80	95	100
SC10	116.9	9.2	3.9	0	20	40	60	80	95	100
SC11	115.4	10.3	4.4	0	20	40	60	80	95	100
SD1	122.4	14.4	6.2	0	20	40	60	80	95	100
SD2	122.7	14.5	6.2	0	20	40	60	80	95	100
SD3	134.6	15.5	5.8	0	20	40	60	80	95	100
SD4	135.7	15.5	5.8	0	20	40	60	80	95	100
SD5	133.2	15.3	5.9	0	20	40	60	80	95	100
SD6	133.2	15.3	5.9	0	20	40	60	80	95	100
SD7	102.2	11.6	6	0	20	40	60	80	95	100
SD8	125.8	14.6	6	0	20	40	60	80	95	100
SD10	84.2	7.2	4.6	0	20	40	60	80	95	100
SD11	103.5	10.2	5	0	20	40	60	80	95	100

Table 6.2. Parameters entered into each SWMM model runs for each subcatchment to test the sensitivity of the model to changes in Horton Infiltration parameters.  $f_o$  = initial infiltration rate (mm/hr),  $f_c$  = final infiltration rate (mm/hr),  $k$  = decay constant (1/hr) under different storm intensity scenarios.

SC	% ISA	$k$	Max Horton Parameters		80 % Max Horton Parameters		60% Max Horton Parameters		40% Max Horton Parameters		20% Max Horton Parameters	
			$f_o$	$f_c$	$f_o$	$f_c$	$f_o$	$f_c$	$f_o$	$f_c$	$f_o$	$f_c$
SA1a	32.6	4.0	254.0	50.8	203.2	40.6	152.4	30.5	101.6	20.3	50.8	10.2
SA1b	45.5	4.0	254.0	50.8	203.2	40.6	152.4	30.5	101.6	20.3	50.8	10.2
SA1	30.8	4.0	254.0	50.8	203.2	40.6	152.4	30.5	101.6	20.3	50.8	10.2
SA2	35.0	4.0	254.0	50.8	203.2	40.6	152.4	30.5	101.6	20.3	50.8	10.2
SA3	49.1	4.0	254.0	50.8	203.2	40.6	152.4	30.5	101.6	20.3	50.8	10.2
SA4	50.9	4.0	254.0	50.8	203.2	40.6	152.4	30.5	101.6	20.3	50.8	10.2
SA5	49.1	4.0	254.0	50.8	203.2	40.6	152.4	30.5	101.6	20.3	50.8	10.2
SA6	39.4	4.0	254.0	50.8	203.2	40.6	152.4	30.5	101.6	20.3	50.8	10.2
SA7,8,11,12	46.2	4.0	254.0	50.8	203.2	40.6	152.4	30.5	101.6	20.3	50.8	10.2
SA9	39.9	4.0	254.0	50.8	203.2	40.6	152.4	30.5	101.6	20.3	50.8	10.2
SA10	34.5	4.0	254.0	50.8	203.2	40.6	152.4	30.5	101.6	20.3	50.8	10.2
SA13	48.9	4.0	254.0	50.8	203.2	40.6	152.4	30.5	101.6	20.3	50.8	10.2
SA14,16	46.4	4.0	254.0	50.8	203.2	40.6	152.4	30.5	101.6	20.3	50.8	10.2
SA15	42.8	4.0	254.0	50.8	203.2	40.6	152.4	30.5	101.6	20.3	50.8	10.2
SA17	49.9	4.0	254.0	50.8	203.2	40.6	152.4	30.5	101.6	20.3	50.8	10.2
SA18	44.5	4.0	254.0	50.8	203.2	40.6	152.4	30.5	101.6	20.3	50.8	10.2
SA19	51.0	4.0	254.0	50.8	203.2	40.6	152.4	30.5	101.6	20.3	50.8	10.2
SA20	50.1	4.0	254.0	50.8	203.2	40.6	152.4	30.5	101.6	20.3	50.8	10.2
SA21,22	45.9	4.0	254.0	50.8	203.2	40.6	152.4	30.5	101.6	20.3	50.8	10.2
SA23	43.6	4.0	254.0	50.8	203.2	40.6	152.4	30.5	101.6	20.3	50.8	10.2
SA24	34.7	4.0	254.0	50.8	203.2	40.6	152.4	30.5	101.6	20.3	50.8	10.2
SB1	7.4	4.0	254.0	50.8	203.2	40.6	152.4	30.5	101.6	20.3	50.8	10.2
SB2	22.5	4.0	254.0	50.8	203.2	40.6	152.4	30.5	101.6	20.3	50.8	10.2
SB3	28.2	4.0	254.0	50.8	203.2	40.6	152.4	30.5	101.6	20.3	50.8	10.2
SB4	23.7	4.0	254.0	50.8	203.2	40.6	152.4	30.5	101.6	20.3	50.8	10.2
SB5	28.9	4.0	254.0	50.8	203.2	40.6	152.4	30.5	101.6	20.3	50.8	10.2
SB6	25.6	4.0	254.0	50.8	203.2	40.6	152.4	30.5	101.6	20.3	50.8	10.2
SB7	30.5	4.0	254.0	50.8	203.2	40.6	152.4	30.5	101.6	20.3	50.8	10.2



Table 6.2. cont.

SC	% ISA	$k$	Max Horton Parameters		80 % Max Horton Parameters		60% Max Horton Parameters		40% Max Horton Parameters		20% Max Horton Parameters	
			$f_o$	$f_c$	$f_o$	$f_c$	$f_o$	$f_c$	$f_o$	$f_c$	$f_o$	$f_c$
SC1	28.8	4.0	254.0	50.8	203.2	40.6	152.4	30.5	101.6	20.3	50.8	10.2
SC2	26.9	4.0	254.0	50.8	203.2	40.6	152.4	30.5	101.6	20.3	50.8	10.2
SC3	27.8	4.0	254.0	50.8	203.2	40.6	152.4	30.5	101.6	20.3	50.8	10.2
SC4	26.5	4.0	254.0	50.8	203.2	40.6	152.4	30.5	101.6	20.3	50.8	10.2
SC5	19.5	4.0	254.0	50.8	203.2	40.6	152.4	30.5	101.6	20.3	50.8	10.2
SC6	33.3	4.0	254.0	50.8	203.2	40.6	152.4	30.5	101.6	20.3	50.8	10.2
SC7	48.0	4.0	254.0	50.8	203.2	40.6	152.4	30.5	101.6	20.3	50.8	10.2
SC8	64.5	4.0	254.0	50.8	203.2	40.6	152.4	30.5	101.6	20.3	50.8	10.2
SC9	35.7	4.0	254.0	50.8	203.2	40.6	152.4	30.5	101.6	20.3	50.8	10.2
SC10	39.4	4.0	254.0	50.8	203.2	40.6	152.4	30.5	101.6	20.3	50.8	10.2
SC11	29.4	4.0	254.0	50.8	203.2	40.6	152.4	30.5	101.6	20.3	50.8	10.2
SD1	43.0	4.0	254.0	50.8	203.2	40.6	152.4	30.5	101.6	20.3	50.8	10.2
SD2	40.3	4.0	254.0	50.8	203.2	40.6	152.4	30.5	101.6	20.3	50.8	10.2
SD3	23.4	4.0	254.0	50.8	203.2	40.6	152.4	30.5	101.6	20.3	50.8	10.2
SD4	23.3	4.0	254.0	50.8	203.2	40.6	152.4	30.5	101.6	20.3	50.8	10.2
SD5	33.3	4.0	254.0	50.8	203.2	40.6	152.4	30.5	101.6	20.3	50.8	10.2
SD6	27.5	4.0	254.0	50.8	203.2	40.6	152.4	30.5	101.6	20.3	50.8	10.2
SD7	40.3	4.0	254.0	50.8	203.2	40.6	152.4	30.5	101.6	20.3	50.8	10.2
SD8	36.8	4.0	254.0	50.8	203.2	40.6	152.4	30.5	101.6	20.3	50.8	10.2
SD10	30.5	4.0	254.0	50.8	203.2	40.6	152.4	30.5	101.6	20.3	50.8	10.2
SD11	28.8	4.0	254.0	50.8	203.2	40.6	152.4	30.5	101.6	20.3	50.8	10.2

subsequent design scenario was represented holding the decay constant,  $k$ , at 4 while the initial and final infiltration rates were decreased by 20%.

Each of the design scenarios was run for storm events of increasing intensity. All were SCS, Type III, 24 hour storm events based on the location of the catchment in Northwest Arkansas (Figure 6.1). The distribution of an SCS, Type III, 24 hour storm event is shown in Figure 6.2. The storms ranged from a minimum of 25 mm (~ 1in.) up to 400mm (~16 in.) Results for each run including predicted peak discharge and total runoff volume were recorded.

To determine the sensitivity of the Mullins Creek SWMM model to changes in impervious area coverage, a similar set up was followed. While all other parameters were held constant to reflect the existing conditions in the catchment, the percent impervious surface was changed from 0% up to 100% and each scenario was run for the same range of storm events as presented above. Results from each model run were recorded and analyzed.

## **Results**

### **Percent Impervious Area**

The results of each scenario: % impervious surface, 0% to 100%, and storm events sized 25mm up to 400mm, were recorded and plotted to examine how a change in percent impervious surface was reflected in peak discharge output (Table 6.3, Figure 6.3) and total runoff output (Table 6.4, Figure 6.4). General trends in the data were then observed. The majority of research papers that discussed the sensitivity of a SWMM model to changes in different parameters, relative sensitivity was discussed, with a focus on which parameters the model was most sensitive to, however, what was not often discussed was how the sensitivity of the model changes based on different conditions.

A key result was that the sensitivity of the model response/output to percent impervious surface was related to the range of percent impervious area where the change was occurring, for example, at the lower end of percent impervious surface (a change from 10 to 20%) or the higher

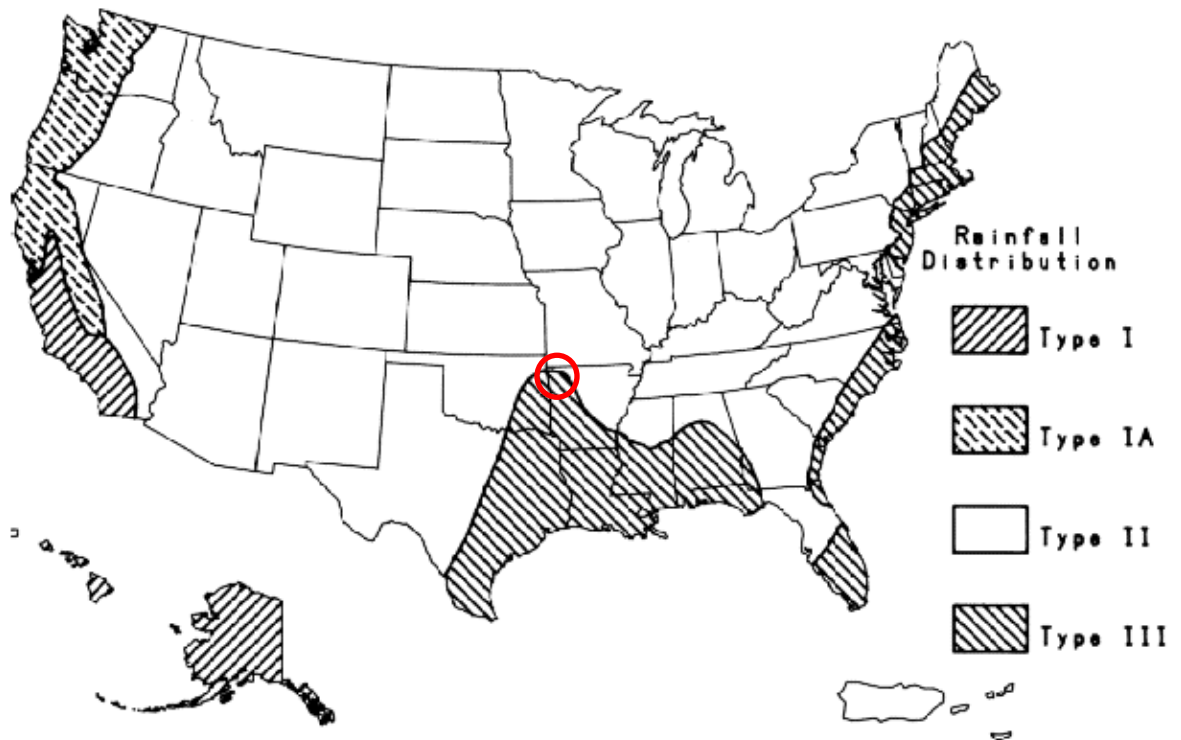


Figure 6.1. Map of SCS rainfall distributions for the United States. The red circle shows the approximate area where the Mullins Creek catchment is located and why SCS Type III storm events were used for the analysis. (Adapted from SCS, 1986).

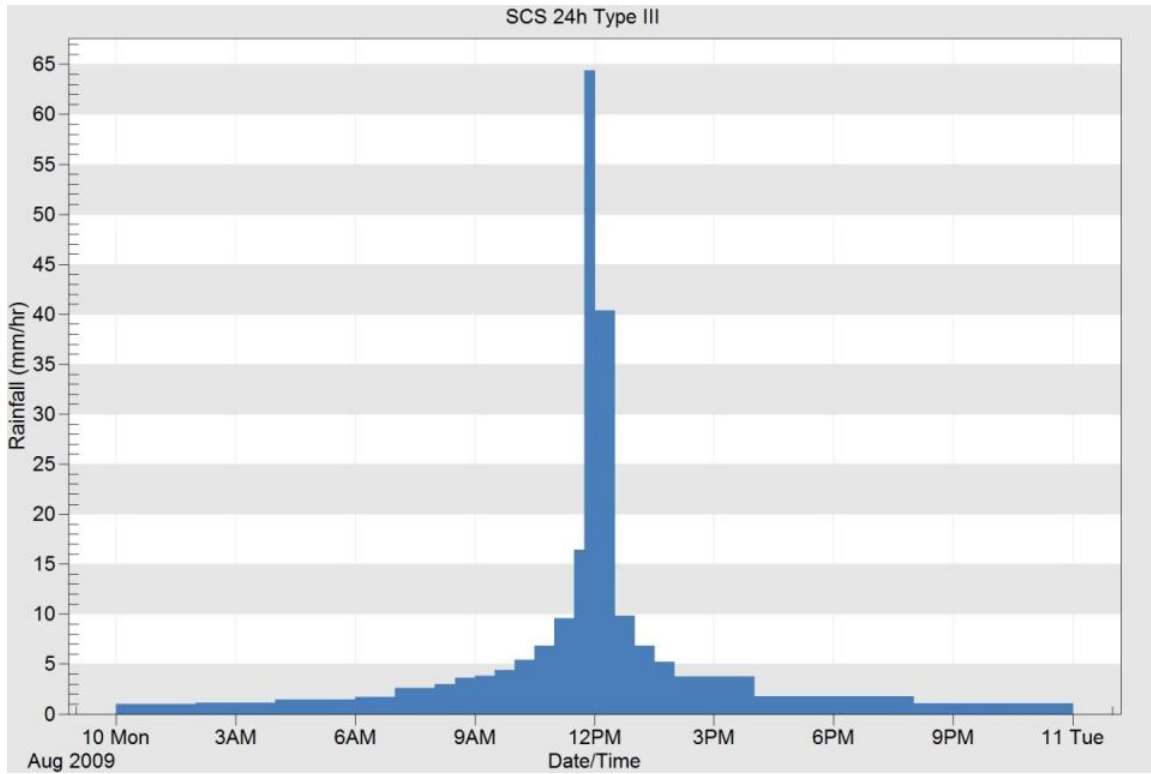


Figure 6.2. Distribution of a 100 mm, SCS Type III, 24 hour storm event (exported from PCSWMM (CHI, 2014)).

Table 6.3. Table of peak discharge predictions (cms) for a range of storm event sizes and over a range of impervious surface percentages for the Mullins Creek catchment model in SWMM.

Rainfall Total	Percent Impervious Surface Area						
	0	20	40	60	80	95	100
25 mm	0.0	2.0	4.4	6.0	7.9	9.2	9.6
50 mm	0.5	4.3	8.9	13.6	18.3	21.4	22.2
100 mm	8.6	15.1	22.6	33.1	43.1	48.6	49.3
150 mm	21.7	31.0	40.2	56.1	70.2	76.9	77.2
200 mm	37.8	49.0	60.8	81.2	98.4	105.4	105.5
250 mm	55.7	67.9	83.3	107.4	126.9	133.9	133.9
300 mm	74.6	87.0	106.9	134.2	155.3	162.3	162.3
350 mm	93.9	106.1	131.3	161.2	183.6	190.7	190.7
400 mm	113.3	125.0	156.1	188.4	211.9	219.1	219.1

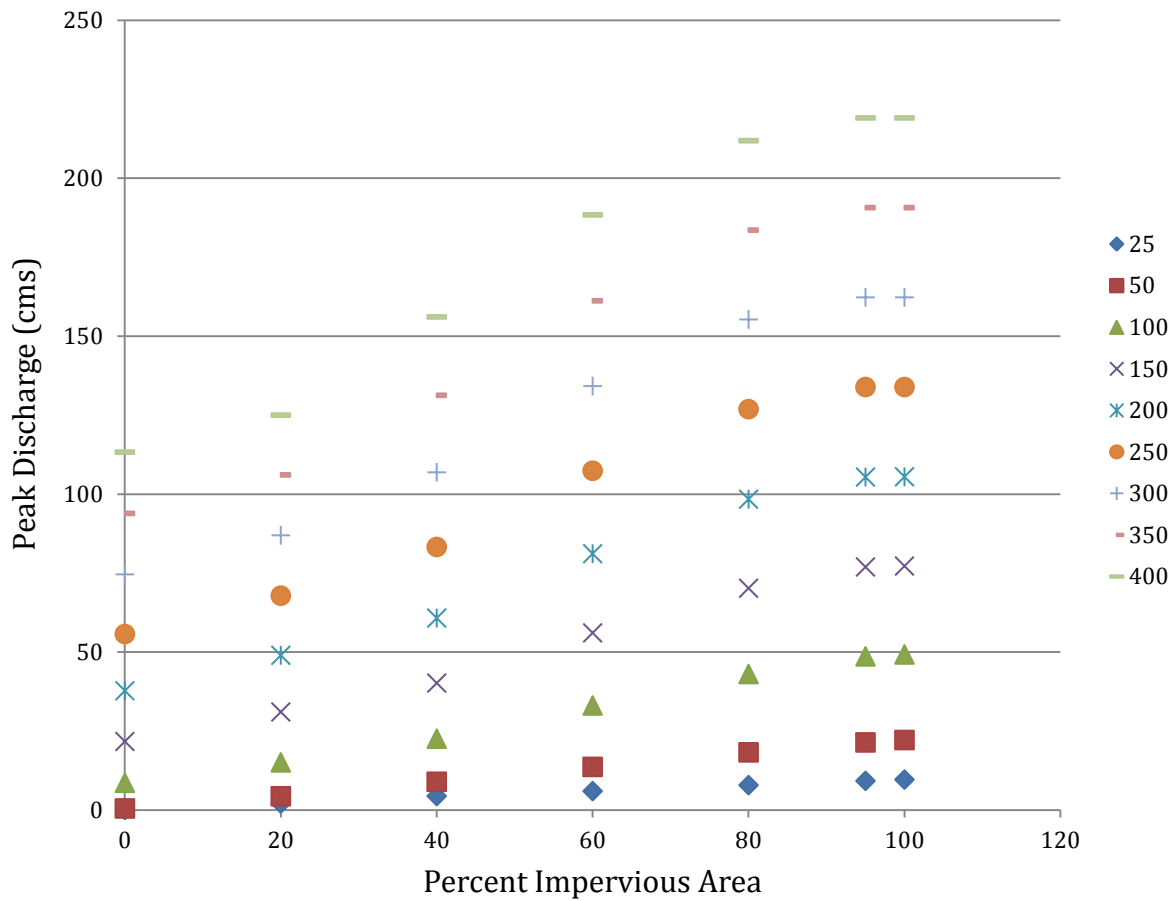


Figure 6.3. Relationship between peak discharge predictions for the Mullins Creek catchment and percent impervious area over a range of SCS Type III, 24 hr design storm events. Each storm event is plotted as a different color/point shape.

Table 6.4. Table of total runoff predictions (m<sup>3</sup>) for a range of storm event sizes and over a range of impervious surface percentages for the Mullins Creek catchment model in SWMM.

Rainfall Total	Percent Impervious Surface Area						
	0	20	40	60	80	95	100
25 mm	4	11210	24230	39160	56000	69580	74220
50 mm	1484	25740	54020	84970	118000	143700	152500
100 mm	35070	85070	138400	194100	251400	294700	308900
150 mm	101100	169400	240900	314800	390200	446800	465500
200 mm	183600	265900	352100	441200	531600	599500	622000
250 mm	276200	370400	469400	571400	674800	752700	778600
300 mm	376400	481100	591200	704500	819500	906300	935100
350 mm	482700	596900	717000	840200	965700	1060000	1092000
400 mm	594200	717000	845900	978600	1113000	1215000	1248000

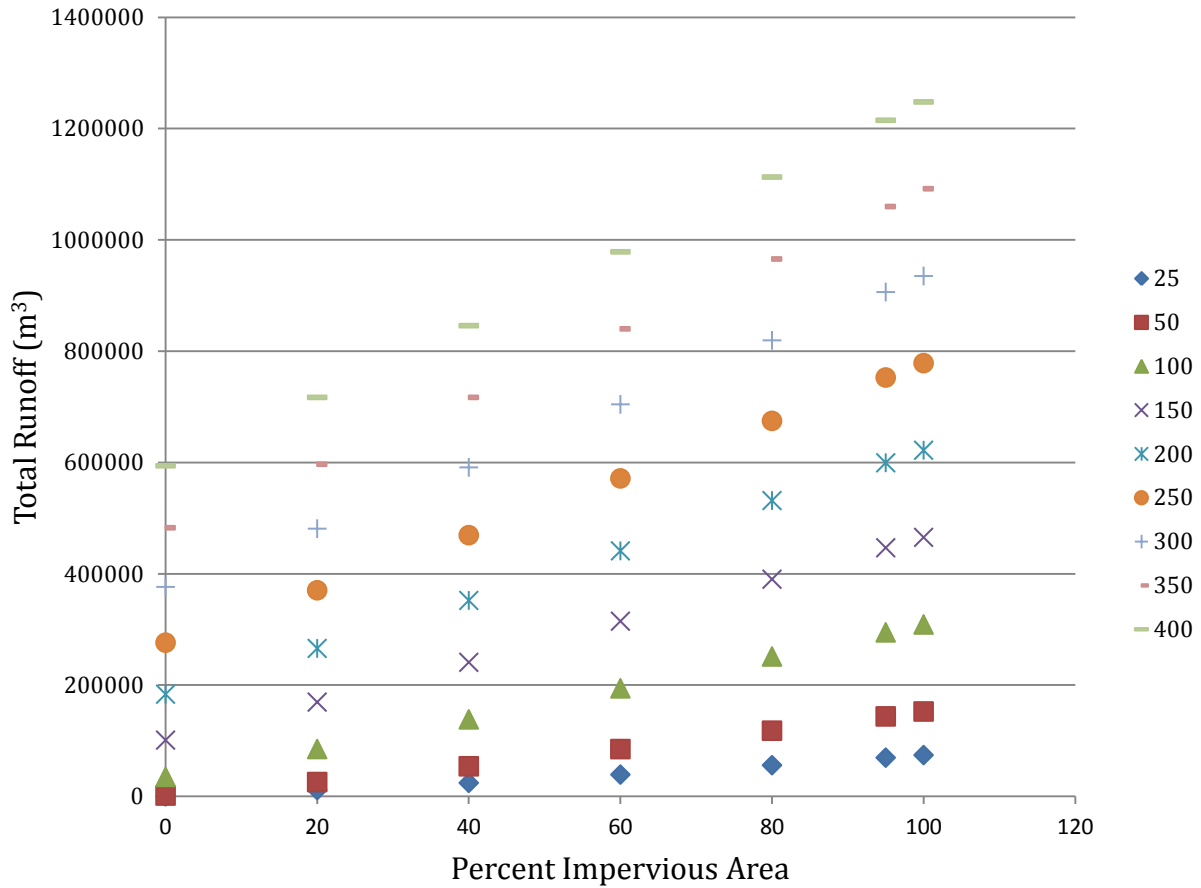


Figure 6.4. Relationship between total runoff predictions for the Mullins Creek catchment and percent impervious area over a range of SCS Type III, 24 hr design storm events. Each storm event is plotted as a different color/point shape.



end of the range (a change from 80 to 90%). The sensitivity of the model output to changes in percent impervious surface was also related to the size of the storm event. The sensitivity of the model to the parameter was also related to if the storm event was small (25mm) or large (400mm), and sometimes in the middle (150mm).

In general, the model output was more sensitive to changes in percent impervious surface that occurred in the lower ranges. The model was most sensitive to changes in percent impervious surface changes from 0 to 10% and became less sensitive the larger the percent impervious surface. The model (peak discharge) output was the most sensitive to changes in % impervious surface for the 25mm and 50mm storm events, and progressively decreased for the larger storm events. For the 400mm storm event, a 10% increase in percent impervious surface only represented an average of a 7.5% increase in peak discharge, but for the 25mm storm event, the average percent increase in peak discharge in response to a 10% increase in impervious surface was 72.7%, almost an order of magnitude greater (Figure 6.5). The sensitivity of total runoff to changes in percent impervious surface showed similar trends. The smaller the storm event, the more sensitive the SWMM output was to changes in percent impervious surface. As the percent impervious surface increased, the model also became less sensitive to these changes (Figure 6.6). On average, across all ranges of percent impervious area and across all modeled storm events, the average percent change in peak discharge as a response to a 10% change in percent impervious surface was 30.9%. On average, across all ranges of percent impervious area and across all modeled storm events, the average percent change in total runoff as a response to a 10% change in percent impervious surface was 18.0%.

### **Horton Infiltration Parameters**

The results of each scenario: Percent of maximum Horton infiltration parameters (from McCuen, 2003), 100% (max infiltration) to 20%, and storm events sized 25mm up to 400mm, were recorded and plotted to examine how a change in percent impervious surface was reflected in peak

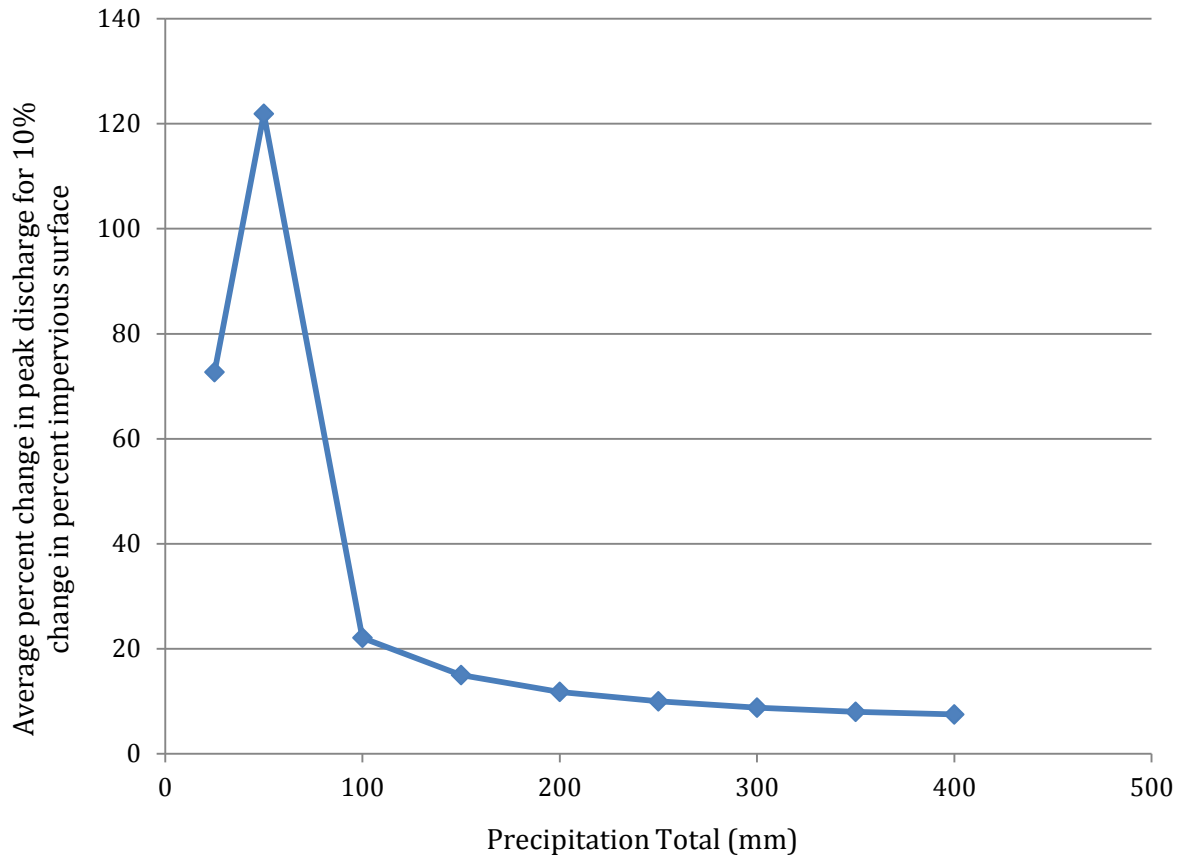


Figure 6.5. Sensitivity of the peak discharge output to changes in percent impervious surface for different storm intensities. The sensitivity of the model to these changes is higher for small storm events and then drops off for larger storm events.

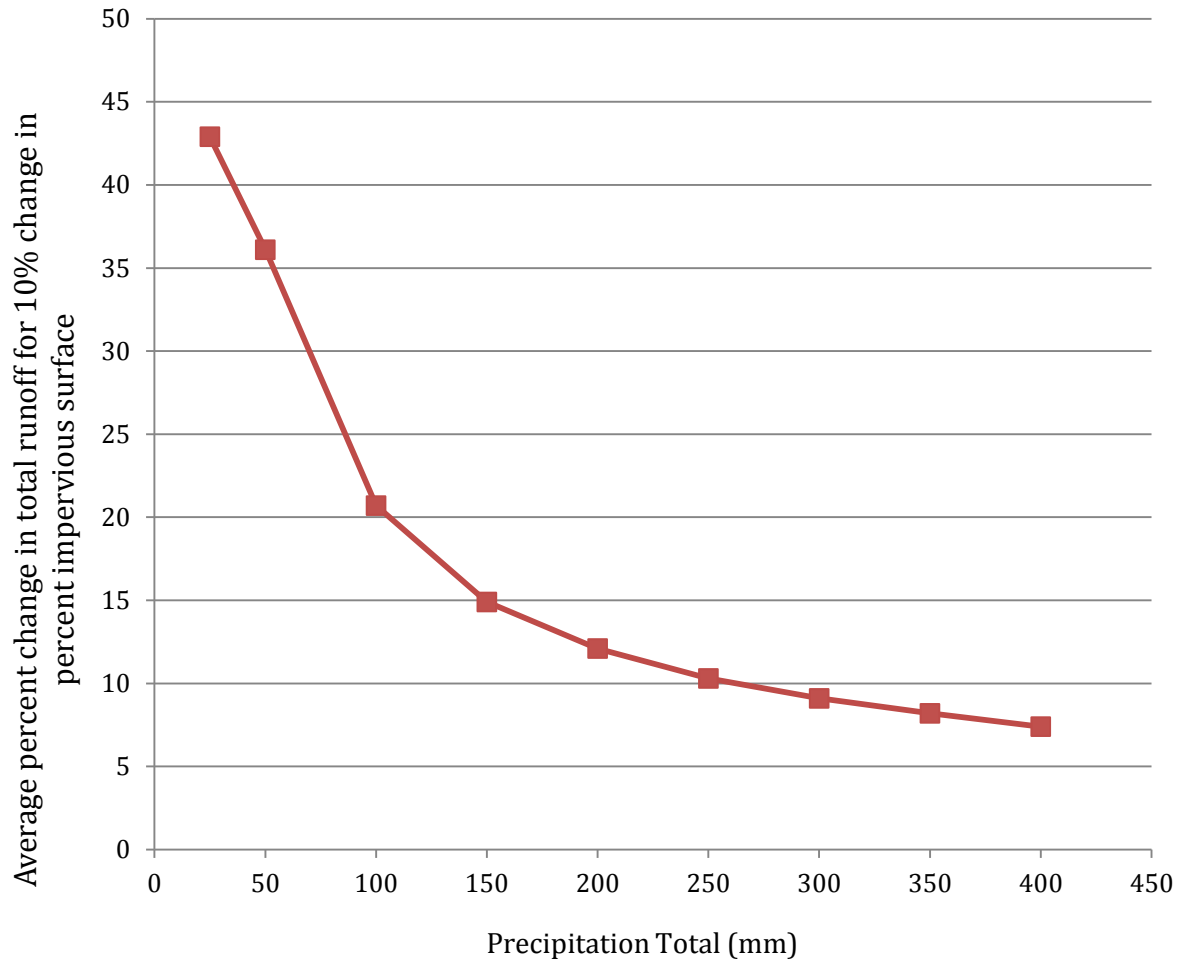


Figure 6.6. Sensitivity of the total runoff output to changes in percent impervious surface for different storm intensities. The sensitivity of the model to these changes is highest for small storm events and then drops off for larger storm events.

discharge output and total runoff output (Table 6.5, 6.6, Figure 6.7, 6.8). General trends in the data were then observed.

Overall, the Mullins Creek SWMM model output was less sensitive to changes in infiltration parameters than in changes in percent impervious surface. The sensitivity of peak discharge to a 10% change in percent of maximum Horton infiltration parameters was 10.8%. The sensitivity of total runoff to a 10% change in percent of maximum Horton infiltration parameters was 6.8%. Unlike for percent impervious area, the model outputs were most sensitive for intermediate storm events and peaked for the 150mm storm for both peak discharge and total runoff outputs (Figure 6.9, and Figure 6.10). Overall the model was less sensitive to changes for smaller storm events than for larger ones. The sensitivity increased as the storm total increased up to the 150mm storm and then slowly decreased.

## **Discussion**

The findings from this sensitivity analysis reflect data presented in the literature stating that the SWMM model is more sensitive to percent imperviousness than to changes in infiltration parameters. As more impervious surfaces cover a catchment, there is a smaller area overall where the infiltration parameters even apply. The results from the changes in percent impervious surface area also reinforce the findings of stream geomorphologists and ecologists who state that a stream system is destabilized at fairly low percents of total impervious area (Booth and Jackson, 1997; Booth, 1990). This is consistent with the model outputs that show more drastic changes in peak discharge and total runoff when the percentages of TIA are lower. There are much larger changes in these values when the TIA changes from 0 to 10% than from 90 to 100%. These small changes in a catchment can dramatically increase peak and total flows resulting in channel instability and erosion. Even though the model is not as sensitive to changes in infiltration parameters, there can be significant differences in peak discharge based on changes in infiltration parameters. For the

Table 6.5. Table of peak discharge predictions (cms) for a range of storm event sizes and over a range of infiltration values for the Mullins Creek catchment model in SWMM.

Rainfall Total	Percent of Maximum Horton Infiltration Values				
	100	80	60	40	20
25 mm	3.2	3.2	3.2	3.2	3.3
50 mm	6.8	6.8	6.8	6.8	7.3
100 mm	13.8	14.0	14.4	16.4	20.8
150mm	20.9	23.6	26.6	31.3	38.0
200 mm	28.3	37.5	42.2	48.5	56.6
250 mm	36.1	53.3	59.9	66.8	75.4
300 mm	45.6	71.4	77.8	85.4	97.0
350 mm	59.5	89.6	96.4	105.8	119.4
400 mm	75.9	107.8	116.9	128.5	142.1

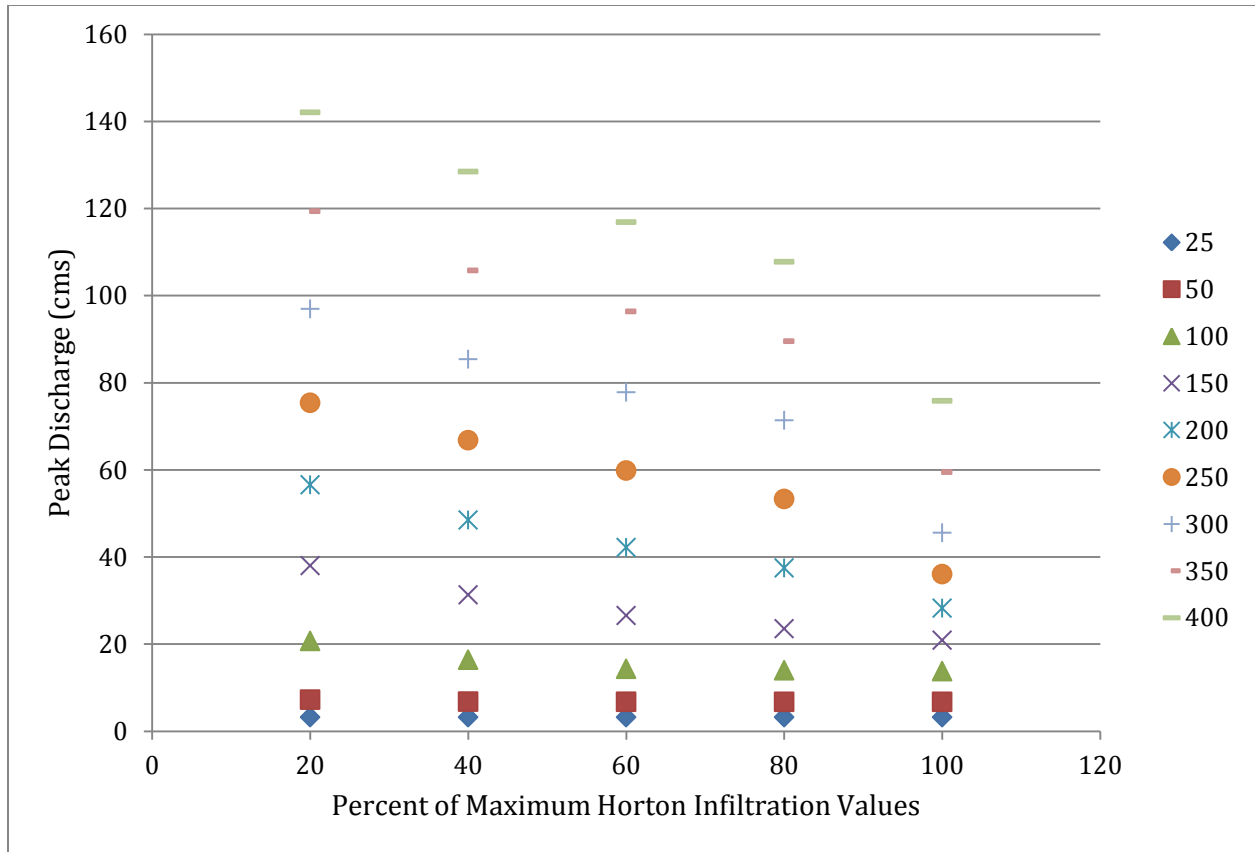


Figure 6.7. Relationship between peak discharge predictions for the Mullins Creek catchment and percent of maximum Horton infiltration parameters over a range of SCS Type III, 24 hr design storm events. Each storm event is plotted as a different color/point shape. The higher the Horton parameters, more infiltration and less runoff is predicted for the pervious areas in the subcatchment.

Table 6.6. Table of total runoff predictions (m<sup>3</sup>) for a range of storm event sizes and over a range of infiltration values for the Mullins Creek catchment model in SWMM.

Rainfall Total	Percent of Maximum Horton Infiltration Values				
	100	80	60	40	20
25 mm	18540	18540	18540	18540	18710
50 mm	38080	38080	38190	38680	44640
100 mm	77160	78940	81820	97820	127700
150mm	116600	132600	153100	180200	228900
200 mm	158200	209700	235100	272100	340600
250 mm	202200	292300	325200	371800	459000
300 mm	250700	380800	418500	475900	583300
350 mm	318000	472700	517200	585500	711900
400 mm	399600	566600	619800	698500	843600

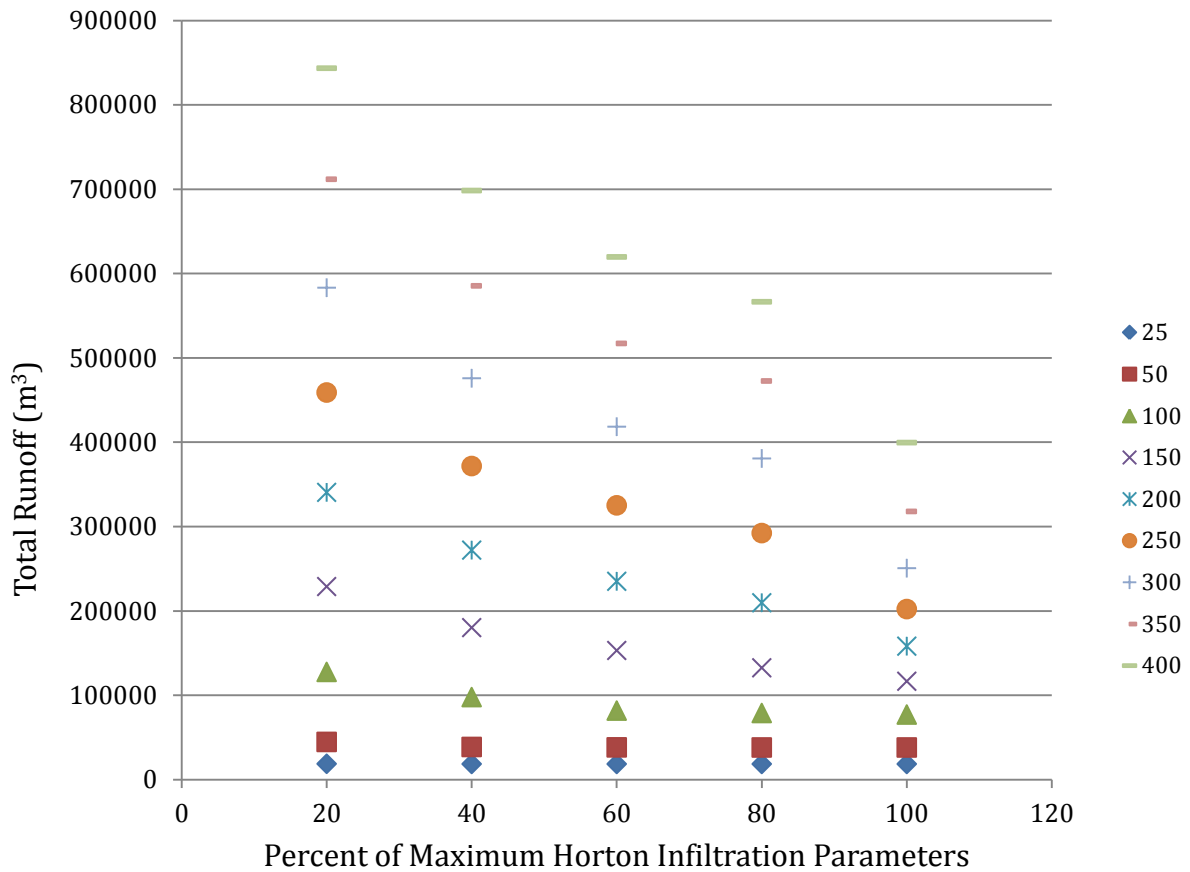


Figure 6.8. Relationship between total runoff predictions for the Mullins Creek catchment and percent of maximum Horton infiltration parameters over a range of SCS Type III, 24 hr design storm events. Each storm event is plotted as a different color/point shape. The higher the Horton parameters, more infiltration and less runoff is predicted for the pervious areas in the subcatchment.



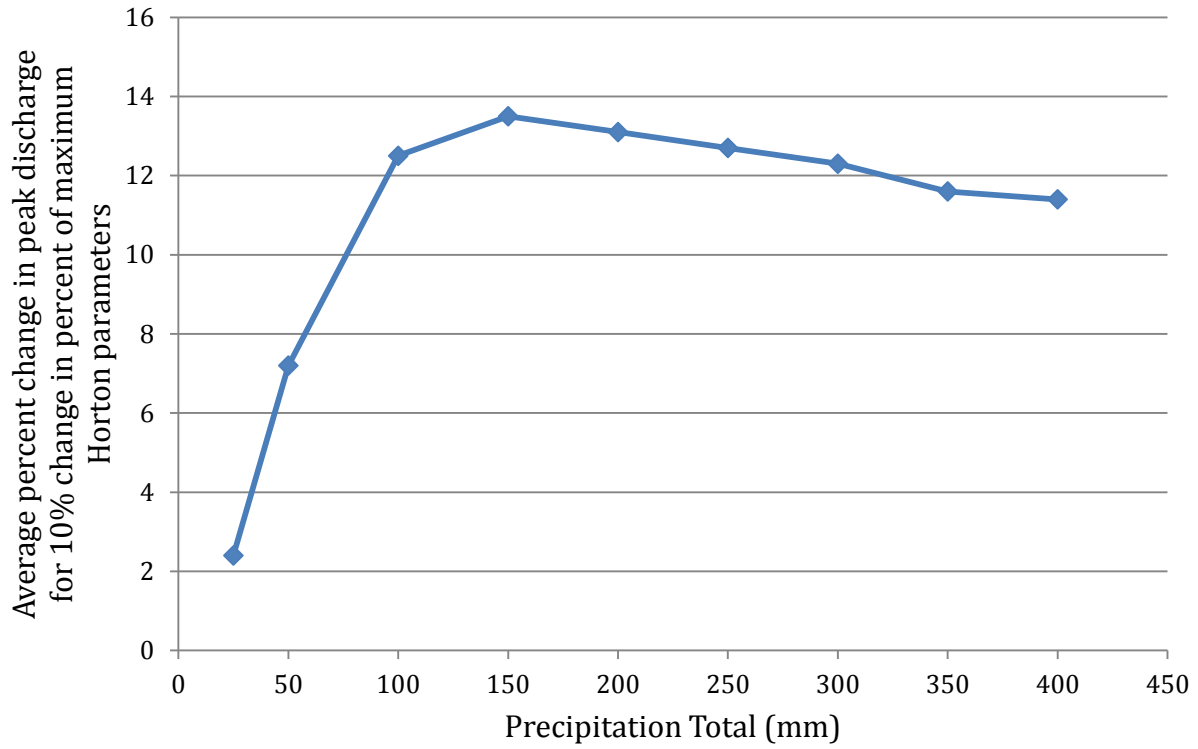


Figure 6.9. Sensitivity of the peak discharge output to changes in percent of Maximum Horton Infiltration Parameters for different storm intensities. The sensitivity of the model to infiltration parameters is highest for the 150 mm storm event, and slowly decreases for progressively larger storm events.

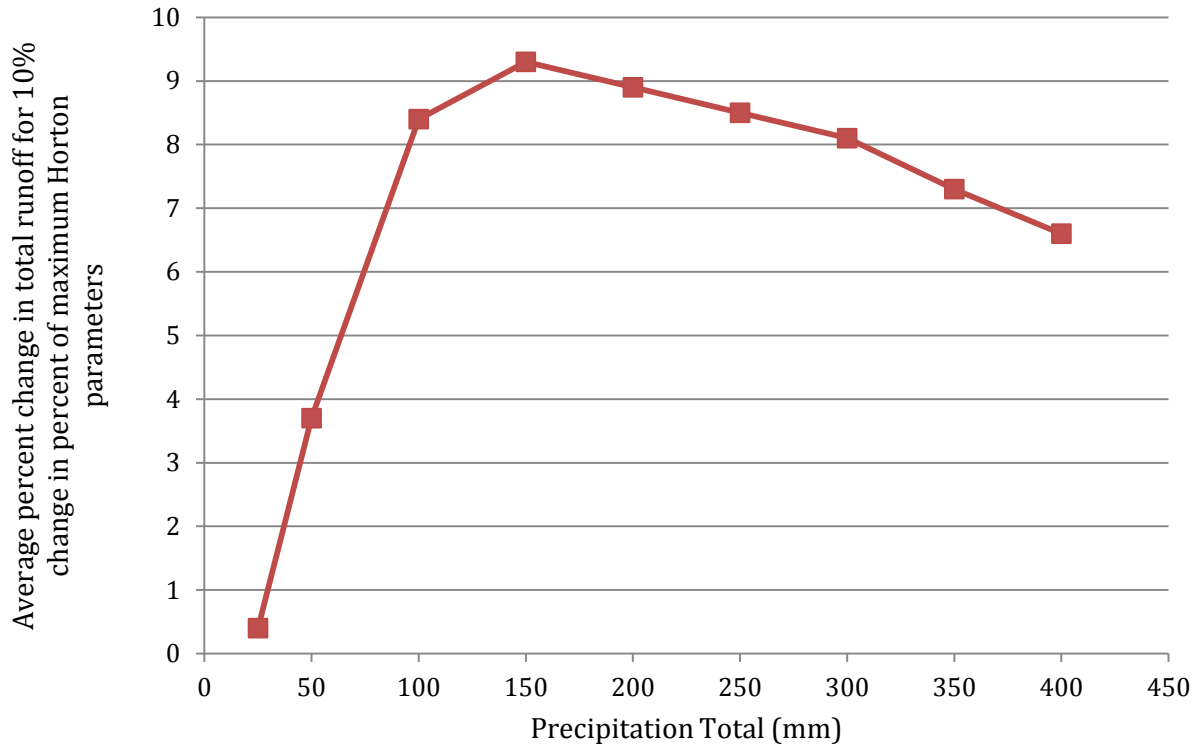


Figure 6.10. Sensitivity of the total runoff output to changes in percent of Maximum Horton Infiltration Parameters for different storm intensities. The sensitivity of the model to infiltration parameters is highest for the 150 mm storm event, and slowly decreases for progressively larger storm events.

Mullins Creek catchment, the inclusion of observed infiltration data resulted in a 54% decrease in infiltration rates which according to the sensitivity analysis could represent a 50% increase in peak discharge and 34% increase in total runoff for the catchment as compared to predicted data. The increases are even more pronounced for larger storm events over 150 mm.

## Chapter 7. Mullins Creek Uncalibrated SWMM Model Validation

### Introduction

For this study, examining the effects of more detailed infiltration and percent impervious surface values for a small urban catchment, the SWMM model was not calibrated. One of the questions to be answered was whether or not accurate predictions of stream response to actual rainfall events could be made without the luxury of observed data. Small urban catchments are ideal candidates for the implementation of stream restoration projects and to study effects of different low impact development (LID) technologies, however, most are not gauged sites so observed runoff data and/or precipitation data may not be available. The same is true when studying undeveloped areas to determine conditions pre- and post-development for stormwater management (Jang, et al., 2007). In their study, Jang, et al. (2007) determined that using SWMM to model pre- and post-development conditions provided a more accurate result than using different models to model the different conditions as has been traditional in North Korea where the study took place. SWMM is a hydrologic model designed to model urban catchments (Rossman, 2010), and limited studies have been conducted to evaluate applicability/accuracy/efficacy in modeling undeveloped catchments. However, based on the results of the studies that have been done, SWMM provides good results modeling natural as well as urban systems. Instead of modeling pre- and post-development conditions, an important use for SWMM is modeling existing and proposed conditions. Proposed changes could include additional development/impervious surface, or disconnection of impervious surfaces and increased infiltration.

Modeling urban systems can be a challenge because of the wide range of land use/land cover (LULC), the heterogeneity of the system, and the complex drainage dynamics of a stormwater drainage network. A model that includes hydrologic as well as hydraulic processes is important for modeling urban systems. As catchments are in the process of being developed, conditions can change practically overnight. However, once development is complete, and conditions in the

catchment are no longer changing, the channel will start to adjust to the new flow dynamics of the system and, if left undisturbed, will reach a new equilibrium state (aka. channel evolution, Simon and Hupp, 1986). In other Ozark headwater streams, urban channels were reported to have greater slopes, and greater cross-sectional areas than their undeveloped counterparts (Shepherd, et al., 2011).

Until they are completely “developed,” many urban streams are dynamically changing in response to changes in the catchment as observed by Keen-Zebert (2007). There is a special challenge when modeling dynamically changing urban systems. Modeling and parameterizing a model for a system that is continuing to change can only be good for a snapshot in time, recognizing that changes in the catchment can occur at a higher temporal resolution than the available datasets. Any observed data that may be used to calibrate/validate the model would have to come from a fairly small window in time that is reflective of when the conditions of interest existed in the catchment.

A university campus is unique in how long the location has been extensively developed, and how dynamically and frequently the LULC can change. A developed residential catchment of the same age would have minimal changes to LULC and percent ISA. Other than the occasional construction of an addition on a home, or a storage shed, conditions would remain fairly stable, especially across an entire catchment. Unlike a residential development, a thriving/growing university campus is extremely dynamic. Buildings become outdated/obsolete and are torn down, existing green space is infilled with higher value dormitories, and classroom buildings. Extensive parking lots are converted from gravel to paved to parking garages. Athletic facilities and fields are constructed and updated. Unlike the residential developments, the receiving waterway in a dynamically changing catchment does not have a chance to recover from or adjust to hydrologic changes.

The goal of this set of model runs was to determine how well the SWMM model predicts the rainfall-runoff relationship in the Mullins Creek catchment without calibration. Four scenarios were run to compare results.

## Methods

All inputs into the SWMM model were held constant except for infiltration and percent impervious area. Four different scenarios were run for each selected observed storm event:

**Scenario 1.** Infiltration parameters for pervious surfaces equal to the predicted Horton parameters without incorporating observed soil infiltration data. Percent impervious surface = estimated directly connected impervious surface values for each subcatchment.

**Scenario 2.** Infiltration parameters included predicted Horton parameters (same as scenario 1). Percent impervious surface = observed total impervious surface values for each subcatchment.

**Scenario 3.** Infiltration parameters include observed infiltration data (see Chapter 4) for highly maintained pervious surfaces in each subcatchment. Percent impervious surface = estimated directly connected impervious surface values for each subcatchment.

**Scenario 4.** Infiltration parameters include observed infiltration data for highly maintained pervious surfaces in each subcatchment. Percent impervious surface = total impervious area as estimated from Percent Imperviousness layer values for each subcatchment.

The average values used in the model for each scenario for each subcatchment A, B, C, and D were presented in Table 7.1. A complete list of parameter inputs for each subcatchment for each model scenario was presented in Appendix C.

### **Observed Runoff Data**

Data downloaded from the U.S. Geological Survey (USGS) site for the gaging station located at the outlet of Mullins Creek (College Branch at MLK Blvd at Fayetteville, AR: 07048480) from 2008 through 2011 were analyzed to identify storm events to use to validate the model. Nine storms over a range of sizes and intensities were identified and used in the validation process. A summary of precipitation and observed runoff parameters are presented in Table 7.2. Storm events ranged from a peak discharge of 4.6 up to 32.2 cms, and a total discharge ranging from about 18,500 m<sup>3</sup> up to 230,000 m<sup>3</sup>. According to the graph, the Mullins Creek catchment had about 2300 m<sup>3</sup> of total runoff for each mm of rainfall ( $R^2 = 0.7345$ ). One storm event was exceptionally large (approximately 230,000 m<sup>3</sup>) and may have skewed the relationship higher than it would have been otherwise. The relationship between total runoff (m<sup>3</sup>) and total precipitation (mm) for the selected events is presented in Figure 7.1.

### **Precipitation Data**

After the dates of the storms to be used for validation were determined, NEXRAD Level III radar rainfall data were downloaded for each storm event from the KINX station located in Tulsa, Oklahoma through the National Oceanic and Atmospheric Association (NOAA) website (NOAA, 2014). These data were then uploaded into PCSWMM, and a Radar Acquisition and Processing (RAP) Project was created. This process creates a theoretical rain gage for each subcatchment based on the radar rainfall. When the model was run, an overall system precipitation hyetograph

Table 7.1. The average infiltration rates and percent impervious surface for four different infiltration/impervious surface scenarios for each main subcatchment.

Scenario 1				
Subcatchment	Initial Infiltration Rate, $f_o$ (mm/hr)	Final Infiltration Rate, $f_c$ (mm/hr)	Decay Constant, $k$ (hr <sup>-1</sup> )	% Imperv
A	237.3	23.3	2.0	43.4
B	247.1	23.7	2.0	23.8
C	224.5	18.0	2.0	34.5
D	246.6	21.3	2.0	32.7

Scenario 2				
Subcatchment	Initial Infiltration Rate, $f_o$ (mm/hr)	Final Infiltration Rate, $f_c$ (mm/hr)	Decay Constant, $k$ (hr <sup>-1</sup> )	% Imperv
A	237.3	23.3	2.0	63.7
B	247.1	23.7	2.0	32.1
C	224.5	18.0	2.0	48.2
D	246.6	21.3	2.0	46.6

Scenario 3				
Subcatchment	Initial Infiltration Rate, $f_o$ (mm/hr)	Final Infiltration Rate, $f_c$ (mm/hr)	Decay Constant, $k$ (hr <sup>-1</sup> )	% Imperv
A	115.4	13.3	5.7	43.4
B	137.9	14.9	5.3	23.8
C	115.4	10.3	4.4	29.4
D	119.8	13.4	5.7	32.7

Scenario 4				
Subcatchment	Initial Infiltration Rate, $f_o$ (mm/hr)	Final Infiltration Rate, $f_c$ (mm/hr)	Decay Constant, $k$ (hr <sup>-1</sup> )	% Imperv
A	115.4	13.3	5.7	63.7
B	137.9	14.9	5.3	32.1
C	91.1	8.7	5.0	48.2
D	119.8	13.4	5.7	46.6



Table 7.2: Summary of observed storm events used for model validation purposes. The total rainfall and peak rainfall intensity were obtained from NEXRAD Level III radar data, and the observed total runoff and peak discharge are from data downloaded from USGS.

Storm Date	Total Rainfall (mm)	Peak Rainfall Intensity (mm/hr)	Observed Total Runoff (m <sup>3</sup> )	Observed Peak Discharge (cms)
12 April 2009	35.2	9.9	44130	4.6
05 August 2009	41.3	42.4	62410	19.1
10 August 2009	19.8	28.9	23840	10.3
21 September 2009	30.3	14.5	65650	9.7
08 October 2009	76.1	30.5	228200	32.2
29 October 2009	34.4	23.9	68020	11.9
27 June 2010	15.2	26.5	18550	5.6
27 February 2011	10.4	89.9	60920	20.7
22 September 2011	32.1	27.6	45250	6.1

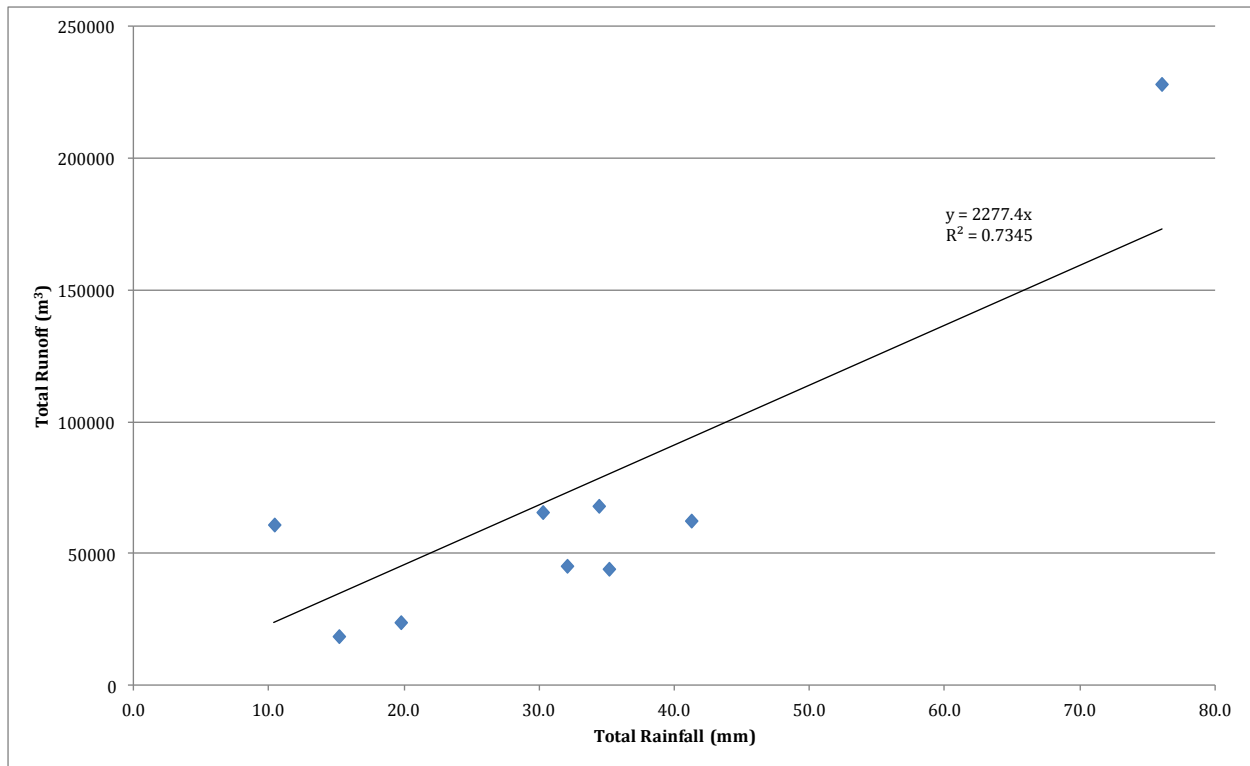


Figure 7.1. Graph of total runoff (m<sup>3</sup>) versus total rainfall (mm) for the storm events selected for validation of the SWMM model.

was created (Figure 7.2). The hyetographs for the remainder of the validation storm events are presented in Appendix B.

### **SWMM Model Runs**

Each storm even was run through four different scenarios as outlined above. The model was run for 48 hours around the precipitation event of interest. The predicted versus observed hydrograph were graphed and the peak discharge (cms) and total discharge (m<sup>3</sup>) were recorded and compared. An example of the predicted versus observed hydrograph is shown in Figure 7.3. The remainder of the predicted versus observed hydrographs are presented in Appendix D. Percent error for the observed versus predicted peak discharge and total runoff were calculated using Equation 12.

$$\text{percent error} = \frac{|\text{predicted} - \text{observed}|}{\text{observed}} \times 100 \quad (12)$$

### **Results and Discussion**

For each model run, the primary results examined were the accuracy of observed versus predicted peak discharge and observed versus predicted total runoff. The lowest peak discharge and total runoff were predicted for scenario 1 (predicted infiltration values, % impervious surface area (ISA) = % DCIA), and the greatest peak discharge and total runoff were predicted for scenario 4 (observed infiltration values, % ISA = % TIA. Overall, the most accurate results were for scenario 4 where predicted peak discharge was within 30% of observed values, and predicted total runoff was within 39.5% of observed values. Accepted percent error for calibrated hydrologic models is around 30% for peak discharge, and 10% for total runoff. These results represent the potential utility of using an uncalibrated SWMM model for a small urban stream system to model existing

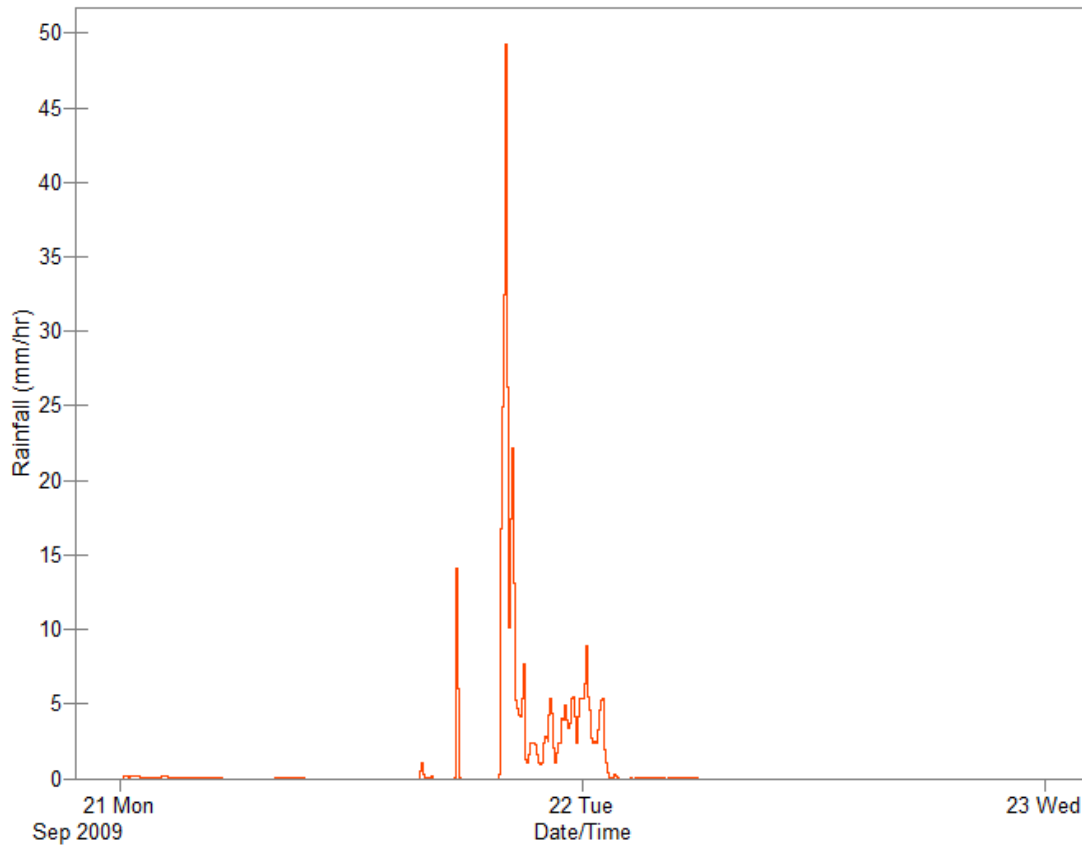


Figure 7.2. A system precipitation hyetograph based on NEXRAD Level III radar data and processed using a Radar Acquisition and Processing (RAP) Project in PCSWMM. For 22 September 2009 storm event.

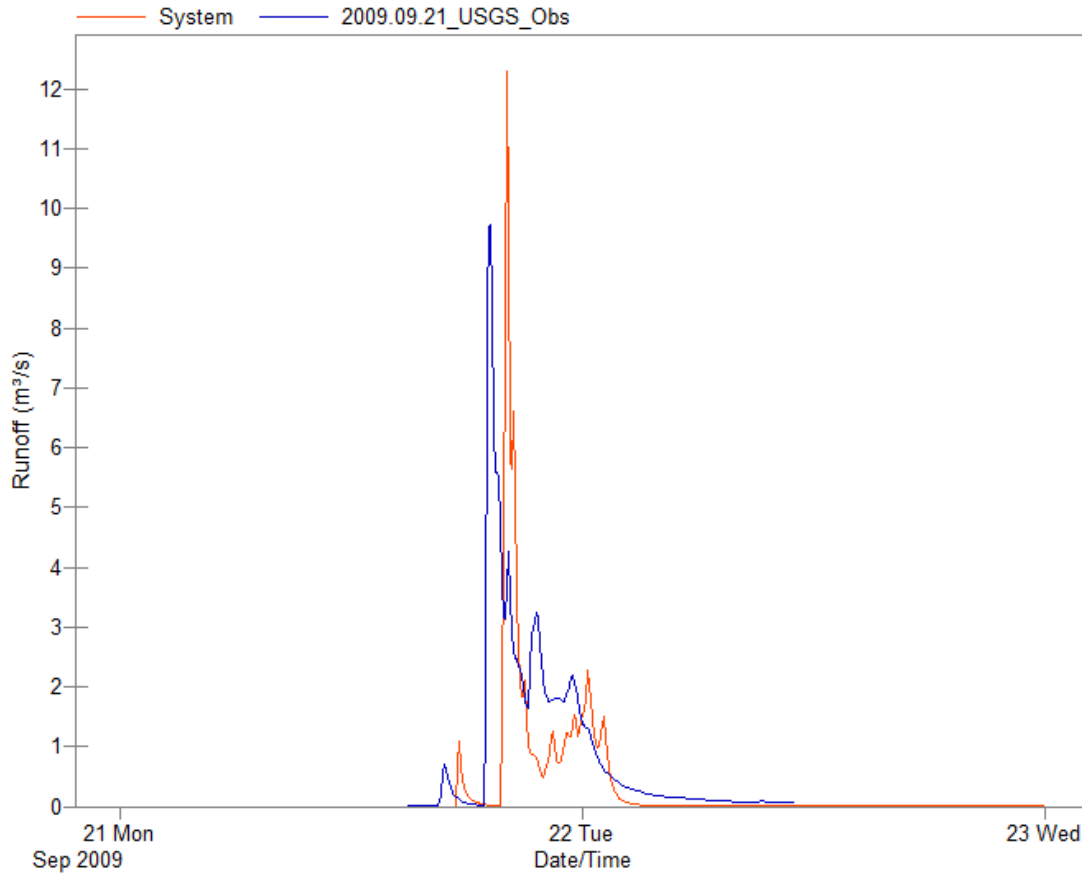


Figure 7.3. Observed versus predicted storm hydrograph. Observed storm hydrograph (discharge over time, cms) from the USGS Gaging Station at the Mullins Creek catchment outlet (blue line) versus the predicted storm hydrograph from the SWMM output, for the 22 September 2009 storm event.

conditions. Once existing conditions are modeled, predicted responses to catchment LULC change could be modeled as well.

With regard to using observed versus predicted infiltration data, the model output was more sensitive to changes in infiltration data when the percent ISA was set to equal percent TIA. Based on predicted versus observed peak discharge and total runoff results for each scenario, the higher the percent of impervious surface in the catchment, the more important the use of observed soil infiltration data in the model. Parameterizing the SWMM model with observed versus predicted infiltration data resulted in minimal change in the accuracy of the peak discharge prediction, however, the predicted results for total runoff were improved by the inclusion of the observed infiltration data.

For scenario 1 and 2, the SWMM model was run using the estimated percent DCIA for the percent ISA parameter. For scenarios 3 and 4, the SWMM model was run using percent TIA for the percent ISA parameter. The model results were more accurate using percent TIA versus percent DCIA. This was an important finding because TIA can be readily estimated for most catchments fairly accurately and with a relatively low level of effort, however, predicting percent DCIA can be a much more complex issue. The modeler would have to make assumptions and/or spend a large amount of time collecting ground reference data to determine what impervious surfaces were directly connected to stormwater drainage networks, and what percent flowed to pervious areas. Even percentages of rooftops that are directly connected must be estimated.

The nine storm events were run through SWMM for the four different infiltration/impervious surface scenarios for a total of 36 model runs. Results for each storm for each run are presented in Table 7.3, 7.4, 7.5, and 7.6.

For five out of nine storm events, the observed versus predicted peak discharges were the most accurate for scenarios 2 and 4, where percent ISA was equal to percent TIA. The first two storm events, 12 April 2009 and 5 August 2009, were removed from calculations of error because

Table 7.3. Observed vs. predicted SWMM model results for the first infiltration scenario. (Percent error is equal to  $|\text{observed} - \text{predicted}|/\text{observed} \times 100$ ).

SWMM Model Scenario 1						
Storm Date	Observed Peak Discharge (cms)	Predicted Peak Discharge (cms)	Percent Error	Observed Total Runoff (m <sup>3</sup> )	Predicted Total Runoff (m <sup>3</sup> )	Percent Error
12 April 2009	4.6	6.0	30.3	44130.0	48040.0	8.9
05 August 2009	19.1	31.3	63.5	62410.0	73050.0	17.0
10 August 2009	10.3	5.3	48.2	23840.0	14660.0	38.5
21 September 2009	9.7	9.1	6.1	65650.0	28270.0	56.9
08 October 2009	32.2	5.5	82.9	228200.0	48920.0	78.6
29 October 2009	11.9	4.7	60.0	68020.0	11010.0	83.8
27 June 2010	5.6	4.3	23.8	18550.0	10950.0	41.0
27 February 2011	20.7	15.5	25.1	60920.0	20540.0	66.3
22 September 2011	6.1	5.6	7.4	45250.0	24270.0	46.4

Table 7.4. Observed vs. predicted SWMM model results for the second infiltration scenario.

SWMM Model Scenario 2						
Storm Date	Observed Peak Discharge (cms)	Predicted Peak Discharge (cms)	Percent Error	Observed Total Runoff (m <sup>3</sup> )	Predicted Total Runoff (m <sup>3</sup> )	Percent Error
12 April 2009	4.6	8.6	88.2	44130.0	70690.0	60.2
05 August 2009	19.1	45.2	136.3	62410.0	107000.0	71.4
10 August 2009	10.3	6.9	33.1	23840.0	21290.0	10.7
21 September 2009	9.7	12.3	26.5	65650.0	41120.0	37.4
08 October 2009	32.2	7.8	75.8	228200.0	71540.0	68.7
29 October 2009	11.9	6.5	45.2	68020.0	16020.0	76.4
27 June 2010	5.6	5.6	0.9	18550.0	15930.0	14.1
27 February 2011	20.7	20.7	0.1	60920.0	29870.0	51.0
22 September 2011	6.1	7.8	28.2	45250.0	35300.0	22.0

Table 7.5. Observed vs. predicted SWMM model results for the second infiltration scenario.

SWMM Model Scenario 3						
Storm Date	Observed Peak Discharge (cms)	Predicted Peak Discharge (cms)	Percent Error	Observed Total Runoff (m <sup>3</sup> )	Predicted Total Runoff (m <sup>3</sup> )	Percent Error
12 April 2009	4.6	7.7	67.9	44130.0	57830.0	31.0
05 August 2009	19.1	46.5	143.1	62410.0	145500.0	133.1
10 August 2009	10.3	5.3	48.2	23840.0	14390.0	39.6
21 September 2009	9.7	9.1	6.1	65650.0	28600.0	56.4
08 October 2009	32.2	5.5	82.8	228200.0	49920.0	78.1
29 October 2009	11.9	4.7	60.0	68020.0	11010.0	83.8
27 June 2010	5.6	4.3	23.8	18550.0	10950.0	41.0
27 February 2011	20.7	15.7	24.2	60920.0	21440.0	64.8
22 September 2011	6.1	5.6	7.4	45250.0	24310.0	46.3

Table 7.6. Observed vs. predicted SWMM model results for the third and final infiltration scenario.

SWMM Model Scenario 4						
Storm Date	Observed Peak Discharge (cms)	Predicted Peak Discharge (cms)	Percent Error	Observed Total Runoff (m <sup>3</sup> )	Predicted Total Runoff (m <sup>3</sup> )	Percent Error
12 April 2009	4.6	10.0	118.6	44130.0	79730.0	80.7
05 August 2009	19.1	59.8	212.7	62410.0	167300.0	168.1
10 August 2009	10.3	6.9	33.6	23840.0	21280.0	10.7
21 September 2009	9.7	12.3	26.5	65650.0	41730.0	36.4
08 October 2009	32.2	7.8	75.7	228200.0	72680.0	68.2
29 October 2009	11.9	6.5	45.3	68020.0	16010.0	76.5
27 June 2010	5.6	5.6	0.8	18550.0	15920.0	14.2
27 February 2011	20.7	20.9	0.8	60920.0	31000.0	49.1
22 September 2011	6.1	7.8	28.1	45250.0	35410.0	21.7



the predicted peak discharge and total runoff were greater than the observed for scenario 1, the scenario for which the least runoff was predicted. For subsequent modeling scenarios, the percent error got progressively worse as the predicted values were even further from the observed values. The percent error for peak discharge was the best for the three storms from 2010 and 2011 (0.8 – 28.1%). Multiple parameters used in the SWMM model were based on a LULC dataset from 2010, so the storm events in 2010 and 2011 may have been during a time when the model parameters matched up the best with existing conditions in the catchment. All of the percentage errors for total runoff were minimized for scenarios 2 and 4 as well.

While peak discharge and total runoff were the output values used to determine the accuracy of the SWMM model, the SWMM model also created a storm hydrograph as an output to compare to the observed hydrograph created from data downloaded from the USGS from the gaging station located at the Mullins Creek catchment outlet (07048480). The storm hydrograph results presented more subtle information on the accuracy of the SWMM model including time of peak, and the reflection of smaller peaks and trends in the hydrographs. One of the most successful runs for the observed versus predicted storm hydrograph (scenario 4) was for the 27 June 2010 storm event (Figure 7.4). While the difference between the time of peak for observed versus predicted was about 55 minutes, the percent error for the peak discharge (0.8%) and total runoff (14.2%) were very low. If the data were shifted to peak at the same time, the outputs would be very similar and represent a successful model run. Not all model runs were as accurate as the 27 June 2010 storm event. The storm event from 5 August 2009 was an example of high percent error for predicted versus observed (scenario 4) (Figure 7.5). The error in the peak discharge was 136.3%, and for total runoff was 71.4%, but the shapes of the hydrographs are similar. The offset of the peak discharge was about 55 minutes as with the 27 June 2010 storm event.

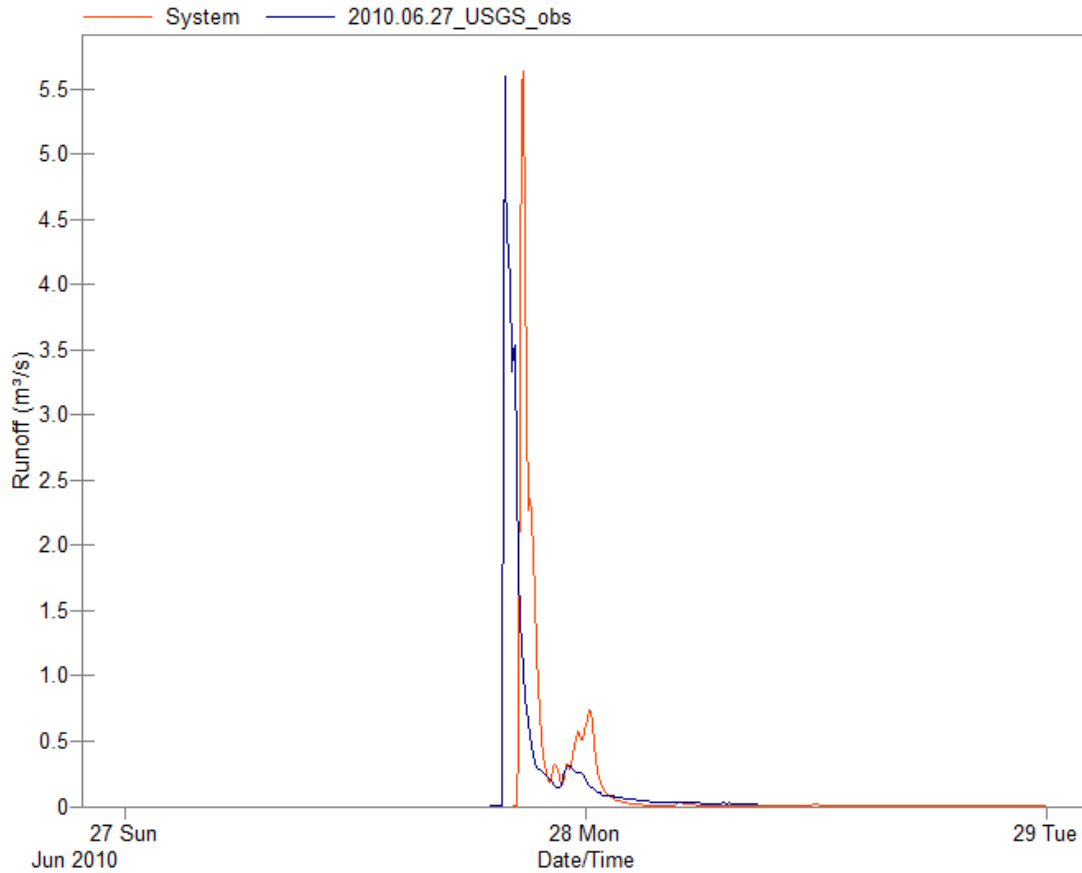


Figure 7.4. Predicted (red line) versus observed (blue line) runoff for Mullins Creek catchment. The predicted runoff hydrograph is based on observed data for infiltration and percent impervious = percent total impervious area (TIA) (Scenario 4). Observed data were downloaded from USGS gaging station data for the Mullins Creek gaging station: 27 June 2010 Storm Event.

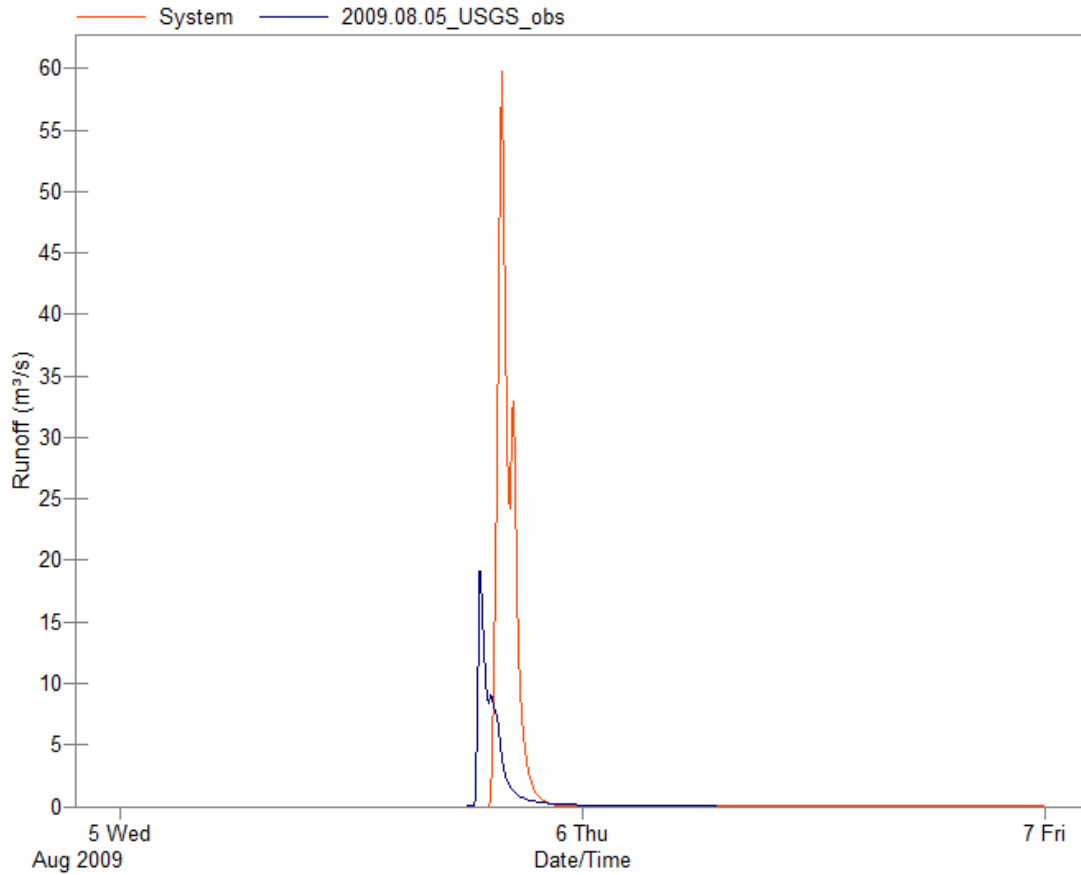


Figure 7.5. Predicted (red line) versus observed (blue line) runoff for Mullins Creek catchment. The predicted runoff hydrograph is based on observed data for infiltration and percent impervious = percent total impervious area (TIA) (Scenario 4). Observed data were downloaded from USGS gaging station data for the Mullins Creek gaging station: 05 August 2009 Storm Event.

Overall, the model performed well for most of the storm events tested when the percent impervious surface is set to equal total impervious area versus directly connected impervious area only. Including the observed soil infiltration data increased the peak discharge and total runoff values predicted by the model, but only a small amount, and not at all for smaller storm events. If a quality comprehensive dataset is available, and it is used appropriately, an uncalibrated SWMM model for a small urban catchment can be used to approximate existing conditions and predict changes in the system in response to changes in the catchment. It is strongly recommended that some observed data (precipitation and runoff) for at least a handful of storm events be collected at any site like this to confirm that predicted results are within a reasonable range of observed.

## Chapter 8. Summary and Conclusions

The Mullins Creek catchment on the University of Arkansas campus in Fayetteville, Arkansas is a dynamically changing urban stream system with a heterogeneous mix of a wide range of land uses/land covers (LULC), an extensive stormwater drainage network, and a highly altered rainfall/runoff regime. It was determined that an EPA Storm Water Management Model (SWMM) could be developed for an urban catchment that could provide useful predictions of existing and future conditions, even without calibration, if a representative set of parameters were extracted for the model from high quality/accurate datasets. However, even with a good quality set of input parameters and sufficient availability of necessary data, the collection of observed data, both precipitation inputs and runoff, is highly recommended to ensure the validity of the urban hydrologic model for the purposes it was developed.

Data were collected for this study to determine if differences in soil characteristics existed for the same soil map unit but under different maintenance regimes. Infiltration rates (overall, initial, final), bulk densities and soil particle size analyses were performed on pairs of sites in the same soil map unit, but under different levels of maintenance: minimally maintained = infrequent disturbance, and highly maintained = frequently disturbed. Infiltration rates were expected to be lower for the highly maintained sites, and the bulk densities were predicted to be higher. Soil particle sizes were predicted to be different for at least some of the pairs of sites given that during development, native top soil can be replaced with non-native soil.

Infiltration rates observed in the highly maintained sites were lower than for the minimally maintained sites. The water levels in the infiltrometers for the minimally maintained sites were more likely to decrease rapidly as the water readily infiltrated into the soil. Incorporating the observed infiltration rates into the SWMM model resulted in a 50% reduction in Horton infiltration parameters for the Mullins Creek subcatchment. Bulk densities were greater for highly maintained sites than minimally maintained sites as a result of compaction during development, and ongoing

compaction from maintenance, foot traffic, and occasional vehicle traffic (i.e. parking for athletic events). The higher bulk densities and lower infiltration rates support research that highly maintained pervious surfaces can behave more like impervious surfaces than their minimally maintained counterparts.

The Mullins Creek catchment has a highly extensive stormwater drainage network which greatly decreases the time of concentration ( $t_c$ ) and lag time of the system. The runoff response to a rainfall event is much more rapid than if the system was undeveloped. The catchment is highly urbanized with over 90% of the catchment categorized as developed in some way (roads, low intensity urban, high intensity urban), and almost 50% of the catchment is covered by impervious surfaces. This high level of impervious surface area in the catchment puts Mullins Creek firmly in the “degraded” or “non-supporting” categories for stream health according to Arnold and Gibbons (1996), and Schueler (1994). The high level of imperviousness of the catchment combined with an extensive stormwater drainage network (50.2 m of pipe per hectare) makes for a highly efficient drainage system with water moving rapidly from the land surface to the receiving waterway.

A SWMM model was developed for the Mullins Creek catchment using available datasets for elevation, LULC, soil map units, percent impervious surface, and information about the stormwater drainage network to parameterize the model. After the model was parameterized using the available datasets, the sensitivity of the model to percent impervious surface, and infiltration rates was examined. While relative sensitivities of the model to changes in different parameters are traditionally reported in the literature, a goal of this sensitivity analysis was to understand how changes in the selected parameters were reflected quantitatively in the model output. Another goal was to understand how the sensitivity of the model output to changes in the selected parameters was affected by the size of the storm event modeled.

The Mullins Creek SWMM model output was more sensitive to changes in percent impervious surface than in changes in the Horton infiltration parameters. A 10% increase in

percent impervious surface resulted in a 30.9% increase in peak discharge, and an 18.0% increase in total runoff. A 10% decrease in Horton infiltration parameters resulted in a 10.8% increase in peak discharge, and a 6.8% increase in total runoff. However, the sensitivity of the model to changes in the selected parameters varied over different size precipitation events. The model outputs (peak discharge and total runoff) were more sensitive to changes in percent impervious surface area for smaller storm events. For a 25 mm storm event, a 10% increase in percent impervious surface area resulted in a peak discharge increase of 72.7% and an increase in total runoff of 42.9%. The sensitivity of the model to changes in percent impervious surface was also higher when the initial percentage of impervious surface was low. For a 25 mm storm event, when the percent impervious surface increased from 20 to 30%, the peak discharge increased by 82.5%, and the total runoff increased by 175.8%. This reflected results presented in the research on the affects that even small percentages of impervious surface in a catchment can have on stream stability, stream health, and the quality of aquatic ecosystems in a receiving waterway (Schueler, 1994; Arnold and Gibbons, 1996; Booth and Jackson, 1997). The Mullins Creek SWMM model output was most sensitive to changes in Horton infiltration rates for moderate to large storm events (> 150 mm) where a 10% decrease in Horton infiltration rates resulted in a 12% increase in peak discharge, and an increase in total runoff of over 9%. When modeling flooding conditions in a catchment, observed soil infiltration data is an important input parameter for obtaining an accurate result and for developing a predictive hydrologic model.

The parameterized Mullins Creek SWMM model was run under four different sets of conditions (scenarios) to determine what inputs would result in the most accurate predicted values. The scenarios are presented in Figure 8.1. The arrows in the figure represent increasing runoff potential for the model parameter inputs. Scenario 1 represents the highest infiltration/lowest runoff potential. The first two observed storm events modeled from 2009 resulted in a peak discharge and total runoff prediction greater than the observed. Therefore, the

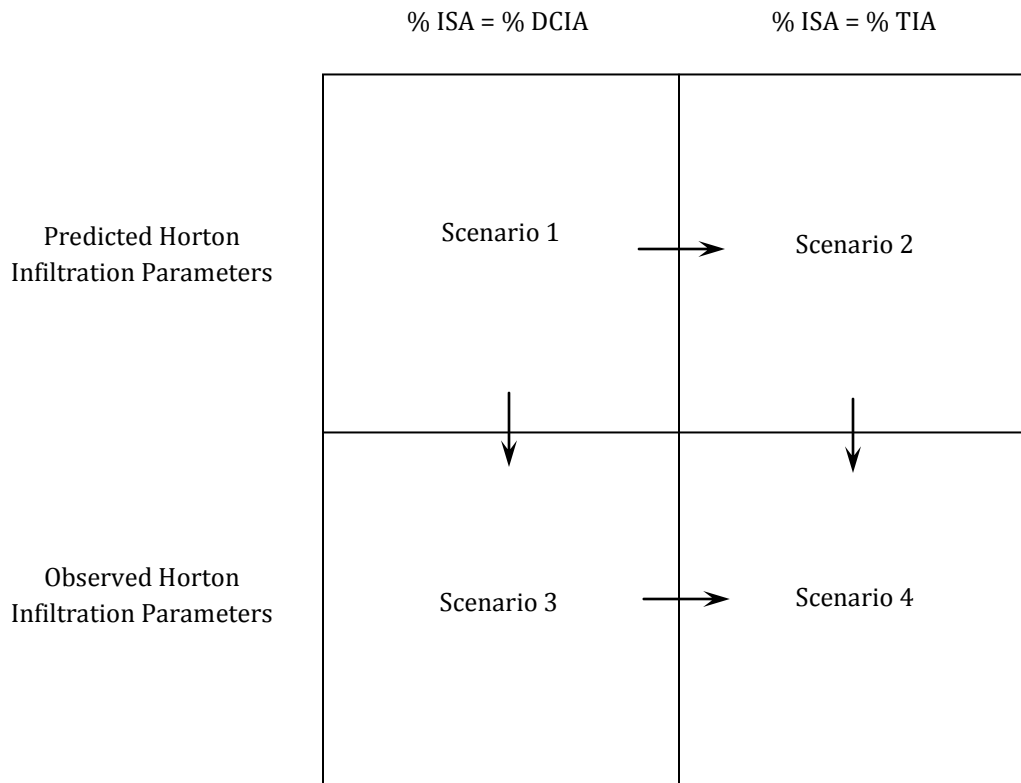


Figure 8.1. Mullins Creek SWMM modeling scenarios for validation of the uncalibrated model. Arrows point to decreasing runoff and increasing runoff potential.



percent error for these storm predictions increase for subsequent modeling scenarios, and were excluded from the analysis. The model performed best for the observed storms in 2010 and 2011. This represented one of the challenges in modeling dynamically changing urban systems. The LULC layer used to parametrize the model was developed from 2010 data. The parameterized model may not have reflected the conditions that existed during the observed storm events in 2009.

For the seven remaining events, modeling scenarios 2 and 4 resulted in the lowest percent error for peak discharge and total runoff in predicted versus observed values. The uncalibrated model performed the best overall for scenario 4 when observed soil infiltration data were incorporated into the model, and percent TIA was used for percent impervious surface area. Collecting accurate data for and determining percent directly connected impervious area (DCIA) is much more of a challenge than determining an accurate percent TIA for a catchment. The time necessary to collect observed infiltration data for a catchment was worth the effort to improve the output for the Mullins Creek SWMM model while more extensive impervious surface connection analysis would not have been helpful to improving model results.

Target values for a calibrated hydrologic model to be considered successful have been listed in the literature as within 10% for total runoff, and within 30% for peak discharge. Results from the uncalibrated Mullins Creek SWMM model run for scenario 4 were an average of 30% error overall for peak discharge, and 39.5% error for total runoff. If the storms of 2010 and 2011 are analyzed separately, the percent error improves for the peak discharge (9.9%) and total runoff (28.3%).

When modeling a dynamically changing urban system, only a small window of data can be used for validation and calibration purposes, and datasets must be selected carefully based on the timeline/conditions the modeler wants to capture. The temporal resolution of the datasets must also be considered if modeling over an extensive time period is the goal. Collecting observed soil infiltration data led to better prediction of peak discharge and total runoff for the Mullins Creek SWMM model, and is important to capturing accurate existing conditions in a catchment. Based on

these results, SWMM can be used to model urban headwater systems with limited observed data available for calibration. For dynamically changing urban systems, a relatively small observed dataset that is collected during the time period of interest may be of greater value than a dataset collected over many decades.

## References

- Akan, A.O., and R.J. Houghtalen. 2003. *Urban Hydrology, Hydraulics and Stormwater Quality – Engineering Applications and Computer Modeling*. Hoboken, New Jersey: John Wiley & Sons, Inc.
- Alley, W.M., and J.E. Veenhuis. 1983. Effective impervious area in urban runoff modeling. *Journal of Hydraulic Engineering* 109(2): 313-319
- Arkansas Geological Survey. 2014. Geology of the Ozark Plateau Region. Little Rock, Arkansas: Arkansas Geological Survey. Retrieved from: [http://www.geology.ar.gov/education/ozark\\_plateaus.htm](http://www.geology.ar.gov/education/ozark_plateaus.htm). Accessed online: 07/22/2014.
- Arkansas State Land Information Board (ASLIB). 2014. Arkansas Centerline File. Little Rock, Arkansas: Arkansas State Land Information Board.
- ASLIB, 2007. 2006 Five Meter Resolution Digital Elevation Model (raster). Little Rock, Arkansas: Arkansas State Land Information Board.
- Arnold, C.L., and C.J. Gibbons. 1996. Impervious surface coverage: The emergence of a key environmental indicator. *Journal of the American Planning Association* 62(2): 243-258.
- Barco, J., K.M. Wong, and M.K. Stenstrom. 2008. Automatic calibration of the U.S. EPA SWMM model for a large urban catchment. *Journal of Hydraulic Engineering* 134(4): 466-474.
- Beaver Water District (BWD). 2010. Beaver Lake and its Watershed. Lowell, Arkansas: Beaver Water District.
- BWD. 2014. Production Data. Lowell, Arkansas: Beaver Water District. Retrieved from: <http://www.bwdh2o.org/about-us/production-data/> Accessed online: 07/21/2014.
- Bedient, P.B., W.C. Huber, and B.E. Vieux. 2008. *Hydrology and Floodplain Analysis*. 4<sup>th</sup> Ed. Upper Saddle River, New Jersey: Prentice Hall.
- Beven, K. 1989. Changing ideas in hydrology – the case of physically-based models. *Journal of Hydrology* 105: 157-172.
- Bhaduri, B., M. Minner, S Tatalovich, and J. Harbor. 2001. Long-term hydrologic impact of urbanization: A tale of two models. *Journal of Water Resources Planning and Management* 127: 13-19.
- Booth, D.B. 1990. Stream-channel incision following drainage-basin urbanization. *Water Resources Bulletin* 26(3): 407-417.
- Booth, D.B. 1991. Urbanization and the natural drainage system – Impacts, solutions, and prognoses. *The Northwest Environmental Journal* 7(1): 93-118.
- Booth, D.B., D. Hartley, and R. Jackson. 2002. Forest cover, impervious-surface area, and the mitigation of stormwater impacts. *Journal of the American Water Resources Association* 38(3): 835-845.

- Booth, D.B., and C. R. Jackson. 1997. Urbanization of aquatic systems: Degradation thresholds, stormwater detention, and the limits of mitigation. *Journal of the American Water Resources Association* 22(5): 1 -20.
- Brabec, E., S. Schulte, and P.L. Richards. 2002. Impervious surfaces and water quality: A review of current literature and its implications for watershed planning. *Journal of Planning Literature* 16(4): 499-514.
- Butler, D., and J.W. Davies. 2004. *Urban Drainage*. 2<sup>nd</sup> Ed. New York, New York: Spon Press.
- Centore, P. 2013. Conversions between the Munsell and sRGB colour systems. Published online: <http://www.99main.com/~centore/ConversionsBetweenMunsellAndRGBsystems.pdf>. Accessed online: 11/22/2014.
- CHI. 2014. PCSWMM 2013 Professional: Version 5.4.1528. Guelph, Ontario, Canada: Computational Hydraulics International.
- Choi, K-S., and J.E. Ball. 2002. Parameter estimation for urban runoff modelling. *Urban Water* 4:31-41.
- City of Fayetteville (COF). 2014. City of Fayetteville Utilities Viewer. Fayetteville, Arkansas: City of Fayetteville. Retrieved from: <http://gis2.accessfayetteville.org/GISPage/Utilities/> arcgis desk. Accessed online: 07/22/2014.
- DeBarry, P.A. 2004. *Watersheds: Processes, Assessment, and Management*. Hoboken, New Jersey: John Wiley & Sons, Inc.
- Denault, C., R.G. Millar, and B.J. Lance. 2006. Assessment of possible impacts of climate change in an urban catchment. *Journal of the American Water Resources Association* 42(3): 685-697.
- Dinicola, R.S. 1989. Characterization and simulation of rainfall-runoff relations for headwater basins in western King and Snohomish Counties, Washington. U.S. Geological Survey Water-Resources Investigation Report 89-4052. Tacoma, Washington: U.S. Geological Survey.
- Espy, W.H., C.W. Morgan, and F.D. Masch. 1966. A study of some effects of urbanization on storm runoff from a small watershed. Report 23. Austin, Texas: Texas Water Development Board.
- ESRI. 2014. ArcGIS Desktop: Release 10.2. Redlands, CA: Environmental Systems Research Institute.
- ESRI. 2008. ArcGIS Desktop Help 9.2. Redlands, CA: Environmental Systems Research Institute. Retrieved from: <http://webhelp.esri.com/arcgisdesktop/9.2/index.cfm?TopicName=welcome> Accessed Online: 11/02/2014.
- Ferguson, B.K. 1994. *Stormwater Infiltration*. Boca Raton, Florida: CRC Press.
- Fletcher, T.D., H. Andrieu, and P. Hamel. 2013. Understanding, management and modelling of urban hydrology and its consequences for receiving waters: A state of the art. *Advances in Water Resources* 51: 261-279.

- FISRWG. 1998. Stream Corridor Restoration: Principles, processes, and Practices. PB98-158348LUW, Washington, D.C.: Federal Interagency Stream Restoration Working Group.
- Formica, S.J., M. Van Eps, T. Morris, J. Beck, A. Cotter, and P. Srivastava. 2004. West Fork White River Watershed – Data Inventory and Nonpoint Source Pollution Assessment. Final Report: FY99 CWA Section 319(h). Little Rock, Arkansas: Arkansas Department of Environmental Quality, Environmental Preservation Division.
- Gardiner, D.T., and R.W. Miller. 2004. *Soils in Our Environment*. 10<sup>th</sup> Ed. Upper Saddle River, New Jersey: Pearson Education, Inc.
- Goldstein, A., K. DiGiovanni, and F. Montalto. 2010. Resolution and sensitivity analysis of a block-scale urban drainage model. In *Proceedings of the World Environmental and Water Resources Congress 2010: Challenges of Change*, R.N. Palmer, Ed. Reston, Virginia: American Society of Civil Engineers.
- Gorham, B. 2012a. 2010 Arkansas 4-meter Resolution Impervious Surface Map. Fayetteville, Arkansas: University of Arkansas, Center for Advanced Spatial Technologies.
- Gorham, B. 2012b. 2010 Arkansas 4-meter Resolution Land-Cover Map. Fayetteville, Arkansas: University of Arkansas, Center for Advanced Spatial Technologies.
- Green, W.H., and G.A. Ampt. 1911. Studies of soil physics, 1: The flow of air and water through soils. *Journal of Agriculture Science* 4(1): 1-24.
- Gregory, J.H., M.D. Dukes, P.H. Jones, and G.L. Miller. 2006. Effect of urban soil compaction on infiltration rate. *Journal of Soil and Water Conservation* 61(3): 117-124.
- Grimm, N.B., J.M. Grove, S.T.A. Pickett, and C.L. Redman. 2000. Integrated approaches to long-term studies of urban ecological systems. *BioScience* 50(7): 571-584.
- Hamilton, G.W., and D.V. Waddington. 1999. Infiltration rates on residential lawns in central Pennsylvania. *Journal of Soil and Water Conservation* 54(3): 564-568.
- Horton, R.E. 1939. Analysis of runoff-plat experiments with varying infiltration-capacity. *Transactions, American Geophysical Union* 20: 693-711.
- Horton, R.E. 1933. The role of infiltration in the hydrologic cycle. *Transactions, American Geophysical Union* 14(1): 446-460.
- Huber, W.C., and R.E. Dickinson. 1988. *Storm Water Management Model, Version 4, User's Manual*, EPA/600/3-88/001a (NTIS PB88-236641/AS), Athens, Georgia: U.S. Environmental Protection Agency.
- Huber, W.C., and R. E. Dickinson. 1992. *Storm Water Management Model User's Manual, Version 4*. Cincinnati, Ohio: U.S. Environmental Protection Agency.
- Jang, S., M. Cho, J. Yoon, Y. Yoon, S. Kim, G. Kim, L. Kim, and H. Aksoy. 2007. Using SWMM as a tool for hydrologic impact assessment. *Desalination* 212: 344-356.

- Keen-Zebert, A. 2007. Channel responses to urbanization: Scull and Mud Creeks in Fayetteville, Arkansas. *Physical Geography* 28(3): 249-260.
- King County. 1993. Issaquah Creek Basin and Nonpoint Action Plan. Seattle, Washington: Department of Public Works, Surface Water Management Division.
- Koehn, K., K.R. Brye, and C. Scarlet. 2011. Quantification of stormwater runoff using a combined GIS and curve number approach: a case study for an urban watershed in the Ozark Highlands, USA. *Urban Water Journal* 8(4): 255-265.
- Konrad, C.P., and D.B. Booth. 2005. Hydrologic changes in urban streams and their ecological significance. *American Fisheries Society Symposium* 47: 157-177.
- Lee, J.G., and J.P. Heaney. 2003. Estimation of urban imperviousness and its impacts on stream water systems. *Journal of Water Resources Planning and Management* 129(5): 419-426.
- Leopold, L.B. 1968. Hydrology for urban land use planning. A guidebook on the hydrologic effects of urban land use. *U.S. Geological Survey Circular 554*. Washington, D.C.: U.S. Geological Survey.
- MacArthur, R., and J.J. DeVries. 1993. *Introduction and application of kinematic wave routing techniques using HEC-1*. Vicksburg, Mississippi: U.S. Army Corps of Engineers.
- May, C.W., R.R. Horner, J.R. Karr, B.W. Mar, and E.B. Welch. 1997. Effects of urbanization on small streams in the Puget Sound lowland ecoregion. *Watershed Protection Techniques* 2(4): 483-494.
- McCoy, K. 2012. Comprehensive drainage study of the upper reach of College Branch in Fayetteville, Arkansas. MS Thesis. Fayetteville, AR: University of Arkansas, Department of Civil Engineering.
- McCuen, R.H. 2005. *Hydrologic Analysis and Design, 3rd Edition*. Upper Saddle River, New Jersey: Prentice Hall.
- Meierdiercks, K.L., J.A. Smith, M.L. Baeck, and A.J. Miller. 2010. Analyses of urban drainage network structure and its impact on hydrologic response. *Journal of the American Water Resources Association* 46(5): 932-943.
- National Climatic Data Center (NCDC). 2014. NEXRAD Level III Data. Asheville, North Carolina: National Oceanic Atmospheric Administration (NOAA). Retrieved from: <https://www.roc.noaa.gov/WSR88D/Level III/Level3Info.aspx> Accessed online: 08/24/2014.
- Natural Resource Conservation Service (NRCS). 1994. STATSGO Soils (polygon). Washington, D.C.: USDA Natural Resources Conservation Service.
- Natural Resource Conservation Service (NRCS). 2014a. National Soil Survey Handbook (NSSH), Title 430-VI. Washington, D.C.: USDA Natural Resources Conservation Service.
- NRCS. 2014b. Soil texture calculator. Retrieved from: [http://www.nrcs.usda.gov/wps/portal/nrcs/detail/soils/survey/?cid=nrcs142p2\\_054167](http://www.nrcs.usda.gov/wps/portal/nrcs/detail/soils/survey/?cid=nrcs142p2_054167), Accessed online: 06/26/2014.

- NRCS. 2014c. Official Soil Series Descriptions (OSDs). Retrieved from:  
[http://www.nrcs.usda.gov/wps/portal/nrcs/detail/soils/survey/class/?cid=nrcs142p2\\_053587](http://www.nrcs.usda.gov/wps/portal/nrcs/detail/soils/survey/class/?cid=nrcs142p2_053587)  
 Accessed online: 06/26/2014.
- NRCS. 2008. Soil quality indicators. Washington, D.C.: USDA Natural Resources Conservation Service.
- NRCS. 2004. Hydrologic Soil-Cover Complexes (Chapter 9). In: Part 630 Hydrology National Engineering Handbook (210-VI-NEH). Washington, D.C.: USDA Natural Resources Conservation Service.
- NRCS. 1994. STATSGO Soils (polygon). Washington, D.C.: USDA Natural Resources Conservation Service.
- Nix, S.J. 1994. *Urban Stormwater Modeling and Simulation*. Boca Raton, Florida: CRC Press, Inc.
- Oliveira, M.T., and I.A. Merwin. 2001. Soil physical conditions in a New York orchard after eight years under different groundcover management systems. *Plant and Soil* 234: 233-237.
- Overton, D.E., and M.E. Meadows. 1976. *Stormwater Modeling*. New York, New York: Academic Press, Inc.
- Park, S.Y., K.W. Less, I.H. Park, and S.R. Ha. 2008. Effect of the aggregation level of surface runoff fields and sewer network for a SWMM simulation. *Desalination* 226: 328-337.
- Paul, M.J., and J.L. Meyer. 2001. Stream in the urban landscape. *Annual Review of Ecological Systems* 32: 333-365.
- Peterson, E.W., and C.M. Wicks. 2006. Assessing the importance of conduit geometry and physical parameters in karst systems using the storm water management model (SWMM). *Journal of Hydrology* 329: 294-305.
- Pitt, R., J. Lantrip, R. Harrison, C.L. Henry and D. Xue. 1999. Infiltration through disturbed urban soils and compost-amended soil effects on runoff quality and quantity. EPA/600/R-00/016. Washington, D.C.: USEPA.
- Pitt, R., S-E. Chen, and S.E. Clark. 2002. Compacted urban soils effects on infiltration and bioretention stormwater control designs. *Proceedings of Ninth International Conference on Urban Drainage*. Portland, Oregon: ASCE.
- Pitt, R., S-E. Chen, S.E. Clark, J. Swenson, and C.K. Ong. 2008. Compaction's impacts on urban storm-water infiltration. *Journal of Irrigation and Drainage Engineering* 134(5): 652-658.
- Pouyat, R.V., I.D. Yesilonis, J. Russel-Anelli, and N.K. Neerchal. 2007. Soil chemical and physical properties that differentiate urban land-use and cover types. *Soil Sci. Soc. Am. J.* 71(3): 1010-1019.
- Rawls, W.J., D.L. Brakensiek, and N. Miller. 1983. Green-Ampt infiltration parameters from soils data. *Journal of Hydraulic Engineering* 109(1): 62-70.

- Rossman, L.A. 2010. *Storm Water Management Model User's Manual, Version 5.0*, EPA/600/R-05/040, Cincinnati, Ohio: U.S. Environmental Protection Agency.
- Roy, A.H., A.D. Rosemond, M.J. Paul, D.S. Leigh, and J.B. Wallace. 2003. Stream macroinvertebrate response to catchment urbanization (Georgia, U.S.A.). *Freshwater Biology* 48: 329-346.
- Roy, A.H., and W.D. Shuster. 2009. Assessing impervious surface connectivity and applications for watershed management. *Journal of the American Water Resources Association* 45(1): 198-209.
- Schade, T.G., and W.D. Shuster. 2005. Paired watershed study of land-use and climate change impact on small streams. In *Proceedings of World Water and Environmental Resources Congress*, R. Walton, Ed. Reston, Virginia: American Society of Civil Engineers.
- Schueler, T. 1994. The importance of imperviousness. *Watershed Protection Techniques* 1(3): 100-111.
- Schueler, T.R. 2000. The compaction of urban soils. *Watershed Protection Techniques* 3(2): 661-665.
- Shepherd, S.L, J.C. Dixon, R.K. Davis, and R. Feinstein. 201. The effect of land use on channel geometry and sediment distribution in gravel mantled bedrock streams, Illinois River watershed, Arkansas. *River Research and Applications* 27(7): 857-866.
- Slonecker, E.T., D.B. Jennings, and D. Garofalo. 2001. Remote sensing of impervious surfaces: A review. *Remote Sensing Reviews* 20: 227-255.
- Shuster, W.D., J. Bonta, H. Thurston, E. Warnemuende, and D. R. Smith. 2005. Impacts of impervious surface on watershed hydrology: A review. *Urban Water Journal* 2(4): 263-275.
- Simon, A. and C.R. Hupp. 1992. Geomorphic and vegetative recovery processes along modified stream channels of West Tennessee. U.S. Geological Survey Open File Report 91-502. Washington, D.C.: U.S. Geological Survey.
- Singh, V.P., and D.A. Woolhiser. 2002. Mathematical modeling of watershed hydrology. *Journal of Hydrologic Engineering* 7(4): 270-292.
- Soil Conservation Service (SCS). 1986. *Urban hydrology for small watersheds*, 2<sup>nd</sup> Ed., Technical Release No. 55. Washington D.C. : USDA Soil Conservation Service.
- Southern Extension and Research Activity (SERA). 2014. Soil test methods from the Southeastern United States. F.J. Sikora and K.P. Moore, Eds. Southern Cooperative Series Bulletin No. 419 (SERA-IEG-6). Lexington, Kentucky: Southern Agricultural Experimental Stations.
- Stankowski, S.J. 1972. Population density as an indirect indicator of urban and suburban land-surface modifications. U.S. Geological Survey Professional Paper 800-B. Washington, D.C.: U.S. Geological Survey.
- Sun, N., M. Hall, B. Hong, and L. Zhang. 2014. Impact of SWMM catchment discretization: Case study in Syracuse, New York. *Journal of Hydrologic Engineering* 19: 223-234.



- Teegavarapu, R.S.V., C. Viswanathan, and L. Ormsbee. 2006. Effect of digital elevation model (DEM) resolution on the hydrological and water quality modeling. In *Proceedings of the World Environmental and Water Resource Congress 2006: Examining the Confluence of Environmental and Water Concerns*, R. Graham, Ed. Reston, Virginia: American Society of Civil Engineers.
- Temprano, J., Ó. Arango, J. Cagiao, J. Suárez, and I. Tejero. 2006. Stormwater quality calibration by SWMM: A case study in Northern Spain. *Water SA* 32(1): 55-63.
- Terstriep, M.L., and J.B. Stall. 1974. The Illinois Urban Drainage Area Simulator, ILLUDAS. Bulletin 58. Urbana, Illinois: Illinois State Water Survey.
- Tsihrintzis, V.A., and R. Hamid. 1998. Runoff quality prediction from small urban catchments using SWMM. *Hydrological Processes* 12: 311-329.
- UDFCD. 2007. Drainage Criteria Manual, Version 1. Denver, Colorado: Urban Drainage and Flood Control District.
- University of Arkansas (UA). 2009. Stormwater Management Plan. Permit: ARR 040028. Fayetteville, Arkansas: University of Arkansas.
- U.S. Geological Survey (USGS). 2009. Medium resolution: national hydrography dataset flowline feature (line). Reston, Virginia: U.S. Geological Survey.
- USGS. 2014. College Branch at MLK Blvd at Fayetteville, AR (07048480) Gaging Station Data. Reston, Virginia. U.S. Geological Survey. Retrieved from: <http://waterdata.usgs.gov/ar/nwis/rt> Accessed online: 9/10/2014.
- Vannote, R.L., G.W. Minshall, K.W. Cummins, J.R. Sedell, and C.E. Cushing. 1980. The river continuum concept. *Canadian Journal of Fisheries and Aquatic Sciences* 37: 130-137.
- Walsh, C.J. 2000. Urban impacts on the ecology of receiving waters: A framework for assessment, conservation and restoration. *Hydrobiologia* 431: 107-114.
- Walsh, C.J., T.D. Fletcher, and A.B. Ladson. 2005a. Stream restoration in urban catchments through redesigning stormwater systems: looking to the catchment to save the stream. *Journal of the North American Benthological Society* 24(3): 690-705.
- Walsh, C.J., A.H. Roy, J.W. Feminella, P.D. Cottingham, P.M. Groffman, and R.P. Morgan. 2005b. The urban stream syndrome: current knowledge and the search for a cure. *Journal of the North American Benthological Society* 24(3): 706-723.
- Walsh, C.J., and J. Kunapo. 2009. The importance of upland flow paths in determining urban effects on stream ecosystems. *Journal of the North American Benthological Society* 28(4): 977-990.
- Wang, K-H., and A. Altunkaynak. 2012. Comparative case study of rainfall-runoff modeling between SWMM and fuzzy logic approach. *Journal of Hydrologic Engineering* 17(2): 283-291.
- Wang, L., J. Lyons, P. Kanehl, and R. Bannerman. 2001. Impacts of urbanization on stream habitat and fish across multiple spatial scales. *Environmental Management* 28(2): 255-266.

- Ward, A.D., and S.W. Trimble. 2004. *Environmental Hydrology*. 2<sup>nd</sup> Ed. New York, NY: CRC Press.
- Wenger, S.J., J.T. Peterson, M.C. Freeman, B.J. Freeman, and D.D. Homans. 2008. Stream fish occurrence in response to impervious cover, historic land use, and hydrogeomorphic factors. *Canadian Journal of Fisheries and Aquatic Sciences* 65: 1250-1264.
- Wigmosta, M.S., L.W. Vail, and D.P. Lettenmaier. 1994. A distributed hydrology-vegetation model for complex terrain. *Water Resources Research* 30(6): 1665-1679.
- Wolkowski, R., and B. Lowery. 2008. Soil compaction: Causes, concerns, and cures (A3367). R-05-2008. Madison Wisconsin: University of Wisconsin Extension.
- Wong, T., D. Knights, and S. Lloyd. 2008. Hydrologic, water quality and geomorphic indicators of catchment effective imperviousness. *Australian Journal of Water Resources* 12(2): 111-120.
- Wu, J.Y., J.R. Thompson, R.K. Kolka, K.J. Franz, and T.W. Stewart. 2013. *Hydrology and Earth System Sciences* 17: 4743-4758.
- Zhao, D., J. Chen, H. Wang, and Q. Tong. 2013. Application of a sampling based on the combined objectives of parameter identification and uncertainty analysis of and urban rainfall-runoff model. *Journal of Irrigation and Drainage Engineering* 139(1): 66-74.

Appendix A: Observed infiltration parameters from field data collection for each site

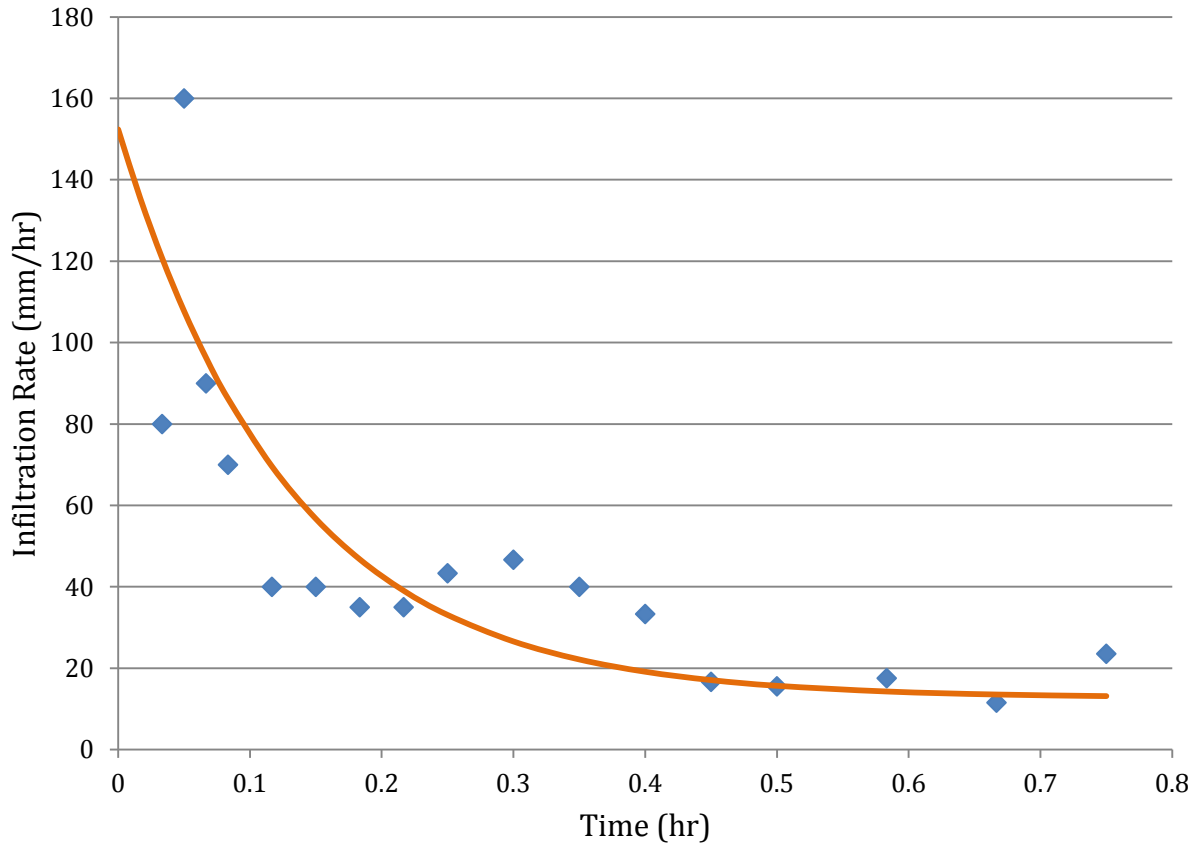


Figure A.1. Graph of observed Horton infiltration data points and the best-fit Horton infiltration curve developed from the observed dataset for the Fayetteville High School (FHS) sampling location. The points are observed infiltration rates during the test, and the line is a best-fit Horton infiltration curve.  $f_c = 12.7$  mm/hr,  $f_o = 152.4$  mm/hr, and  $k = 7.7$  1/hr.

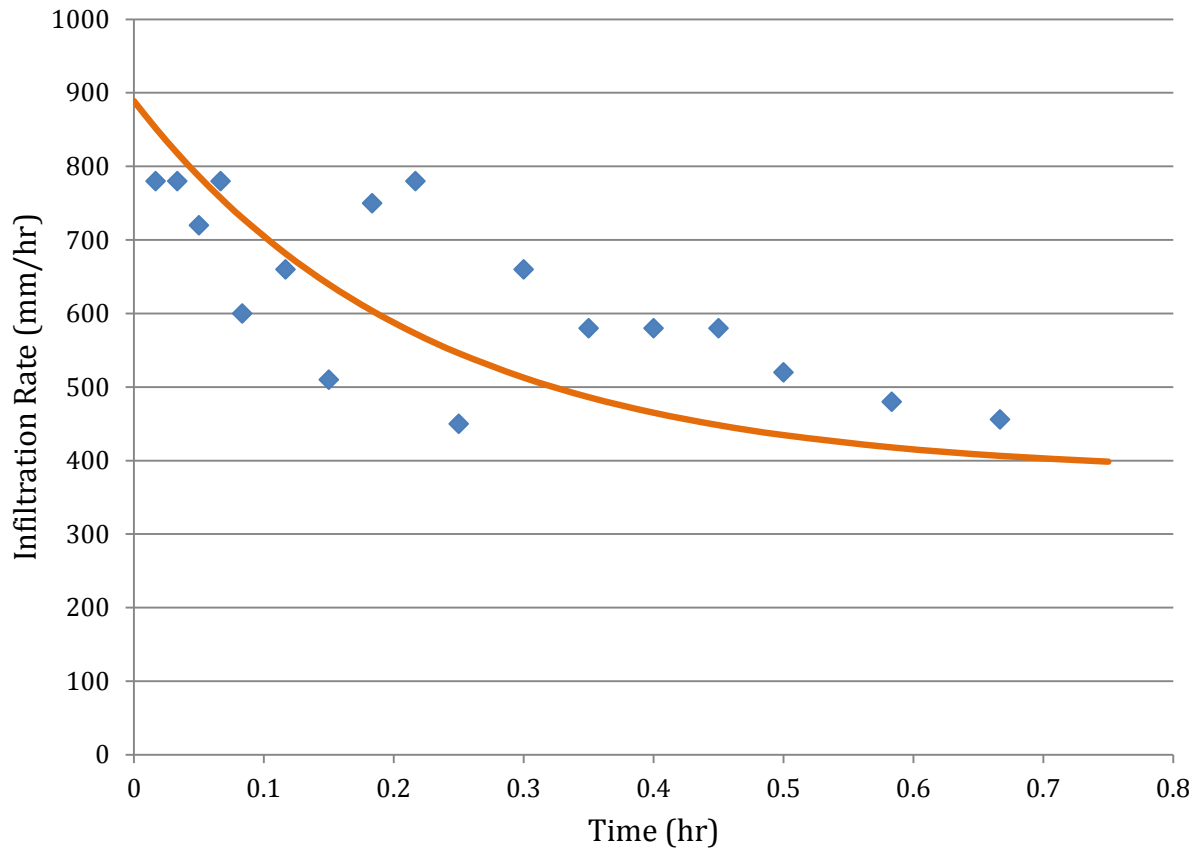


Figure A.2. Graph of observed Horton infiltration data points and the best-fit Horton infiltration curve developed from the observed dataset for the Leflar sampling location. The points are observed infiltration rates during the test, and the line is a best-fit Horton infiltration curve.  $f_c = 381$  mm/hr,  $f_o = 889$  mm/hr, and  $k = 6.5$  1/hr.

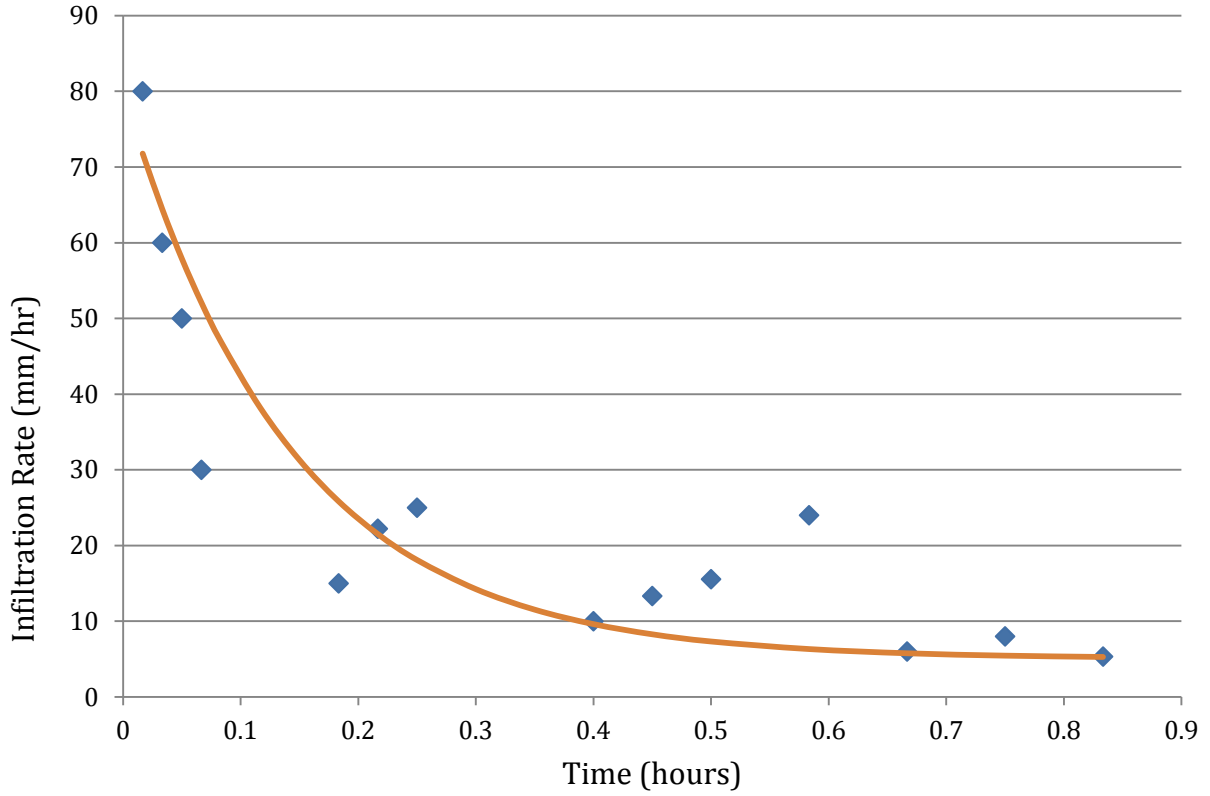


Figure A.3. Graph of observed Horton infiltration data points and the best-fit Horton infiltration curve developed from the observed dataset for the Maple Hill sampling location. The points are observed infiltration rates during the test, and the line is a best-fit Horton infiltration curve.  $f_c = 5.1$  mm/hr,  $f_o = 80.0$  mm/hr, and  $k = 7.0$  1/hr.

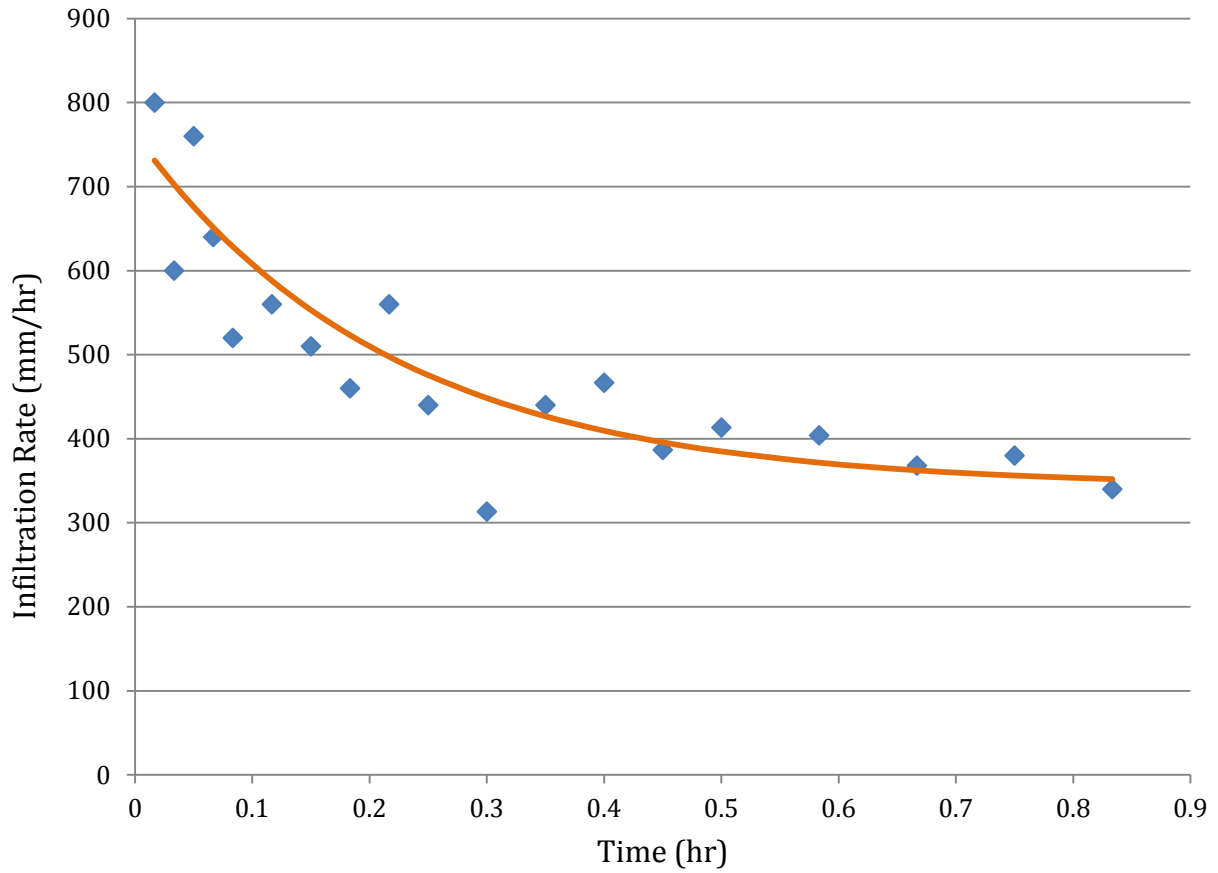


Figure A.4. Graph of observed Horton infiltration data points and the best-fit Horton infiltration curve developed from the observed dataset for the Lewis Avenue sampling location. The points are observed infiltration rates during the test, and the line is a best-fit Horton infiltration curve.  $f_c = 343$  mm/hr,  $f_o = 762$  mm/hr, and  $k = 4.6$  1/hr.

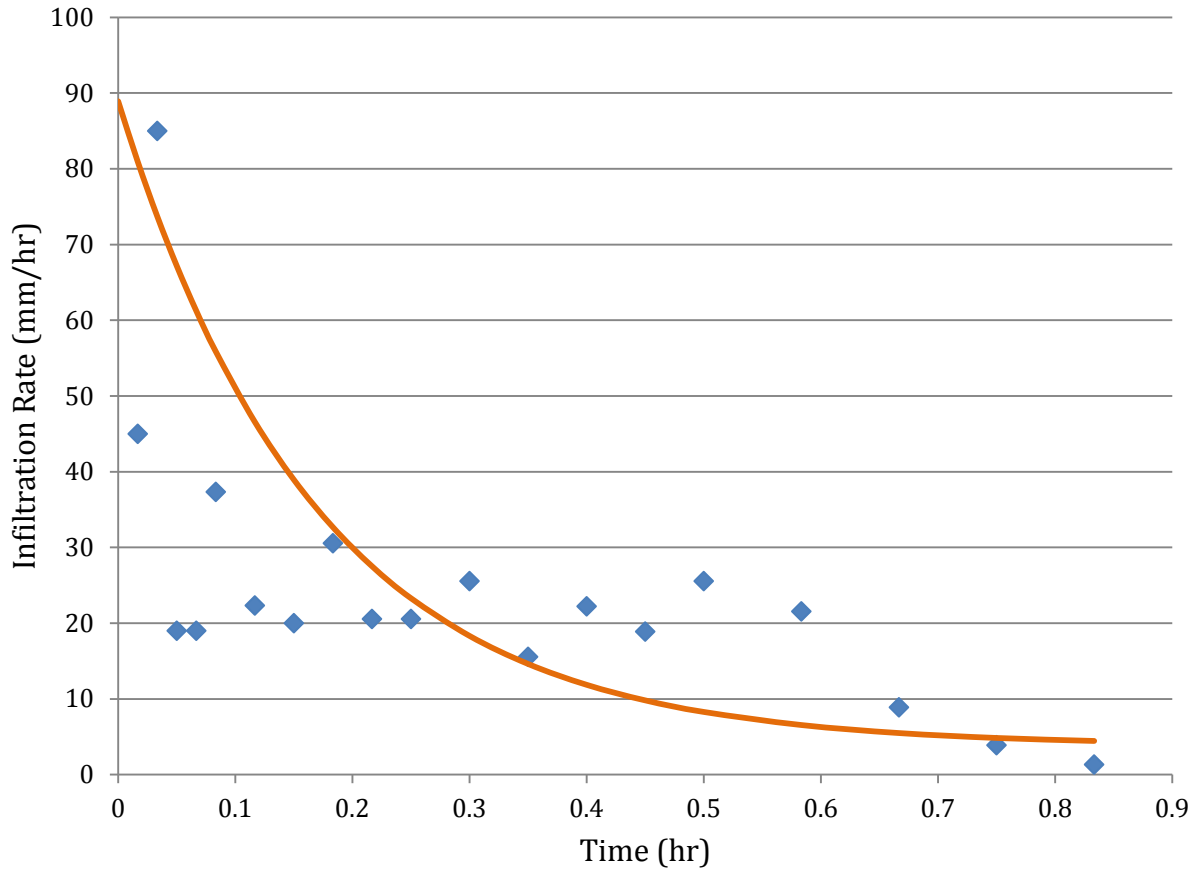


Figure A.5. Graph of observed Horton infiltration data points and the best-fit Horton infiltration curve developed from the observed dataset for the Reynold's Center sampling location. The points are observed infiltration rates during the test, and the line is a best-fit Horton infiltration curve.  $f_c = 3.8$  mm/hr,  $f_o = 88.9$  mm/hr, and  $k = 5.9$  1/hr.

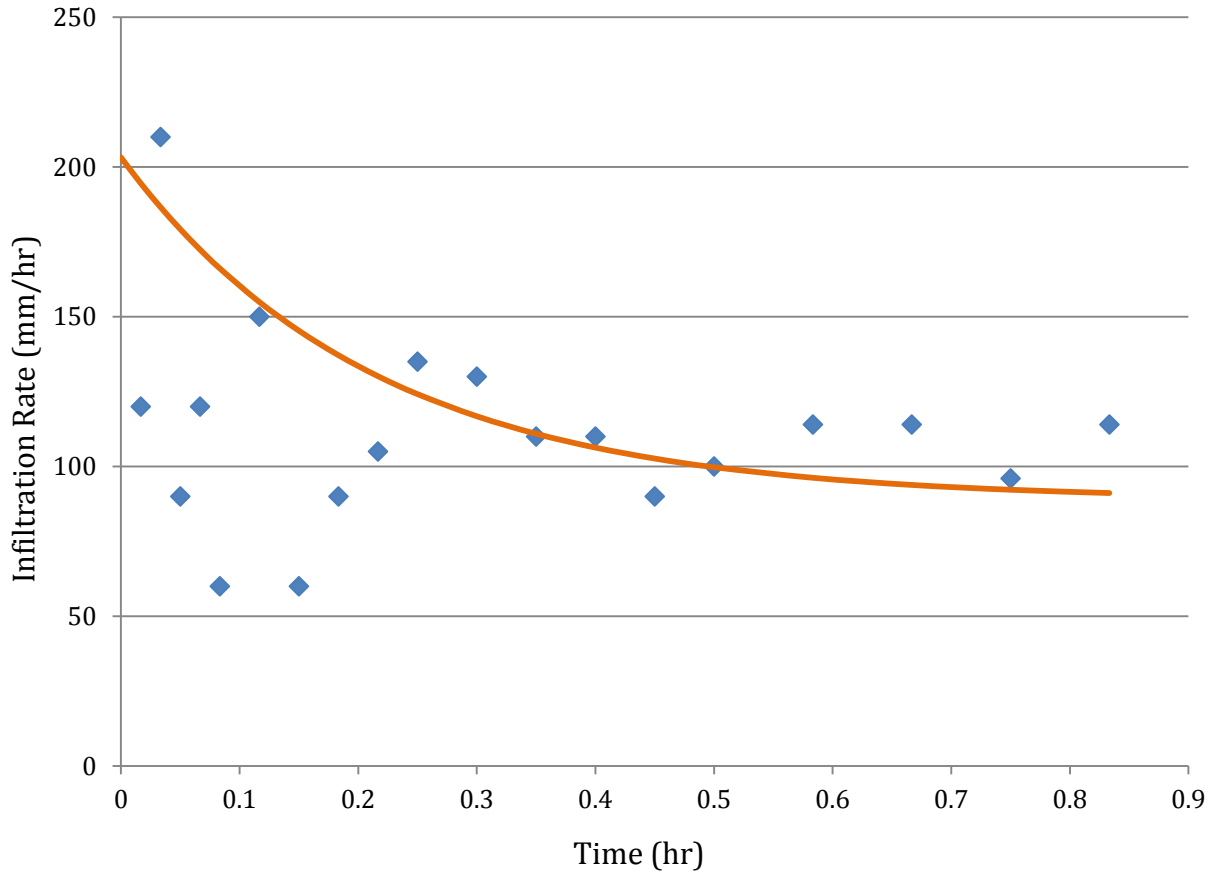


Figure A.6. Graph of observed Horton infiltration data points and the best-fit Horton infiltration curve developed from the observed dataset for the Pratt Place sampling location. The points are observed infiltration rates during the test, and the line is a best-fit Horton infiltration curve.  $f_c = 88.9$  mm/hr,  $f_o = 203.2$  mm/hr, and  $k = 4.7$  1/hr.



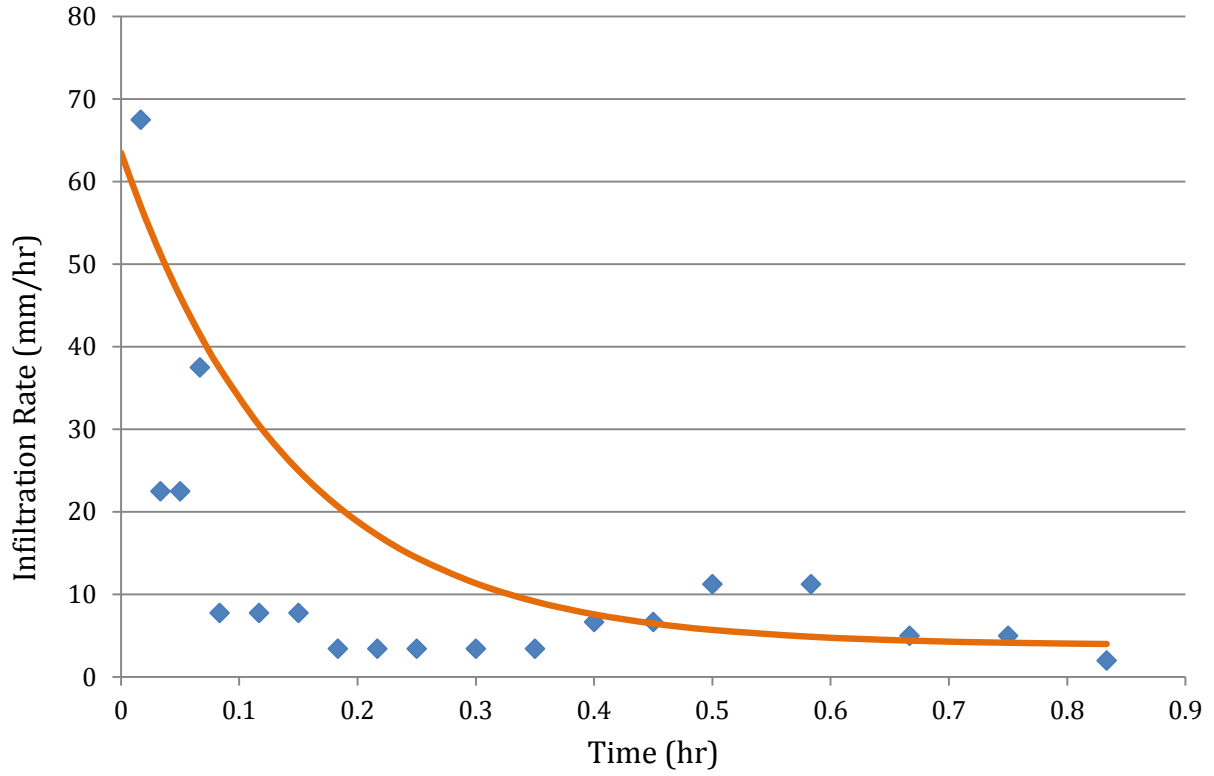


Figure A.7. Graph of observed Horton infiltration data points and the best-fit Horton infiltration curve developed from the observed dataset for the SW Gardens sampling location. The points are observed infiltration rates during the test, and the line is a best-fit Horton infiltration curve.  $f_c = 3.8$  mm/hr,  $f_o = 63.5$  mm/hr, and  $k = 6.9$  1/hr.

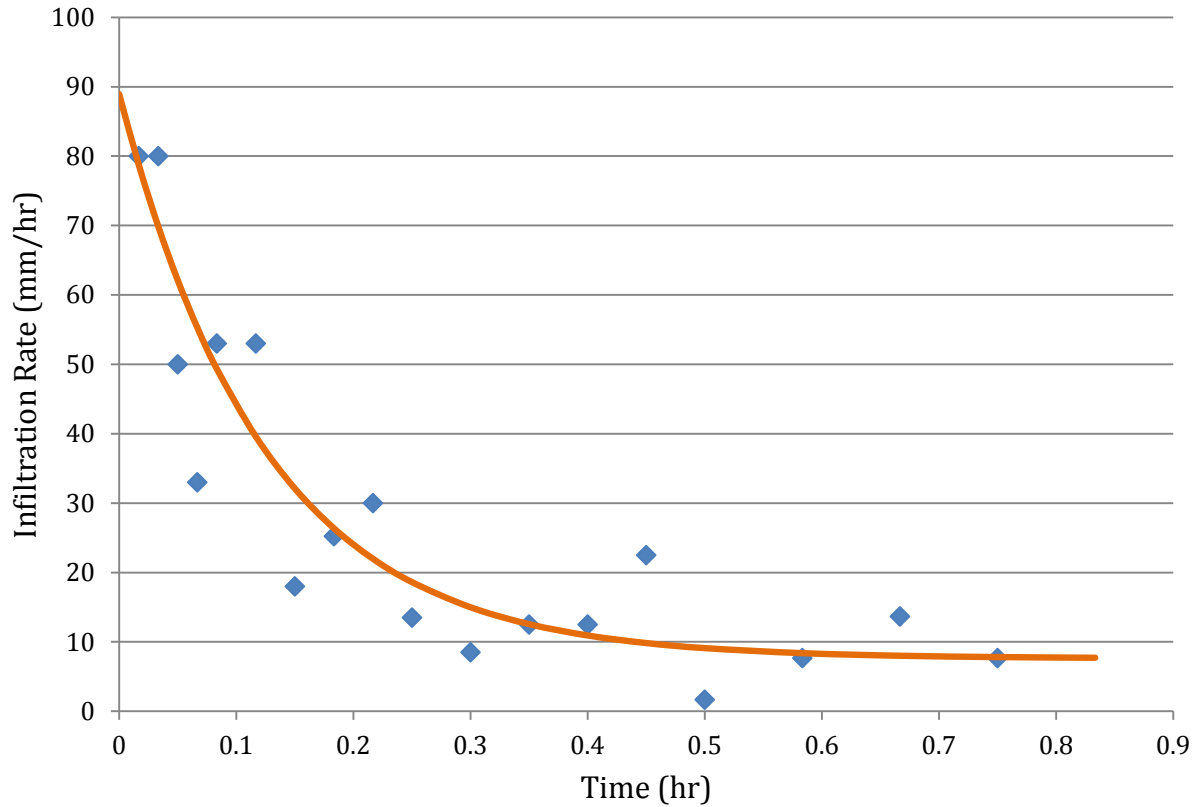


Figure A.8. Graph of observed Horton infiltration data points and the best-fit Horton infiltration curve developed from the observed dataset for the UA Chicken Farm sampling location. The points are observed infiltration rates during the test, and the line is a best-fit Horton infiltration curve.  $f_c = 7.6$  mm/hr,  $f_o = 88.9$  mm/hr, and  $k = 8.0$  1/hr.

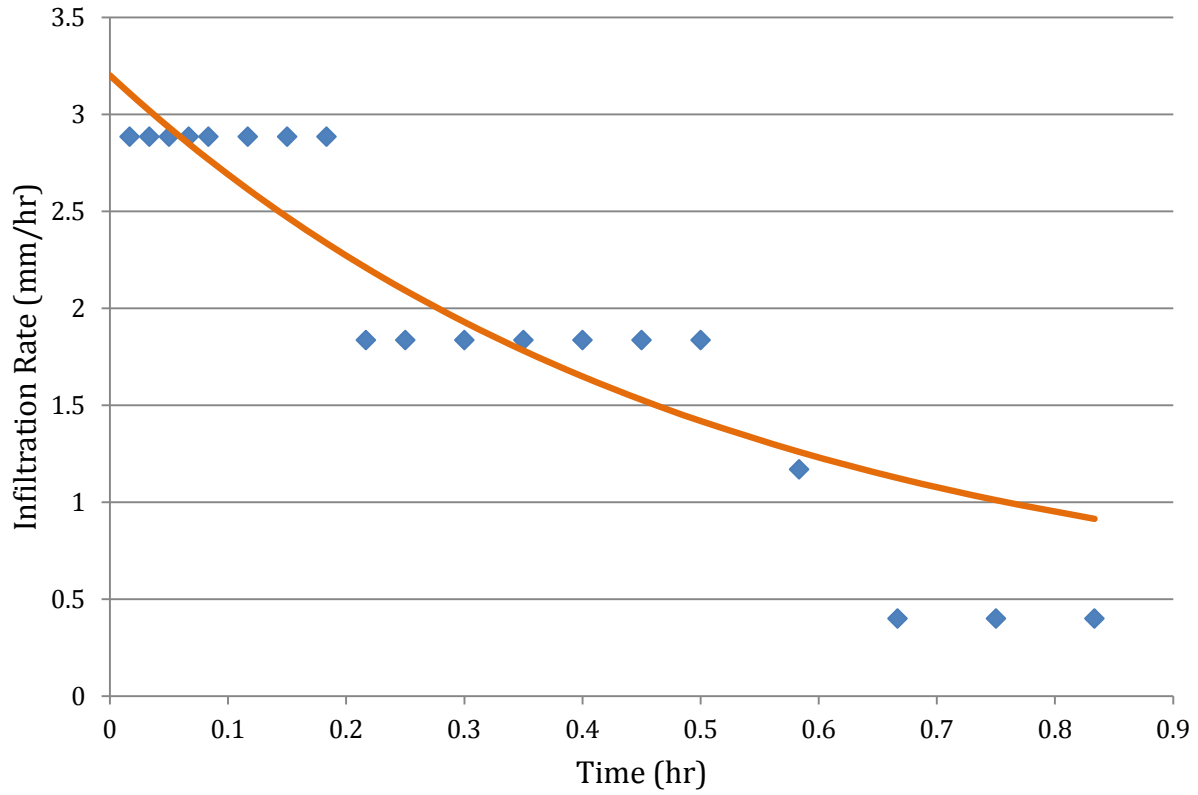


Figure A.9. Graph of observed Horton infiltration data points and the best-fit Horton infiltration curve developed from the observed dataset for the Central Gardens sampling location. The points are observed infiltration rates during the test, and the line is a best-fit Horton infiltration curve.  $f_c = 0.4$  mm/hr,  $f_o = 3.2$  mm/hr, and  $k = 1.4$  1/hr.

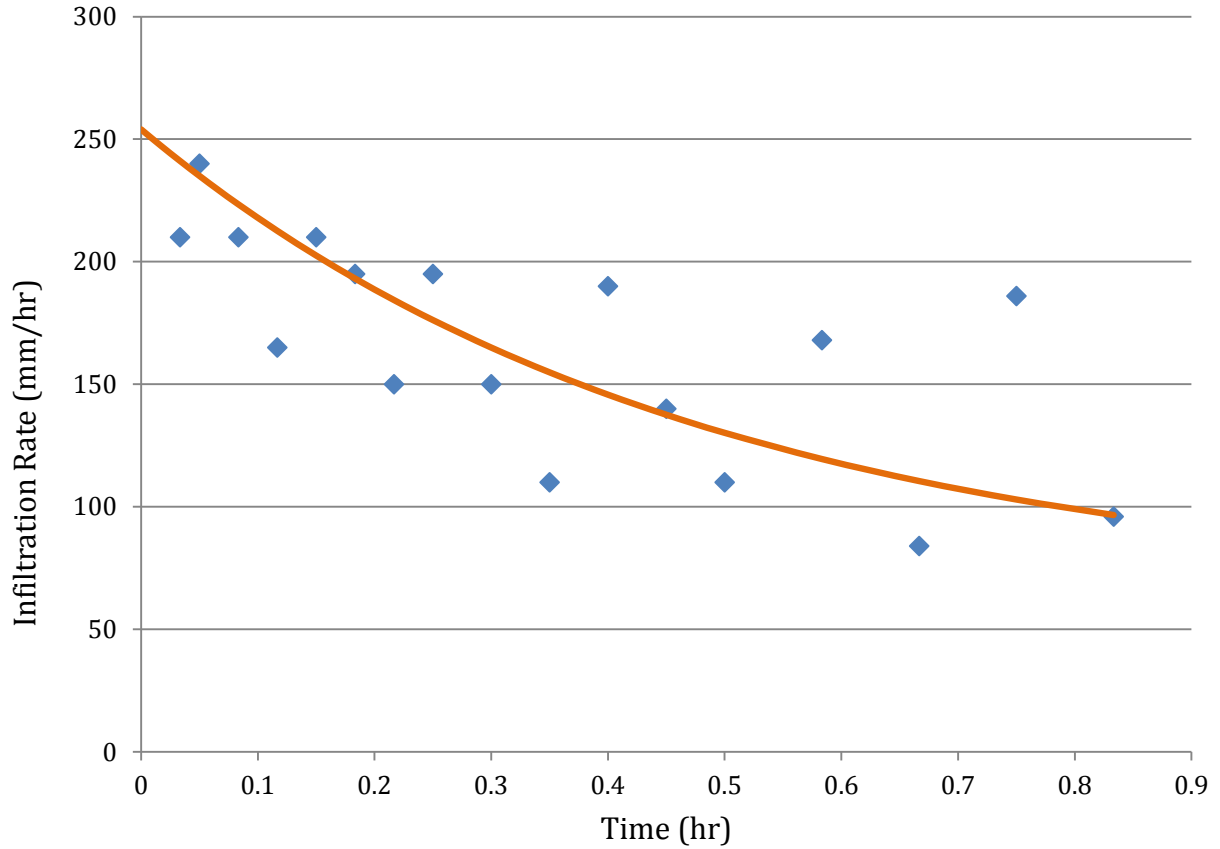


Figure A.10. Graph of observed Horton infiltration data points and the best-fit Horton infiltration curve developed from the observed dataset for the Mullins Creek South sampling location. The points are observed infiltration rates during the test, and the line is a best-fit Horton infiltration curve.  $f_c = 63.5$  mm/hr,  $f_o = 254$  mm/hr, and  $k = 2.1$  1/hr.

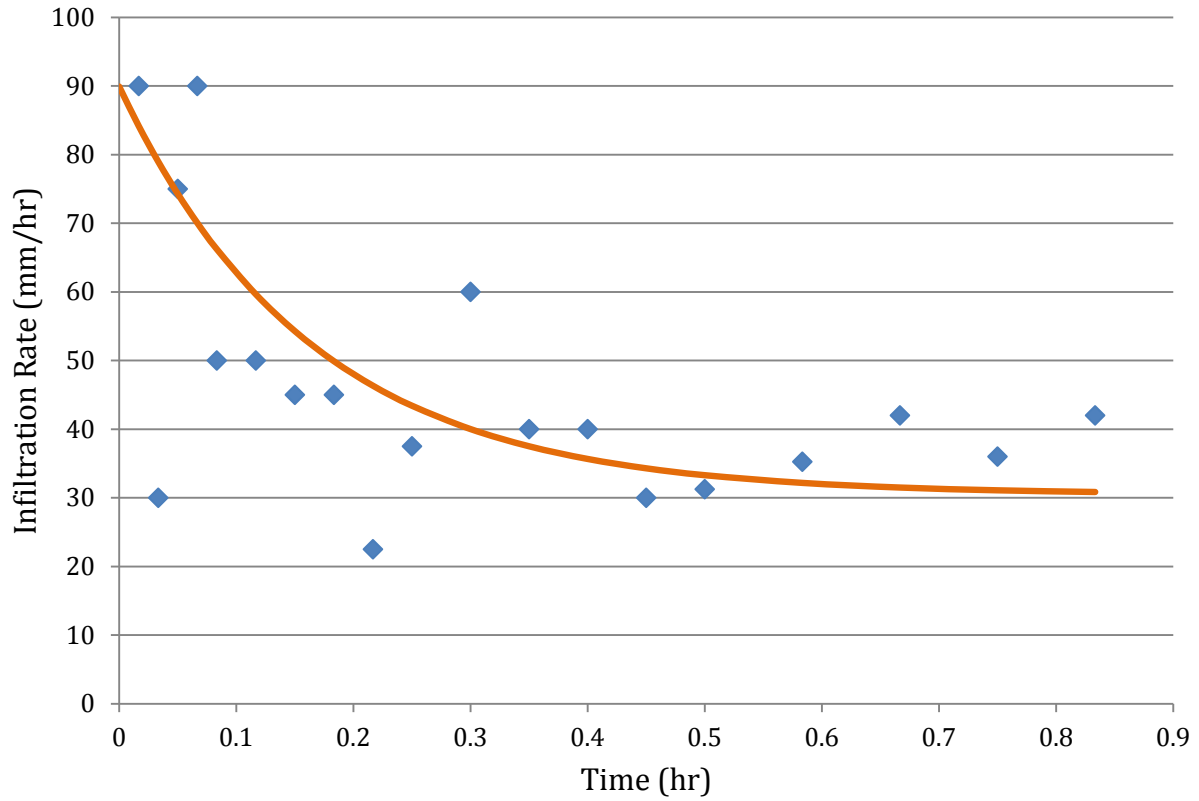


Figure A.11. Graph of observed Horton infiltration data points and the best-fit Horton infiltration curve developed from the observed dataset for the Lot 56B sampling location. The points are observed infiltration rates during the test, and the line is a best-fit Horton infiltration curve.  $f_c = 30.5$  mm/hr,  $f_o = 89.9$  mm/hr, and  $k = 6.1$  1/hr.

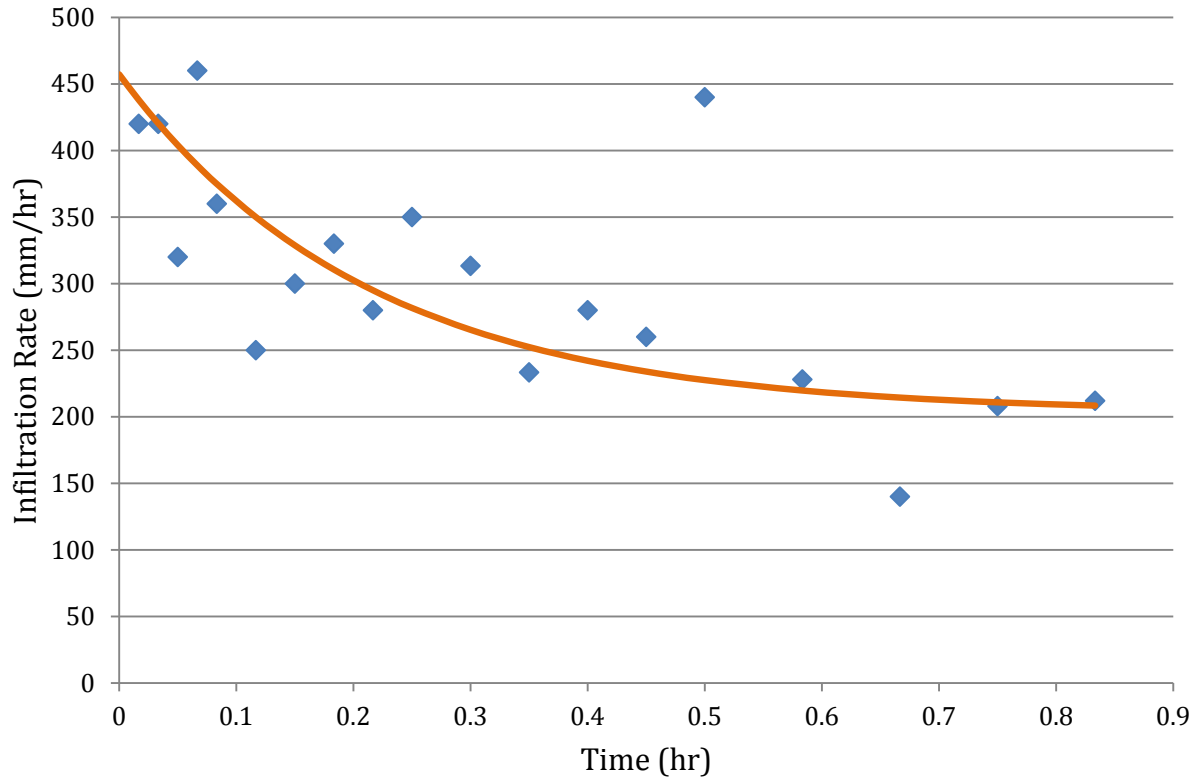


Figure A.12. Graph of observed Horton infiltration data points and the best-fit Horton infiltration curve developed from the observed dataset for the Oakland-Zion sampling location. The points are observed infiltration rates during the test, and the line is a best-fit Horton infiltration curve.  $f_c = 203$  mm/hr,  $f_o = 457$  mm/hr, and  $k = 4.7$  1/hr.

## Appendix B. Rainfall distribution for selected storm events in the Mullins Creek catchment

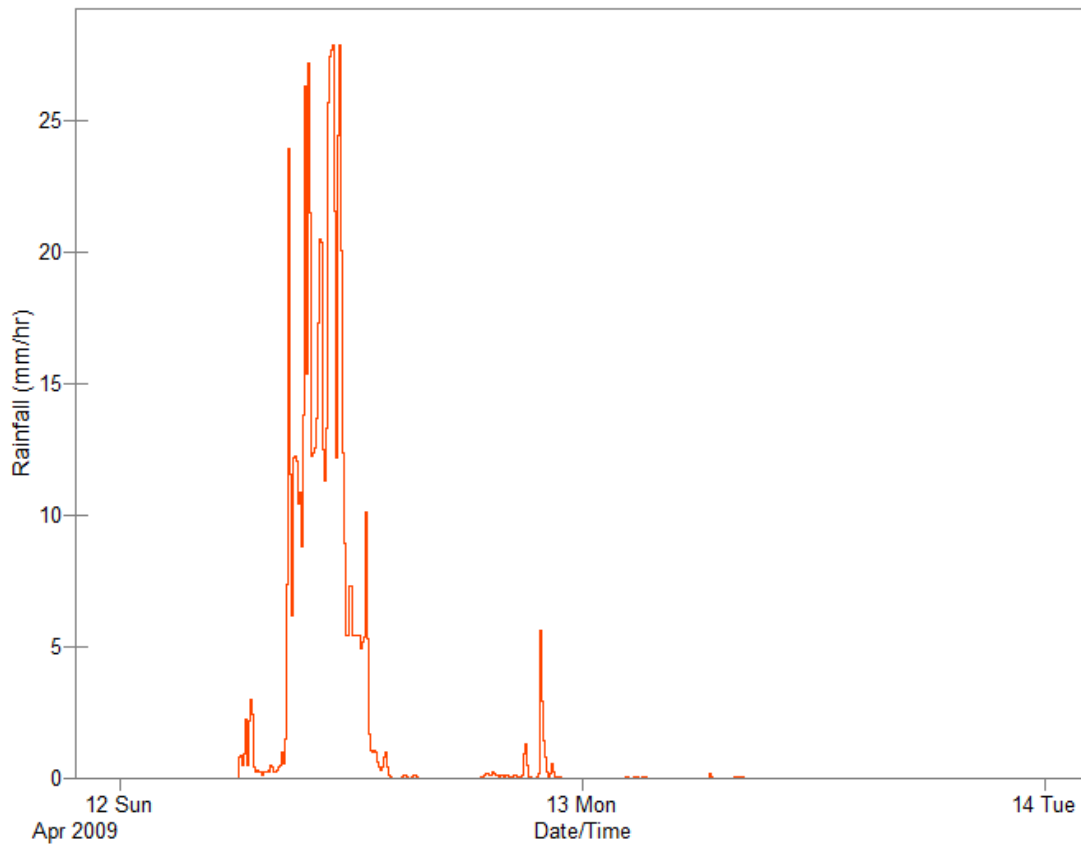


Figure B.1. Rainfall hyetograph for Mullins Creek catchment from PCSWMM system results, NEXRAD Level III inputs, 12 April 2009 storm event.

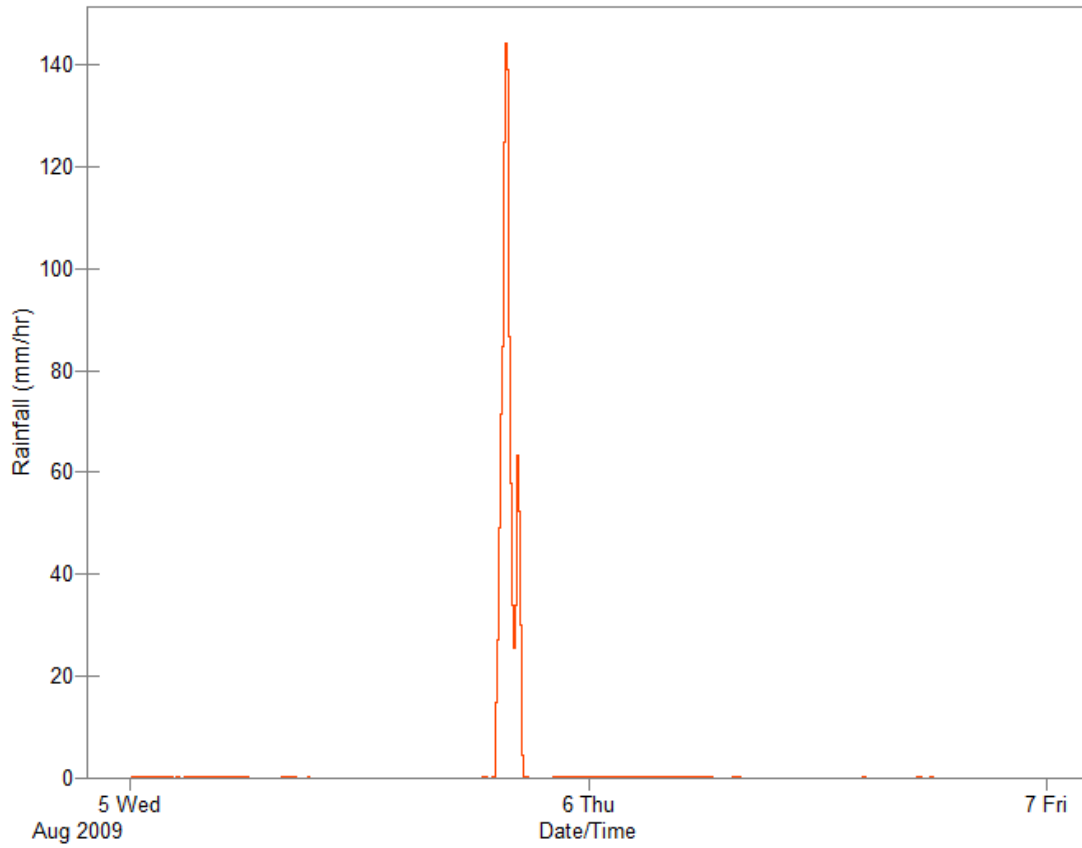


Figure B.2. Rainfall hyetograph for Mullins Creek catchment from PCSWMM system results, NEXRAD Level III inputs, 05 August 2009 storm event.



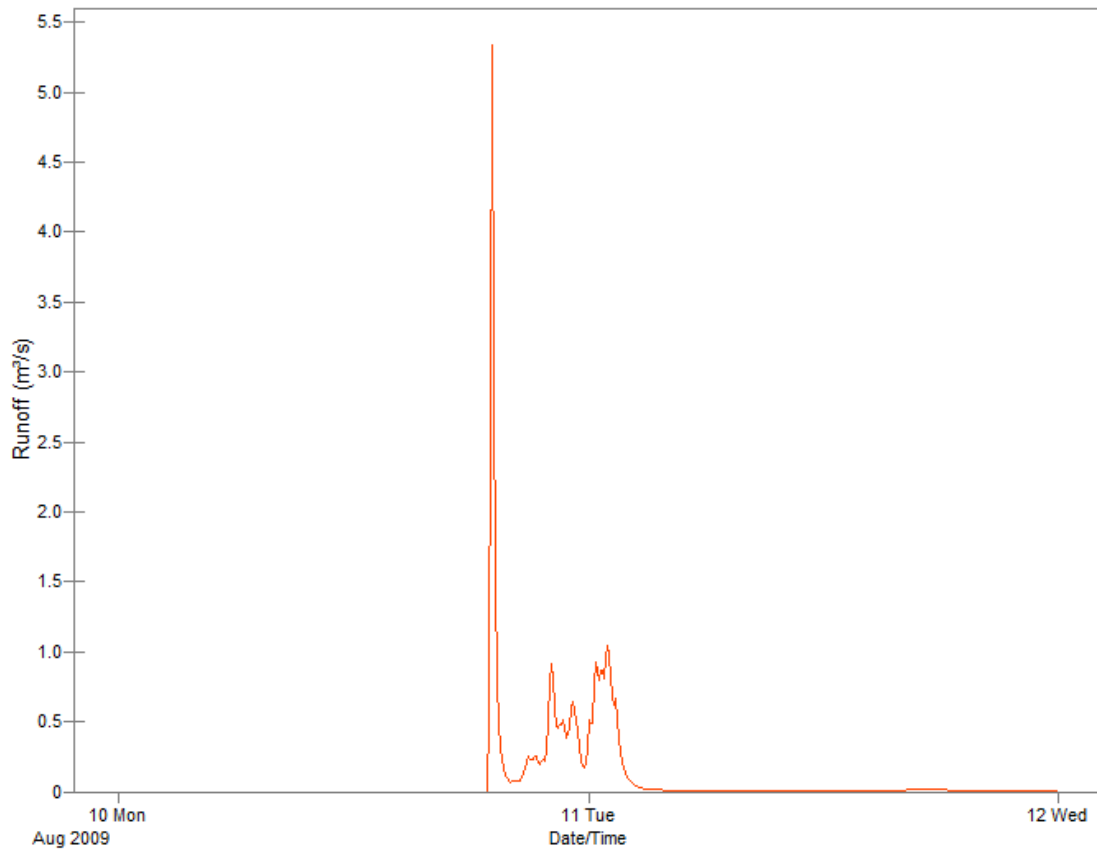


Figure B.3. Rainfall hyetograph for Mullins Creek catchment from PCSWMM system results, NEXRAD Level III inputs, 10 August 2009 storm event.

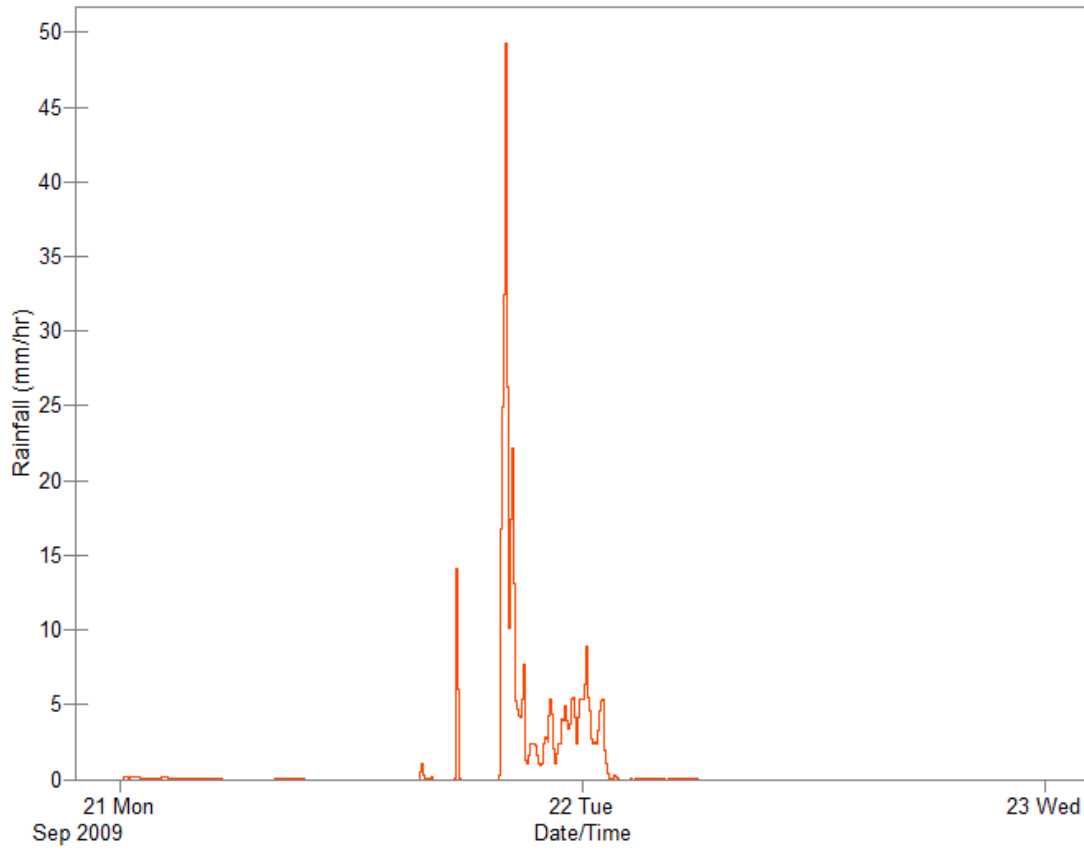


Figure B.4. Rainfall hyetograph for Mullins Creek catchment from PCSWMM system results, NEXRAD Level III inputs, 21 September 2009 storm event.

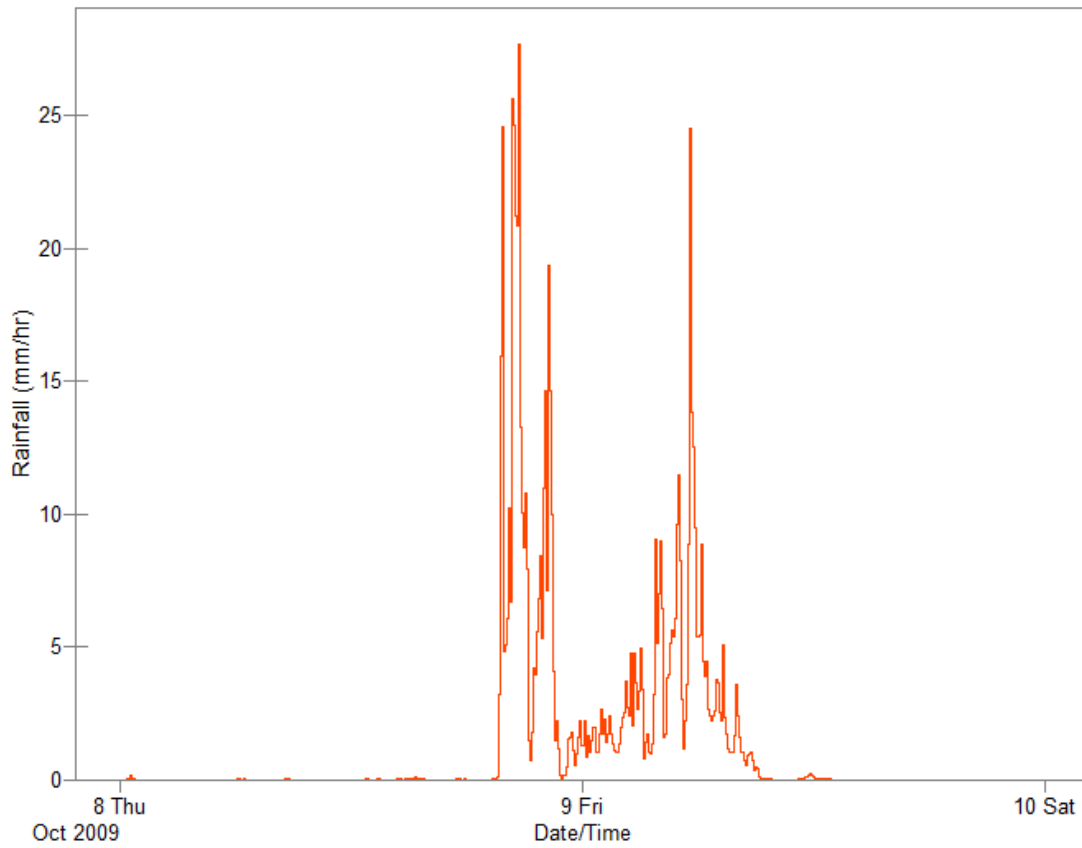


Figure B.5. Rainfall hyetograph for Mullins Creek catchment from PCSWMM system results, NEXRAD Level III inputs, 08 October 2009 storm event.

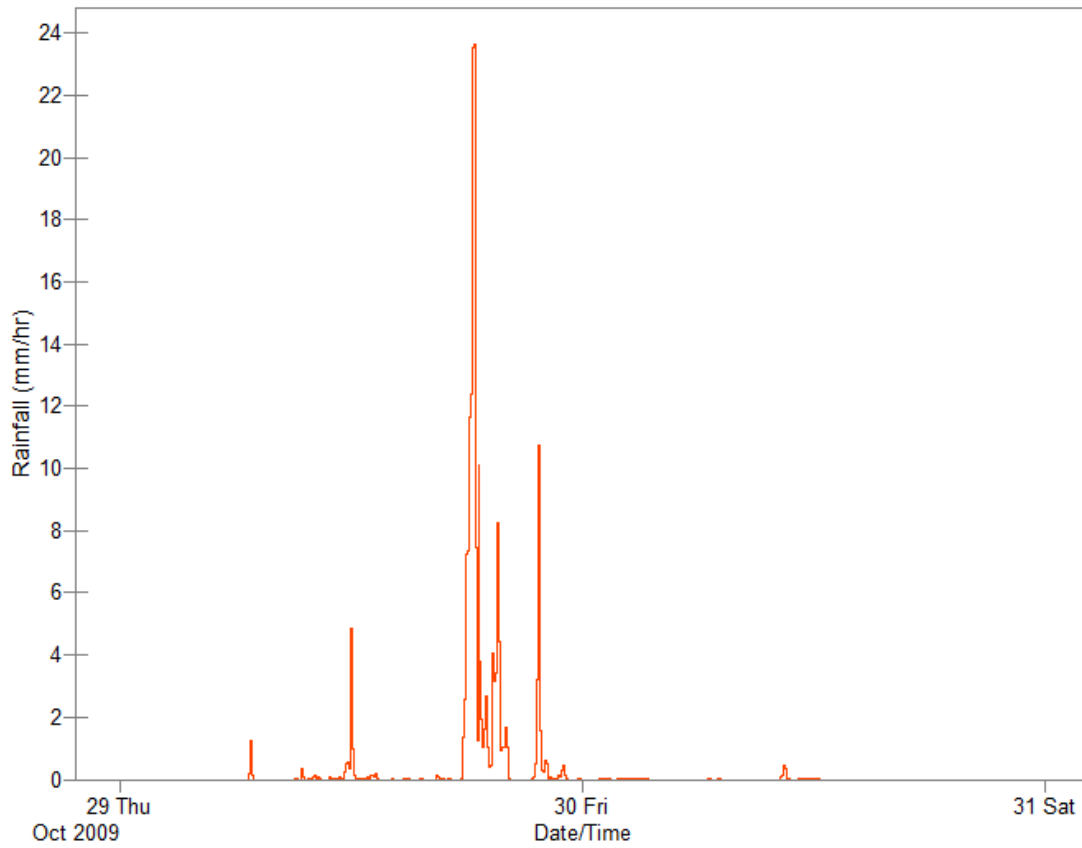


Figure B.6. Rainfall hyetograph for Mullins Creek catchment from PCSWMM system results, NEXRAD Level III inputs, 29 October 2009 storm event.

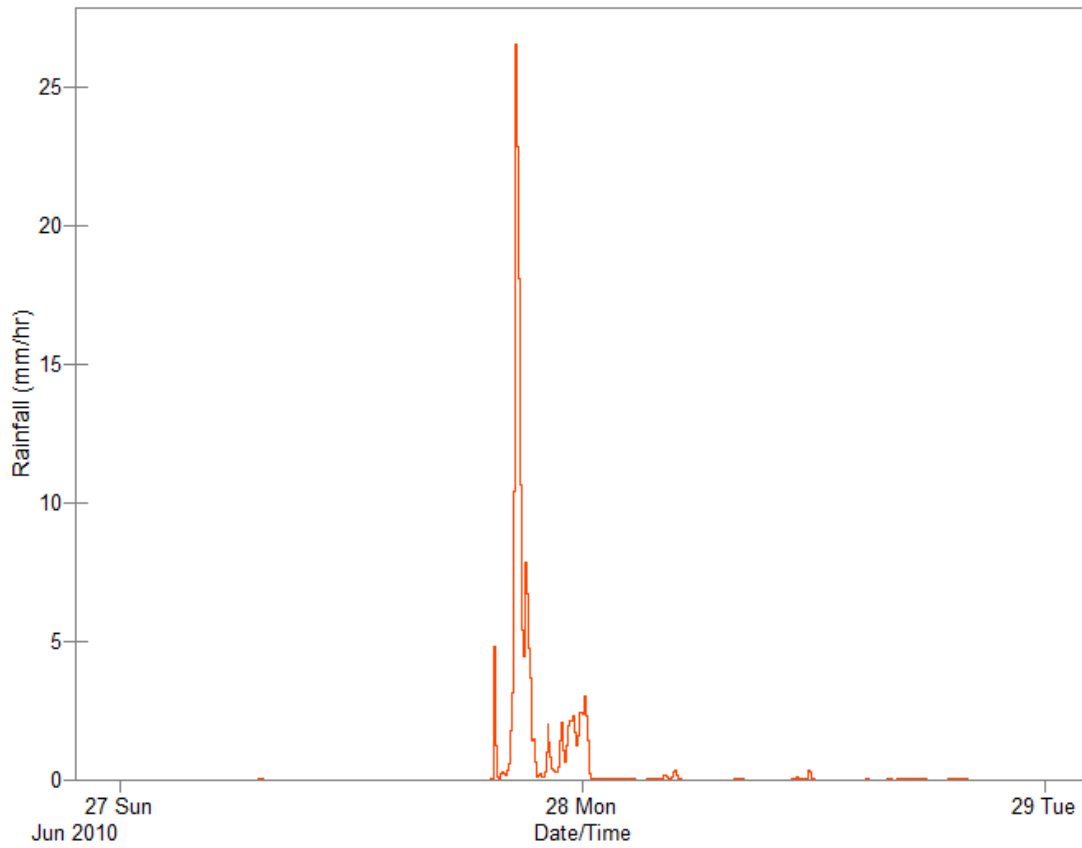


Figure B.7. Rainfall hyetograph for Mullins Creek catchment from PCSWMM system results, NEXRAD Level III inputs, 27 June 2010 storm event.

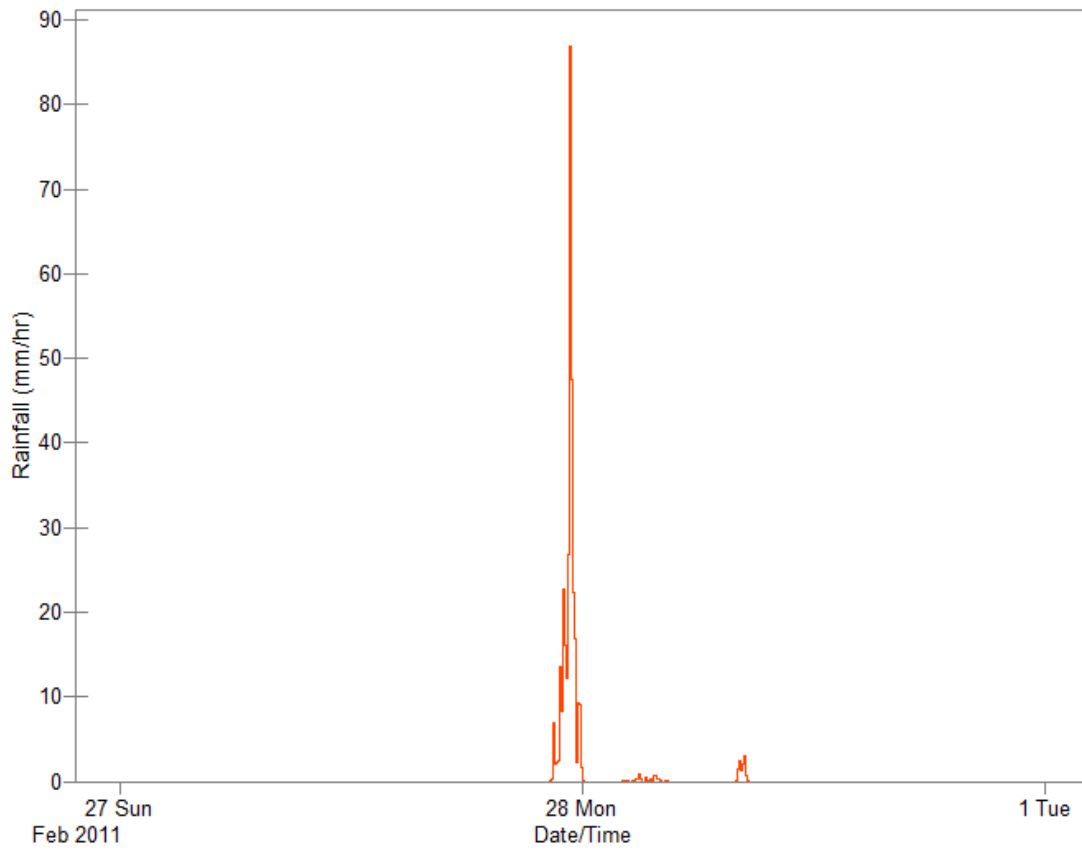


Figure B.8. Rainfall hyetograph for Mullins Creek catchment from PCSWMM system results, NEXRAD Level III inputs, 27 February 2011 storm event.

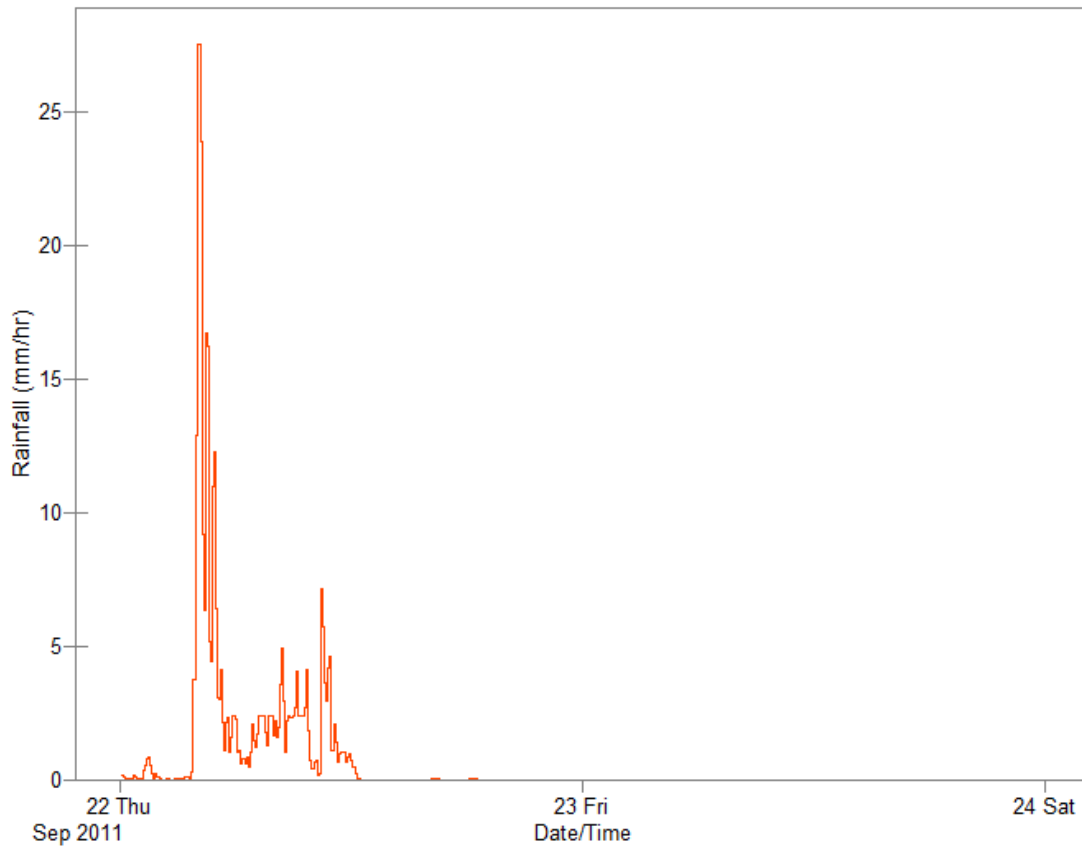


Figure B.9. Rainfall hyetograph for Mullins Creek catchment from PCSWMM system results, NEXRAD Level III inputs, 22 September 2011 storm event.

**Appendix C: Infiltration and percent impervious area input parameters for validation of SWMM model to observed storm events.**

Table C.1. Input parameters for each subcatchment for model scenario 1: predicted infiltration based on soil texture, and percent impervious area equal to percent directly connected impervious area.

Subcatchment	Initial Infiltration Rate, $f_o$ (mm/hr)	Final Infiltration Rate, $f_c$ (mm/hr)	Decay Constant, $k$ (hr <sup>-1</sup> )	% Imperv
SA1a	254.0	25.4	2.0	32.6
SA1b	254.0	25.4	2.0	45.5
SA1	254.0	25.4	2.0	30.8
SA2	254.0	25.4	2.0	35.0
SA3	254.0	25.4	2.0	49.1
SA4	254.0	25.4	2.0	50.9
SA5	254.0	25.4	2.0	49.1
SA6	254.0	25.4	2.0	39.4
SA7,8,11,12	254.0	25.4	2.0	46.2
SA9	254.0	25.4	2.0	39.9
SA10	137.2	15.2	2.0	34.5
SA13	104.1	12.7	2.0	48.9
SA14,16	252.3	25.0	2.0	46.4
SA15	253.5	25.3	2.0	42.8
SA17	252.8	25.1	2.0	49.9
SA18	239.7	21.8	2.0	44.5
SA19	254.0	25.4	2.0	51.0
SA20	234.1	20.4	2.0	50.1
SA21,22	250.9	24.6	2.0	45.9
SA23	237.9	21.4	2.0	43.6
SA24	225.9	18.4	2.0	34.7

Subcatchment	Initial Infiltration Rate, $f_o$ (mm/hr)	Final Infiltration Rate, $f_c$ (mm/hr)	Decay Constant, $k$ (hr <sup>-1</sup> )	% Imperv
SB1	254.0	25.4	2.0	7.4
SB2	254.0	25.4	2.0	22.5
SB3	254.0	25.4	2.0	28.2
SB4	254.0	25.4	2.0	23.7
SB5	246.2	23.4	2.0	28.9
SB6	247.7	23.8	2.0	25.6
SB7	219.8	16.9	2.0	30.5



Table C.1. cont.

Subcatchment	Initial Infiltration Rate, $f_o$ (mm/hr)	Final Infiltration Rate, $f_c$ (mm/hr)	Decay Constant, $k$ (hr <sup>-1</sup> )	% Imperv
SC1	246.6	23.5	2.0	28.8
SC2	250.2	24.4	2.0	26.9
SC3	223.4	17.8	2.0	27.8
SC4	229.1	19.2	2.0	26.5
SC5	203.2	12.7	2.0	19.5
SC6	210.7	14.6	2.0	33.3
SC7	244.9	23.1	2.0	48.0
SC8	218.2	16.5	2.0	64.5
SC9	203.2	12.7	2.0	35.7
SC10	215.4	15.7	2.0	39.4
SC11	224.3	18.0	2.0	29.4

Subcatchment	Initial Infiltration Rate, $f_o$ (mm/hr)	Final Infiltration Rate, $f_c$ (mm/hr)	Decay Constant, $k$ (hr <sup>-1</sup> )	% Imperv
SD1	254.0	25.4	2.0	43.0
SD2	254.0	2.5	2.0	40.3
SD3	254.0	25.4	2.0	23.4
SD4	254.0	25.4	2.0	23.3
SD5	254.0	25.4	2.0	33.3
SD6	254.0	25.4	2.0	27.5
SD7	243.0	22.7	2.0	40.3
SD8	252.6	25.1	2.0	36.8
SD10	216.8	16.1	2.0	30.5
SD11	229.9	19.4	2.0	28.8

Table C.2. Input parameters for each subcatchment for model scenario 2: predicted infiltration based on soil texture, and percent impervious area equal to percent total impervious area.

Subcatchment	Initial Infiltration Rate, $f_o$ (mm/hr)	Final Infiltration Rate, $f_c$ (mm/hr)	Decay Constant, $k$ (hr <sup>-1</sup> )	% Imperv
SA1a	254.0	25.4	2.0	45.2
SA1b	254.0	25.4	2.0	68.6
SA1	254.0	25.4	2.0	45.9
SA2	254.0	25.4	2.0	46.4
SA3	254.0	25.4	2.0	72.0
SA4	254.0	25.4	2.0	74.1
SA5	254.0	25.4	2.0	73.7
SA6	254.0	25.4	2.0	56.7
SA7,8,11,12	254.0	25.4	2.0	71.8
SA9	254.0	25.4	2.0	58.1
SA10	137.2	15.2	2.0	47.6
SA13	104.1	12.7	2.0	73.6
SA14,16	252.3	25.0	2.0	71.9
SA15	253.5	25.3	2.0	58.7
SA17	252.8	25.1	2.0	74.1
SA18	239.7	21.8	2.0	67.0
SA19	254.0	25.4	2.0	74.7
SA20	234.1	20.4	2.0	74.3
SA21,22	250.9	24.6	2.0	69.0
SA23	237.9	21.4	2.0	60.6
SA24	225.9	18.4	2.0	53.7

Subcatchment	Initial Infiltration Rate, $f_o$ (mm/hr)	Final Infiltration Rate, $f_c$ (mm/hr)	Decay Constant, $k$ (hr <sup>-1</sup> )	% Imperv
SB1	254.0	25.4	2.0	8.3
SB2	254.0	25.4	2.0	31.8
SB3	254.0	25.4	2.0	37.6
SB4	254.0	25.4	2.0	33.0
SB5	246.2	23.4	2.0	38.4
SB6	247.7	23.8	2.0	34.9
SB7	219.8	16.9	2.0	40.5

Table C.2. cont.

Subcatchment	Initial Infiltration Rate, $f_o$ (mm/hr)	Final Infiltration Rate, $f_c$ (mm/hr)	Decay Constant, $k$ (hr <sup>-1</sup> )	% Imperv
SC1	246.6	23.5	2.0	39.3
SC2	250.2	24.4	2.0	36.6
SC3	223.4	17.8	2.0	39.5
SC4	229.1	19.2	2.0	38.2
SC5	203.2	12.7	2.0	19.3
SC6	210.7	14.6	2.0	46.8
SC7	244.9	23.1	2.0	69.8
SC8	218.2	16.5	2.0	83.8
SC9	203.2	12.7	2.0	55.3
SC10	215.4	15.7	2.0	57.6
SC11	224.3	18.0	2.0	44.4

Subcatchment	Initial Infiltration Rate, $f_o$ (mm/hr)	Final Infiltration Rate, $f_c$ (mm/hr)	Decay Constant, $k$ (hr <sup>-1</sup> )	% Imperv
SD1	254.0	25.4	2.0	59.4
SD2	254.0	2.5	2.0	57.0
SD3	254.0	25.4	2.0	34.5
SD4	254.0	25.4	2.0	33.6
SD5	254.0	25.4	2.0	44.7
SD6	254.0	25.4	2.0	39.3
SD7	243.0	22.7	2.0	60.8
SD8	252.6	25.1	2.0	51.2
SD10	216.8	16.1	2.0	44.7
SD11	229.9	19.4	2.0	40.9

Table C.3. Input parameters for each subcatchment for model scenario 3: predicted infiltration based on observed soil infiltration characteristics, and percent impervious area equal to percent directly connected impervious area.

Subcatchment	Initial Infiltration Rate, $f_o$ (mm/hr)	Final Infiltration Rate, $f_c$ (mm/hr)	Decay Constant, $k$ (hr <sup>-1</sup> )	% Imperv
SA1a	131.3	15.2	5.9	32.6
SA1b	108.3	13.3	6.7	45.5
SA1	127.6	14.9	6.1	30.8
SA2	133.0	15.3	5.9	35.0
SA3	106.4	13.1	6.7	49.1
SA4	104.5	12.9	6.8	50.9
SA5	102.8	12.8	6.9	49.1
SA6	121.9	14.4	6.2	39.4
SA7,8,11,12	102.8	12.8	6.9	46.2
SA9	254.0	25.4	2.0	39.9
SA10	137.2	15.2	2.0	34.5
SA13	104.1	12.7	2.0	48.9
SA14,16	100.6	12.4	6.8	46.4
SA15	122.8	14.4	6.2	42.8
SA17	101.4	11.0	5.6	49.9
SA18	92.3	10.5	6.0	44.5
SA19	103.2	12.8	6.8	51.0
SA20	77.9	8.8	6.0	50.1
SA21,22	104.1	12.6	6.6	45.9
SA23	101.4	11.0	5.6	43.6
SA24	86.0	8.5	5.2	34.7

Subcatchment	Initial Infiltration Rate, $f_o$ (mm/hr)	Final Infiltration Rate, $f_c$ (mm/hr)	Decay Constant, $k$ (hr <sup>-1</sup> )	% Imperv
SB1	187.5	19.9	4.1	7.4
SB2	137.1	15.7	5.8	22.5
SB3	136.7	15.6	5.8	28.2
SB4	137.0	15.7	5.8	23.7
SB5	127.3	14.0	5.5	28.9
SB6	129.5	14.3	5.5	25.6
SB7	110.3	9.4	4.3	30.5

Table C.3. cont.

Subcatchment	Initial Infiltration Rate, $f_o$ (mm/hr)	Final Infiltration Rate, $f_c$ (mm/hr)	Decay Constant, $k$ (hr <sup>-1</sup> )	% Imperv
SC1	126.2	13.9	5.6	28.8
SC2	132.2	14.8	5.6	26.9
SC3	88.4	8.3	5.0	27.8
SC4	92.4	9.3	5.3	26.5
SC5	47.3	3.1	4.5	19.5
SC6	58.2	4.7	4.7	33.3
SC7	98.2	11.5	6.3	48.0
SC8	57.9	5.6	5.3	64.5
SC9	69.1	4.5	4.1	35.7
SC10	116.9	9.2	3.9	39.4
SC11	115.4	10.3	4.4	29.4

Subcatchment	Initial Infiltration Rate, $f_o$ (mm/hr)	Final Infiltration Rate, $f_c$ (mm/hr)	Decay Constant, $k$ (hr <sup>-1</sup> )	% Imperv
SD1	122.4	14.4	6.2	43.0
SD2	122.7	14.5	6.2	40.3
SD3	134.6	15.5	5.8	23.4
SD4	135.7	15.5	5.8	23.3
SD5	133.2	15.3	5.9	33.3
SD6	133.2	15.3	5.9	27.5
SD7	102.2	11.6	6.0	40.3
SD8	125.8	14.6	6.0	36.8
SD10	84.2	7.2	4.6	30.5
SD11	103.5	10.2	5.0	28.8

Table C.4. Input parameters for each subcatchment for model scenario 4: predicted infiltration based on observed soil infiltration characteristics, and percent impervious area equal total impervious area.

Subcatchment	Initial Infiltration Rate, $f_o$ (mm/hr)	Final Infiltration Rate, $f_c$ (mm/hr)	Decay Constant, $k$ (hr <sup>-1</sup> )	% Imperv
SA1a	131.3	15.2	5.9	45.2
SA1b	108.3	13.3	6.7	68.6
SA1	127.6	14.9	6.1	45.9
SA2	133.0	15.3	5.9	46.4
SA3	106.4	13.1	6.7	72.0
SA4	104.5	12.9	6.8	74.1
SA5	102.8	12.8	6.9	73.7
SA6	121.9	14.4	6.2	56.7
SA7,8,11,12	102.8	12.8	6.9	71.8
SA9	254.0	25.4	2.0	58.1
SA10	137.2	15.2	2.0	47.6
SA13	104.1	12.7	2.0	73.6
SA14,16	100.6	12.4	6.8	71.9
SA15	122.8	14.4	6.2	58.7
SA17	101.4	11.0	5.6	74.1
SA18	92.3	10.5	6.0	67.0
SA19	103.2	12.8	6.8	74.7
SA20	77.9	8.8	6.0	74.3
SA21,22	104.1	12.6	6.6	69.0
SA23	101.4	11.0	5.6	60.6
SA24	86.0	8.5	5.2	53.7

Subcatchment	Initial Infiltration Rate, $f_o$ (mm/hr)	Final Infiltration Rate, $f_c$ (mm/hr)	Decay Constant, $k$ (hr <sup>-1</sup> )	% Imperv
SB1	187.5	19.9	4.1	8.3
SB2	137.1	15.7	5.8	31.8
SB3	136.7	15.6	5.8	37.6
SB4	137.0	15.7	5.8	33.0
SB5	127.3	14.0	5.5	38.4
SB6	129.5	14.3	5.5	34.9
SB7	110.3	9.4	4.3	40.5

Table C.4. cont.

Subcatchment	Initial Infiltration Rate, $f_o$ (mm/hr)	Final Infiltration Rate, $f_c$ (mm/hr)	Decay Constant, $k$ (hr <sup>-1</sup> )	% Imperv
SC1	126.2	13.9	5.6	39.3
SC2	132.2	14.8	5.6	36.6
SC3	88.4	8.3	5.0	39.5
SC4	92.4	9.3	5.3	38.2
SC5	47.3	3.1	4.5	19.3
SC6	58.2	4.7	4.7	46.8
SC7	98.2	11.5	6.3	69.8
SC8	57.9	5.6	5.3	83.8
SC9	69.1	4.5	4.1	55.3
SC10	116.9	9.2	3.9	57.6
SC11	115.4	10.3	4.4	44.4

Subcatchment	Initial Infiltration Rate, $f_o$ (mm/hr)	Final Infiltration Rate, $f_c$ (mm/hr)	Decay Constant, $k$ (hr <sup>-1</sup> )	% Imperv
SD1	122.4	14.4	6.2	59.4
SD2	122.7	14.5	6.2	57.0
SD3	134.6	15.5	5.8	34.5
SD4	135.7	15.5	5.8	33.6
SD5	133.2	15.3	5.9	44.7
SD6	133.2	15.3	5.9	39.3
SD7	102.2	11.6	6.0	60.8
SD8	125.8	14.6	6.0	51.2
SD10	84.2	7.2	4.6	44.7
SD11	103.5	10.2	5.0	40.9

**Appendix D. Mullins Creek catchment predicted runoff (from the hydrologic model) versus observed runoff (from USGS gaging station 07048480) for selected events used for model validation.**

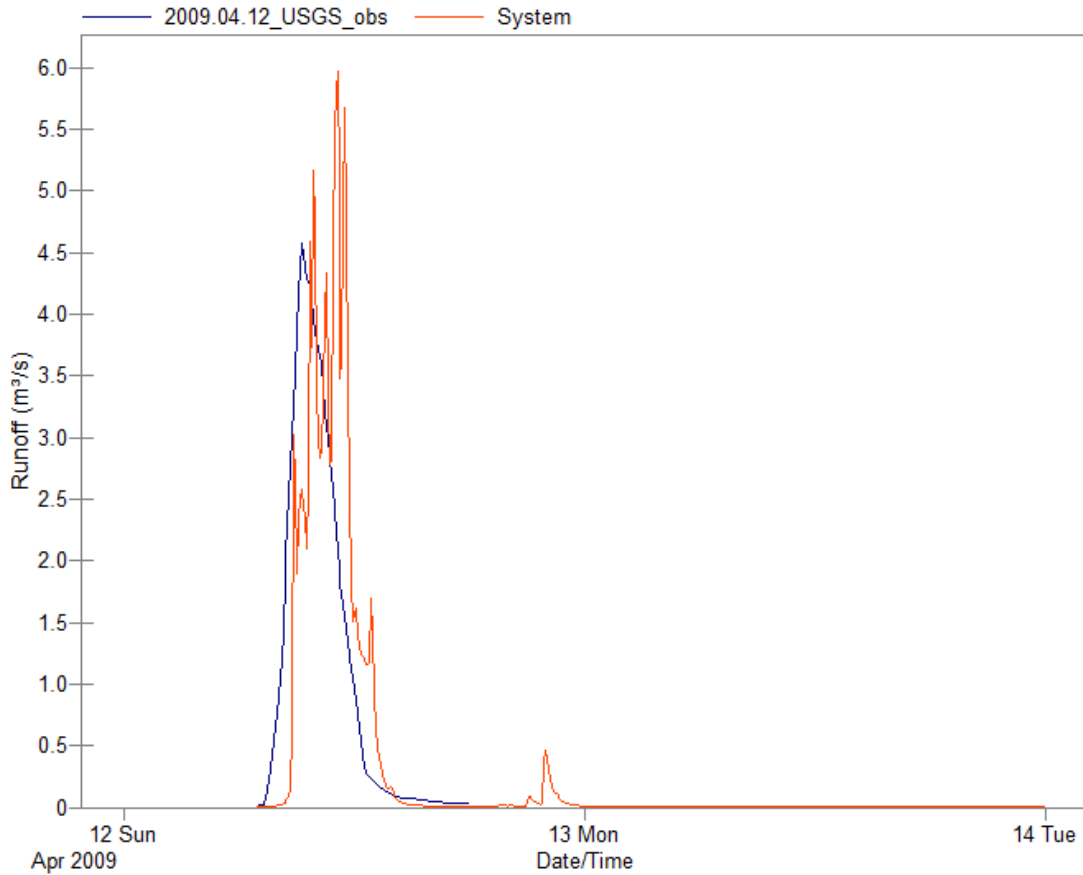


Figure D.1a. Predicted (red line) versus observed (blue line) runoff for Mullins Creek catchment. The predicted runoff hydrograph is based on predicted data for infiltration and percent impervious = percent directly connected impervious surface (Scenario 1). Observed data were downloaded from USGS gaging station data for the Mullins Creek gaging station: 12 April 2009 Storm Event.



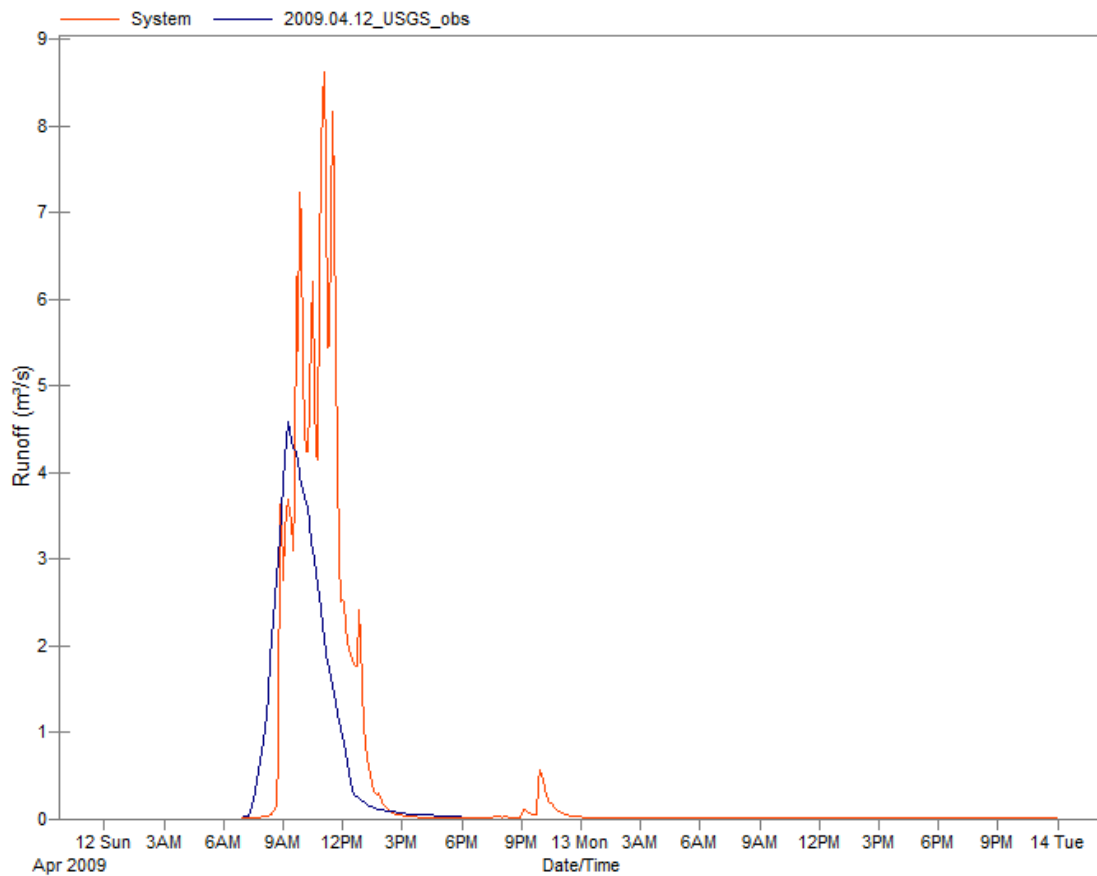


Figure D.1b. Predicted (red line) versus observed (blue line) runoff for Mullins Creek catchment. The predicted runoff hydrograph is based on observed data for infiltration and percent impervious = percent total impervious surface (TIA) (Scenario 2). Observed data were downloaded from USGS gaging station data for the Mullins Creek gaging station: 12 April 2009 Storm Event.

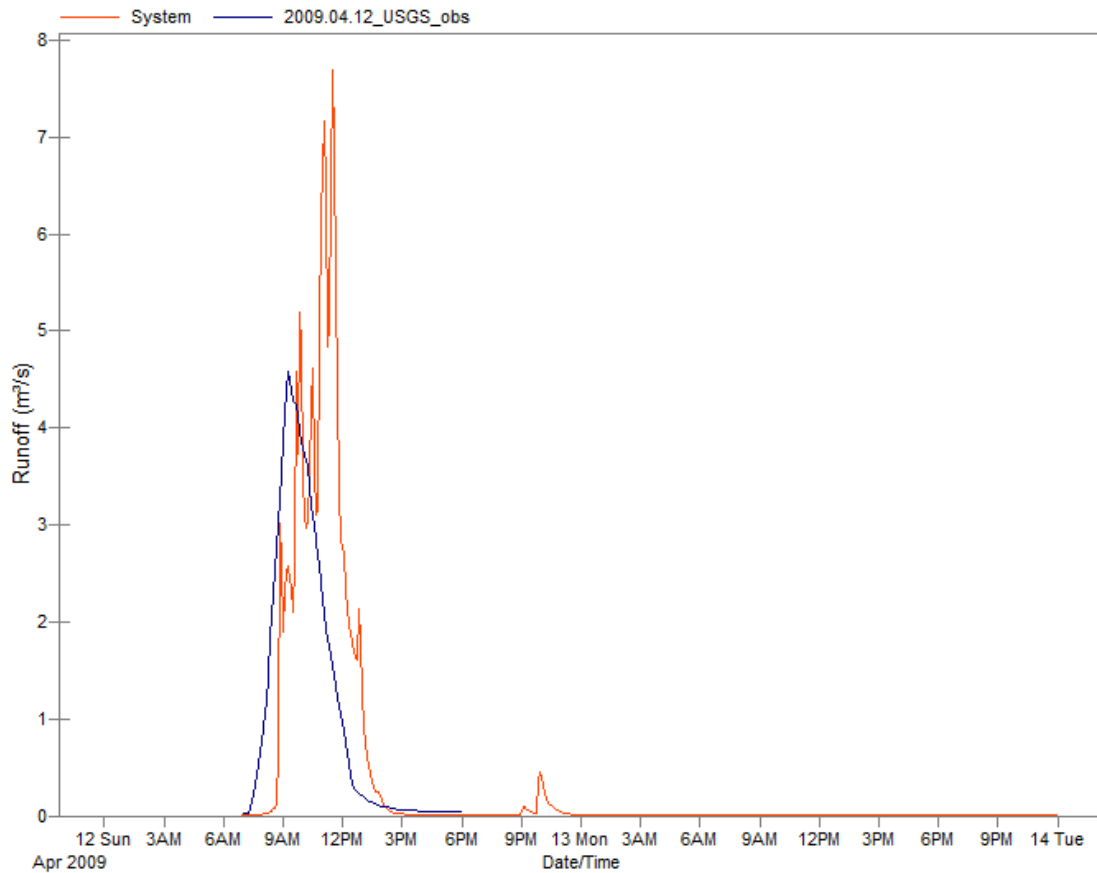


Figure D.1c. Predicted (red line) versus observed (blue line) runoff for Mullins Creek catchment. The predicted runoff hydrograph is based on observed data for infiltration and percent impervious = percent directly connected impervious surface (Scenario 3). Observed data were downloaded from USGS gaging station data for the Mullins Creek gaging station: 12 April 2009 Storm Event.

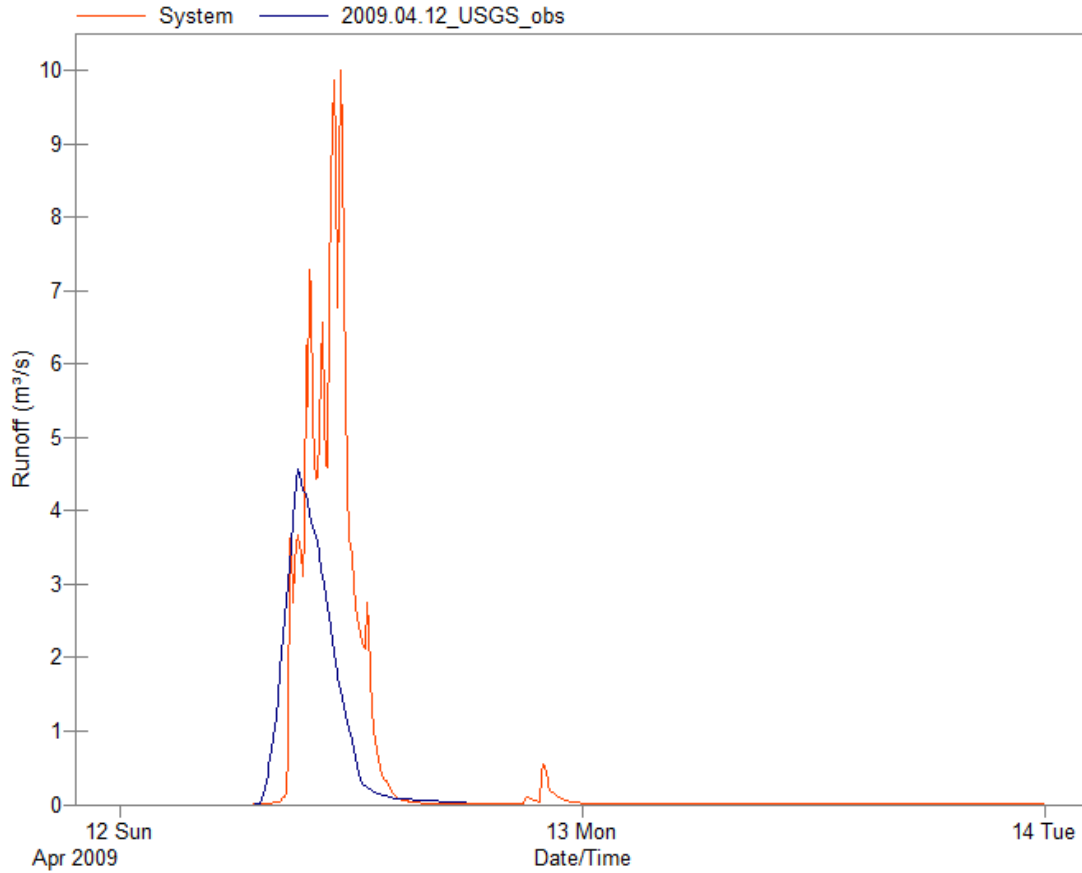


Figure D.1d. Predicted (red line) versus observed (blue line) runoff for Mullins Creek catchment. The predicted runoff hydrograph is based on observed data for infiltration and percent impervious = percent total impervious area (TIA) (Scenario 4). Observed data were downloaded from USGS gaging station data for the Mullins Creek gaging station: 12 April 2009 Storm Event.

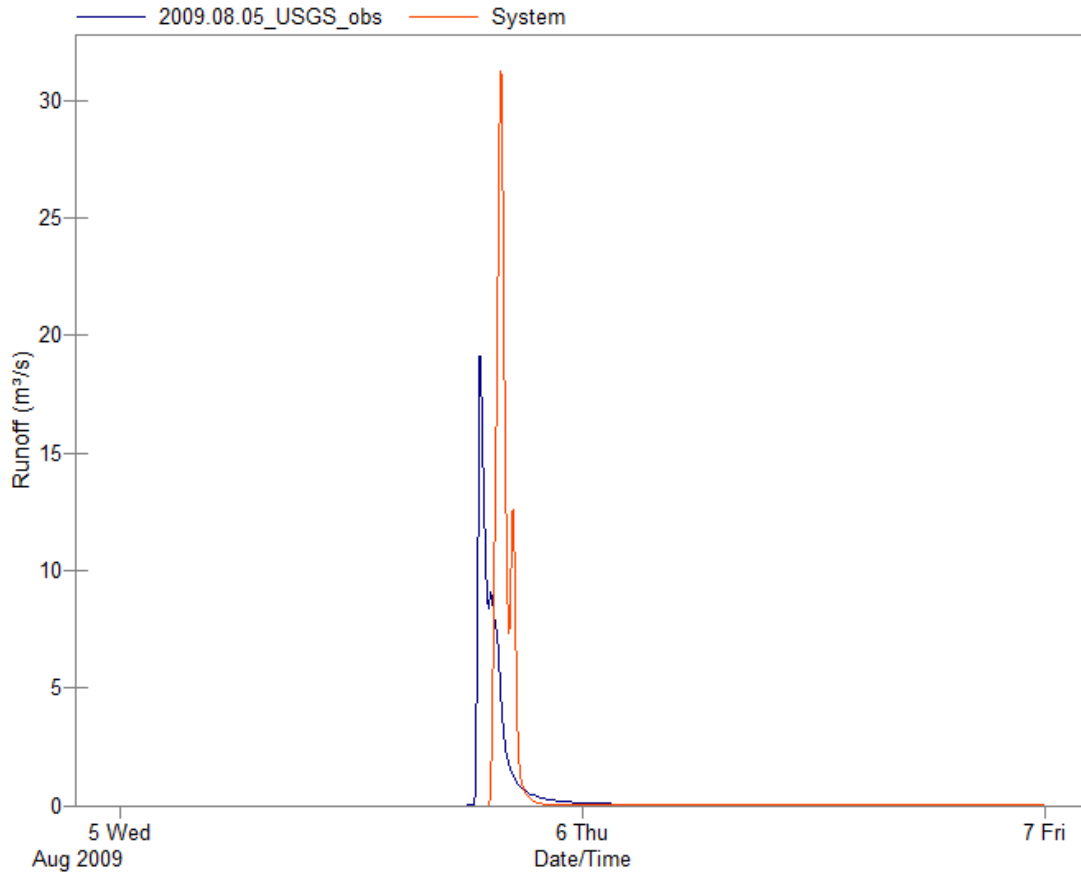


Figure D.2a. Predicted (red line) versus observed (blue line) runoff for Mullins Creek catchment. The predicted runoff hydrograph is based on predicted data for infiltration and percent impervious = percent directly connected impervious surface (Scenario 1). Observed data were downloaded from USGS gaging station data for the Mullins Creek gaging station: 05 August 2009 Storm Event.

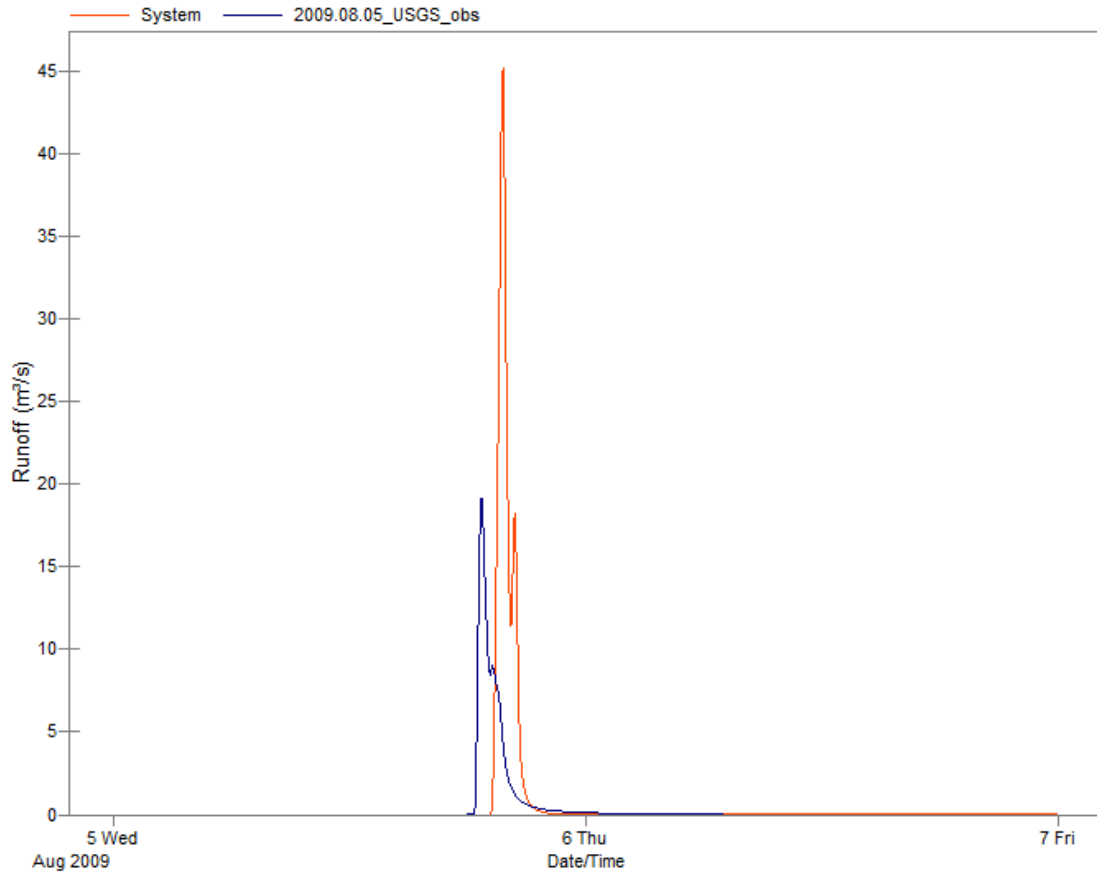


Figure D.2b. Predicted (red line) versus observed (blue line) runoff for Mullins Creek catchment. The predicted runoff hydrograph is based on observed data for infiltration and percent impervious = percent total impervious surface (TIA) (Scenario 2). Observed data were downloaded from USGS gaging station data for the Mullins Creek gaging station: 05 August 2009 Storm Event.

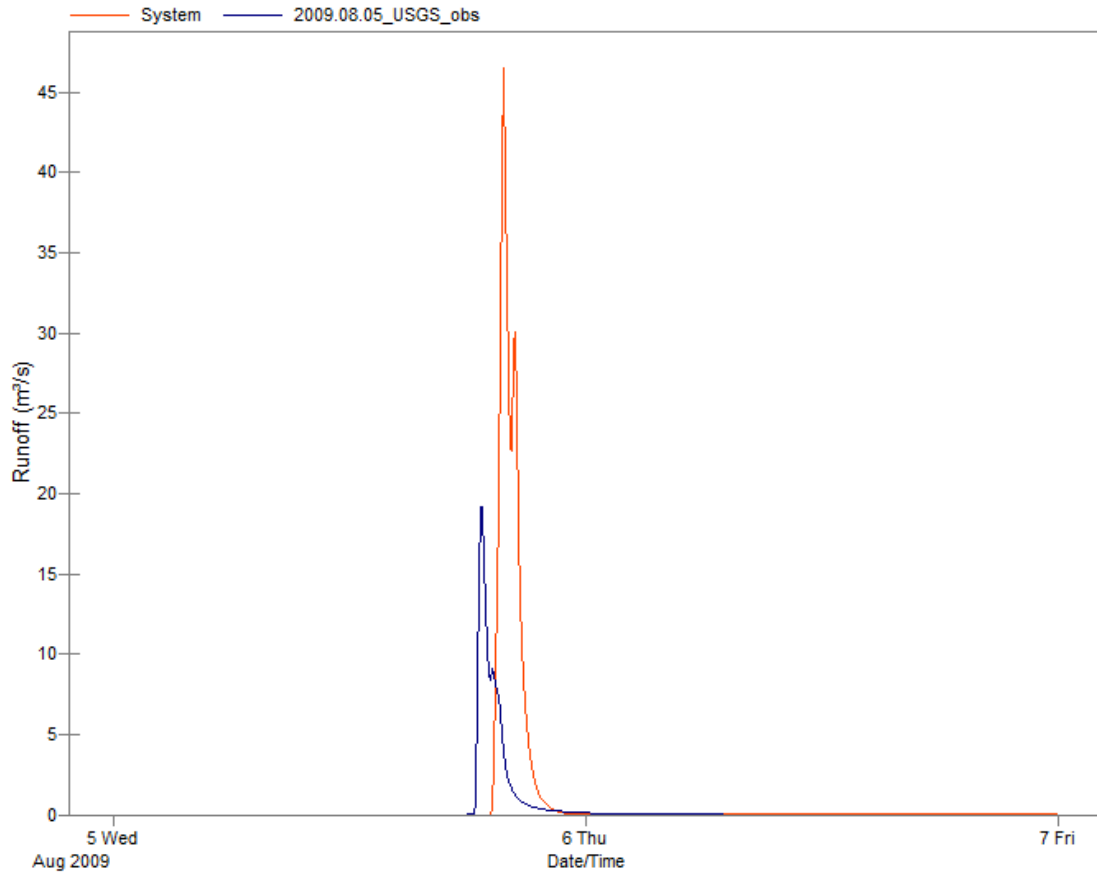


Figure D.2c. Predicted (red line) versus observed (blue line) runoff for Mullins Creek catchment. The predicted runoff hydrograph is based on observed data for infiltration and percent impervious = percent directly connected impervious surface (Scenario 3). Observed data were downloaded from USGS gaging station data for the Mullins Creek gaging station: 05 August 2009 Storm Event.

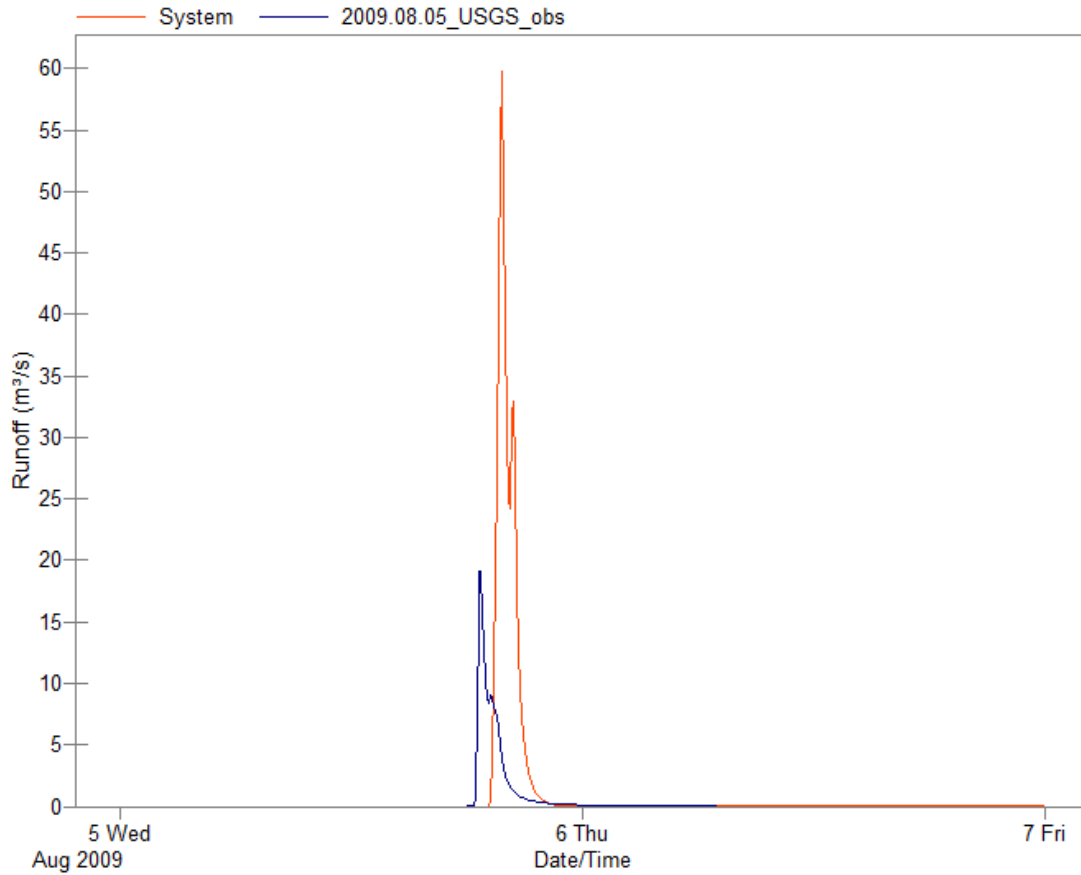


Figure D.2d. Predicted (red line) versus observed (blue line) runoff for Mullins Creek catchment. The predicted runoff hydrograph is based on observed data for infiltration and percent impervious = percent total impervious area (TIA) (Scenario 4). Observed data were downloaded from USGS gaging station data for the Mullins Creek gaging station: 05 August 2009 Storm Event.

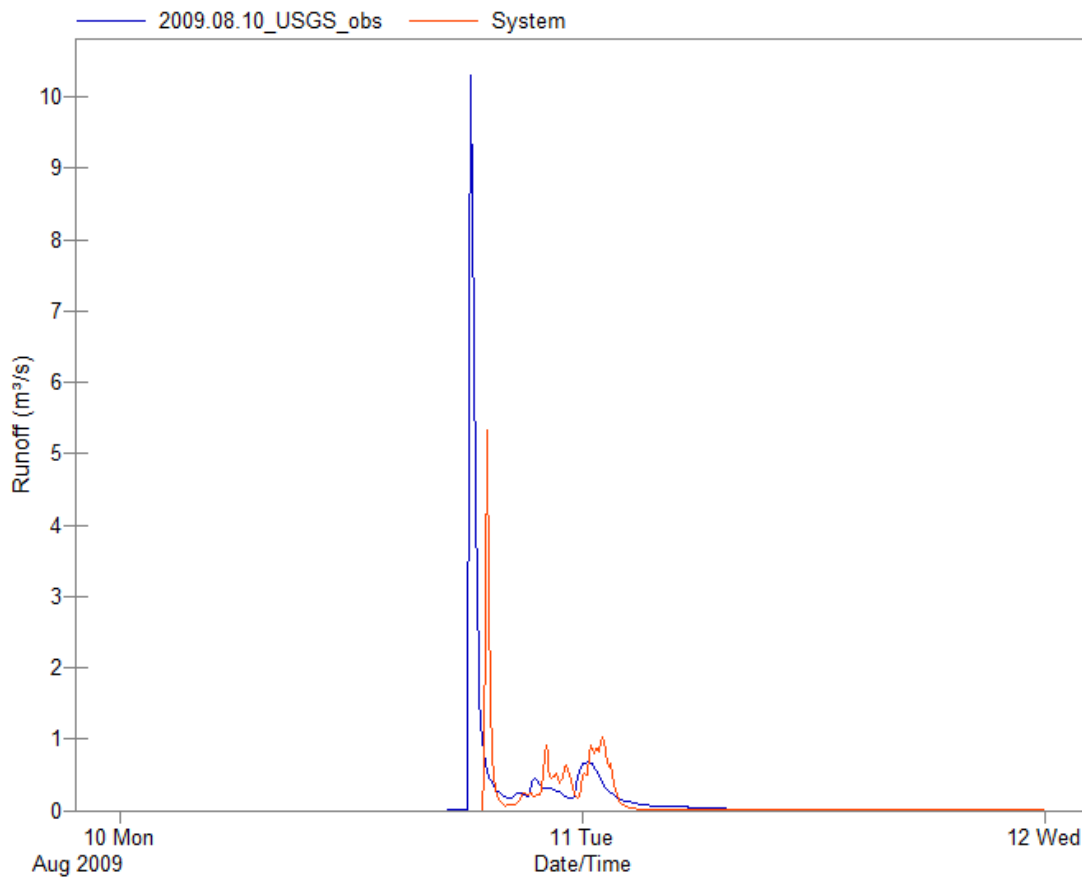


Figure D.3a. Predicted (red line) versus observed (blue line) runoff for Mullins Creek catchment. The predicted runoff hydrograph is based on predicted data for infiltration and percent impervious = percent directly connected impervious surface (Scenario 1). Observed data were downloaded from USGS gaging station data for the Mullins Creek gaging station: 10 August 2009 Storm Event.



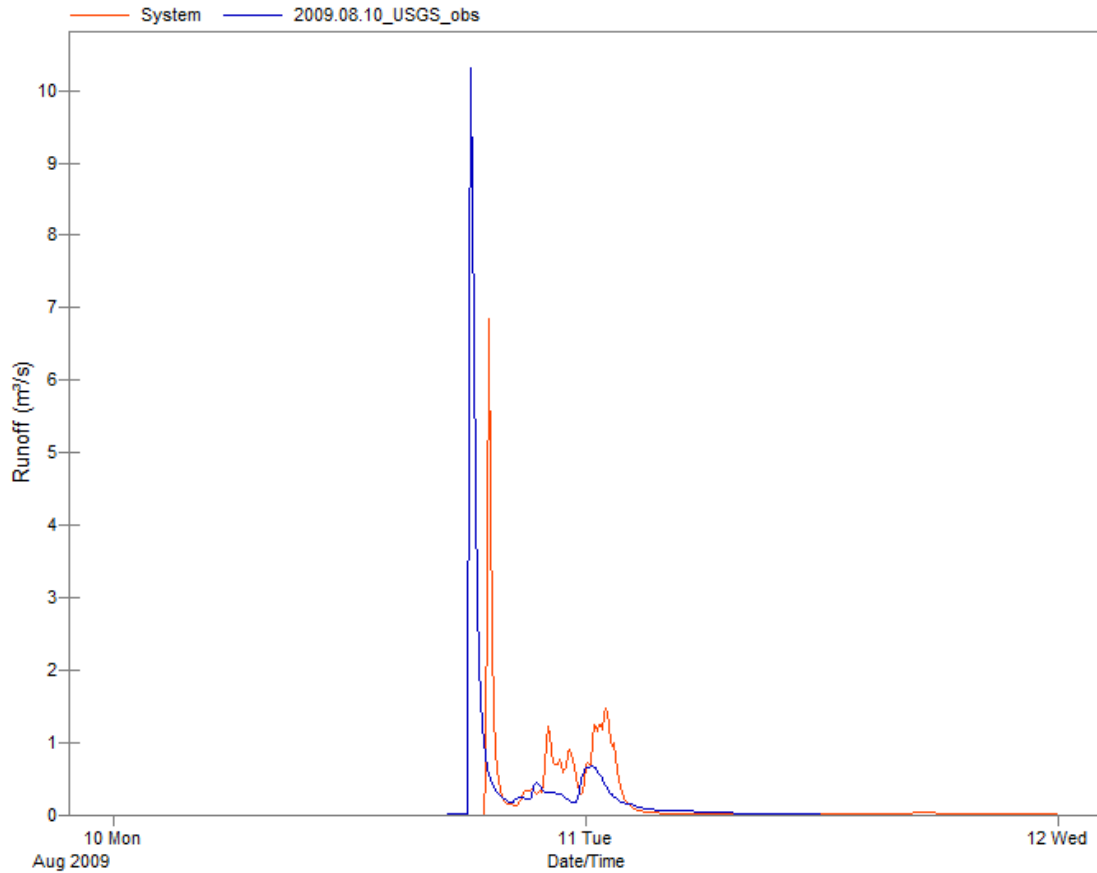


Figure D.3b. Predicted (red line) versus observed (blue line) runoff for Mullins Creek catchment. The predicted runoff hydrograph is based on observed data for infiltration and percent impervious = percent total impervious surface (TIA) (Scenario 2). Observed data were downloaded from USGS gaging station data for the Mullins Creek gaging station: 10 August 2009 Storm Event.

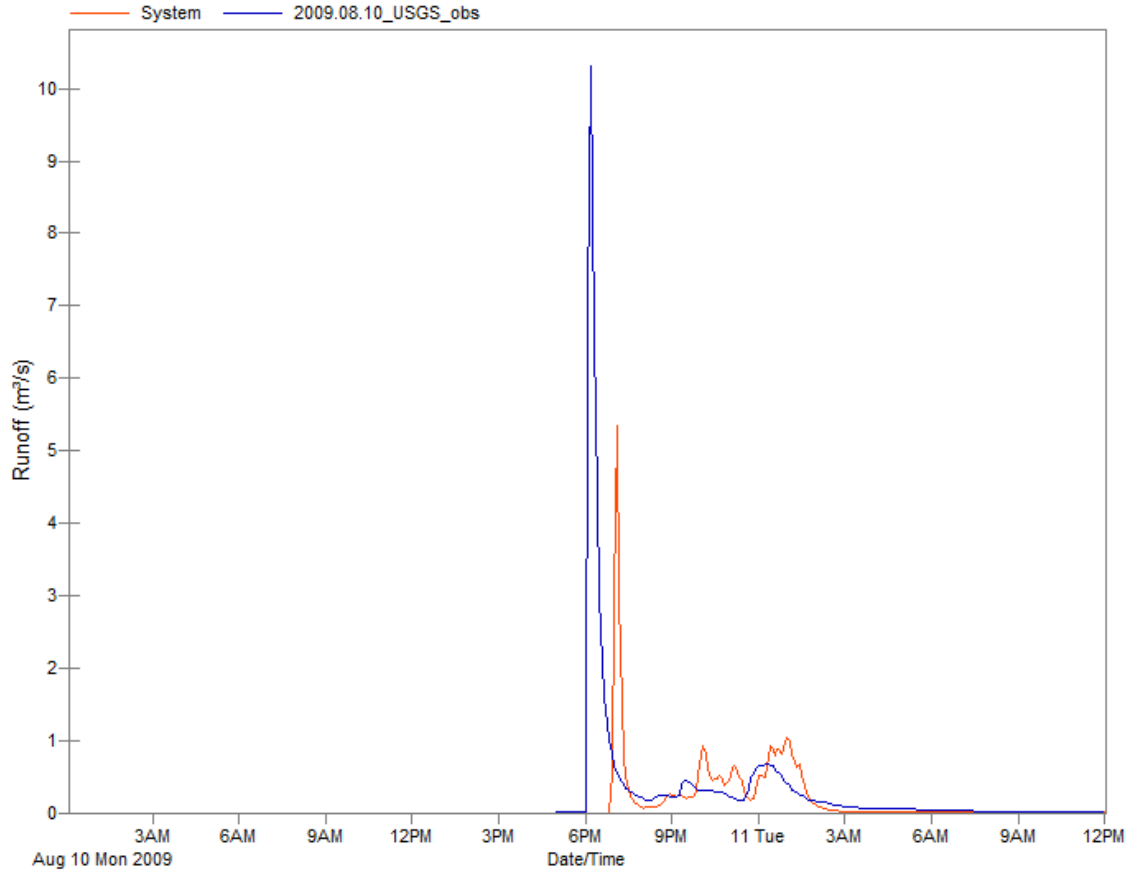


Figure D.3c. Predicted (red line) versus observed (blue line) runoff for Mullins Creek catchment. The predicted runoff hydrograph is based on observed data for infiltration and percent impervious = percent directly connected impervious surface (Scenario 3). Observed data were downloaded from USGS gaging station data for the Mullins Creek gaging station: 10 August 2009 Storm Event.

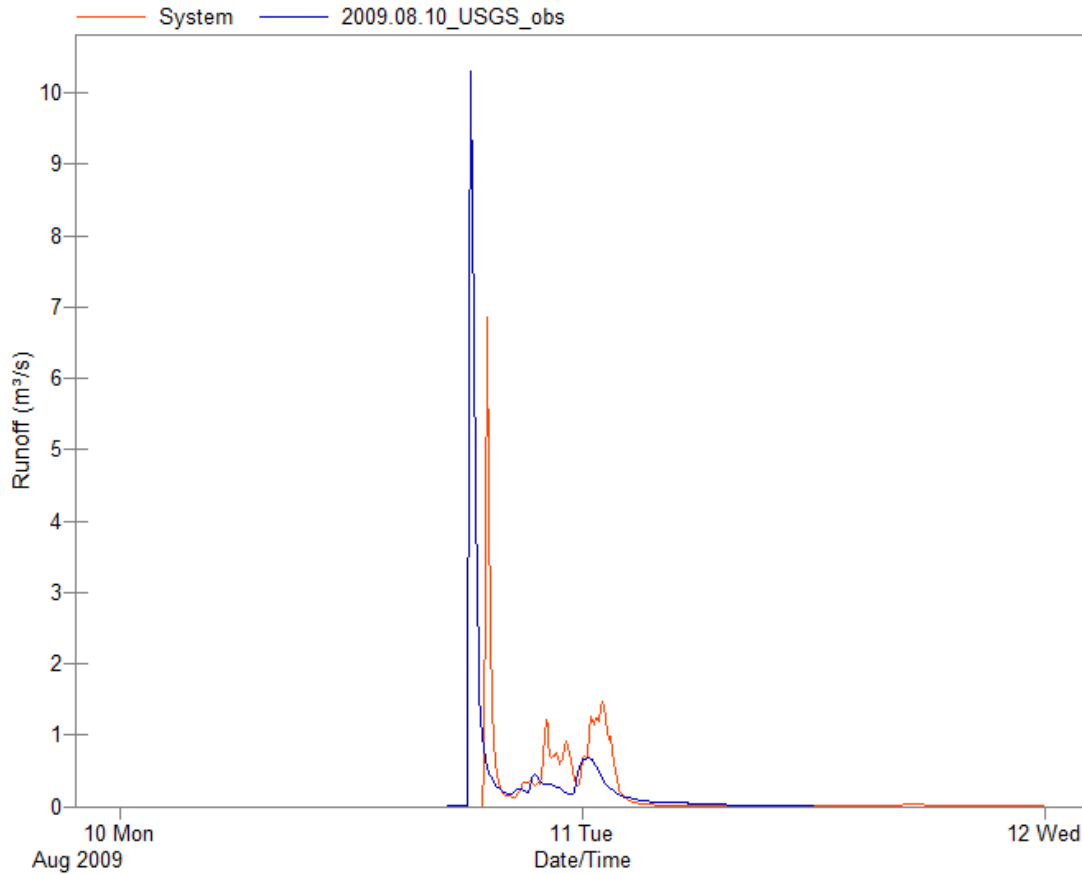


Figure D.3d. Predicted (red line) versus observed (blue line) runoff for Mullins Creek catchment. The predicted runoff hydrograph is based on observed data for infiltration and percent impervious = percent total impervious area (TIA) (Scenario 4). Observed data were downloaded from USGS gaging station data for the Mullins Creek gaging station: 10 August 2009 Storm Event.

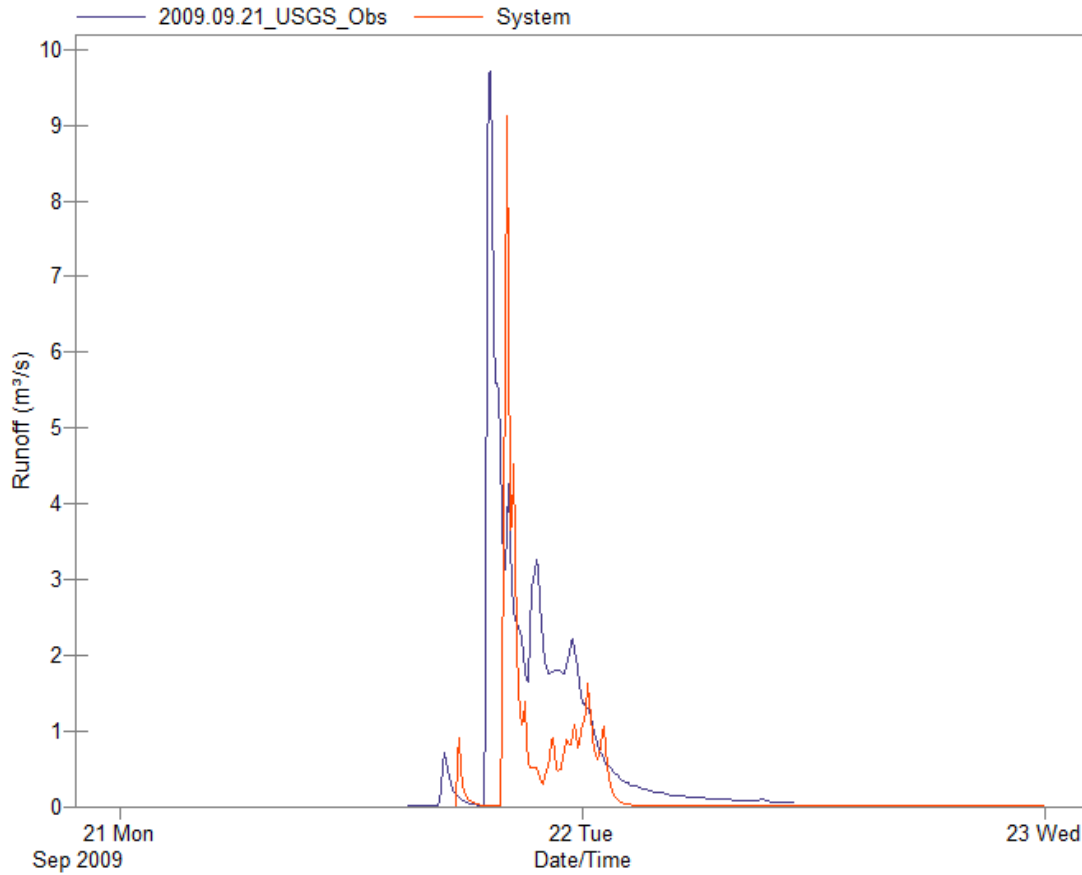


Figure D.4a. Predicted (red line) versus observed (blue line) runoff for Mullins Creek catchment. The predicted runoff hydrograph is based on predicted data for infiltration and percent impervious = percent directly connected impervious surface (Scenario 1). Observed data were downloaded from USGS gaging station data for the Mullins Creek gaging station: 21 September 2009 Storm Event.

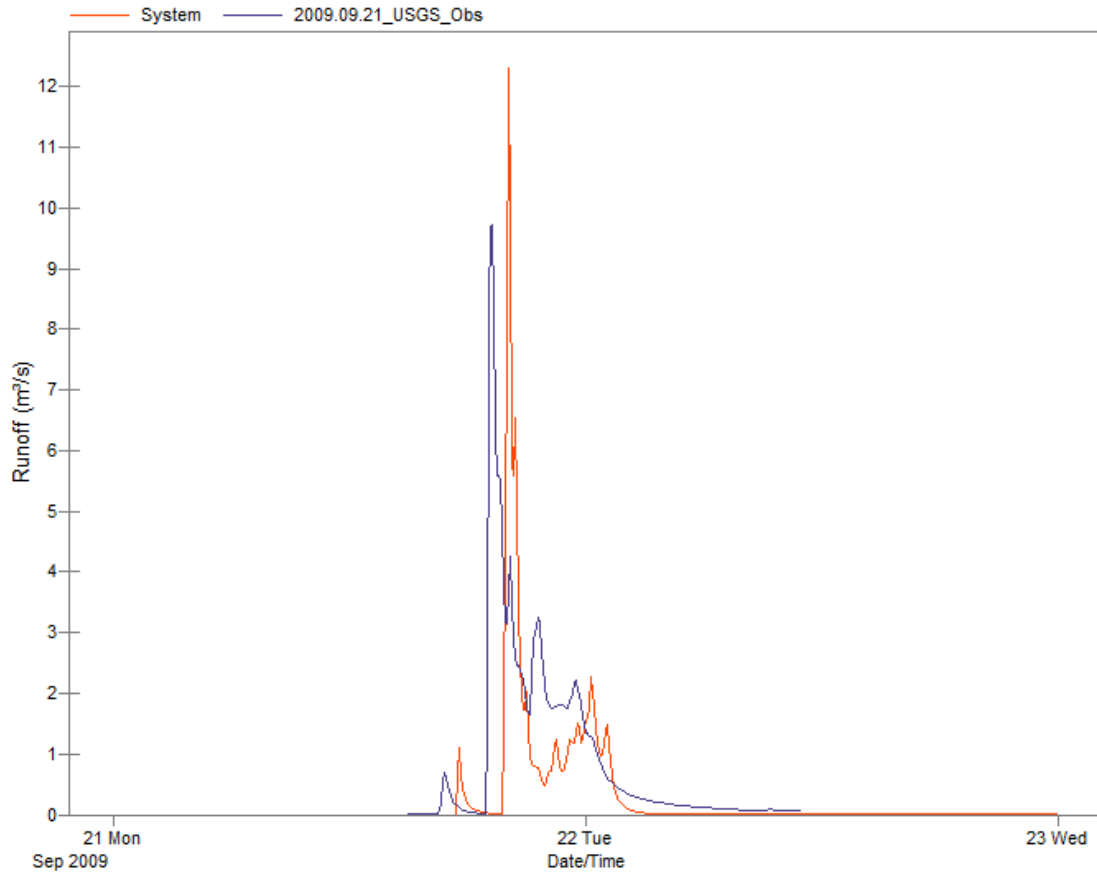


Figure D.4b. Predicted (red line) versus observed (blue line) runoff for Mullins Creek catchment. The predicted runoff hydrograph is based on observed data for infiltration and percent impervious = percent total impervious surface (TIA) (Scenario 2). Observed data were downloaded from USGS gaging station data for the Mullins Creek gaging station: 21 September 2009 Storm Event.

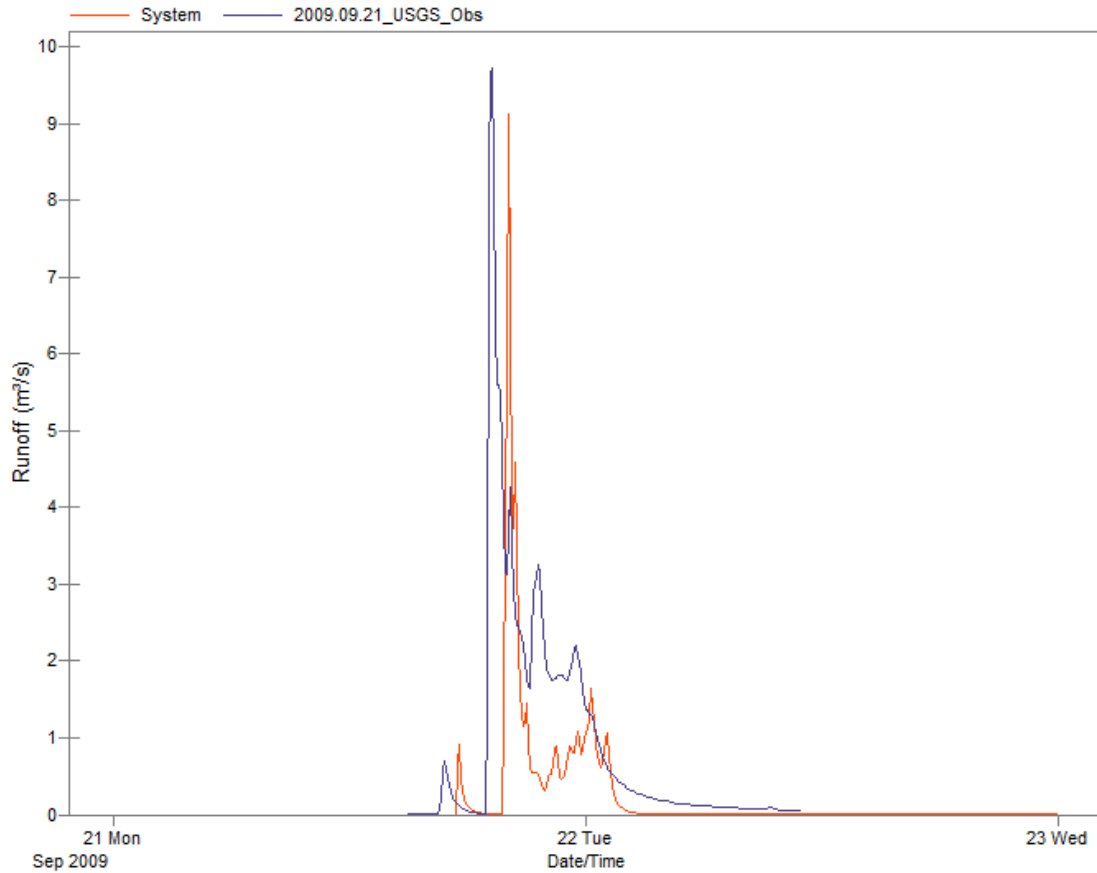


Figure D.4c. Predicted (red line) versus observed (blue line) runoff for Mullins Creek catchment. The predicted runoff hydrograph is based on observed data for infiltration and percent impervious = percent directly connected impervious surface (Scenario 3). Observed data were downloaded from USGS gaging station data for the Mullins Creek gaging station: 21 September 2009 Storm Event.

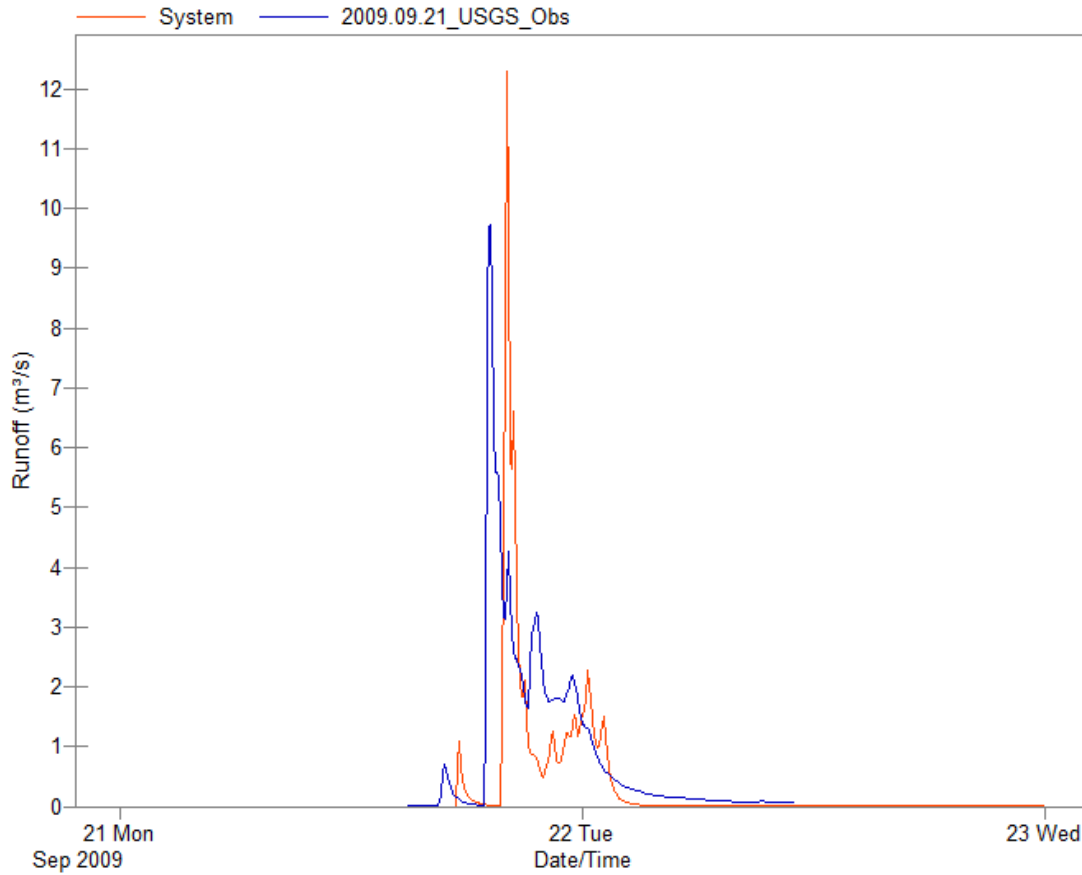


Figure D.4d. Predicted (red line) versus observed (blue line) runoff for Mullins Creek catchment. The predicted runoff hydrograph is based on observed data for infiltration and percent impervious = percent total impervious area (TIA) (Scenario 4). Observed data were downloaded from USGS gaging station data for the Mullins Creek gaging station: 21 September 2009 Storm Event.

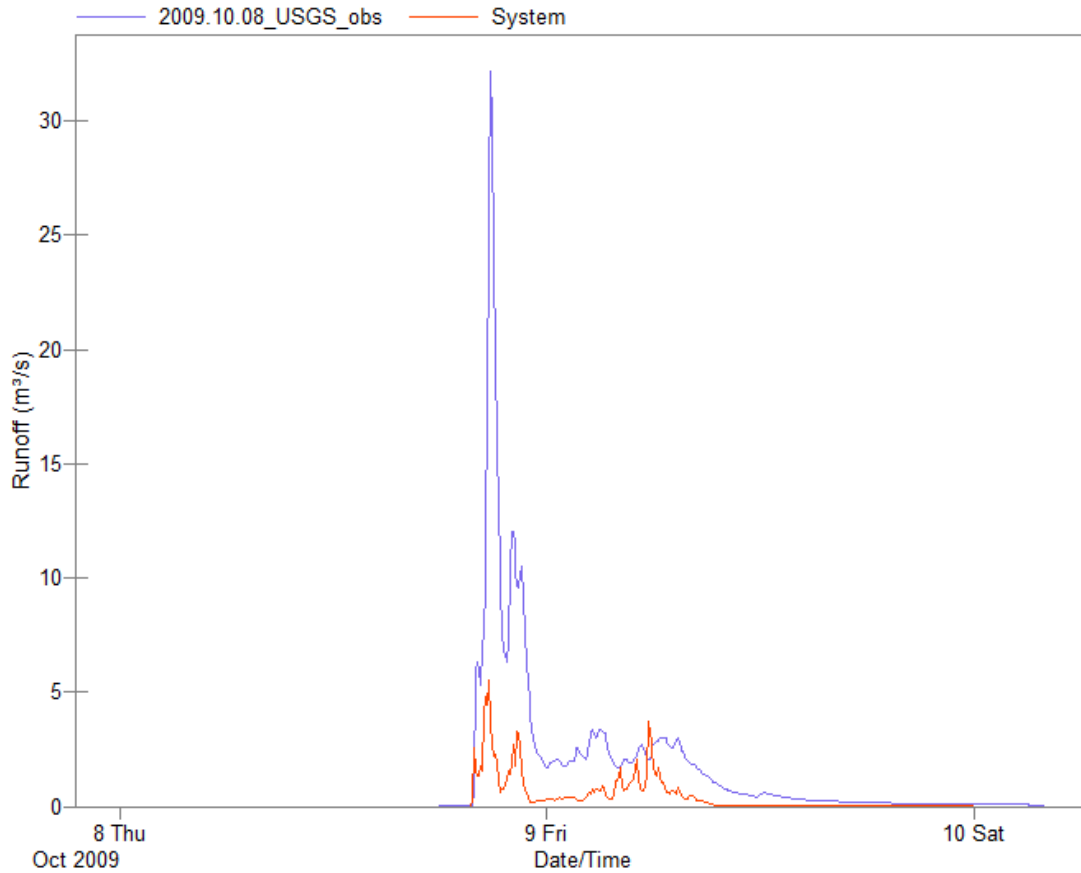


Figure D.5a. Predicted (red line) versus observed (blue line) runoff for Mullins Creek catchment. The predicted runoff hydrograph is based on predicted data for infiltration and percent impervious = percent directly connected impervious surface (Scenario 1). Observed data were downloaded from USGS gaging station data for the Mullins Creek gaging station: 08 October 2009 Storm Event.



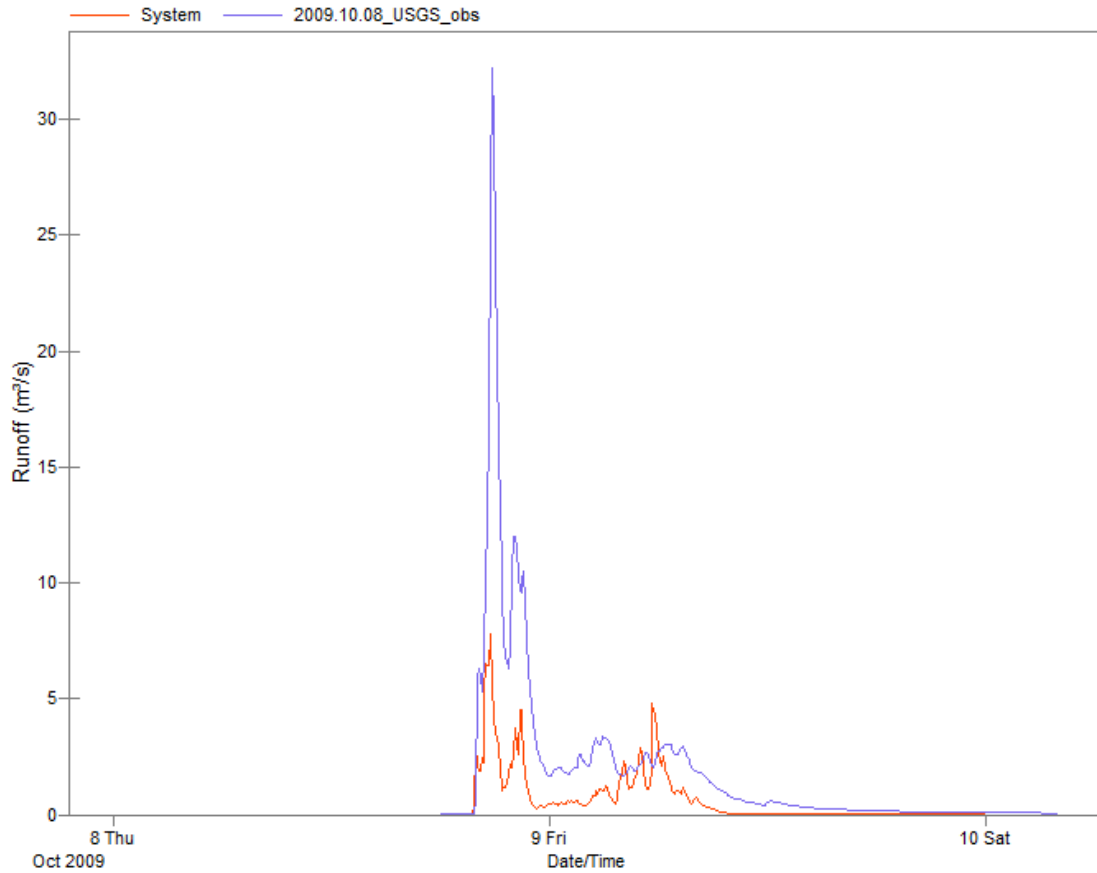


Figure D.5b. Predicted (red line) versus observed (blue line) runoff for Mullins Creek catchment. The predicted runoff hydrograph is based on observed data for infiltration and percent impervious = percent total impervious surface (TIA) (Scenario 2). Observed data were downloaded from USGS gaging station data for the Mullins Creek gaging station: 08 October 2009 Storm Event.

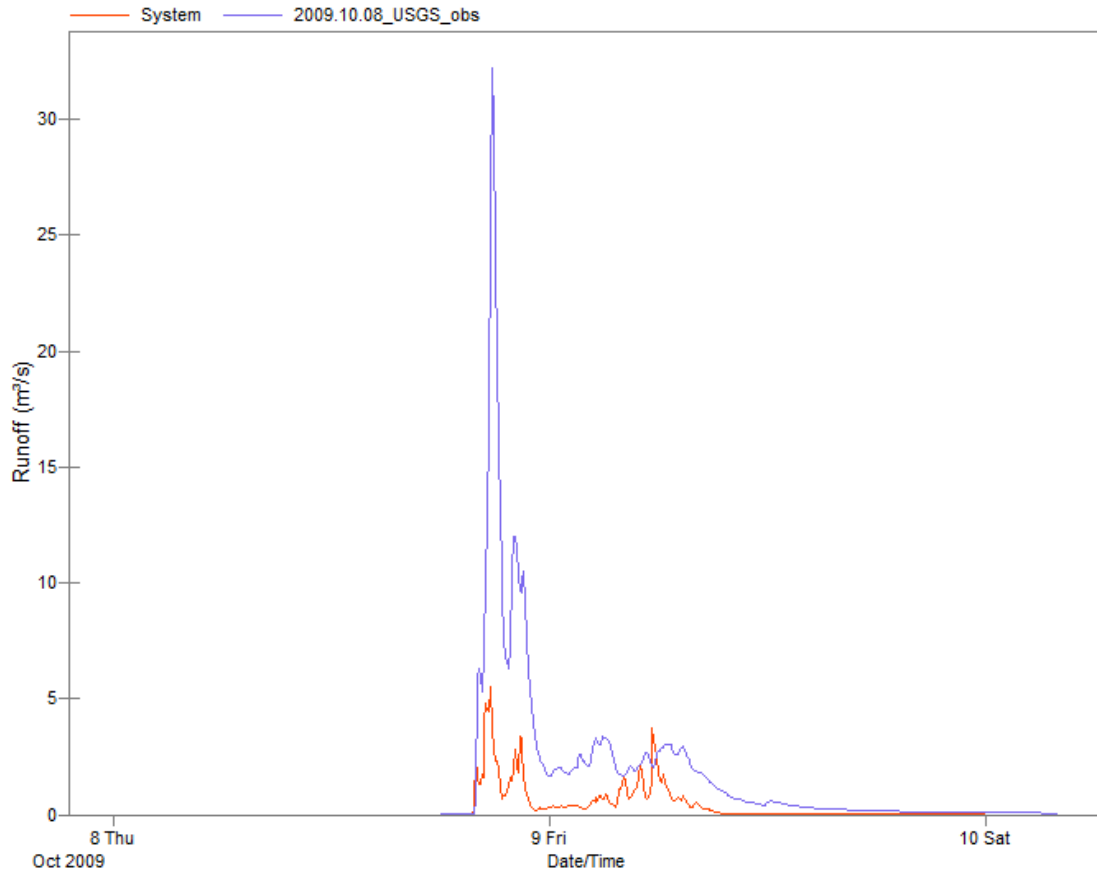


Figure D.5c. Predicted (red line) versus observed (blue line) runoff for Mullins Creek catchment. The predicted runoff hydrograph is based on observed data for infiltration and percent impervious = percent directly connected impervious surface (Scenario 3). Observed data were downloaded from USGS gaging station data for the Mullins Creek gaging station: 08 October 2009 Storm Event.

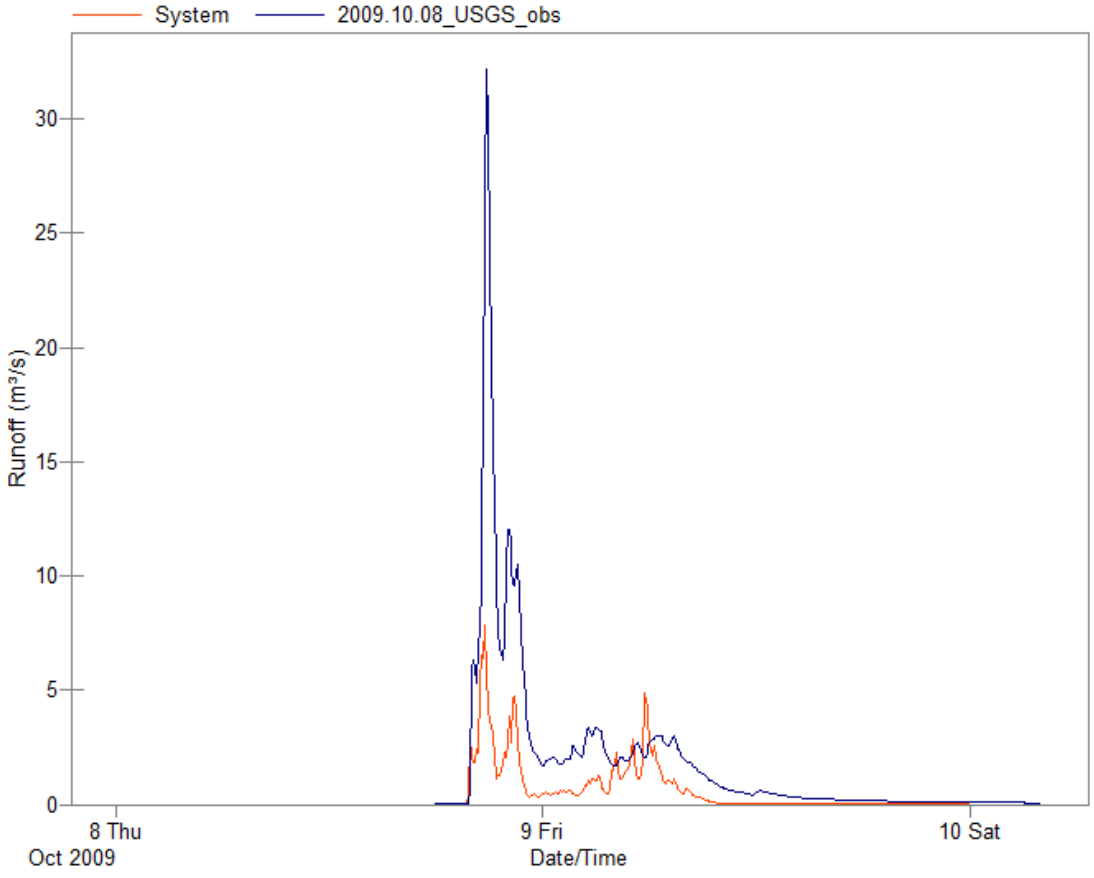


Figure D.5d. Predicted (red line) versus observed (blue line) runoff for Mullins Creek catchment. The predicted runoff hydrograph is based on observed data for infiltration and percent impervious = percent total impervious area (TIA) (Scenario 4). Observed data were downloaded from USGS gaging station data for the Mullins Creek gaging station: 08 October 2009 Storm Event.

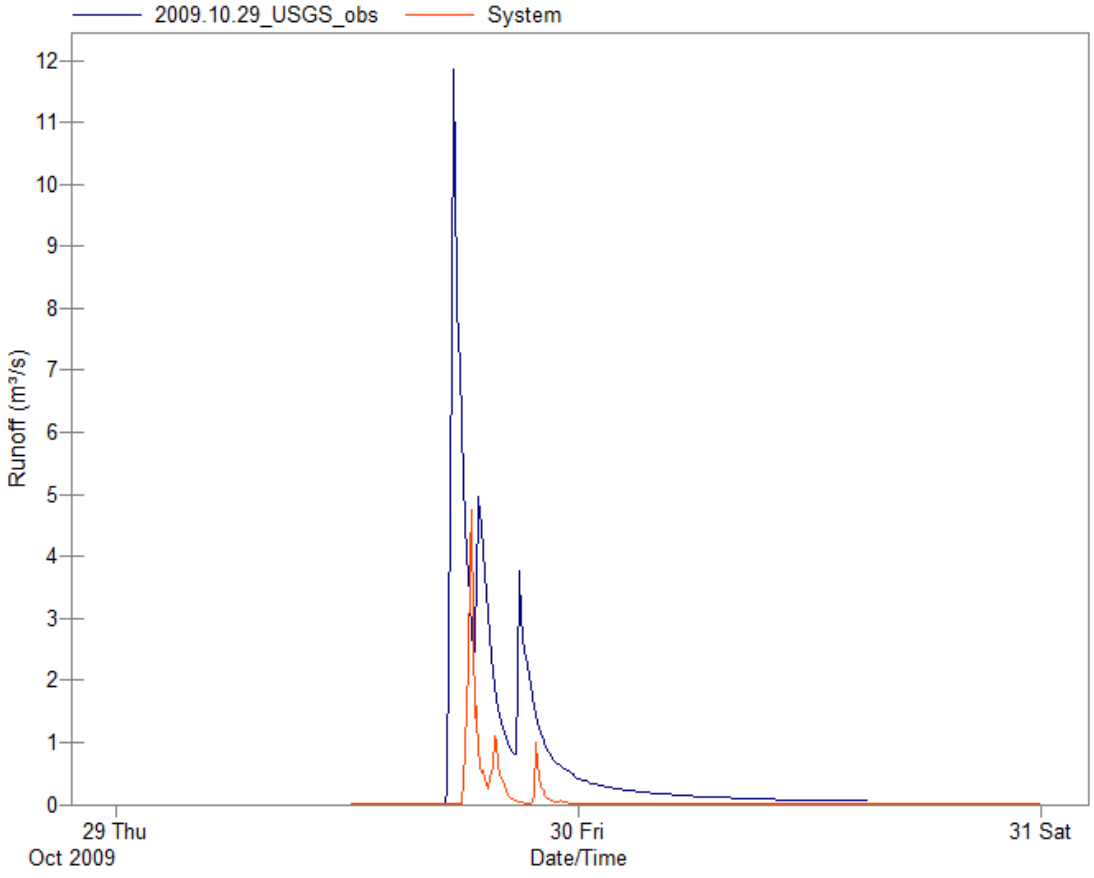


Figure D.6a. Predicted (red line) versus observed (blue line) runoff for Mullins Creek catchment. The predicted runoff hydrograph is based on predicted data for infiltration and percent impervious = percent directly connected impervious surface (Scenario 1). Observed data were downloaded from USGS gaging station data for the Mullins Creek gaging station: 29 October 2009 Storm Event.

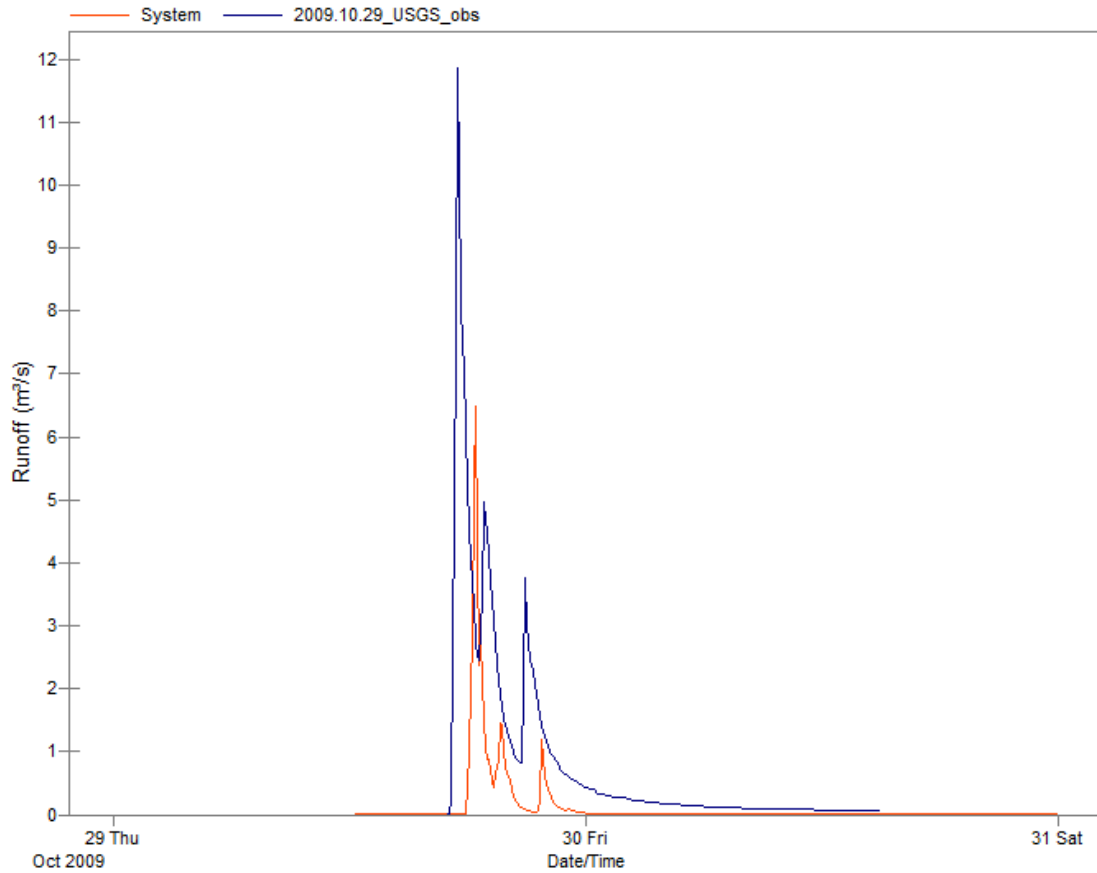


Figure D.6b. Predicted (red line) versus observed (blue line) runoff for Mullins Creek catchment. The predicted runoff hydrograph is based on observed data for infiltration and percent impervious = percent total impervious surface (TIA) (Scenario 2). Observed data were downloaded from USGS gaging station data for the Mullins Creek gaging station: 29 October 2009 Storm Event.

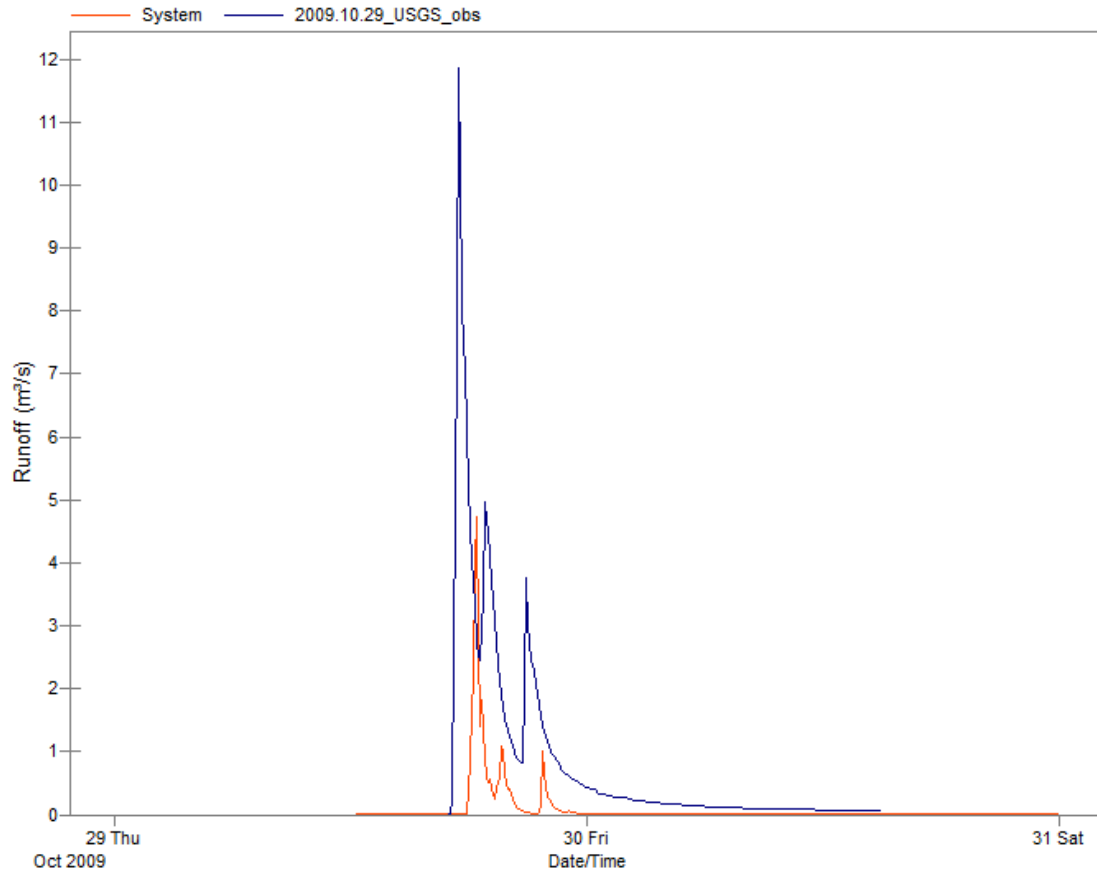


Figure D.6c. Predicted (red line) versus observed (blue line) runoff for Mullins Creek catchment. The predicted runoff hydrograph is based on observed data for infiltration and percent impervious = percent directly connected impervious surface (Scenario 3). Observed data were downloaded from USGS gaging station data for the Mullins Creek gaging station: 29 October 2009 Storm Event.

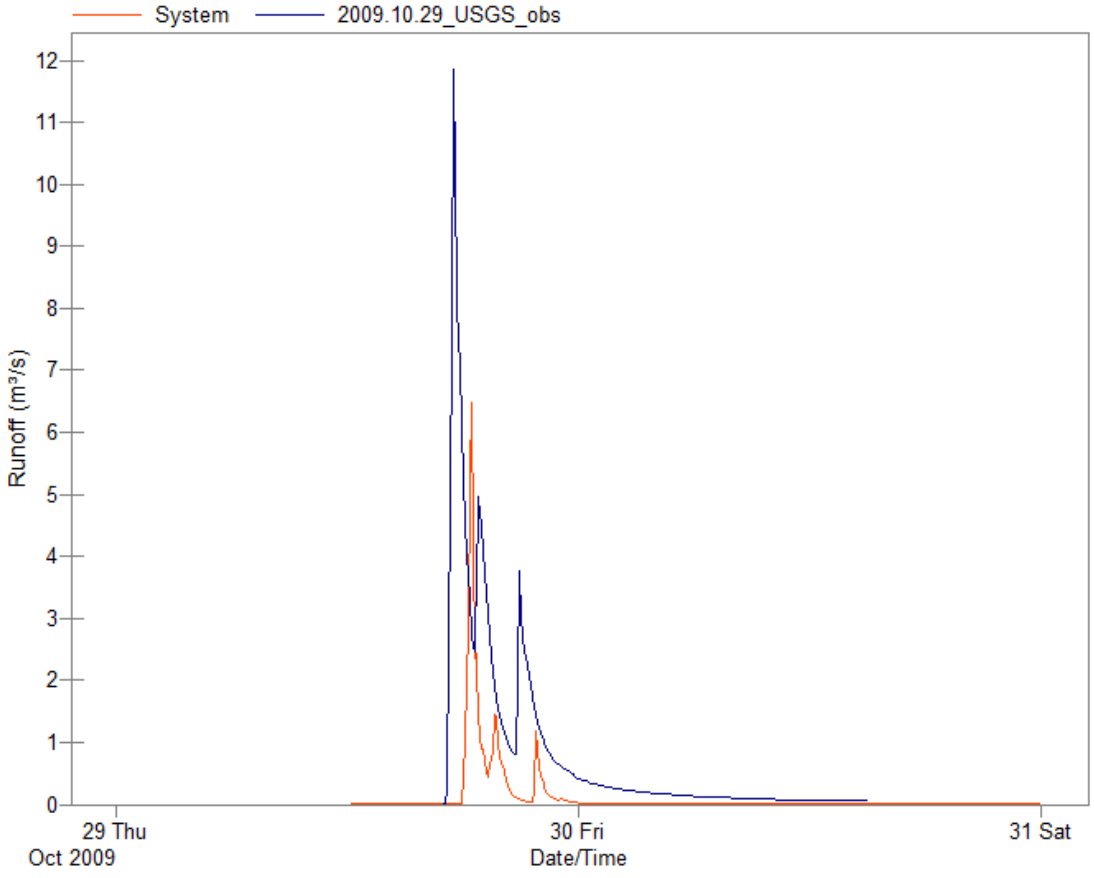


Figure D.6d. Predicted (red line) versus observed (blue line) runoff for Mullins Creek catchment. The predicted runoff hydrograph is based on observed data for infiltration and percent impervious = percent total impervious area (TIA) (Scenario 4). Observed data were downloaded from USGS gaging station data for the Mullins Creek gaging station: 29 October 2009 Storm Event.

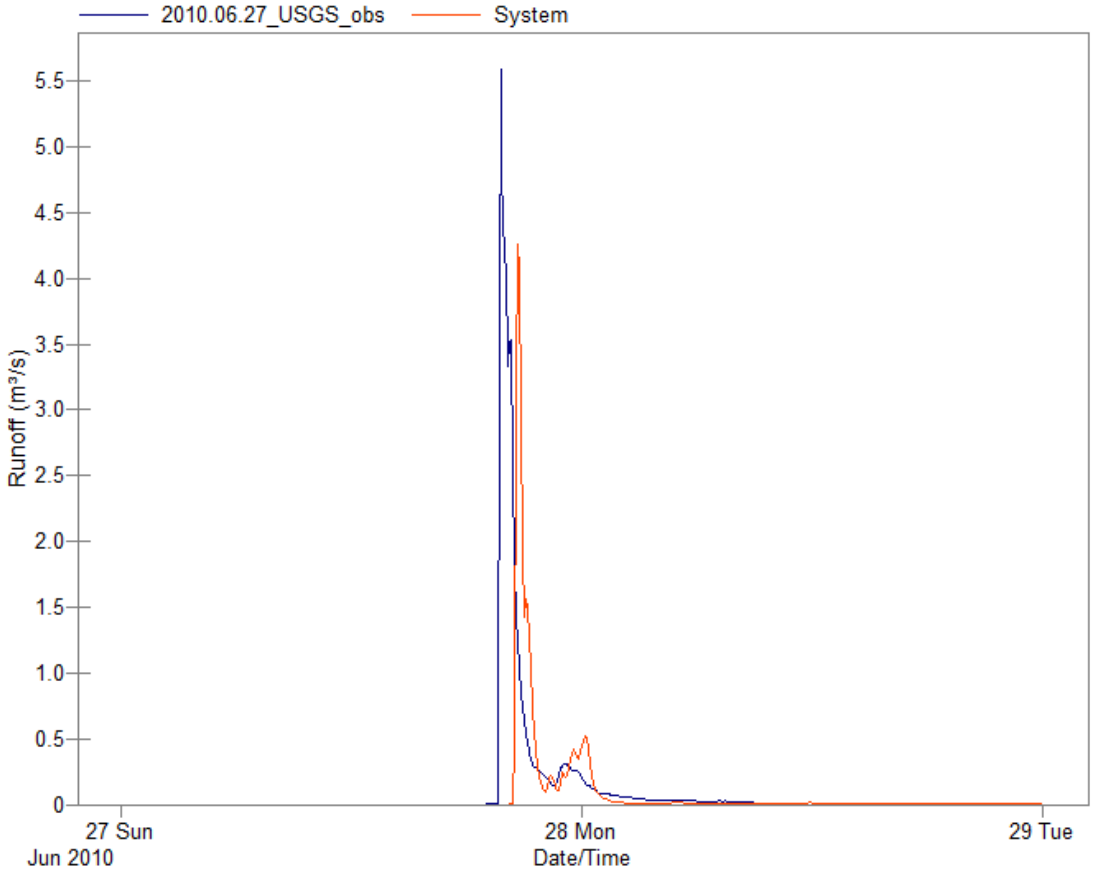


Figure D.7a. Predicted (red line) versus observed (blue line) runoff for Mullins Creek catchment. The predicted runoff hydrograph is based on predicted data for infiltration and percent impervious = percent directly connected impervious surface (Scenario 1). Observed data were downloaded from USGS gaging station data for the Mullins Creek gaging station: 27 June 2010 Storm Event.



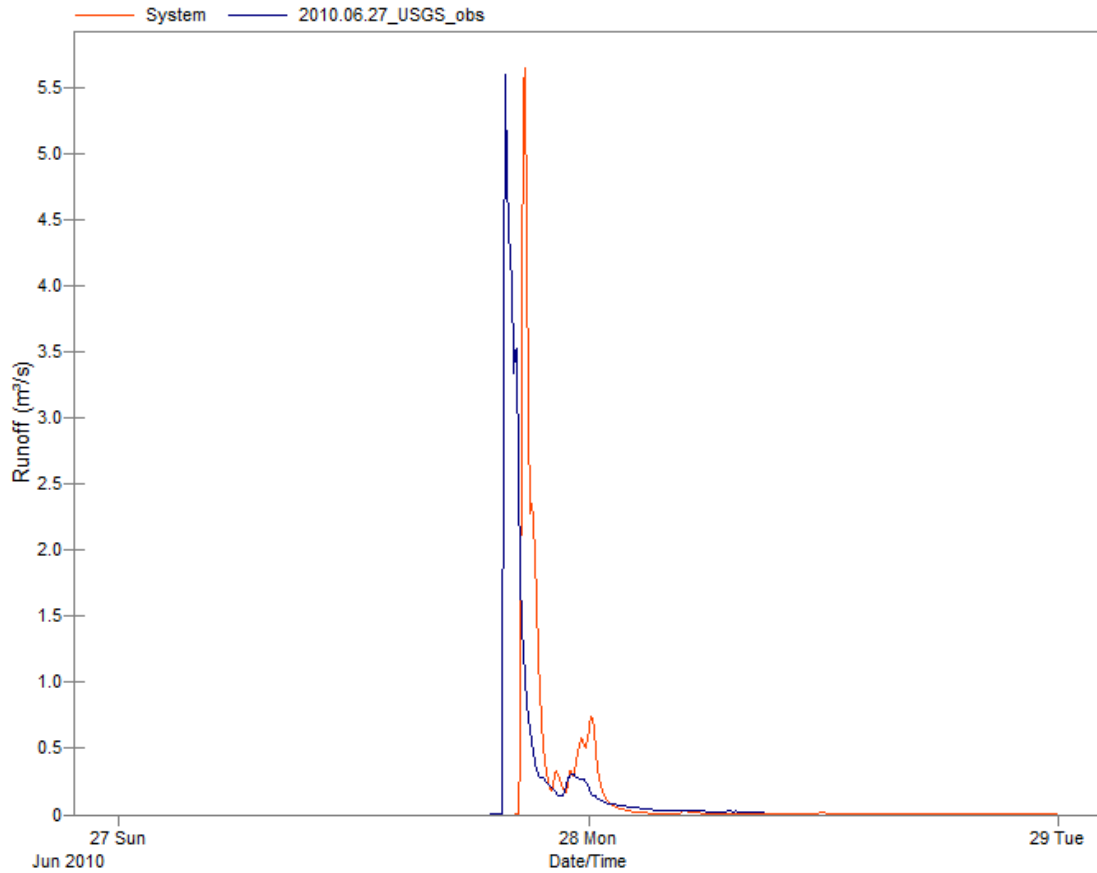


Figure D.7b. Predicted (red line) versus observed (blue line) runoff for Mullins Creek catchment. The predicted runoff hydrograph is based on observed data for infiltration and percent impervious = percent total impervious surface (TIA) (Scenario 2). Observed data were downloaded from USGS gaging station data for the Mullins Creek gaging station: 27 June 2010 Storm Event.

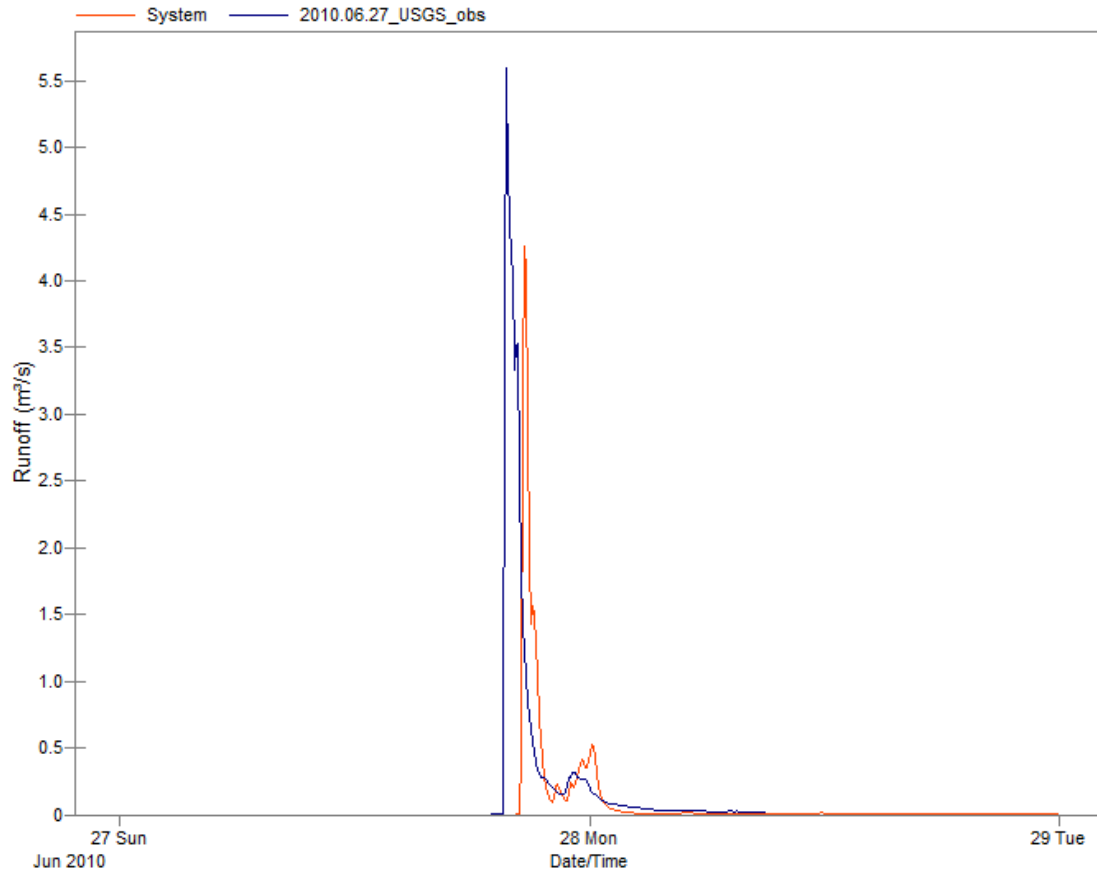


Figure D.7c. Predicted (red line) versus observed (blue line) runoff for Mullins Creek catchment. The predicted runoff hydrograph is based on observed data for infiltration and percent impervious = percent directly connected impervious surface (Scenario 3). Observed data were downloaded from USGS gaging station data for the Mullins Creek gaging station: 27 June 2010 Storm Event.

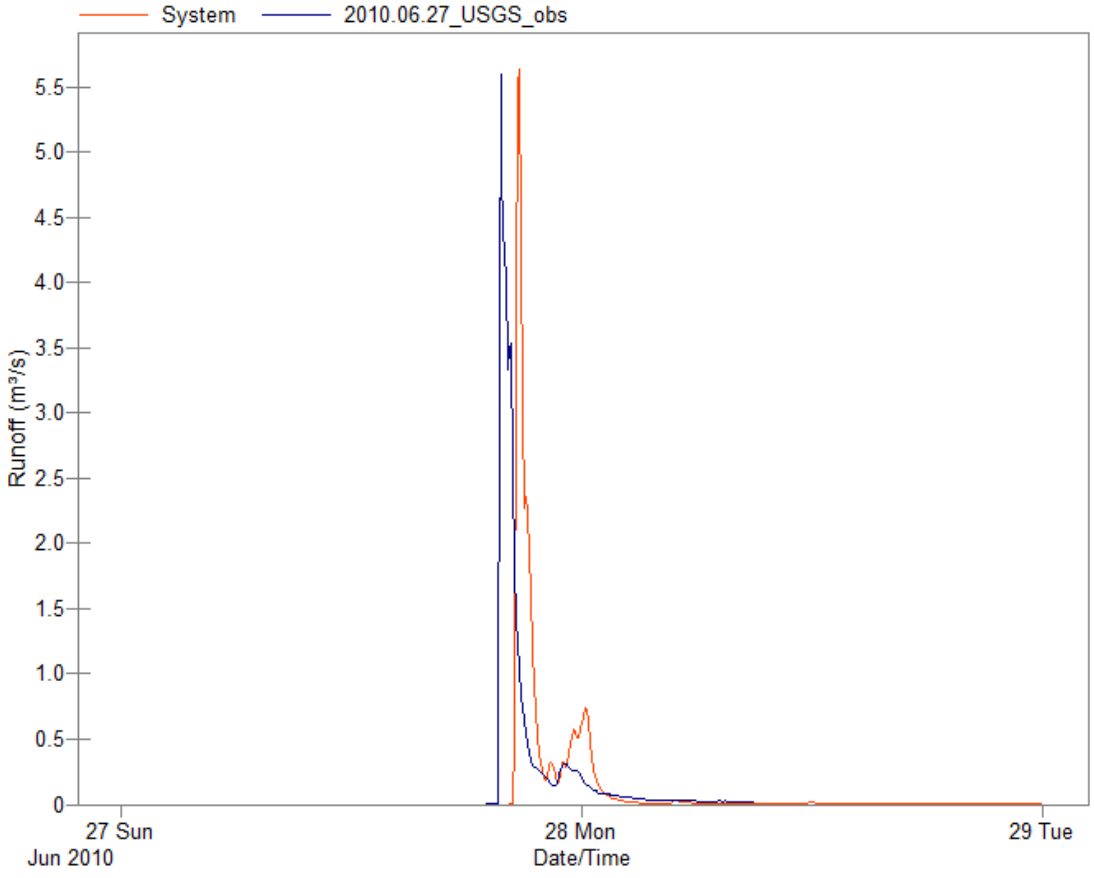


Figure D.7d. Predicted (red line) versus observed (blue line) runoff for Mullins Creek catchment. The predicted runoff hydrograph is based on observed data for infiltration and percent impervious = percent total impervious area (TIA) (Scenario 4). Observed data were downloaded from USGS gaging station data for the Mullins Creek gaging station: 27 June 2010 Storm Event.

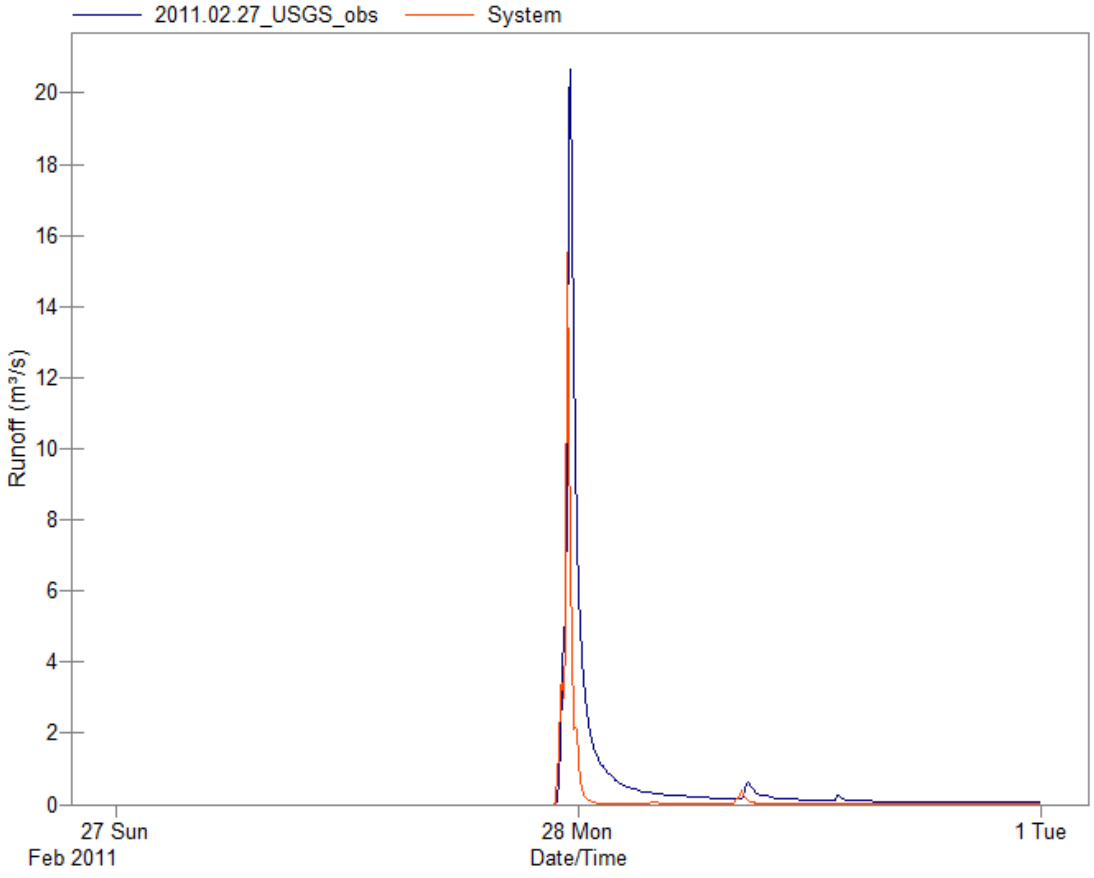


Figure D.8a. Predicted (red line) versus observed (blue line) runoff for Mullins Creek catchment. The predicted runoff hydrograph is based on predicted data for infiltration and percent impervious = percent directly connected impervious surface (Scenario 1). Observed data were downloaded from USGS gaging station data for the Mullins Creek gaging station: 27 February 2011 Storm Event.

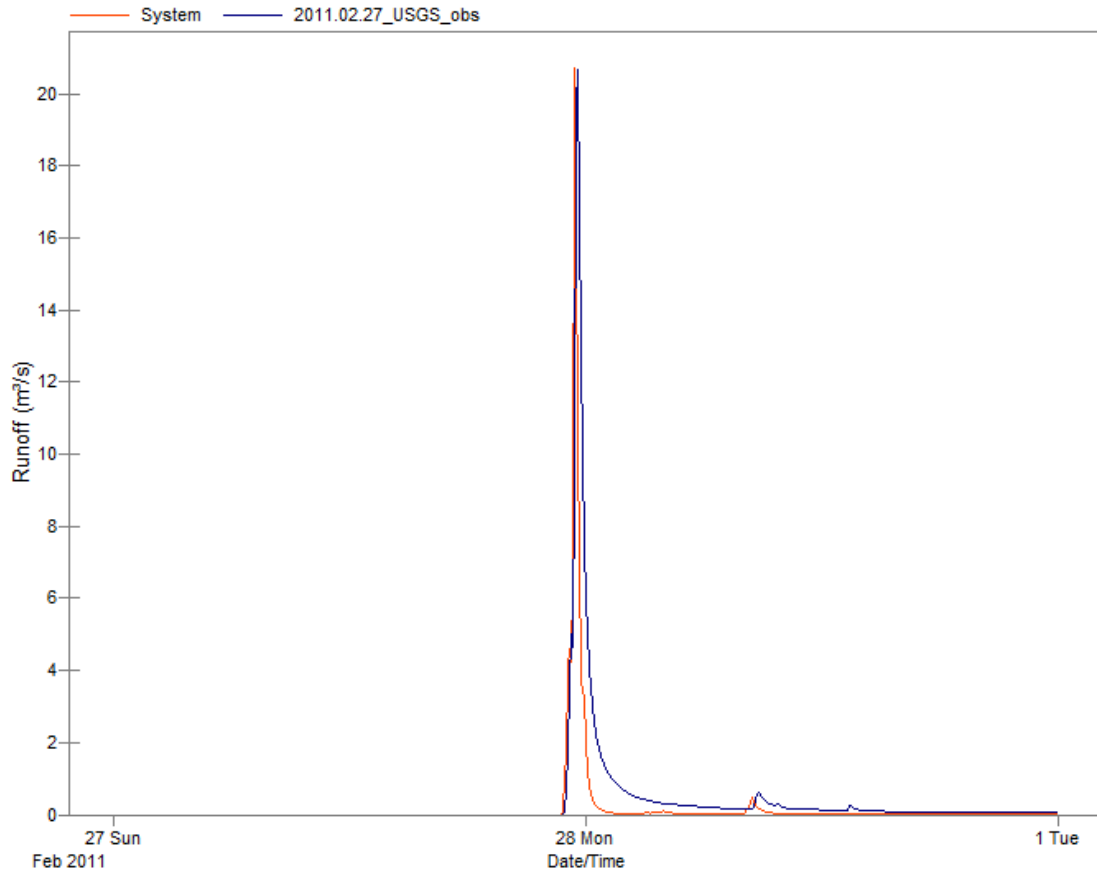


Figure D.8b. Predicted (red line) versus observed (blue line) runoff for Mullins Creek catchment. The predicted runoff hydrograph is based on observed data for infiltration and percent impervious = percent total impervious surface (TIA) (Scenario 2). Observed data were downloaded from USGS gaging station data for the Mullins Creek gaging station: 27 February 2011 Storm Event.

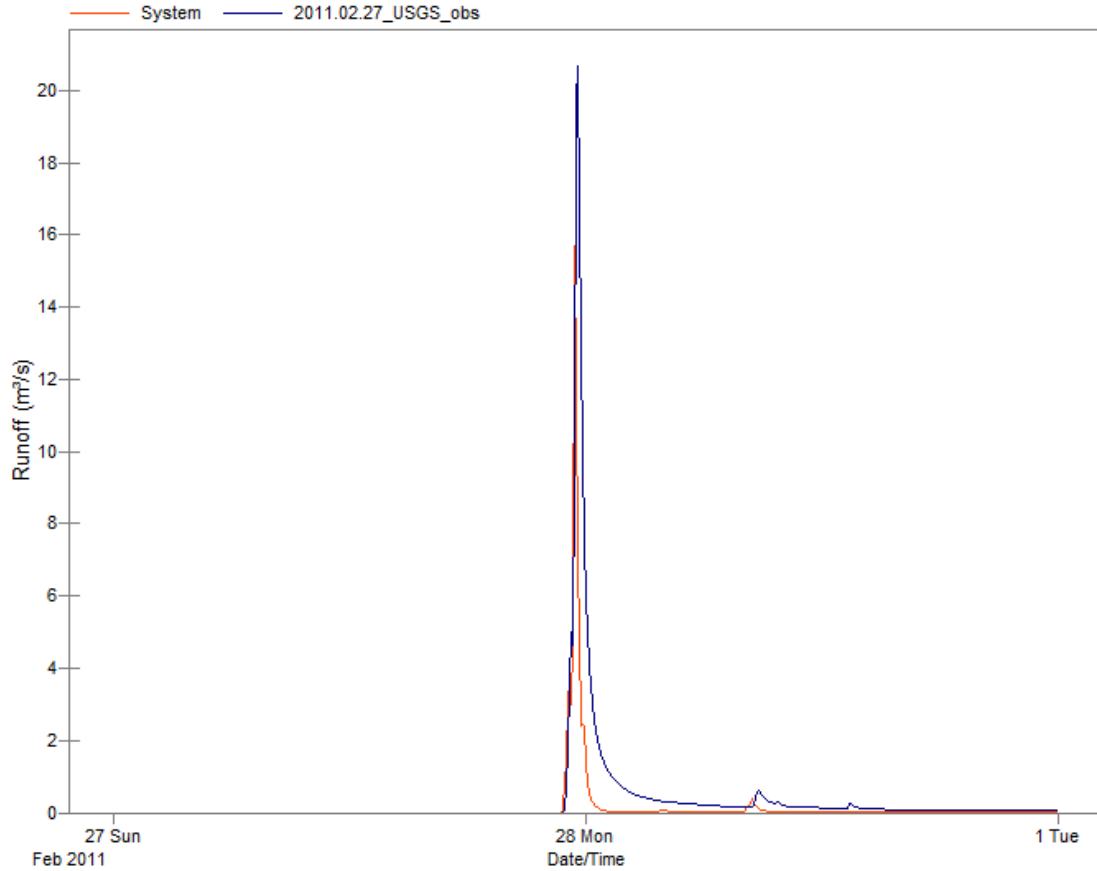


Figure D.8c. Predicted (red line) versus observed (blue line) runoff for Mullins Creek catchment. The predicted runoff hydrograph is based on observed data for infiltration and percent impervious = percent directly connected impervious surface (Scenario 3). Observed data were downloaded from USGS gaging station data for the Mullins Creek gaging station: 27 February 2011 Storm Event.

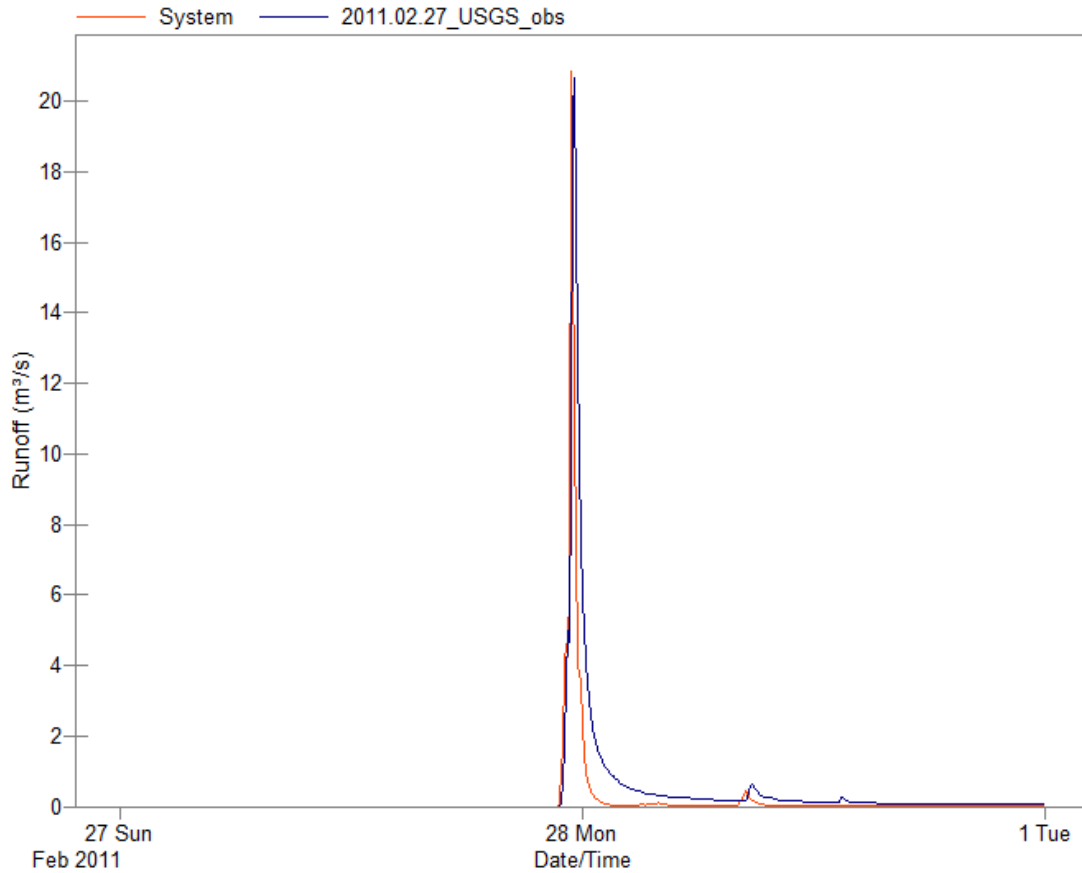


Figure D.8d. Predicted (red line) versus observed (blue line) runoff for Mullins Creek catchment. The predicted runoff hydrograph is based on observed data for infiltration and percent impervious = percent total impervious area (TIA) (Scenario 4). Observed data were downloaded from USGS gaging station data for the Mullins Creek gaging station: 27 February 2011 Storm Event.

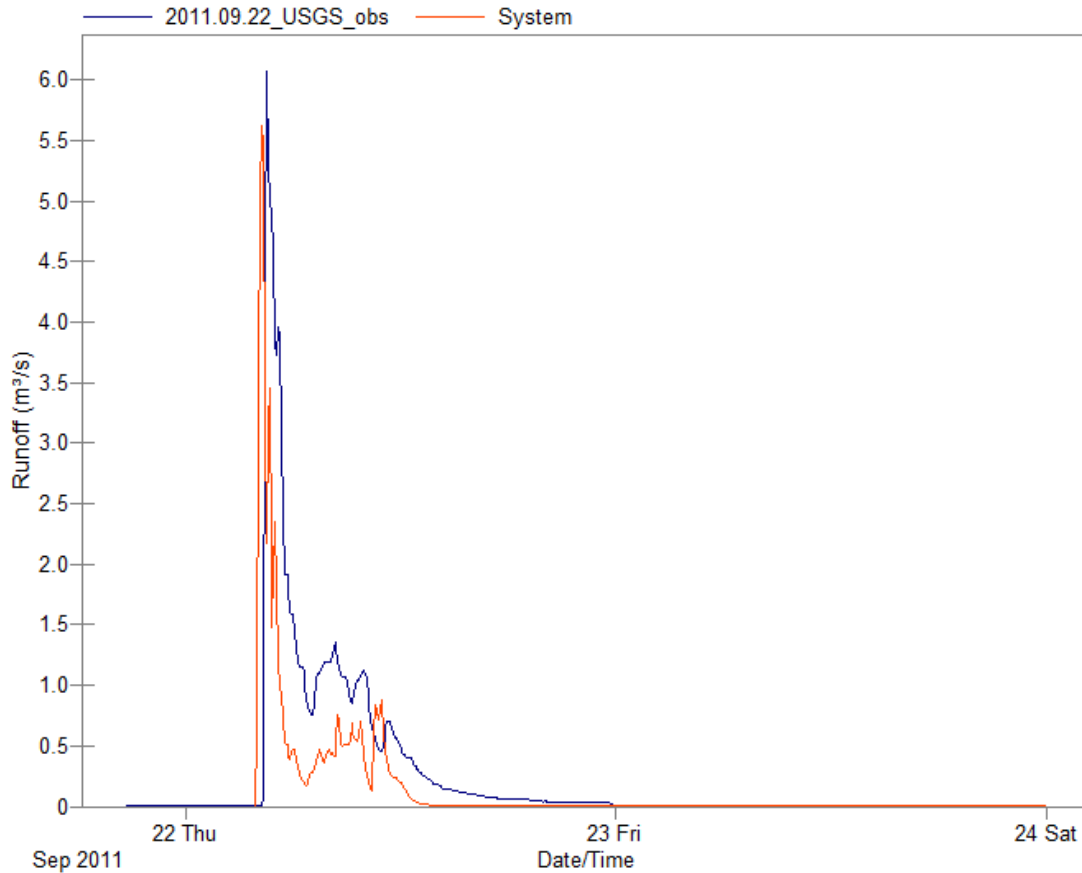


Figure D.9a. Predicted (red line) versus observed (blue line) runoff for Mullins Creek catchment. The predicted runoff hydrograph is based on predicted data for infiltration and percent impervious = percent directly connected impervious surface (Scenario 1). Observed data were downloaded from USGS gaging station data for the Mullins Creek gaging station: 22 September 2011 Storm Event.



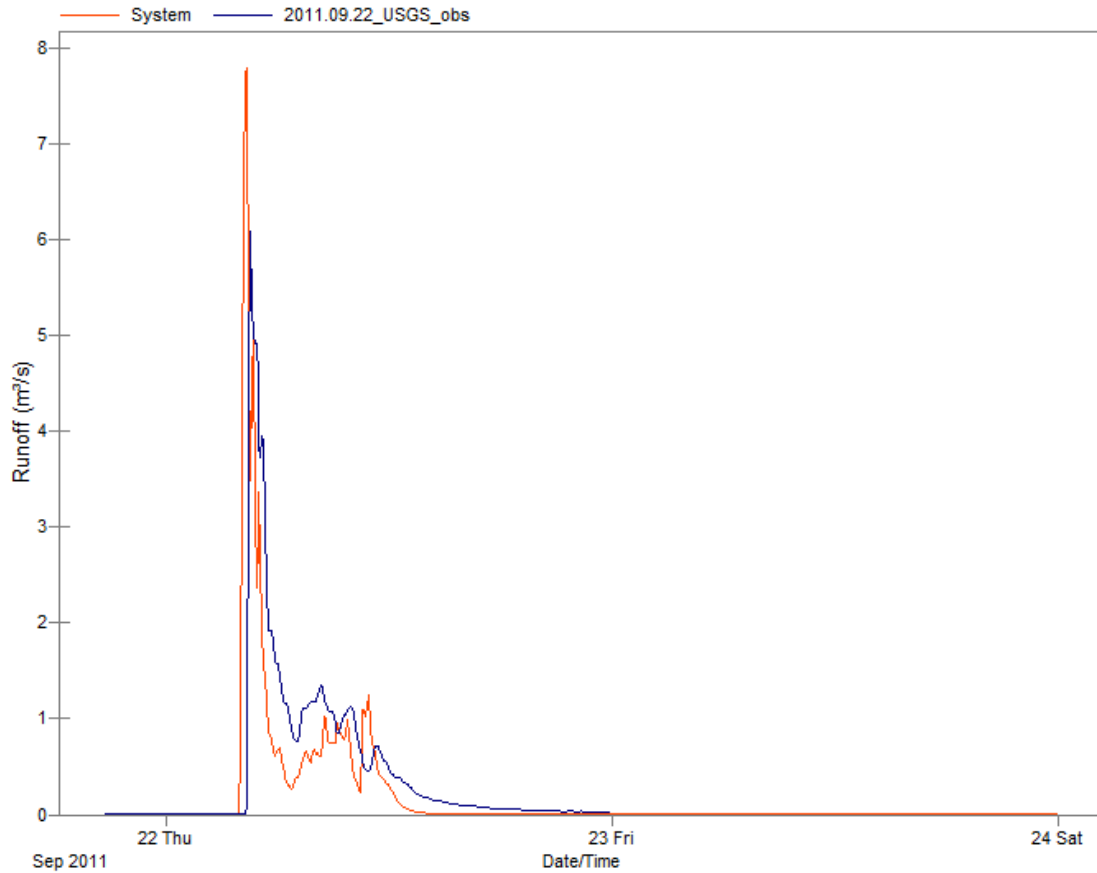


Figure D.9b. Predicted (red line) versus observed (blue line) runoff for Mullins Creek catchment. The predicted runoff hydrograph is based on observed data for infiltration and percent impervious = percent total impervious surface (TIA) (Scenario 2). Observed data were downloaded from USGS gaging station data for the Mullins Creek gaging station: 22 September 2011 Storm Event.

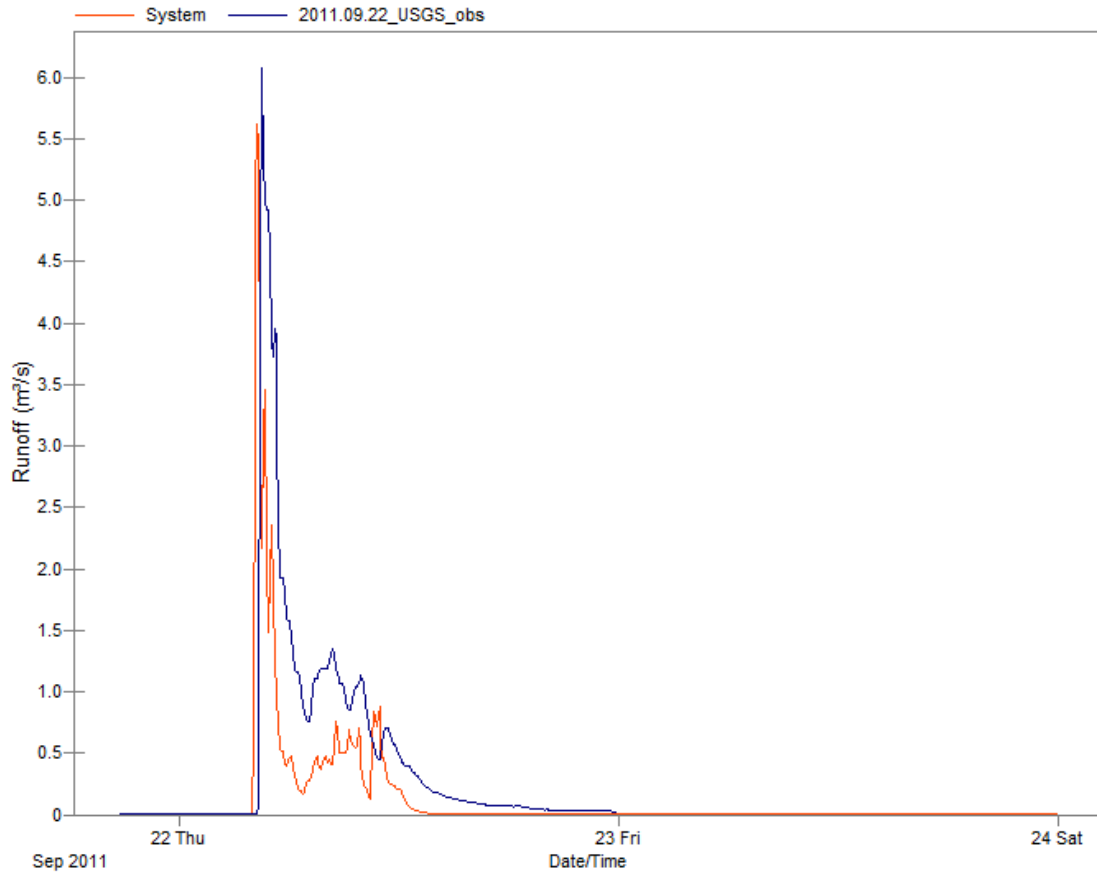


Figure D.9c. Predicted (red line) versus observed (blue line) runoff for Mullins Creek catchment. The predicted runoff hydrograph is based on observed data for infiltration and percent impervious = percent directly connected impervious surface (Scenario 3). Observed data were downloaded from USGS gaging station data for the Mullins Creek gaging station: 22 September 2011 Storm Event.

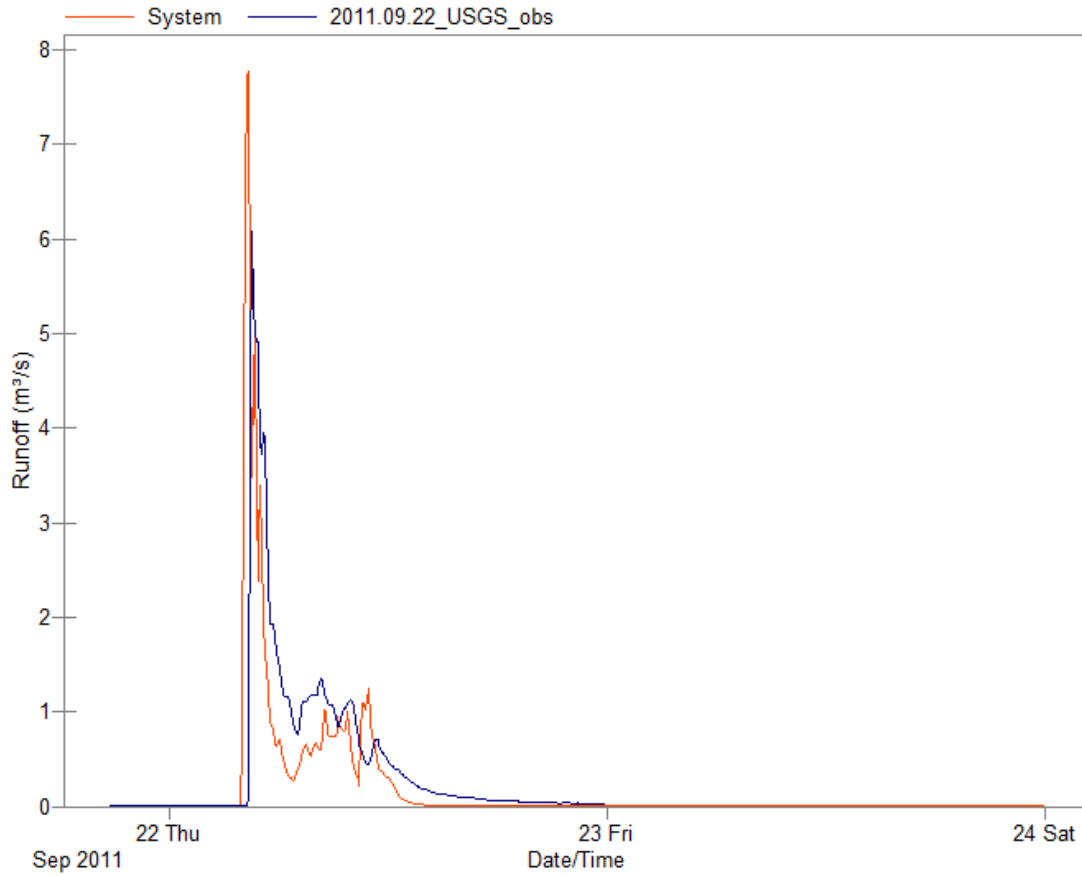


Figure D.9d. Predicted (red line) versus observed (blue line) runoff for Mullins Creek catchment. The predicted runoff hydrograph is based on observed data for infiltration and percent impervious = percent total impervious area (TIA) (Scenario 4). Observed data were downloaded from USGS gaging station data for the Mullins Creek gaging station: 22 September 2011 Storm Event.